Gas Shale Potential of Devonian Strata, Northeastern British Columbia

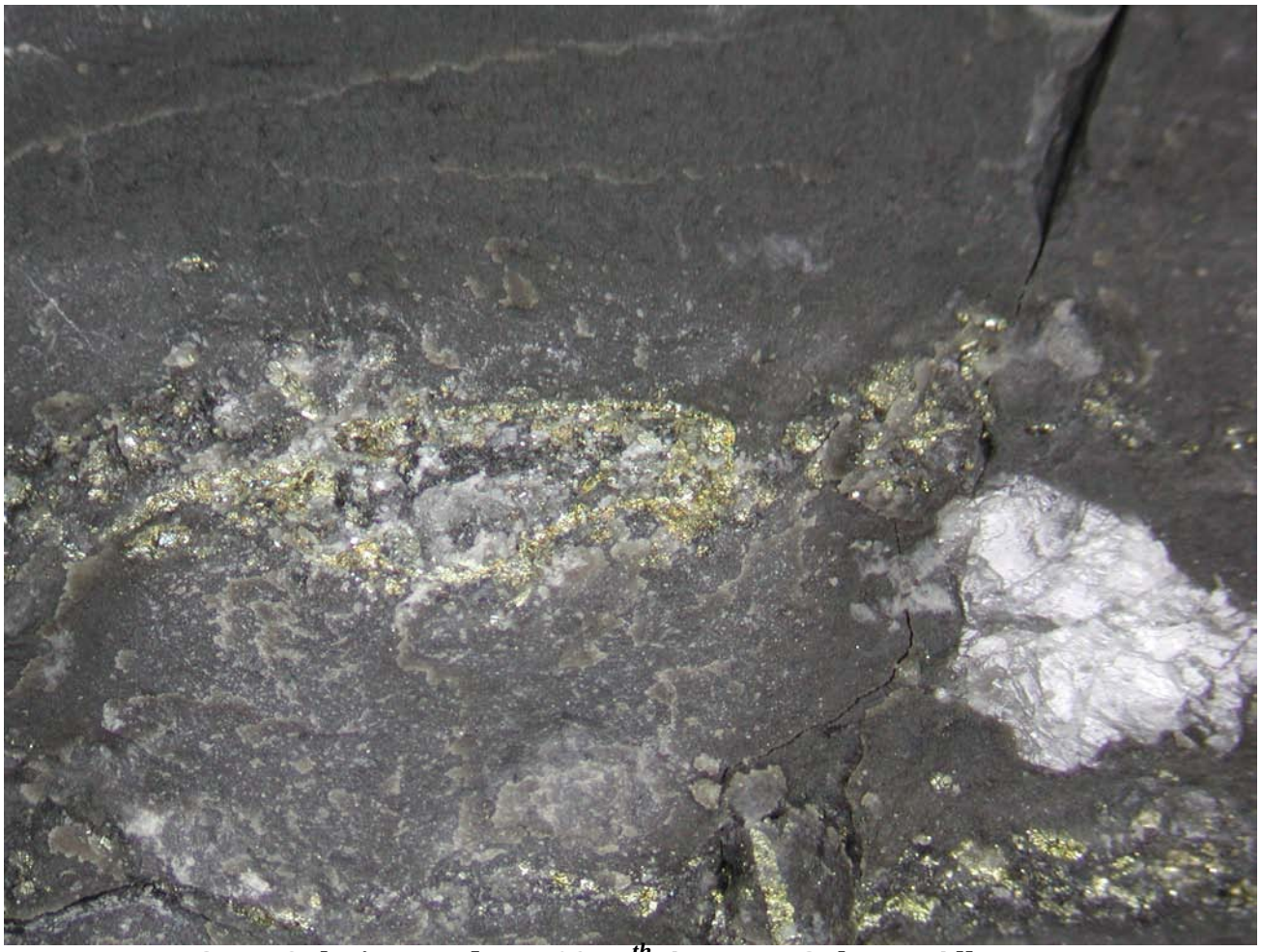

CBM Solutions Ltd 2908 12th Ave NW Calgary, Alberta

CONTENTS

LIST OF FIGURES

LIST OF TABLES

SUMMARY

Formation	# of Core Wells	Average Thickness (m)	Average TOC (wt%)	Average Porosity (%)	Mineralogy	Average Gas Capacity at 11 MPa (cc/g)
Exshaw	4	5-10	5.0	4.4	Quartz, Kolinite, Illite	1.3
Besa River	2	450-500	4.3	4.6	Quartz, Kolinite, Illite	0.8
Fort Simpson	3	475-525	0.4	3.3	Quartz, Kolinite, Illite	0.3
Muskwa	8	15-25	3.1	3.2	Quartz, Kolinite, Illite	0.7

Table 1. Summary data for each formation analyzed.

SCOPE

CBM Solutions undertook an this assessment of gas shale potential for the British Columbia Ministry of Energy and Mines, Oil and Gas Division, Resource Development and Geoscience Branch. This data provides the results of a multifaceted evaluation of the gas shale potential within Devonian strata of northeastern British Columbia. The study focuses on the organic content, thermal maturity, sorption capacity and clay mineralogy of the Exshaw, Besa River, Fort Simpson and Muskwa formations of northeastern British Columbia. Areas of interest include parts of the Liard Plateau and Basin and Prophet Trough in northeastern BC, and western extensions of the Peace River Arch/ Embayment in eastern central BC.

INTRODUCTION

With increasing demand for natural gas, exploration focus is shifting to unconventional resources. Projections for conventional reserves predict a serious decline which falls well

short of future demands for natural gas. Devonian shales of northeastern British Columbia provide potential for large scale reserves within organic rich intervals.

The purpose of this study is to determine the gas capacity and potential gas in place within the Besa River, Exshaw, Fort Simpson and Muskwa formations. Additional this study provide pertinent mineralogical data that will help assess the ease with which the shales maybe completed (fraced) which is being increasingly recognized as a key factor to successful exploitation. To determine the zones with the highest potential for gas in place, a sampling program was initiated to determine, sorption capacity, total organic carbon (TOC), porosity, thermal maturity (using Rock-Eval pyroloysis) clay mineralogy (using x-ray diffraction), aerial extent and shale zone thickness. The results are provided in the following sections on an individual formation basis.

GEOLOGIC SETTING

Devonian-Carboniferous strata of north-eastern British Columbia and Alberta were deposited in ramp and basin settings on the convergent western margin of North America (Richards, 1989). Tectonic elements at this time comprised the westward-deepening Alberta cratonic platform bounded to the west by a deep, linear, north-south orientated depression, the Prophet Trough (Figure 1; Richards, 1989), which passed southward into the Antler Foreland Basin of western United States (Poole, 1974; Richards, 1989). The Devonian-Carboniferous interval is marked by the Antler Orogeny in western United States and Caribou Orogeny in eastern British Columbia. During the Caribou Orogeny, depositional style, geometry, lithology and distribution of Devonian-Carboniferous strata were controlled by large-scale tectonic readjustments of the cratonic platform superimposed on lower frequency eustatic sea-level changes (*e.g.*, Johnson *et al.*, 1985; Morrow and Geldsetzer, 1988; Bond and Kominz, 1991; Savoy and Mountjoy, 1995).

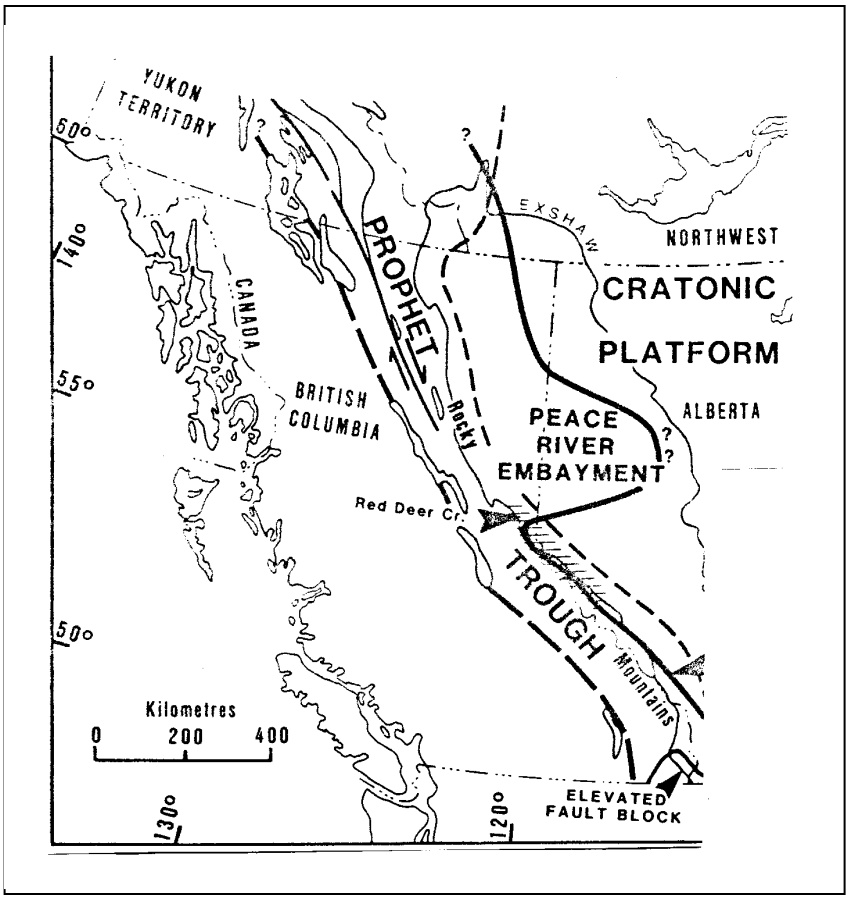

Figure 1. Structural elements for deposition of Devonian shales (Gordey et al, 1991).

Upper Devonian (Famennian) subsurface strata of northeastern British Columbia and western Alberta consist of a series of stacked cyclical ramp and shelf carbonates and associated evaporites (Wabamun Group). Mixed siliciclastic-carbonate Wabamun to upper Exshaw strata of the Western Canada Sedimentary Basin were deposited in a broad, epicontinental sea on the Alberta - Hay River cratonic platform, in an embayment north of the Peace River Arch area of central Alberta and within the Prophet Trough and Liard Basin in eastern British Columbia (Richards, 1989). These rocks are coeval with Palliser Formation strata exposed in the Rocky Mountain Front Ranges. In northeastern British Columbia the ramp carbonates shale out into the Besa River shales in the Liard Basin. Shelf sediments of the Exshaw and Duvernay (Muskwa – Duvernay equivalent)

Formations occur on the Hay River and Alberta inner shelf areas, separated by the Peace River Arch. The most basinward sediments are contained in the Liard Basin and in outer shelf or basin slope settings in northeastern British Columbia. The Smoky River Sub-basin was developed on the Alberta inner shelf area just south of the Peace River Arch. Along the deformed belt, the Sukunka Uplift in the northern Rocky Mountains separates deeper sediments of the Liard Basin from those of the Sassenach Sub-basin in southeastern British Columbia.

The Kootenay Terrane, an arc/plutonic belt rimming the western part of the Prophet Trough, was episodically exposed from Famenian to Viséan times, and it has been proposed that this rim was formed by the convergence of the Kootenay pericratonic and other terranes to the North American continent. Alternatively, extensional, and strike-slip tectonism have been proposed in Prophet Trough subsidence (Gordey et al, 1987). In southern British Columbia, the Prophet Trough was associated with Devonian-Carboniferous aged metamorphism, volcanism, granitoid plutonism and tectonism which were related to an episode of compression and easterly-directed subduction which coincided with the Antler Orogeny in the western United States. (Poole, 1974; Richards, 1989; Richards *et al.*, 1993; Smith *et al.*, 1993). Volcanic tuffs of the Upper Devonian Exshaw and Lower Carboniferous Banff formations of Alberta and British Columbia provide additional evidence for possible convergence (Richards and Higgins, 1988; Richards, 1989; Savoy and Mountjoy, 1995). Mesozoic metamorphism and complex structural deformation in British Columbia has masked accurate interpretation of tectonic style affecting the Prophet Trough.

REGIONAL SETTING AND TECTONIC STYLES

Devonian-Carboniferous strata of the Alberta cratonic platform, predominantly platform and ramp carbonates, thicken and become argillaceous westward into the Prophet Trough (Richards, 1989). Overlying the carbonates of the Palliser/Wabamun Group, terrigenous clastic sediments are predominantly deep water shales, bedded chert and minor carbonate

with continental provenance (Exshaw and Besa River formations), but include westerly derived coarse clastics of the Earn Group (Gordey et al. 1987). The presence of both extensive organic rich shales and Earn Group clastics suggests that the Prophet Trough existed as a rimmed basin during much of Late Devonian – early Carboniferous time, a result of periods of uplift to the west in the pericratonic Kootenay terrane.

Prophet Trough shale occurrences in British Columbia can be subdivided into northern, Liard Plateau and Basin assemblages, and central and southern Peace River Arch and Foothills assemblages.

Liard Plateau and Liard Basin

The Liard Plateau straddles the British Columbia – Yukon border, occupying the westernmost extent of the Hay River platform and eastern flank of the Prophet Trough. From the Cambrian to the Late Silurian the Liard Plateau area underwent continuous subsidence and deposition as part of the western miogeocline. In Late Silurian time, there is some evidence that the seas withdrew briefly, possibly in response to the Caledonian Orogeny. By Early Devonian time the seas transgressed to the east without a major break in carbonate/shale deposition through to the Late Devonian. Near the end of the late Devonian, uplift occurred in the Toad River area of British Columbia. This uplift may have extended northward into the area of the Beaver River (Beavercrow) High. This Late Devonian uplift caused a thickened Upper Devonian succession in the northern and eastern parts of the Liard Plateau. The farthest basinward (westward) sediments are known are in the Liard Basin, an asymmetric north-trending structural trough located immediately east of the Cordilleran fold and thrust belt and west of the Bovie Lake fault. Late Paleozoic sedimentation records recurrent movement on that fault (west side down). The Liard Basin is 80 km wide by 200 km long and has over 5000 m of Paleozoic and Mesozoic sedimentary fill (Monahan, 1996).

In the Carboniferous, a thick succession of shale (the Etanda Formation) was deposited in the northern and western parts of the Liard Plateau. This shale is associated with sandstone and siltstone of Banffian age (the Clausen and Yohin formations), and carbonates of Late Carboniferous age (Prophet Formation).

Foothills - Western Peace River Arch

A thick sequence (up to 6 km) of pre-Windermere Proterozoic sediments, underlies the western extension of the Peace River Arch in the Foothills of the Carbon Creek area (northern flank of Peace River Arch). The south-eastward disappearance of the older Proterozoic succession probably reflects a transverse step in the older Proterozoic sedimentary basin that likely coincides with the Hay River Fault. The Sukunka Uplift, an outboard high to the Peace River Embayment, had several hundred metres of east-side down motion in the Carbon Creek area during the late Paleozoic. Structurally high areas are preserved north of the Peace River Arch and possibly reflect pre-Middle Devonian compressive deformation due to a thinner crust (Ross and Stephenson, 1989). Further evidence of this deformation is provided by extensive northeast-southwest transverse faulting in the area of the Peace River Arch (Sikabonyi and Rogers, 1959).

Late Paleozoic Faulting: In the Peace River Arch area, Wabamun conventional oil and gas fields occur in, and are associated with, faulted horst structures. These features occur at the northern edge of the Smoky River Sub-basin, broaching the crestal portions of the Peace River Arch. Most reservoirs occur in fault-controlled, hydrothermal, white dolomites (Stoakes, 1992). Two dominant fault trends are recognized in this area: northwest-trending synthetic extension faults with hanging-wall movement down to the southwest, but possibly linked at depth with a detachment extending to the continental margin (see also McClay et al., 1989), and northeast-southwest transverse faults, possibly associated with compression (Churcher and Majid, 1989). The extensional faults were

involved in the formation of the extensional Peace River rift basin (Peace River Embayment) after Wabamun deposition.

Carboniferous strata (Besa River – Debolt formations) recording episodes of late Paleozoic block faulting and pronounced subsidence followed by regression and differential uplift, are extensively preserved in the foothills of British Columbia's Trutch and Halfway map areas and in the adjacent plains. Western occurrences, transected by northwest-striking block faults, were deposited in the latest Famennian to Pennsylvanian Prophet Trough. To the east, Carboniferous deposition occurred on the cratonic platform and in the Peace River Embayment. The embayment axis, developed on the Devonian Peace River Arch during the Mississippian, opens westward into Prophet Trough and is characterized by block faults recording recurrent late Paleozoic movement. On the cratonic platform and in the Peace River Embayment, abrupt thickness changes in the Exshaw/Banff interval record the onset of late Paleozoic block faulting and subsidence.

Mesozoic Deformation: The change from thick-skinned reactivated normal faults (northern Foothills) to thin-skinned reactivated normal faults at the north end of the Sukunka Uplift suggests the orientation of late Paleozoic normal faults may have influenced the deep structural style of the fold and thrust belt. Seismic, surface and well data from the foothills of the Carbon Creek area, northeastern British Columbia show that the Foothills are thin-skinned with structures having formed above a major detachment in the Upper Devonian-Carboniferous Besa River Formation. Middle Devonian and older strata underlying the Besa River detachment were not deformed during Cretaceous-Eocene contractional deformation. Detachment folds, thrust faults and related fault-bend folds and tip folds dominate the structural style of Carboniferous (Besa River) to Triassic strata with local detachments within the Upper Carboniferous, lower Triassic, and upper Triassic indicated by structural discordance (Eaton et al, 1999).

The present-day disposition of Wabamun oil and gas fields is probably the result of inversion of the Peace River basin in Laramide time by reactivation of the extensional

fault system in contraction. Similar tectonics possibly created the Parkland gas field at the western edge of the Peace River Arch in northeast British Columbia.

DEVONIAN – CARBONIFEROUS STRATIGRAPHY

Formations of interest in this study are the Givetian to Visean Besa River Formation, the Upper Famenian to Lower Tournaisian Exshaw Formation, and the Upper Devonian Fort Simpson and Muskwa formations. These formations include laterally persistent black shale deposits that are stratigraphically equivalent to the Devonian black shales of the eastern United States which are important gas shales resources.

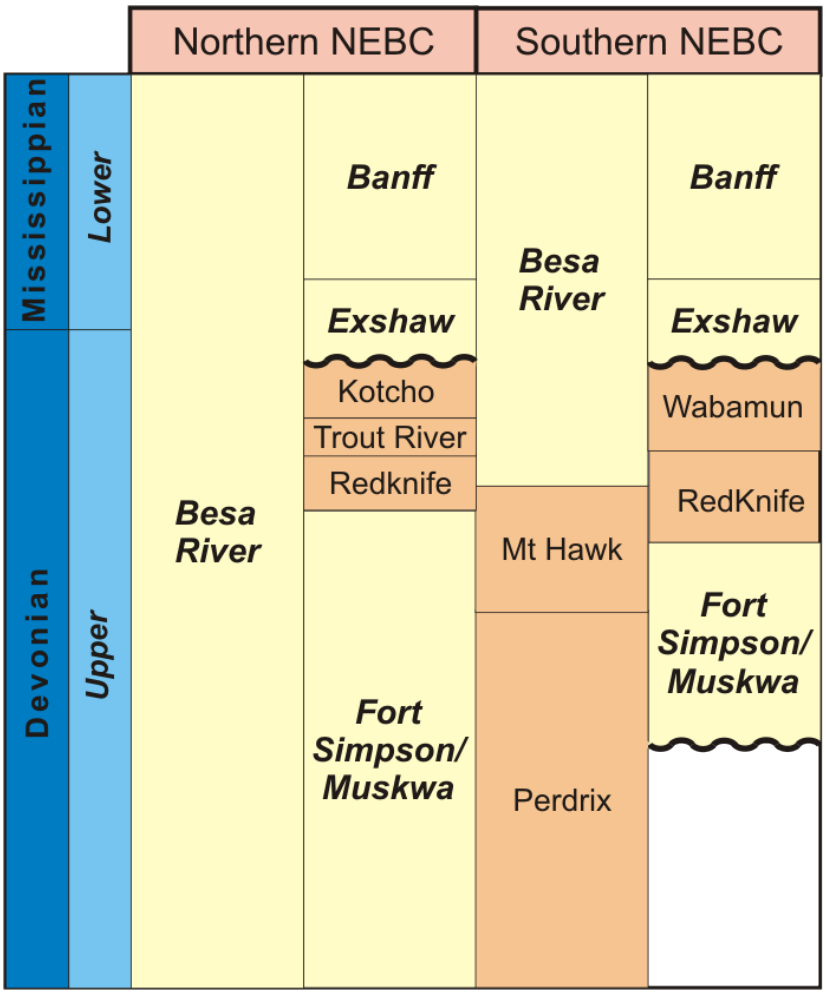

Figure 2. Devonian to Lower Mississippian stratigraphy of the study area (modified from Core Labs, 2001).

METHODOLOGY

The Exshaw, Besa River, Fort Simpson and Muskwa formations were sampled in a total of 17 cored wells (Table 2). Within each cored well, samples were collected for adsorption isotherms, Total Organic Carbon (TOC), Rock-Eval, porosity and clay mineralogy.

Formation	Well Name	Location (UWI)
Besa River	Dunedin	d-075-E/094-N-08
Besa River	La Biche	b-055-E/094-O-13
Exshaw	Kaiser Doe	06-06-081-14-W6
Exshaw	Parkland	10-26-081-16W6
Exshaw	Golata	08-29-083-15W6
Exshaw	Sikanni Chief	b-092-D/094-I-04
Ft Simpson	Sikanni Chief	b-092-D/094-I-04
Ft Simpson	Junior	c-60-E/094-I-11
Ft Simpson	Kotcho	c-032-K/094-I-14
Ft Simpson/Upper Muskwa	Helmet	b-049-G/094-P-07
Muskwa	Equatorial Boat	a-077-D/094-I-04
Muskwa/Otter Park	Snake River	c-028-D/094-O-01
Muskwa/Otter Park	South Kotcho	c-098-G/094-I-14
Muskwa/Slave Point	HZ Kotcho	d-012-C/094-P-03
Lower Muskwa/Slave Point	Walrus	b-086-L/094-I-16
Lower Muskwa/Slave Point	Fort Nelson	c-070-I/094-J-10
Lower Muskwa/Slave Point	Dilly	a-088-F/094-P-12

Table 2. Cored wells that were sampled and analyzed in this study.

Adsorption Isotherms

Gas capacities for each formation have been determined using adsorption isotherms. The classic theory used to describe the Type I isotherm for microporous materials with small external surface area is based on the Langmuir equation (Langmuir, 1916). The Type I isotherm displays a steep increase in adsorption at low relative pressures due to enhanced adsorption caused by the overlapping adsorption potentials between walls of pores whose diameters are commensurate in size with the adsorbate molecule. The Type I isotherm then flattens out into a plateau region at higher relative pressure, which is believed to be

due to the completion of a monolayer of adsorbed gas. The micropore volume is then thought to be filled by only a few molecular layers of adsorbate, and further uptake is limited by the dimensions of the micropores.

The Langmuir model assumes that a state of dynamic equilibrium is established between the adsorbate vapor and the adsorbent surface and that adsorption is restricted to a single monolayer (Gregg and Sing, 1982). The adsorbent surface is thought to be composed of a regular array of energetically homogeneous adsorption sites upon which an adsorbed monolayer is assumed to form. The rate of condensation is assumed to be equal to the rate of evaporation from the adsorbed monolayer at a given relative pressure and constant temperature. The Langmuir equation takes the following form:

$$\frac{P}{V} = \frac{1}{BV_m} + \frac{P}{V_m}$$

Where P is the equilibrium pressure, V is the volume of gas adsorbed at equilibrium, V_m is the volume of adsorbate occupying a monolayer, and B is an empirical constant. A plot of P/V Vs relative pressure should yield a straight line whose slope will yield V_m from which the surface area may be obtained.

The Langmuir Isotherm can be written:

$$V(P) = \frac{V_L P}{P_L + P}$$

P = gas pressure
V(P) = predicated amount of gas adsorbed at P
V_L = Langmuir volume parameter
P_L = Langmuir pressure parameter
The difference between the measured amount of gas adsorbed (V(P)) and that predicted using the Langmuir Equation (Vi(P)) is a measure of error and is given as:

Err(P) = Vi(P) - V(P)

This error may be positive or negative. The square of the error is always positive and is a measure of the how well the calculated isotherm matches the data. This error can be calculated for each point and summed giving a measure of the overall error:

$$SSE = \sum_{i=1}^{N} Err_i^2$$

N= number of measured points.

All of the adsorption isotherms analyzed were run at an average temperature of 30^{o}C, allowing direct comparison of all adsorption isotherms analyzed in this study. Based on regional hydrostatic pressure gradients, an average gradient of 11.1 kPa/m (0.49 psi/ft) was used to calculate the corresponding reservoir pressures for each analyzed sample

Total Organic Carbon

The total organic carbon content of rocks is obtained by heating a 20-30 mg sample in a furnace and combusting the organic matter to carbon dioxide. The amount of carbon dioxide liberated is proportional to the amount of carbon liberated in the furnace, which in turn is related to the carbon content of the rock. The carbon dioxide liberated is measured using infrared spectroscopy.

Many source rocks also include inorganic sources of carbon such as carbonates and most notably calcite, dolomite and siderite. These minerals break down at high temperature, generating carbon dioxide and thus their presence must be corrected in order to determine the organic carbon content. The amount of carbonate is determined by acid digestion

(normally 50% HCl) and the carbon dioxide generated is measured using infrared spectroscopy. Total organic carbon is determined by subtracting the inorganic carbon fraction from the total carbon content (carbon dioxide).

TOC = TC - TIC.

TC= total carbon
TIC= total inorganic carbon
TOC = total organic carbon

Wireline Logs and Total Organic Carbon Correlations

Wireline logs may be used to identify organic rich zones and to semi quantitatively predict total organic carbon. In this study, measured total organic carbon data is overlain on gamma ray, density/neutron and sonic logs (if available) to determine the relationship between organic carbon and geophysical responses.

Gamma ray logs respond to radioactivity in detrital minerals and uranium, which is often associated with organic matter enrichment during deposition in oxygen-deficient conditions. Radioactive elements (U, Th and K) often bind into the organic fraction of the clay mineral matrix resulting in high gamma ray response on geophysical logs.

Rock-Eval Pyrolysis

Kerogen Type

The type of kerogen by definition is determined by the elemental ratios of H/C and O/C of the kerogen. Alternatively the HI and OI measured from Rock-Eval® (Peters, 1986) analyzes are used as proxies for the elemental ratios.

The majority of the samples analyzed in this study plot on a Van Krevelan diagram in the region of Type III kerogen because the kerogen is hydrogen poor and oxygen poor or oxygen values are very low. For highly mature organic matter such as most strata in this study, the hydrogen index and oxygen indices are low because of the elevated maturity level irrespective of kerogen type and thus differentiating kerogen type may not be possible (Tissot and Welte, 1984).

Rock-Eval Pyrolyses

Rock Eval pyrolysis comprises programmed heating in helium of a crushed sample (<100 mg). The amount of the free hydrocarbons contained in the sample and the hydrocarbon- and oxygen-containing compounds (CO_2) that are volatilized during the cracking of the organic matter during programmed heating up to 550ºC are determined.

The free hydrocarbons are determined from isothermally heating the sample at 300°C. The generated hydrocarbons are measured by a flame ionization detector and is referred to as the S_1 peak (Figure 3). The temperature is then increased from 300° to 550°C and hydrocarbons released from this thermal cracking are measured as the S_2 peak at the flame ionization detector. The temperature at which S_2 reaches its maximum rate of hydrocarbon generation is referred to as T_{max}. CO_2 generated from the OM in the 300°-390°C range is measured by a thermal conductivity detector and is referred to as the S_3 peak.

In summary, Rock Eval provides the following data:

S_1 = amount of free hydrocarbons in sample (in milligrams of hydrocarbon per gram of rock). If S_1 >1 mg/g suggests oil or contamination of samples by hydrocarbons.
S_2 = amount of hydrocarbons generated through thermal cracking- provides measure of quantity of hydrocarbons that the rock has the potential of producing through diagenesis.
S_3 = the amount of CO_2 (in milligrams CO_2 per gram of rock) produced during pyrolysis of organic matter. S_3 reflects the amount of oxygen in the OM.

T_{max} = the temperature at which the maximum rate of generation of hydrocarbons occurs during pyrolysis. T_{max} is an indicator of the level of diagenesis of the OM.

A number of important parameters are calculated from Rock-Eval pyrolysis:
HI = hydrogen index (HI = [100 x S_2]/TOC).
OI = oxygen index (OI = [100 x S_3]/TOC).
PI = production index (PI = S_1/[S_1 + S_2]). PI is used to characterize the evolution level of the organic matter.
PC = pyrolyzable carbon (PC = 0.083 x [S_1 + S_2]). Carbon content of hydrocarbons volatilized and pyrolyzed during the analysis.

Kerogen type and degree of maturation of the organic matter can be estimated by cross-plotting of HI and OI on a van Krevelan diagram with the caveat outlined above that at very maturities differentiating kerogen types may not be possible.

The level of diagenesis at which the oil window occurs varies with kerogen type. In general T_{max} = <430°C represents immature organic matter; T_{max} = 435°-450°C defined the oil window; T_{max} > 450°C indicates strata are over mature. In very mature samples the S_2 may be so small that a Tmax value may be spurious.

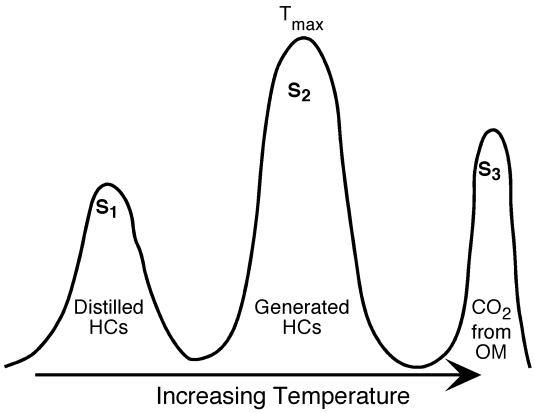

Figure 3. Idealized gas generation trace from Rock-Eval analyzes.

Clay Mineralogy

Determining the clay mineralogy of shale samples is important in order to predict if the shales are water sensitive and the mechanical properties (ultimate strength and brittleness) of the shales. Shales samples are comprised primarily of the clay minerals illite, kaolinite, mixed layer illite-smectite and smectite. In addition, quartz, feldspar and carbonate minerals can form a significant portion of the shales mineralogy. The Devonian shales analyzed in this study are typically comprised of a high percentage of quartz along with varying proportions of illite and kaolinite. Some of the samples consist of a small percentage of smectite or degraded illite (water sensitive clays) which may cause formation damage during drilling and completion.

In order to determine the clay mineralogy within each formation of interest, select samples were collected and analyzed using x-ray diffraction. The samples were ground to – 2 μm and smeared on a glass slide in an ethanol paste and allowed to dry. Each sample was x-rayed between 3^{o} and 60° using a Cu X-ray tube. In order to obtain relative semiquantitative mineral percentages on peaks, the following calculation was used:

weight % = (Peak intensity (counts per second))/sum of Peak Intensity for all peaks used) * 100.

X-ray diffraction analyzes of samples that include clay minerals is semi-quantitative because of the variable d-spacing of the clays. Approximate relative abundance of clays have been estimated based on peak heights and correcting for Lorentz polarization. More sophisticated quantitative techniques such as Rietveld analyzes cannot be applied to clays without standards made with clays of the composition of those studied.

Porosity

When analysing shales for potential gas in place, storage capacity within the porosity must be considered. Porosity measurements were made on every isotherm sample in order to determine the free gas capacity in porosity. A sub-sample from each isotherm sample was analyzed using mercury immersion and helium pycnometry. The bulk density is determined based on Archimedes principal. Because mercury is a non wetting fluid with high surface tension, it will not move into the pore structures at low pressure. The skeletal density is measured by helium pycnometry. The ratio of mercury to helium density provides the fractional porosity within the sample. The porosity is measured on air dried samples. For calculating free gas capacity the assumption is made that S_W=0 and a correction is applied for space occupied by sorbed gas.

RESULTS

Exshaw Formation

Lithology and Stratigraphy

In the Liard Basin the Uppermost Devonian – Mississippian carbonate-shale succession includes all strata from the Exshaw to Debolt (Prophet) formations, and comprises two basin-filling sequences 400 to 500 m thick (Monahan, 1997). Regionally, the Exshaw includes both uppermost Devonian and Mississippian strata, but in the study area the Exshaw and part of the overlying Banff may be entirely Devonian in age (Richards et al, 1994). The lower prograding Exshaw sequence unconformably overlies Kotcho Formation carbonates in the east, and Lower Besa River Formation shales in the western plateau. In the westernmost Liard Basin, Besa River shales are stratigraphically equivalent to Exshaw, Banff and Prophet Formations. The Exshaw core examined in this

study consisted of shale that is black, hard, carbonaceous and locally sheared. Silty layers and laminae and massive pyrite are common features observed in the Exshaw core within the study area. In the Parkland 10-26-81-16W6 core, localized fractures and brecciation were infilled by carbonate precipitate.

In east-central British Columbia, Palliser carbonates are sharply to gradationally overlain by black, laminated, organic-rich, mudrocks of the Exshaw Formation. The latest Devonian transgressive episode led to the demise of the Big Valley carbonate ramp and subsequent deposition of Exshaw mudrocks (Savoy, 1992). These mudrocks are equivalent to the black shale member of the Exshaw Formation in outcrop at the Jura Creek type-section (Macqueen and Sandberg, 1970). The black shale member is abruptly to gradationally overlain by the bioturbated siltstone member of the Exshaw Formation, and correlates with identical lithologies in the Rocky Mountain Front Ranges (Macqueen and Sandberg, 1970; Richards and Higgins, 1988). A eustatic sea-level fall at the Devonian-Carboniferous boundary (Sandberg, *et al.*, 1988) terminated deposition of organic-rich mudrocks and was followed by sedimentation of organic-lean mudrocks on the distal sediment-starved palaeocontinental shelf. These silt to sand sized clastics were deposited during a regressive event which resulted in westward shoreface progradation.

The Exshaw Formation is overlain by black shales of the lower Banff Formation in the Canadian Cordillera and Alberta cratonic platform (Richards, 1989; Savoy, 1992). Latest Famennian Palliser/Wabamun carbonate shelf strata pass westward into the Besa River shales deeper water equivalents in the Prophet Trough and shallow to the east into intertidal and supratidal evaporites of the Stettler Formation in the subsurface on the Interior Platform of southeastern Alberta (Geldsetzer, 1982; Higgins *et al.*, 1991; Richards *et al.*, 1991; Richards *et al.*, 1993, p. 9). On geophysical logs, the Exshaw Formation is characterized by high gamma ray radiation (Figure 4).

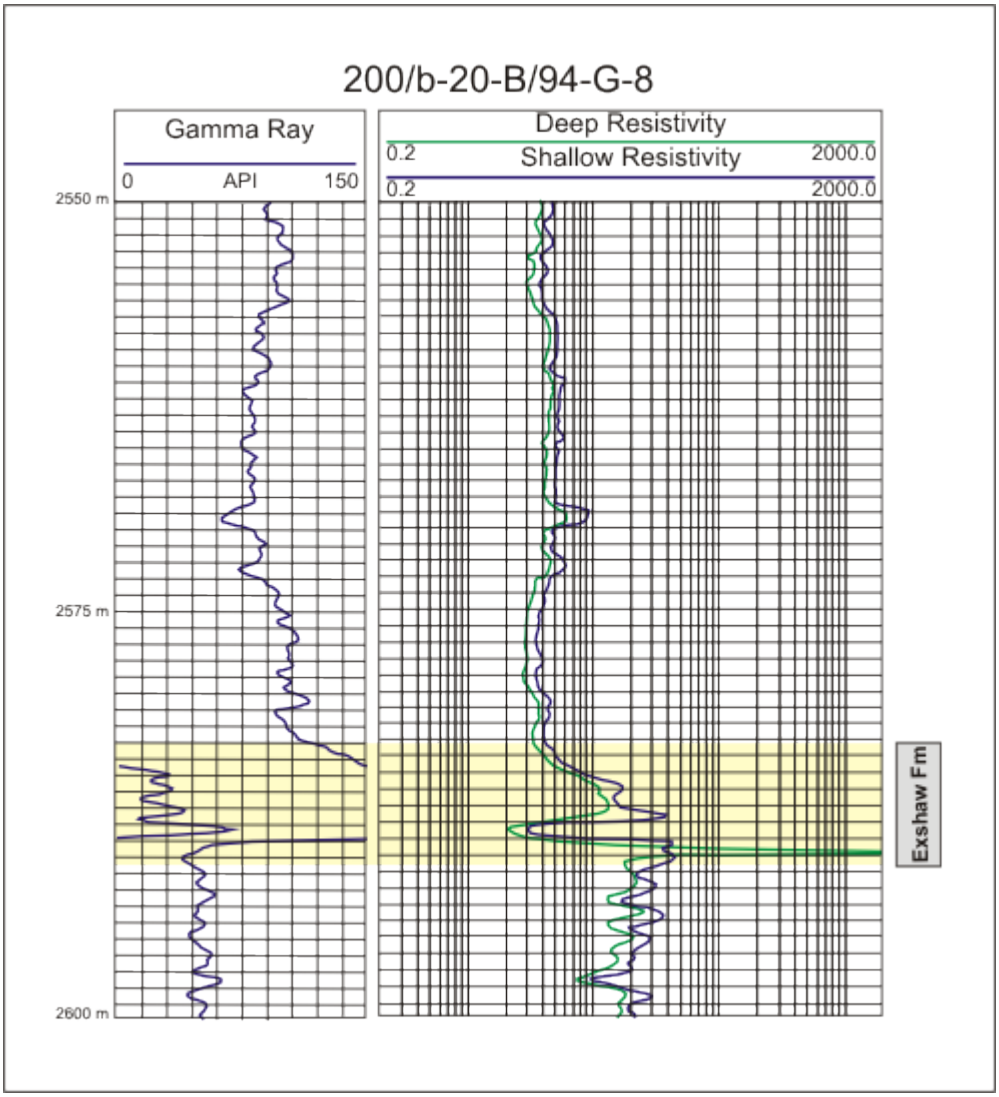

Figure 4. Typical log signature for the Exshaw Formation. High gamma ray response is characteristic.

Lateral Extent and Thickness

The Exshaw Formation is present throughout northeastern British Columbia. The highest density of wells penetrating the Exshaw occur in the northeast corner of the study area (Figure 5). From the available well data, (consisting of approximately 1200 Exshaw Formation intersections) the Exshaw Formation thickens from east to west. The thinnest intersection of the Exshaw shale is approximately 1 m and occurs in the northeast corner of the study area (Figure 8). The maximum thickness of the Exshaw Formation is approximately 80 m and occurs in both the northwest and southwest portion of the study area (Figure 8). In the far south portion of the study area (NTS block 93), well control is limited to two wells.

Structurally, the Exshaw Formation dips from north to south (Figure 9). The deepest intersections of the Exshaw Formation occur in the Peace River Arch block and reach depths of approximately 3000 m. The shallowest intersections recorded in the study area are approximately 120 m and occur primarily in the northeast.

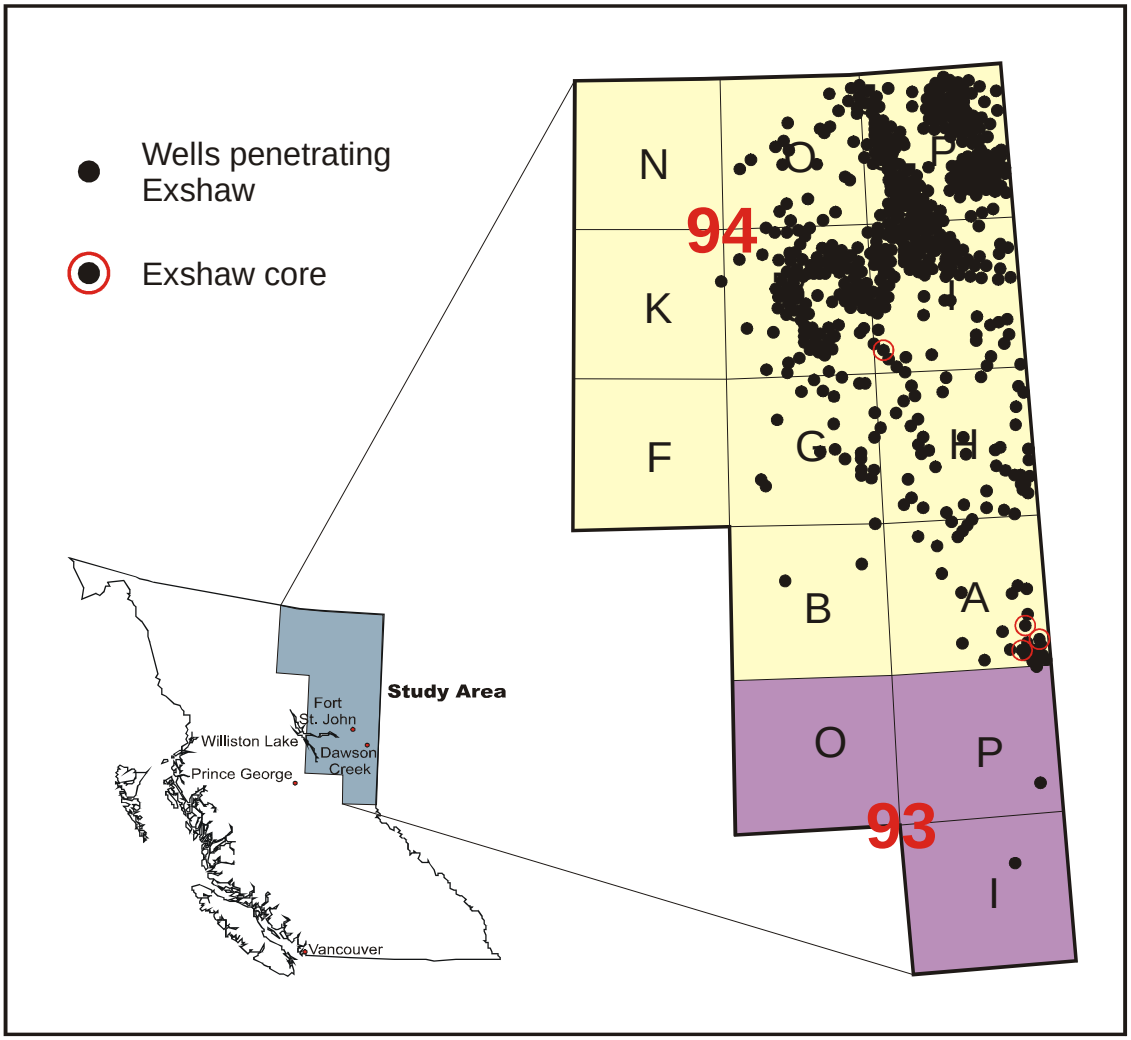

Figure 5. Distribution of wells penetrating the Exshaw Formation. Red circles indicate wells with core.

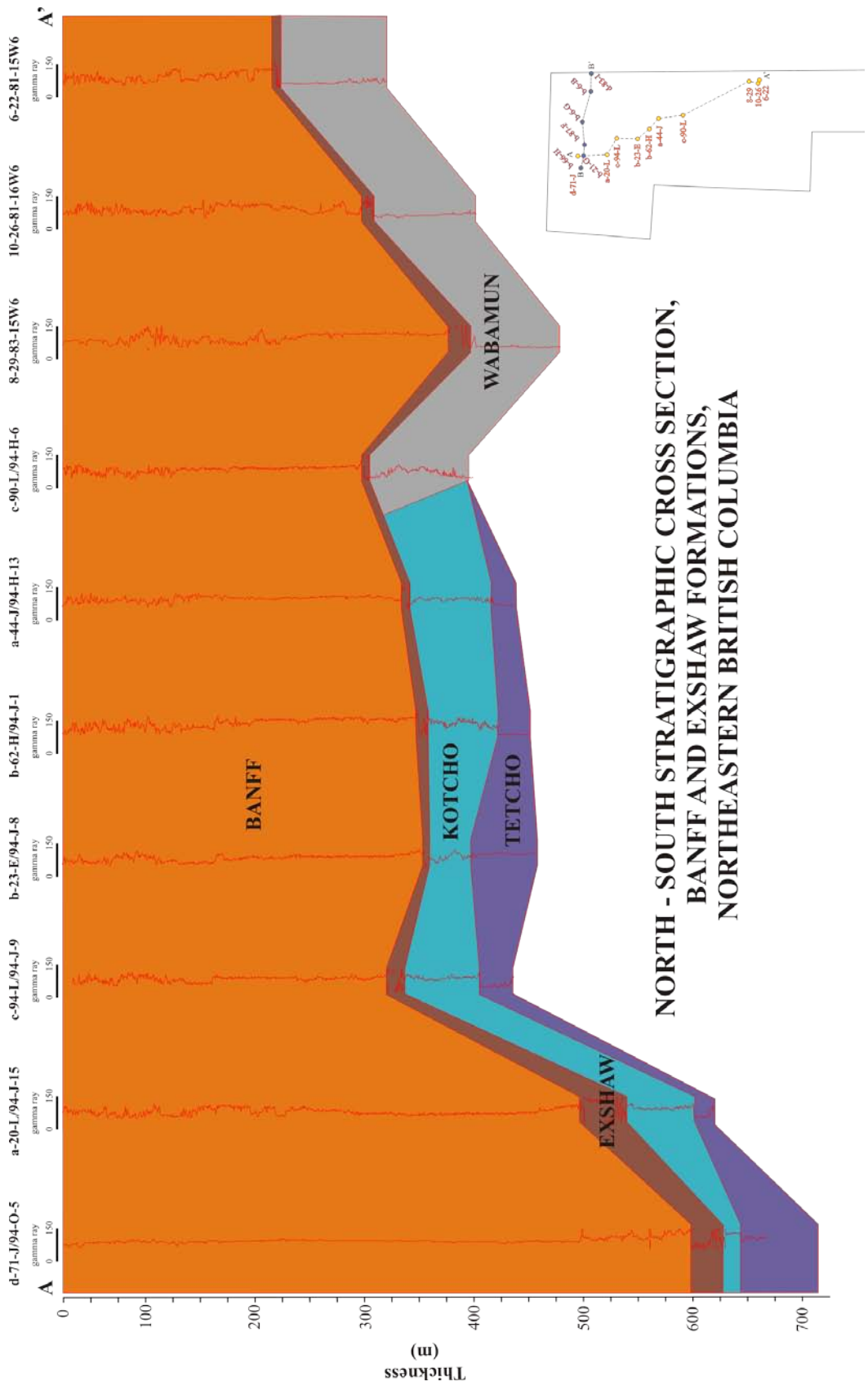

Figure 6. North to south stratigraphic cross section of the Banff and Exshaw formations (A – A').

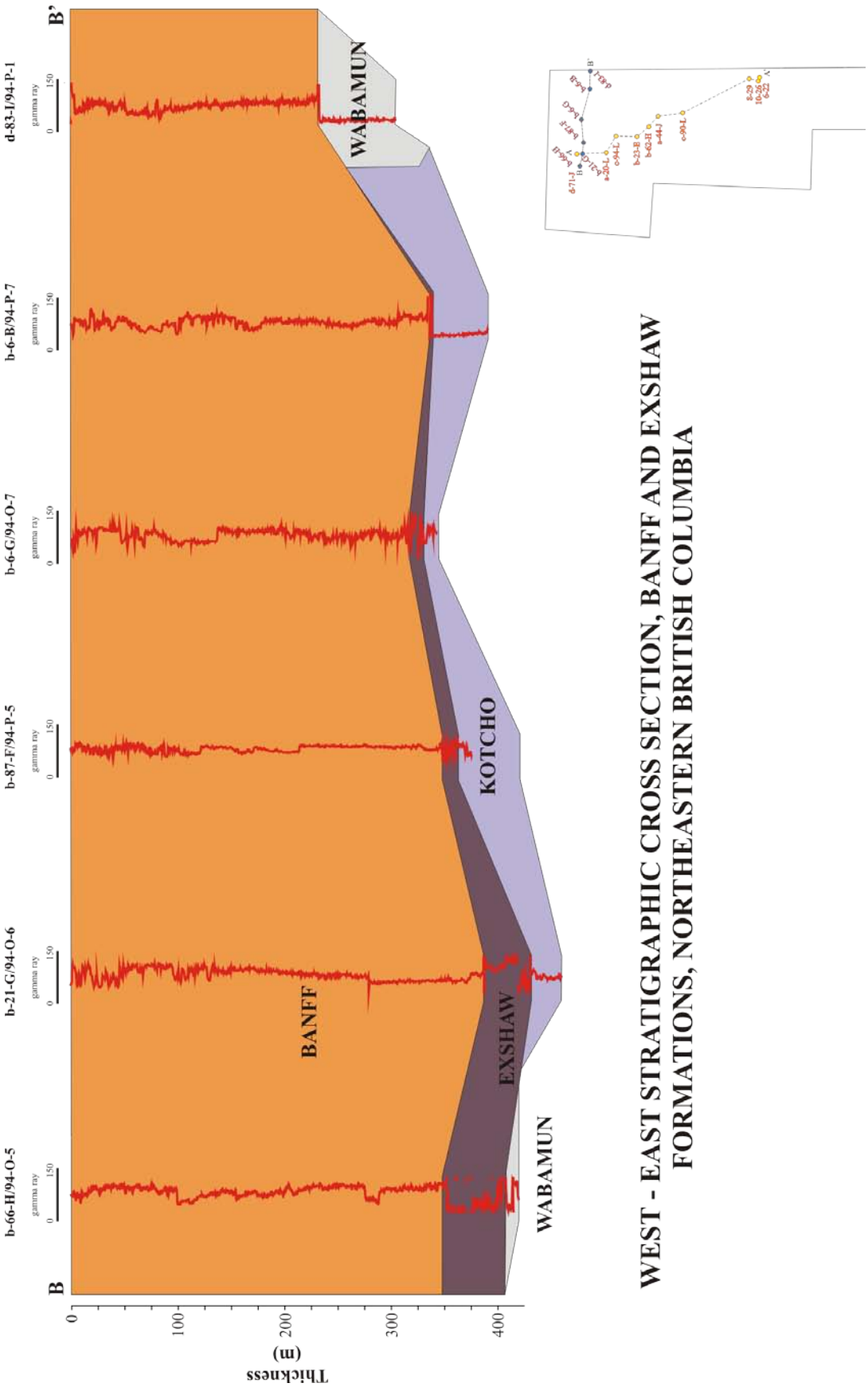

Figure 7. West to east stratigraphic cross section of the Banff and Exshaw formations (B – B').

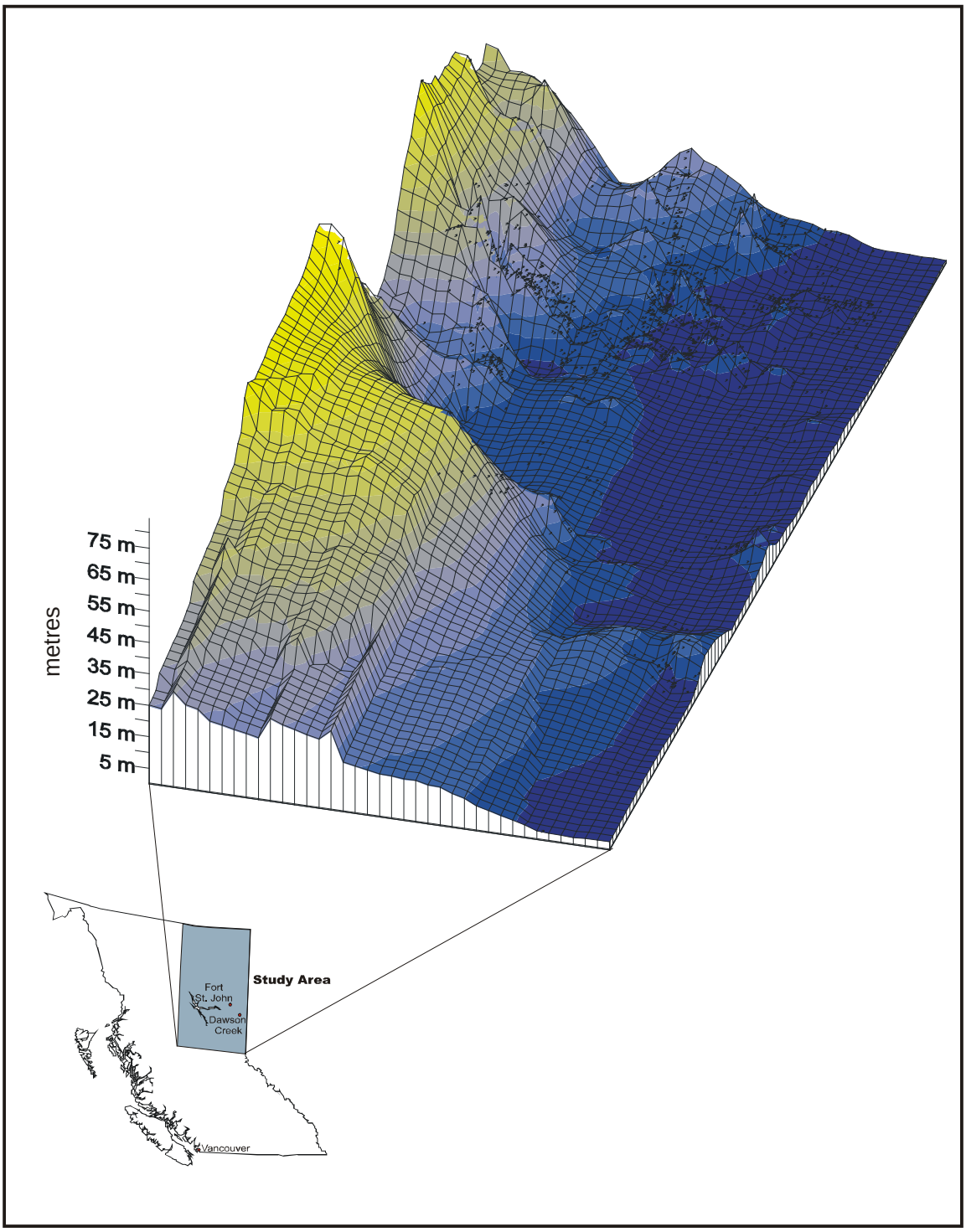

Figure 8. Isopach map of the Exshaw Formation.

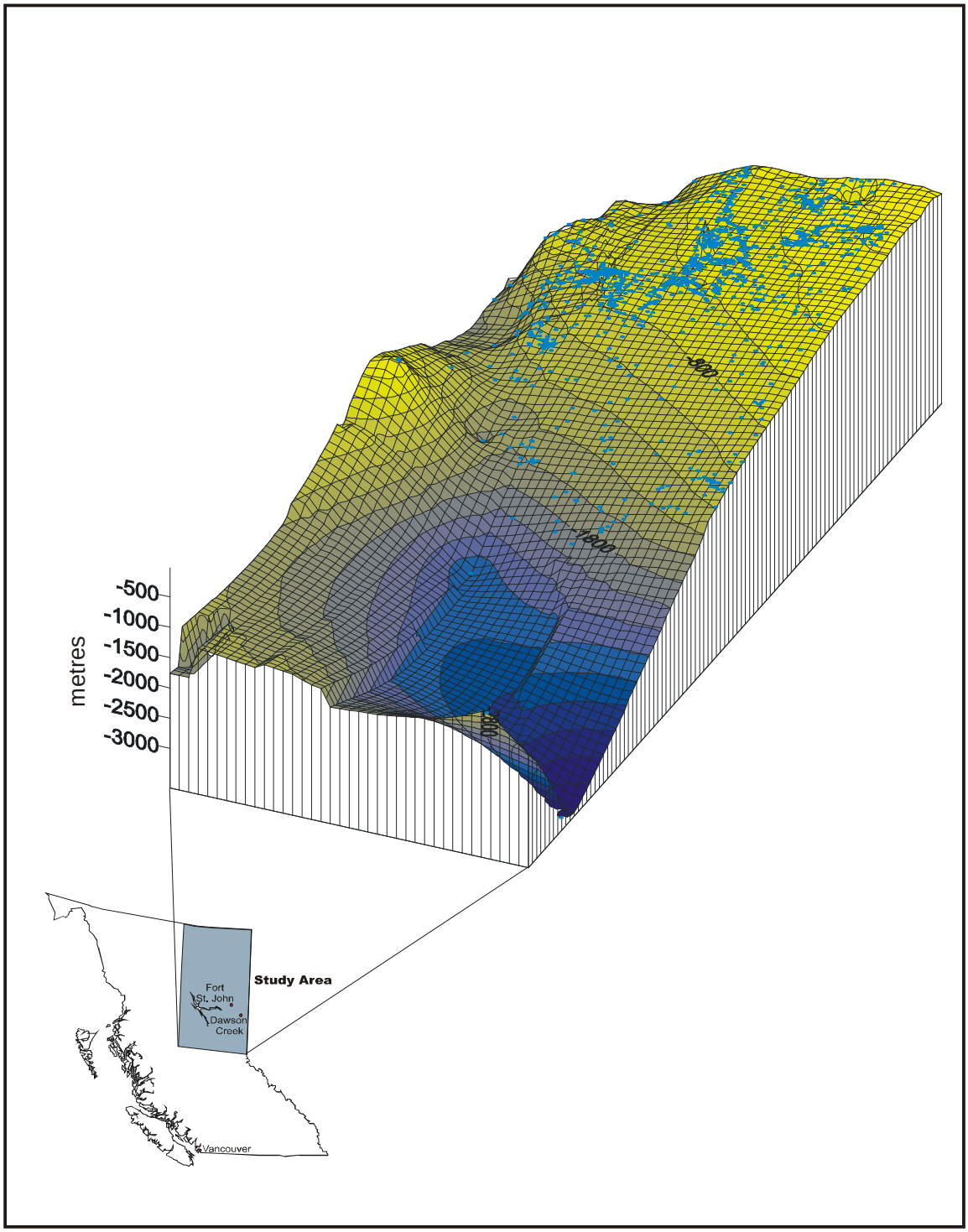

Figure 9. Upper surface of the Exshaw Formation showing the drill depths from surface.

Total Organic Carbon

Total organic carbon (TOC) measurements were made on 22 samples from 4 wells (Table 3). Three of the cored wells are located in the township and range block in the southwest portion of the study area and one well is in the centre of the study area. On average, the analyzed Exshaw Formation shale samples show an organic carbon content of 5.02% (by weight).

For the Parkland 10-26-81-16W6 core, the average TOC (wt%) for core 7 (3371.2 – 3373.15 m; Figure 10) is 5.3%. These samples represent the organic rich interval of the Exshaw Formation which is characterized by a high gamma ray response. An attempt was made to correlate TOC content with gamma ray and sonic responses; however, a direct correlation is not evident. A lack of correlation is most likely due to high organic content variability over small vertical scales (mm to cm scales) which is not reflected in the samples collected.

The average TOC (wt%) for the Golata 8-29-83-15W6 core 8 (3385.90 – 3391.00 m) is 5.2%. Within core 8, the samples range in TOC from 1.6 – 8.0 wt%. The lower TOC values reflect the transition form the underlying carbonate-rich Wabamun into the Exshaw Formation (Figure 11). The Exshaw Formation shale in the Golata well is dark grey, dense and contains carbonate-infilled fractures. The TOC contents do not vary consistently with gamma ray intensities or sonic log travel times.

The Kaiser Doe 6-6-81-14W6 TOC sample was collected at a depth of 3303.80 m and has a TOC (wt%) content of 1.3%. The sample is located within the transition from the Wabamun Formation into the Exshaw Formation (Figure 12). The sampled core in the Kaiser Doe well is dense, calcareous/dolomite-rich shale with abundant stylolites and localized calcite infilled fractures.

The Sikanni Chief b-92-D/94-I-4 samples have an average TOC (wt%) of 0.4%. The Exshaw Formation shales in this region overlay the Kotcho carbonates (Figure 13). TOC

data from samples in the Sikanni Chief well correlate with an increase in gamma ray intensities and neutron counts/second. The shales are light to medium grey, highly calcareous and fissile. Features include rare carbonaceous/coaly fragments, very minor microfracturing and occasional thin pyrite lenses.

Table 3. Total organic carbon measured on Exshaw shale samples.

Well	Depth m	Total Carbon %	Inorganic Carbon %	Organic Carbon %
Parkland 10-26-81-16W6	3371.20	5.33	0.14	5.19
	3371.50	5.71	0.07	5.64
	3371.80	5.21	0.16	5.05
	3372.10	6.27	0.60	5.67
	3372.40	6.15	0.67	5.48
	3373.10	5.01	0.13	4.88
	3373.15	5.16	0.13	5.03
Golata 8-29-83-15W6	3386.20	8.00	6.38	1.62
	3386.50	6.98	0.35	6.63
	3386.80	7.53	3.07	4.46
	3387.10	8.48	1.46	7.02
	3387.40	9.31	7.75	1.56
	3387.70	3.44	0.21	3.23
	3387.75	8.13	0.80	7.33
	3387.80	5.27	0.82	4.45
	3387.85	6.50	1.01	5.49
	3387.90	8.90	0.89	8.01
	3387.95	8.37	1.35	7.02
	3388.00	6.36	0.89	5.47
	3388.30	6.74	1.85	4.89
	3388.60	7.36	2.37	4.99
Kaiser Doe 6-6-81-14W6	3303.80	6.69	5.37	1.32
Sikanni Chief b-92-D/94-I-4	1573.00	2.06	2.06	<0.05
	1573.30	1.79	1.53	0.26
	1573.60	1.63	1.36	0.27
	1573.90	1.62	1.30	0.32
	1574.20	2.12	1.83	0.29
	1574.50	1.68	1.45	0.23
	1574.80	1.92	1.58	0.34
	1575.10	1.26	1.09	0.17
	1575.40	0.92	0.62	0.30
	1575.70	1.00	0.86	0.14
	1576.00	1.26	0.95	0.31
	1576.30	1.57	1.27	0.30
	1576.60	3.52	3.02	0.50
	1576.90	1.75	1.36	0.39
	1577.20	3.23	2.45	0.78
	1577.50	1.71	1.31	0.40
	1577.80	2.98	2.06	0.92
	1578.10	4.06	3.58	0.48

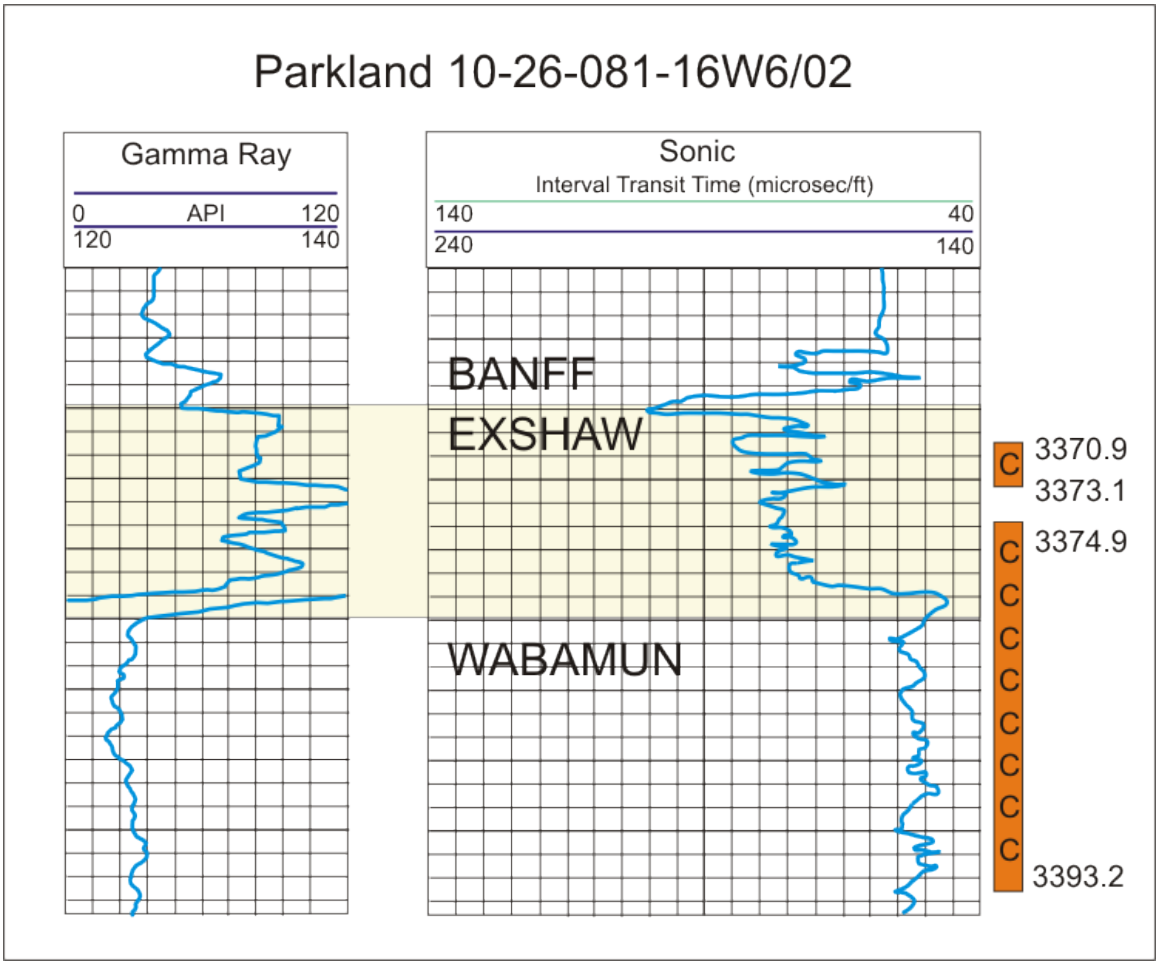

Figure 10. Gamma ray and Sonic log signature for Parkland 10-26-81-16W6, showing Exshaw core (core #7) from 3385.90 – 3391.00 m. "C" indicates core intervals.

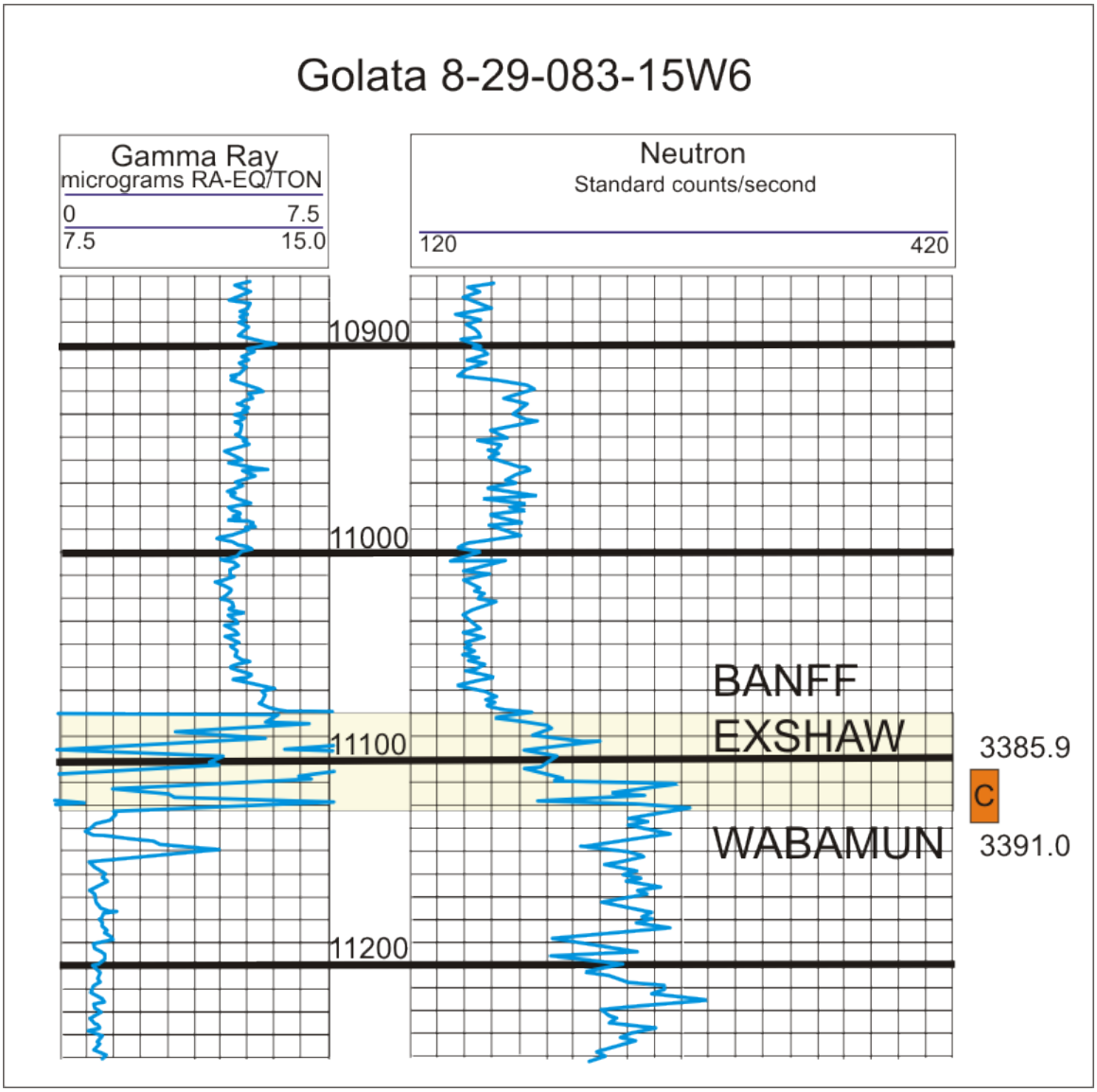

Figure 11. Gamma ray and Sonic log signature for Golata 8-29-83-15W6 showing Exshaw core (core #8) from 3370.90 - 3373.10 m. "C" indicates core interval.

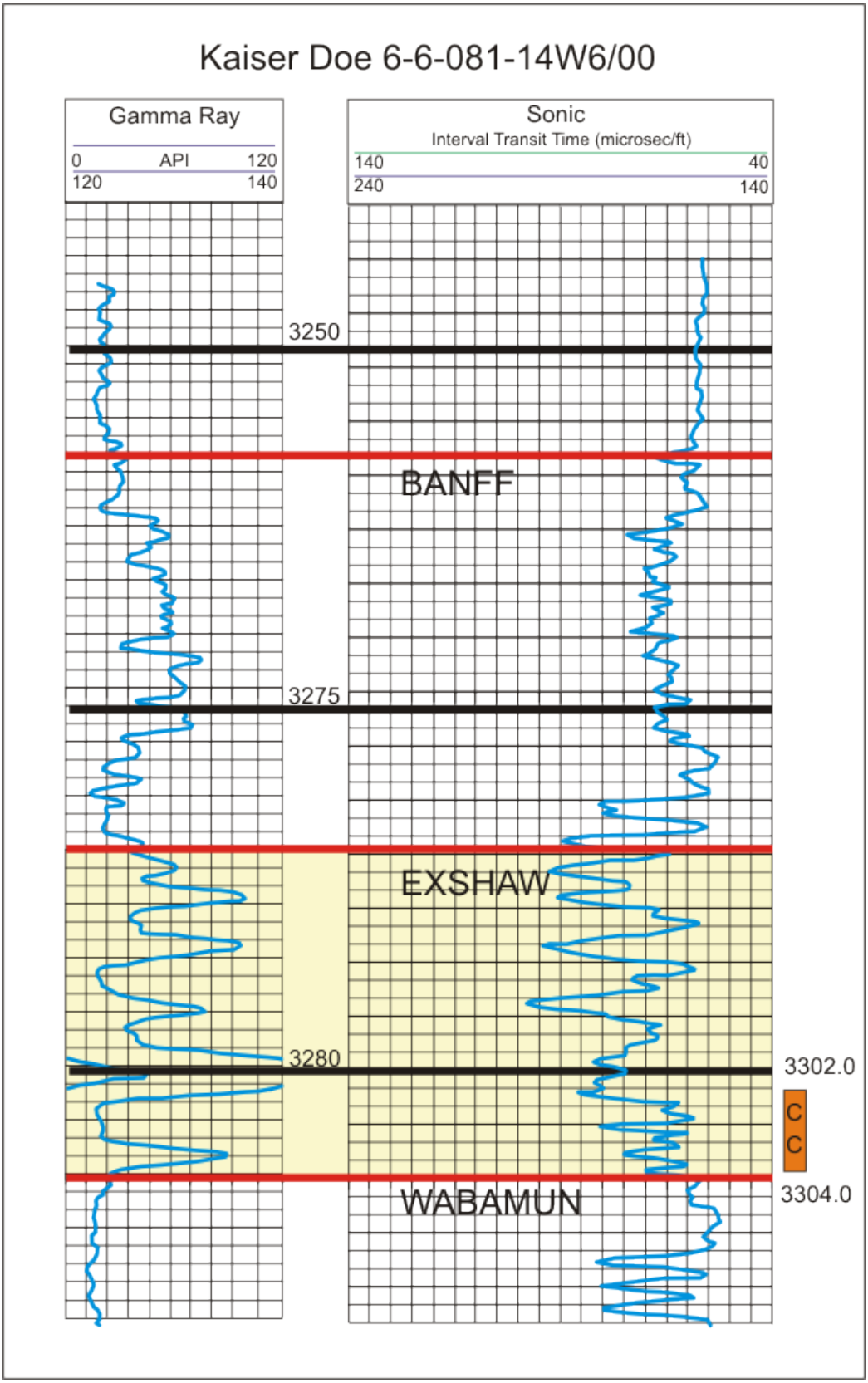

Figure 12. Gamma ray and Sonic log signature for Kaiser Doe 6-6-81-14W6, showing core (core #1) from 3302.00 – 3304.00 m. "C" indicates core interval.

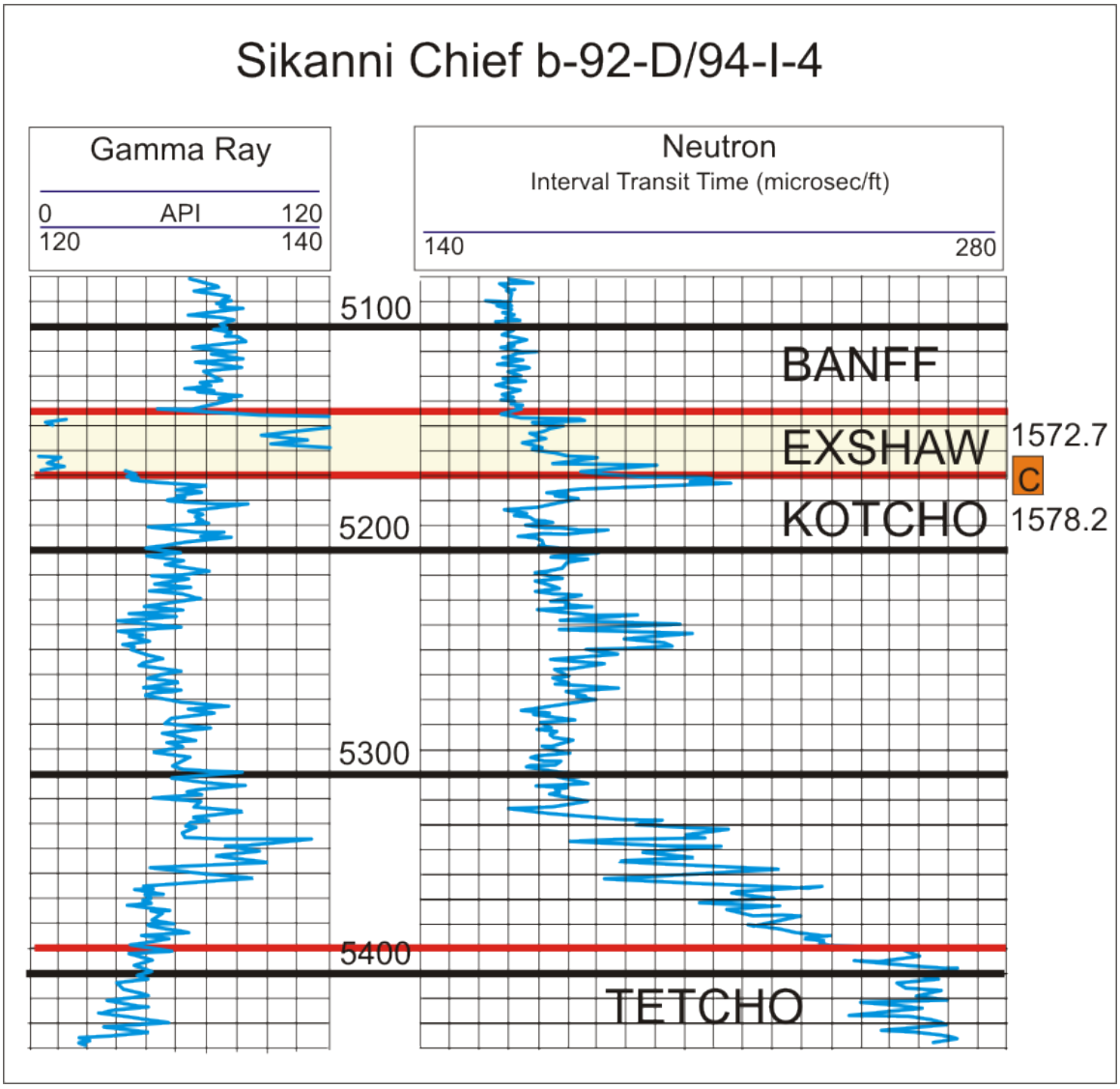

Figure 13. Gamma ray and Neutron log signature for Sikanni Chief b-92-D/94-I-4 showing core (core #9) from 1572.70 – 1578.20 m. "C" indicates core interval.

Thermal Maturity and Organic Matter Type

Select Exshaw shale samples were analyzed using Rock-Eval pyrolysis to determine both the thermal maturity and organic matter type. Table 4 shows the Rock-Eval data for seven analyzed samples from three wells. The low S2 values measured in all of the samples suggest that the shales are very mature. As a result, the Tmax values are suspect and cannot be used reliably to determine an absolute maximum thermal exposure.

All of the analyzed samples plot in the Type III organic matter range (Figure 14). The samples measured from the Sikanni Chief b-92-D well have considerably higher hydrogen and oxygen indices and lower TOC values, indicative of the Banff Formation.

Depth	Tmax	S1	S2	S3	PI	S2/S3	PC(%)	TOC(%)	HI	OI
Sikahni Chief b-92-D										
1573.8	433	0.01	0.02	0.46	0.30	0.04	0.01	0.13	15	354
1574.6	476	0.01	0.02	0.41	0.22	0.05	0.00	0.20	10	205
1576.0	491	0.01	0.05	0.45	0.19	0.11	0.00	0.15	33	300
Golata 8-29										
3388.15	605	0.03	0.15	0.34	0.15	0.44	0.02	6.65	3	5
3388.15	604	0.02	0.08	0.37	0.17	0.22	0.01	6.55	2	6
3390.1	344	0.11	0.11	0.34	0.49	0.32	0.02	1.11	10	31
Parkland 10-26										
3371.2	604	0.02	0.15	0.70	0.10	0.21	0.02	5.68	3	12
3372.0	399	0.21	0.40	0.30	0.33	1.33	0.05	6.29	7	5
3372.0	392	0.24	0.54	0.18	0.29	3.00	0.07	6.18	9	3

Table 4. Rock-Eval data for Exshaw shale samples.

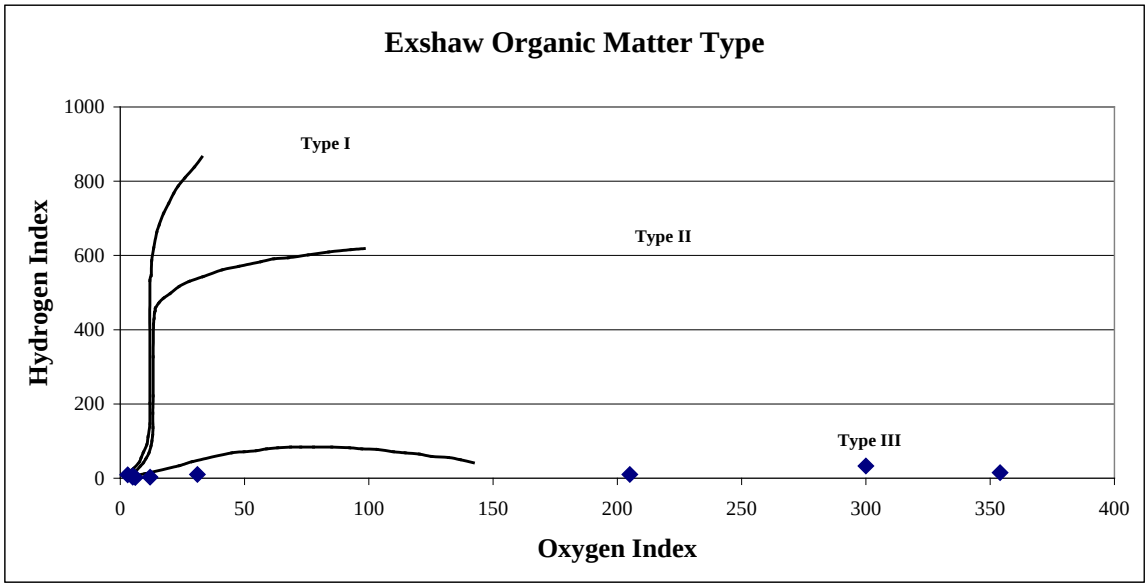

Figure 14. Van Krevelen diagram showing the organic matter of the Exshaw Formation shales. The level of maturity is so high that it is not possible to type the kerogen based on the Van Krevelen plot.

Porosity

Five shale samples from Exshaw and Banff formations were analyzed for total porosity (Table 5). The analyzes show that the range of porosity is from 2.8 to 6.9% with an average value of 4.4%. Assuming the formation is saturated, the pore space in the shale provides additional gas storage capacity which may significantly increase the potential gas in place. The effect of porosity on gas capacity in place is discussed in a later section.

Sample	Depth (m)	Formation	Hg Bulk Density (cc/g)	He Skeletal Density (cc/g)	Std Dev.	Porosity	
						Fraction	Percent
Golata 8-29-83-15W6	3888.15	Exshaw	2.58	2.77	0.004	0.069	6.94
Golata 8-29-83-15W6	3390.1	Exshaw	2.70	2.78	0.007	0.026	2.64
Golata 8-29-83-15W6	3386.55	Exshaw	2.51	2.58	0.003	0.028	2.83
Sikanni Chief b-92-D/94-I-4	1573.8	Exshaw	2.58	2.73	0.007	0.055	5.46
Sikanni Chief b-92-D/94-I-4	1574.6	Exshaw	2.61	2.72	0.005	0.040	4.01

Table 5. Porosity of select Exshaw/Banff samples.

Sorption Capacity

In order to quantify the sorbed gas capacity in place, adsorption isotherms were completed on 7 samples from 4 wells in northeastern British Columbia. Based on drilling depths, intersections of the Exshaw Formation range from approximately 100 m in the northeast corner of the study area to 3500 m in the southeast corner of the study area. Using the drill depth range of 100 m to 3500 m, the calculated reservoir pressures range from 1110 to 38850 kPa (160 to 5600 psi). The TOC contents of the samples ranges from 0.13% to 6.65%. The low TOC samples are representative of the transition from the Exshaw Formation to the overlying Banff Formation. By having a range in TOC values, the importance of organic content on capacity can be highlighted. The average TOC measured for all of the Exshaw Formation sampled collected for this study is approximately 5%.

All adsorption data (gas capacity data) is presented at both reservoir pressure and a standard pressure of 11 MPa (1600 psi) (Table 6). The average TOC value of 5% is represented at a depth of 3371.95 m in the Parkland 10-26-81-16W6. At a reservoir pressure of 33 MPa (4760 psi), the gas capacity (not accounting for porosity) is 1.6 cc/g (51.9 scf/ton). At a standard pressure of 11 MPa, the gas capacity is 1.3 cc/g (41.6 scf/ton) (Figure 15). Table 5 provides the gas capacity data for each Exshaw Formation sample at both reservoir pressure and a standard pressure of 11 MPa. In comparison, a low TOC sample (0.20%) characteristic of the transition from the Exshaw Formation to the Banff Formation has a maximum gas capacity of 0.09 cc/g (2.9 scf/ton) which is achieved at a pressure of 7.5 MPa (1100 psi).

Because there is significant porosity in the Exshaw samples, the gas capacity may increase significantly if free gas capacity is considered and water saturation is less than 1. In figure 16, the gas capacities have been calculated to show the effect of porosity on gas capacity. End members of 2% and 6% porosity have been used to calculate the gas capacity in a 5% TOC sample. At 11 MPa pressure, the gas capacity with 2% porosity is 2.3 cc/g (74 scf/ton) which is a 77% increase over the sorbed gas capacity. With 6%

porosity, the gas capacity is 4.5 cc/g (143 scf/ton) which is a 246% increase over the sorbed gas capacity.

Several of the samples with low TOC contents do not plot as a normal Type I isotherm. At low pressures, the sorption capacity is zero or nearly zero, but with increasing pressure the sorption capacity begins to rise steadily. Once the sorption capacity begins to increase, it surpasses the saturation capacity typical of a sample with less than 1% TOC. At this time, the reasoning for this effect is uncertain but may be partially due to gas saturation in water (samples are run at equilibrium moisture and therefore have water within the matrix of the sample) or at low pressure capillary pressures may block access to pores which are available at higher pressures.

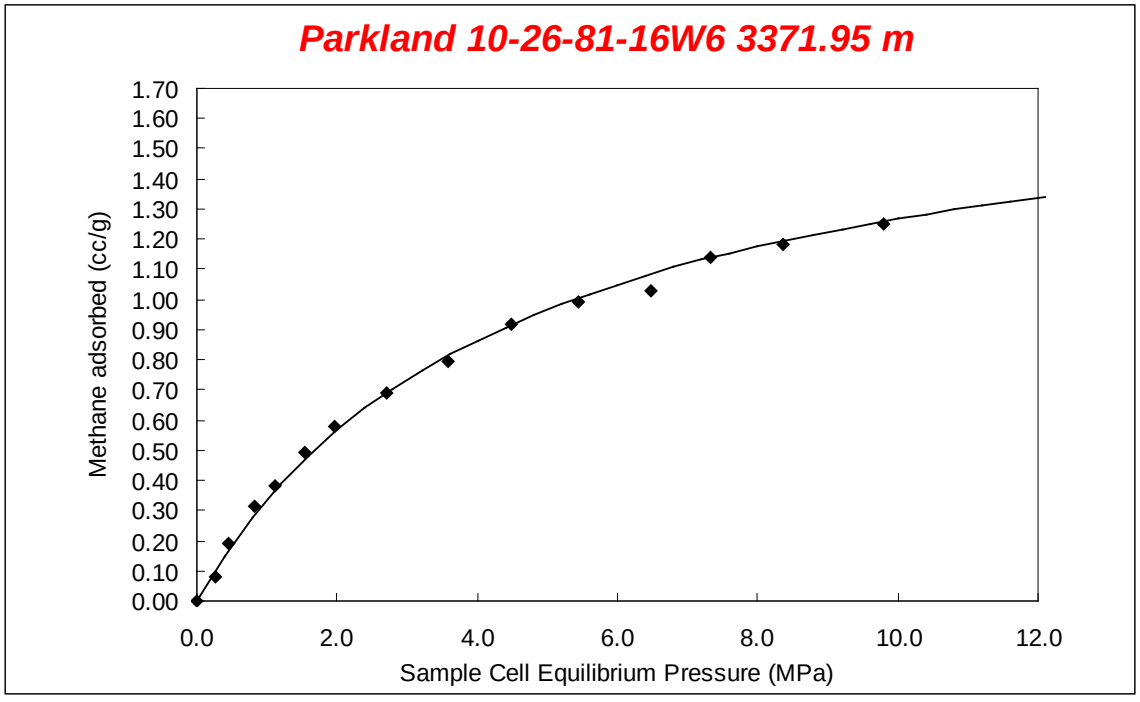

Figure 15. Adsorption isotherm for a shale sample from the Exshaw Formation. Sample has a TOC content of 5.02%. Gas capacity for pressures greater than 10 MPa is extrapolated using the Langmuir equation.

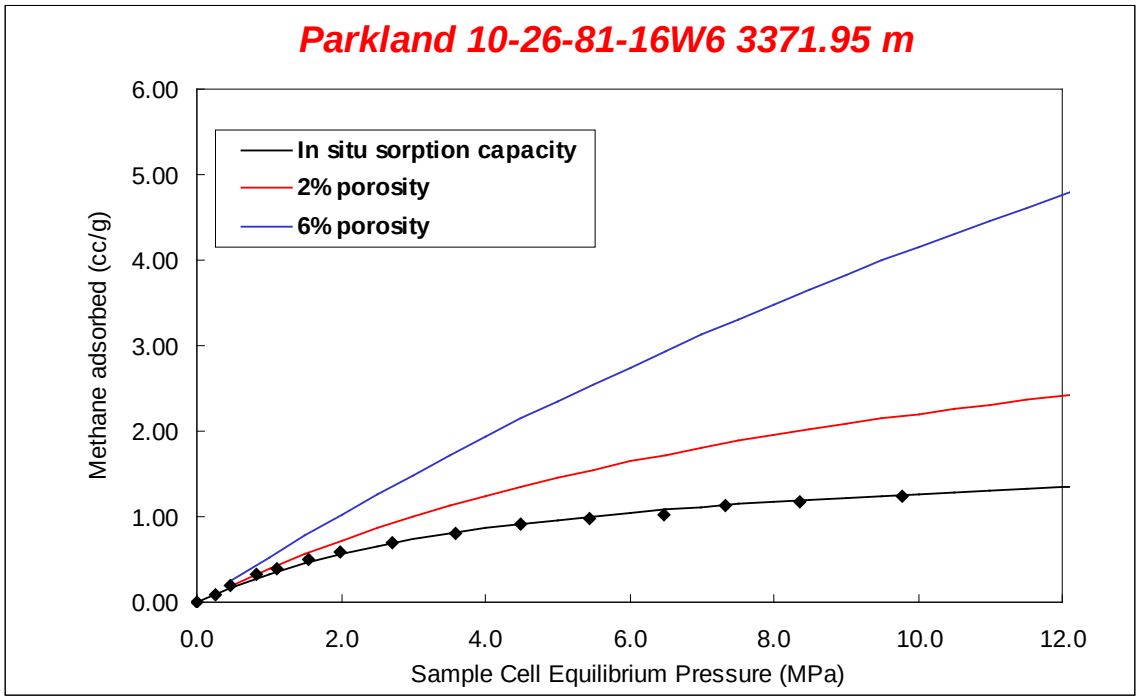

Figure 16. Sorbed plus free gas capacity in a 5% TOC sample.

Well Name	Location	Depth (m)	Reservoir Pressure (psi)	Reservoir Pressure (kPa)	Gas Capacity (cc/g)	Gas Capacity @ 11 Mpa (cc/g)	TOC
Exshaw							
Golata	8-29-83-15W6	3388.15	4780	32956	2.1	1.5	6.65
		3390.10	4783	32975	0.1	0.1	1.11
Sikanni Chief	b-92-D/94-I-4	1573.80	2220	15308	1.0	1.0	0.13
		1574.60	2221	15316	0.1	0.1	0.20
Parkland	10-26-081-16W6	3371.95	4757	32798	1.6	1.3	5.68
		3372.40	4758	32803	0.9	0.8	6.24
Kaiser Doe	6-6-81-14W6	3303.80	4661	32136	1.1	0.7	0.70

Table 6. Variation in sorption capacity with total organic carbon content for Exshaw and Banff formation shale samples. Capacities are given at reservoir pressure and a standard pressure of 11 MPa.

Clay Mineralogy

To determine clay mineralogy of the Exshaw Formation, x-ray diffraction (XRD) analyzes was completed on 3 samples from 2 cored wells. Table 7 shows a summary of the x-ray diffraction data. X-ray diffraction traces for each sample are shown in Appendix B. All of the analyzed samples consist primarily of quartz with the dominant

clay minerals being kaolinite and illite. Two of the samples (Golata 3386.55 and Sikanni Chief 1573.8) show a minor component of degraded illite which is water sensitive and may swell during drilling and completion if water based fluids are used. Sample 3390.1 m from the Golata 8-29-83-15W6 well shows a high percentage of dolomite which is expected as the sample was collected within the transition from the Wabamun Formation (carbonate-rich) into the Exshaw Formation.

EXSHAW XRD			**Mineralogy (% Relative)**					
Name	**Location**	**Depth (m)**	**Illite/Mica (d=10.00)**	**Kaolinite (d=7.10)**	**Quartz (d=4.23)**	**Calcite (d=3.03)**	**Pyrite (d=2.71)**	**Dolomite (d=2.89)**
Golata	8-29-83-15W6	3386.55	10	13	71	0	6	0
		3390.10	2	2	43	0	3	49
Sikanni Chief	b-92-D/94-I-4	1573.80	14	15	62	0	0	5

Table 7. Relative mineralogy percentages determined from XRD analyzes. "d" refers to the d-spacing of the principal plane of each mineral that was used to (semi-) quantify the relative abundances. Shaded regions show degraded illite which has a range of d spacings.

Gas Capacity in Place

Because gas capacities are highly variable due to changing organic contents, reservoir pressures, formation thicknesses and porosity, gas in place numbers must be calculated based on a range of reservoir properties. On average, the organic rich zone of the Exshaw Formation is 5 m thick, therefore this value is used for the gas in place calculations. Table 8 provides gas capacity in place numbers using an average TOC content of 5% and varying reservoir pressures and porosities. The gas capacity in place values are calculated using an average bulk density of 2.60 cc/g which is measured using mercury immersion.

Porosity (%)	TOC (%)	Shale Thickness (m)	Pressure (MPa)	Resources (cc/cm2)	Resources (bcf/section)	Average Gas Content (scf/ton)	Average Gas Content (cc/g)	Density (g/cc)
0	5	5.0	11.0	1690	**1.55**	42	1.3	2.60
2	5	5.0	11.0	3003	**2.75**	74	2.3	2.60
6	5	5.0	11.0	5811	**5.31**	143	4.5	2.60
0	5	5.0	33.0	2106	**1.93**	52	1.6	2.60
2	5	5.0	33.0	4459	**4.08**	110	3.4	2.60
6	5	5.0	33.0	11622	**10.63**	286	8.9	2.60

Table 8. Gas capacity in place based on an average of 5% TOC content at two different reservoir pressures. Also shown is the variation in gas capacity with increasing porosity.

Conclusions

The Exshaw Formation is a thin organic rich shale interval which is widely distributed throughout northeastern British Columbia. Maximum thickness of the Exshaw Formation in northeastern British Columbia reaches 86 m. Typically, the high organic interval (characterized by high gamma ray response) is between 2 and 10 metres thick averaging 5 metres in the study area. Maximum total organic carbon (TOC) contents reach 6% by weight with an average of 5%. Within the upper and lower transition zones of the Exshaw Formation, TOC contents typically fall to 1% or less. Due to the high organic contents, the Exshaw shales have potential for high sorbed gas capacity. A sample with 5% TOC can hold 1.6 cc/g at a typical reservoir pressure of 33 MPa. With porosity in the range of 2% to 6%, the free gas potential, assuming saturation, can increase the gas capacity by 75% to 250% over the sorbed gas capacity. Localized fracturing and occasional silty intervals within the Exshaw Formation may increase the flow potential into borehole intersections.

Besa River Formation

Lithology and Stratigraphy

The Besa River Formation consists primarily of a dark gray to black shale facies. Lateral variations in both thickness and facies changes create difficulty in defining the stratigraphy of the Besa River Formation within northeastern British Columbia and the Yukon (Kidd 1963). In the Liard Plateau up to 2256 m of dark grey to black, thinly bedded, fissile, calcareous, pyritic and cherty shale of the Besa River Formation (Givetian to Visean) conformably overlie the Muskwa Member. Higher in the trough succession, chert-dominant slope deposits of the Tournaisian to upper Viséan Prophet Formation overlie and pass southwestward (basinward) into the Besa River Formation. Conformably overlying the Devonian Besa River Shale in most of the study area and the Kotcho in the extreme east are up to 425 m of Carboniferous medium grey to black, non-calcareous, bituminous and micaceous, fissile basinal shale interbedded with medium grey, fine- to very fine-grained quartzose, cherty, tight siltstone, sandstone and limestone assigned to the Etanada and Exshaw formations. This shale represents the basinal equivalent of the Carboniferous clastics and carbonates. The organic richness of the shale makes it an excellent source rock candidate for hydrocarbons trapped in the Carboniferous clastic and carbonate reservoirs. The Besa River Formation characteristically shows zones with high gamma ray response throughout the interval (Figure 17).

In the Liard Basin the Famennian part of the Besa River shales grades eastward into carbonates and shales of the Tetcho and overlying Kotcho formations. These sediments interfinger with shallow-water shelf carbonates of the Stettler Formation via a ramp relationship. Westward, both the Tetcho and Kotcho grade into shales of the Besa River equivalent to the First Black Shale.

The Besa River Shale is attributed to be the zone of décollement in northeast British Columbia. The Besa River Shale has been identified as a source rock zone and a potential fractured reservoir. (In the Beaver River, Kotaneelee, and Pointed Mountain fields (Yukon Territory), the First Black Shale marker is contained within the Besa River Formation. To date, there are no discovered Besa River (Muskwa) gas resources documented in British Columbia. In south-east Yukon Territory, the Middle Devonian Besa River (Muskwa) fractured shale play is a sour(?) dry conventional gas play. Laramide antiforms structurally complicated by normal, reserve and thrust faults form the trap for this play. The organic-rich Besa River (Muskwa) shale provides the seal for the reservoir and is the source of gas. The reservoir unit is composed of fractured shale. The wells in the Beaver River field tested slightly sour gas from this zone at initial rates up to 0.10 106m3/d (3.6 MMcf/d), with no water. The gas rates declined quickly indicating limited reservoir extent. The gas is generally 96 to 98% methane with 1 to 2% H2S. Further play potential lies to the south and east of the study area.

West and south of the Peace River Arch, at the base of the Prophet Trough succession, the upper part of the Middle Devonian to Tournaisian Besa River Formation comprises basinal shale passing eastward into uppermost Famennian to lower Tournaisian basinal shale and overlying ramp carbonates of the Exshaw and Banff formations. The basal detachment to the fold and thrust belt runs in the basal part of the Besa River Formation in the Foothills at Carbon Creek and the Besa River shales are strongly deformed, folded and faulted (McMechan, 2002).

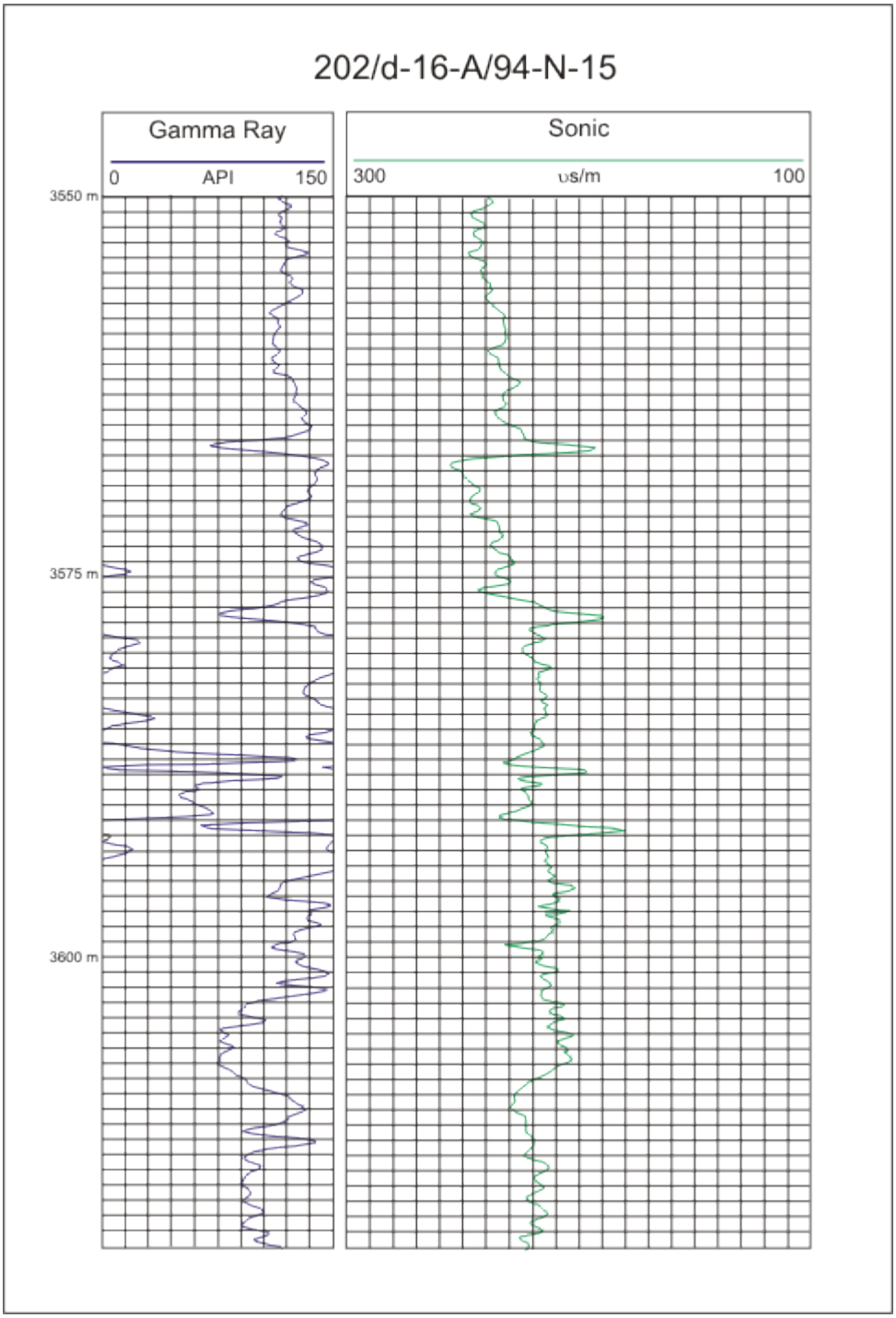

Figure 17. Typical log signature in the Besa River Formation.

Lateral Extent and Thickness

Very few wells penetrate the Besa River Formation and even fewer wells have core in the Besa River. The data for this study is limited to 11 wells which penetrate the Besa River Formation, of which two wells have core (Figure 18). Further data is available from previous studies in the public domain. Thickness up to 1600 m have been reported for the Besa River Formation (Richards, 1989)

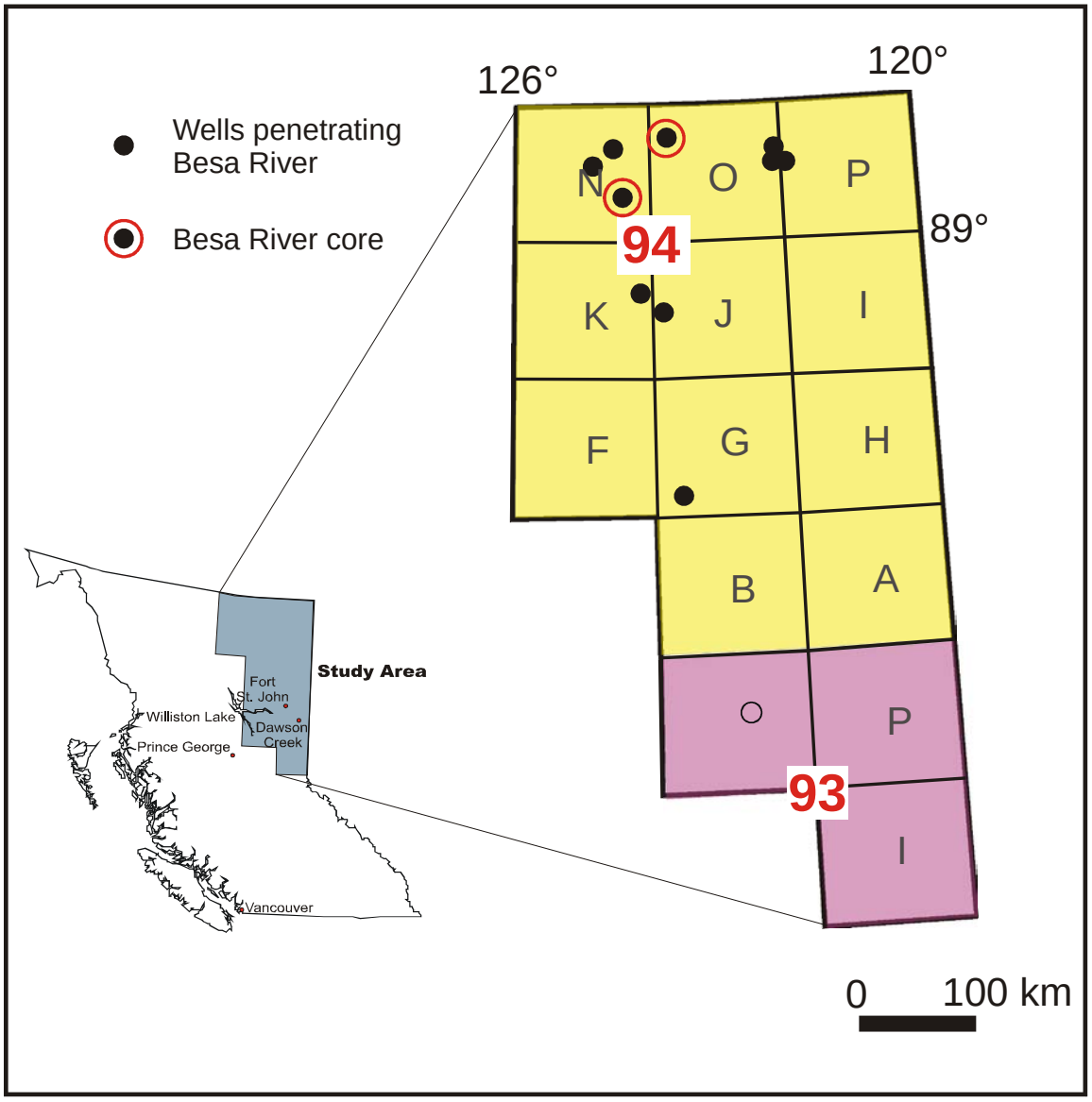

Figure 18. Distribution of wells penetrating the Besa River Formation. Red circles indicate wells with core.

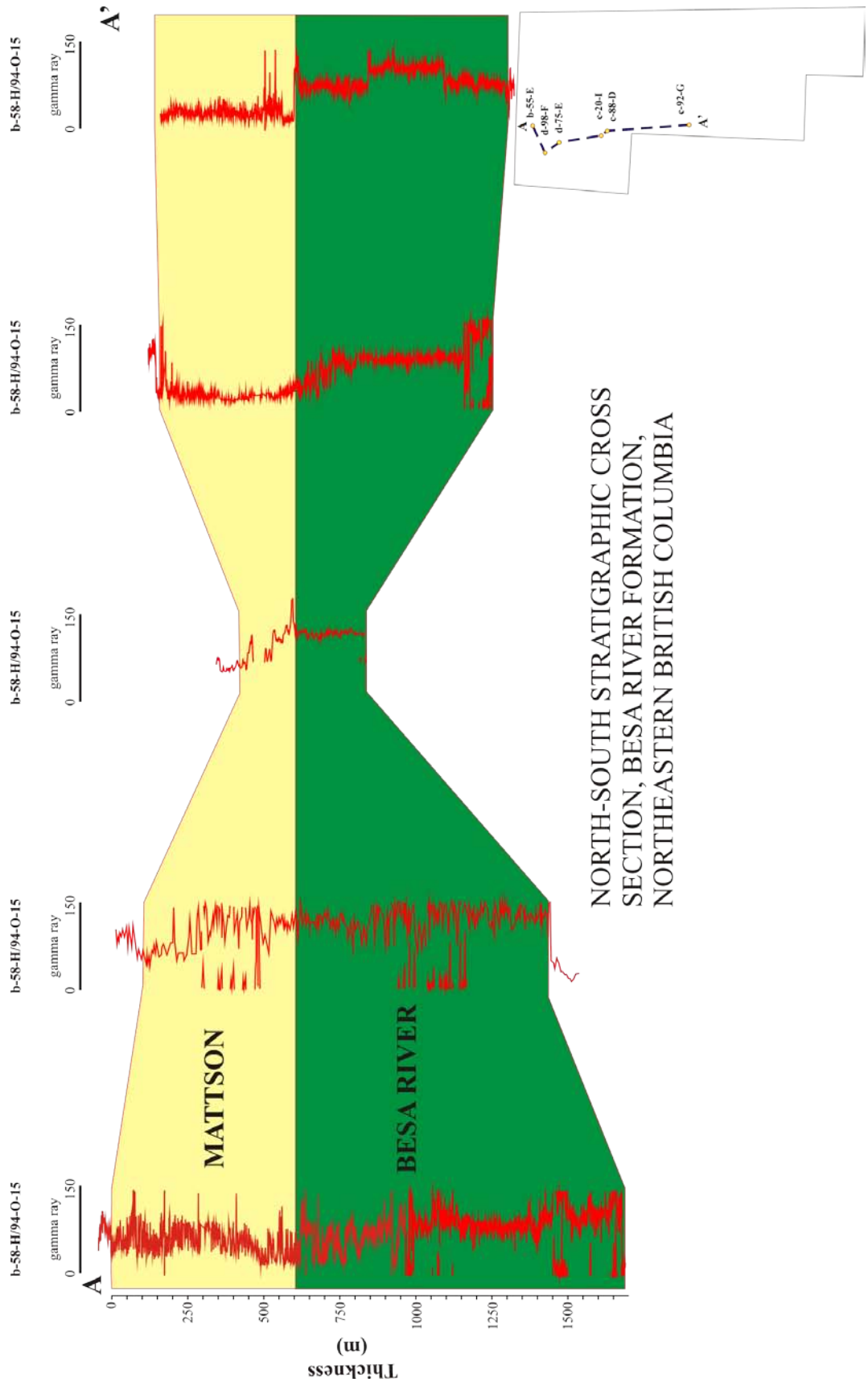

Figure 19. North to south stratigraphic cross section of the Besa River Formation (A – A').

Total Organic Carbon

For the Besa River Formation, a total of 64 samples from two cored wells were run for TOC (Table 9). In northeastern British Columbia, very few wells penetrate the Besa River Formation, and only one well has a full geophysical log section from top to bottom in the Besa River Formation. As a result, limited data is available to correlate TOC to geophysical logs. From the limited cores available, TOC analyzes show that the Besa River includes organic-rich intervals (> 2 wt% TOC).

For Dunedin d-75-E/94-N-8, the average TOC (wt%) for core 15 (3687.0 – 3702.0 m), core 16 (3773.2 – 3775.7 m) and core 17 (3889.7 – 3895.5 m) are 4.0%, 3.4%, and 7.8% respectively (Figure 20 shows the location of core samples). Core 15 is transitional from the Mattson Formation to the Besa River Formation and consists of interbedded shale, sandstone and siltstone. The TOC contents for cores 15 (3687.0 – 3702.0 m) and 16 (3773.2 – 3775.7 m) are highly variable due to vertical facies changes within the section. In general, the soft, fissile, black shale samples from Dunedin d-75-E/94-N-8, core 17 (3889.7 – 3895.5 m) contain the highest and most consistent organic carbon content values. The TOC contents do not correlate with gamma ray intensities, which is most likely due to a data set and log signatures that do not reflect the small scale variability within the section. Density and neutron logs are not available for Dunedin d-75-E/94-N-8.

The average TOC for the La Biche b-55-E core is 3.20 wt%. The TOC contents are variable due to the vertical facies changes. The only log available is the neutron log which shows a strong correlation of increasing neutron counts per second with increasing organic content (Figure 21) signifying the relationship between TOC content and the amount of hydrogen present.

Well	Depth m	Total Carbon %	Inorganic Carbon %	Organic Carbon %
Dunedin d-75-E/94-N-8	3687.00	0.62	0.29	0.33
	3687.60	2.65	0.68	1.97
	3688.20	2.92	0.79	2.13
	3689.10	4.97	0.10	4.87
	3690.00	3.02	0.17	2.85
	3690.90	6.86	0.39	6.47
	3692.10	5.29	0.13	5.16
	3693.00	5.73	2.76	2.97
	3693.90	4.89	2.00	2.89
	3695.10	4.24	0.50	3.74
	3696.00	7.46	7.41	0.05
	3696.90	3.07	0.40	2.67
	3698.10	6.43	0.50	5.93
	3699.00	9.12	0.34	8.78
	3699.90	5.35	0.51	4.84
	3700.50	9.99	2.14	7.85
	3701.10	5.49	0.86	4.63
	3702.00	4.05	0.14	3.91
	3773.20	2.24	<0.05	2.24
	3773.48	4.26	<0.05	4.26
	3773.50	1.85	<0.05	1.85
	3773.80	3.35	0.05	3.30
	3774.10	3.45	0.12	3.33
	3774.40	3.77	0.17	3.60
	3774.70	4.17	0.19	3.98
	3775.00	4.09	<0.05	4.09
	3775.30	4.32	<0.05	4.32
	3889.70	5.49	0.87	4.62
	3890.00	4.71	<0.05	4.71
	3890.30	4.67	<0.05	4.67
	3890.60	6.47	0.36	6.11
	3890.90	6.35	0.22	6.13
	3891.20	6.13	<0.05	6.13
	3891.50	5.61	<0.05	5.61
	3891.80	6.35	0.06	6.29
	3892.10	6.63	0.06	6.57
	3892.40	6.97	0.17	6.80
	3892.70	6.03	<0.05	6.03
	3893.00	6.74	0.05	6.69
	3893.30	6.36	<0.05	6.36
	3893.60	6.93	0.44	6.49
	3893.90	6.79	<0.05	6.79
	3894.20	6.45	0.06	6.39
	3894.50	6.14	0.08	6.06
	3894.80	5.83	0.06	5.77
	3895.10	5.40	<0.05	5.40
	3895.40	5.23	0.09	5.14
	3895.70	5.14	0.12	5.02

Well	Depth m	Total Carbon %	Inorganic Carbon %	Organic Carbon %
La Biche b-55-E/94-N-13	3044.50	4.03	<0.05	4.03
	3044.80	3.83	<0.05	3.83
	3045.10	2.95	0.05	2.90
	3045.40	3.64	0.25	3.39
	3045.70	4.91	0.16	4.75
	3046.00	3.43	0.13	3.30
	3046.30	3.76	0.33	3.43
	3046.60	3.27	0.21	3.06
	3046.90	4.35	0.28	4.07
	3047.20	4.18	0.23	3.95
	3047.50	3.58	0.22	3.36
	3047.80	2.68	0.13	2.55
	3048.10	1.99	0.10	1.89
	3048.40	2.58	0.10	2.48
	3048.70	2.37	0.10	2.27
	3049.00	2.32	0.35	1.97

Table 9. Total Organic Carbon results for Besa River core samples.

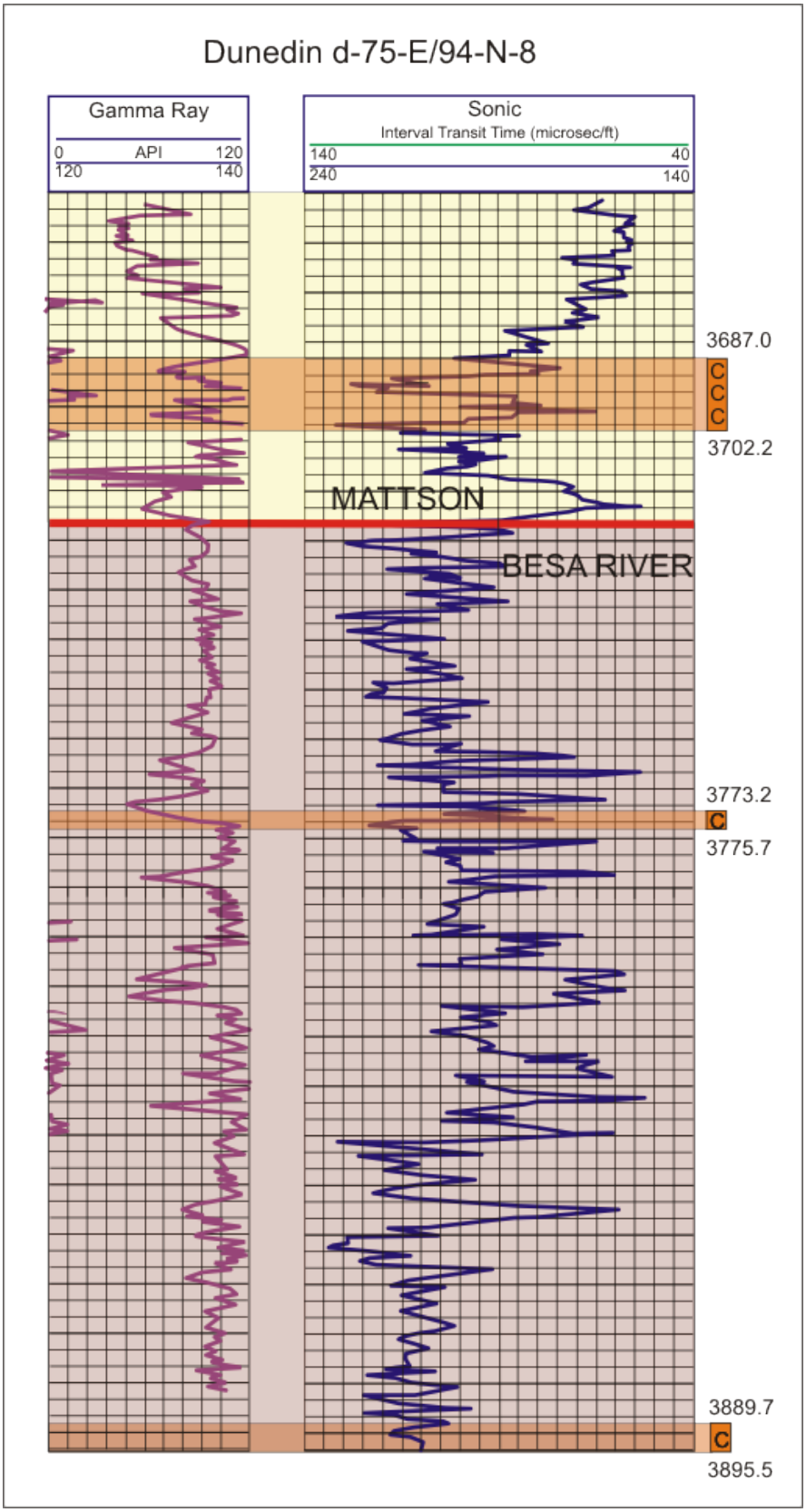

Figure 20. Core locations and gamma ray and sonic log signatures for Dunedin d-75-E/94-N-8. "C" indicates core intervals.

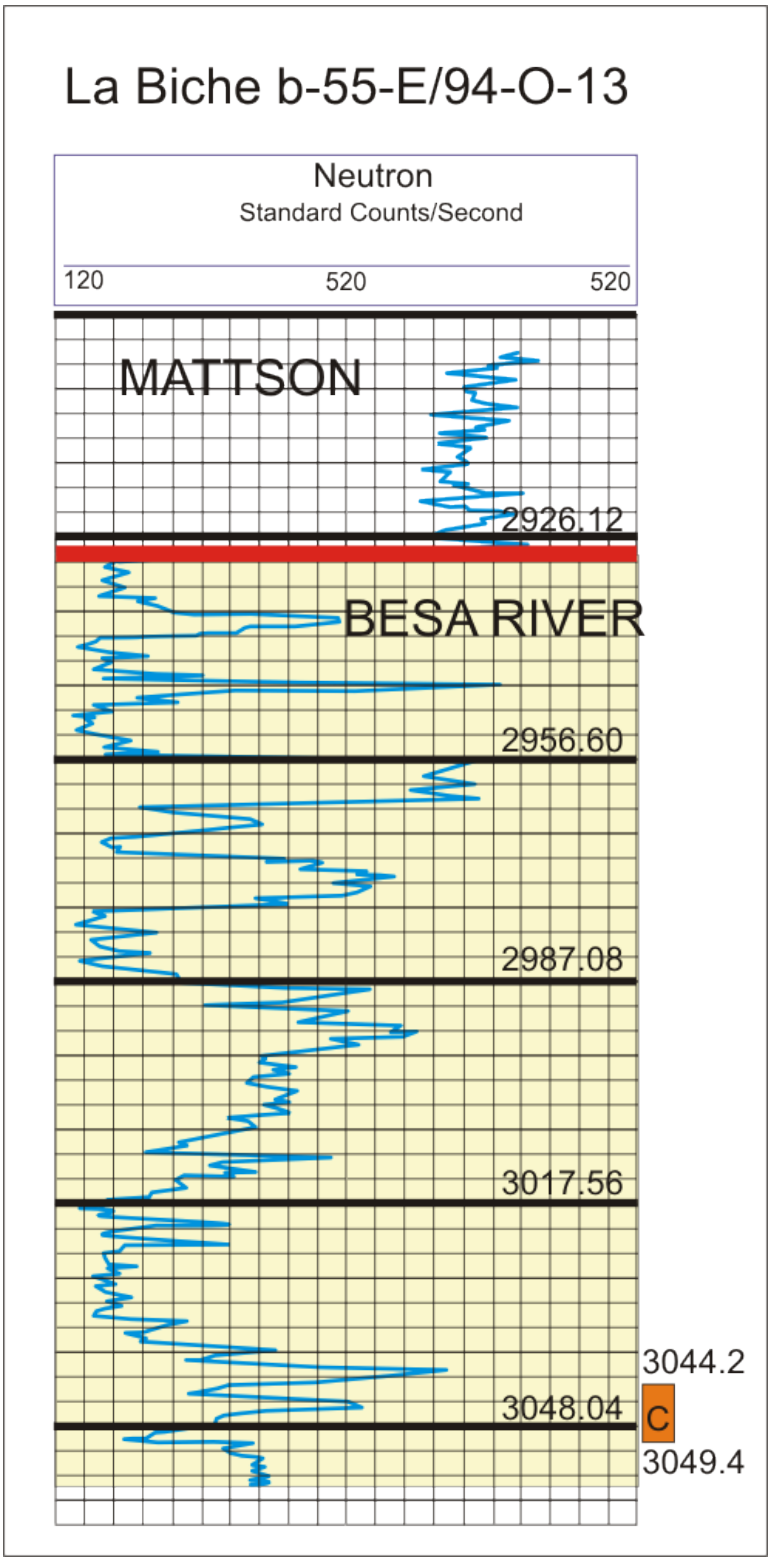

Figure 21. Gamma ray and Sonic log signature for well La Biche b-55-E/94-O-13, showing core 16 from 3044.20 – 3049.40 m. "C" indicates core intervals.

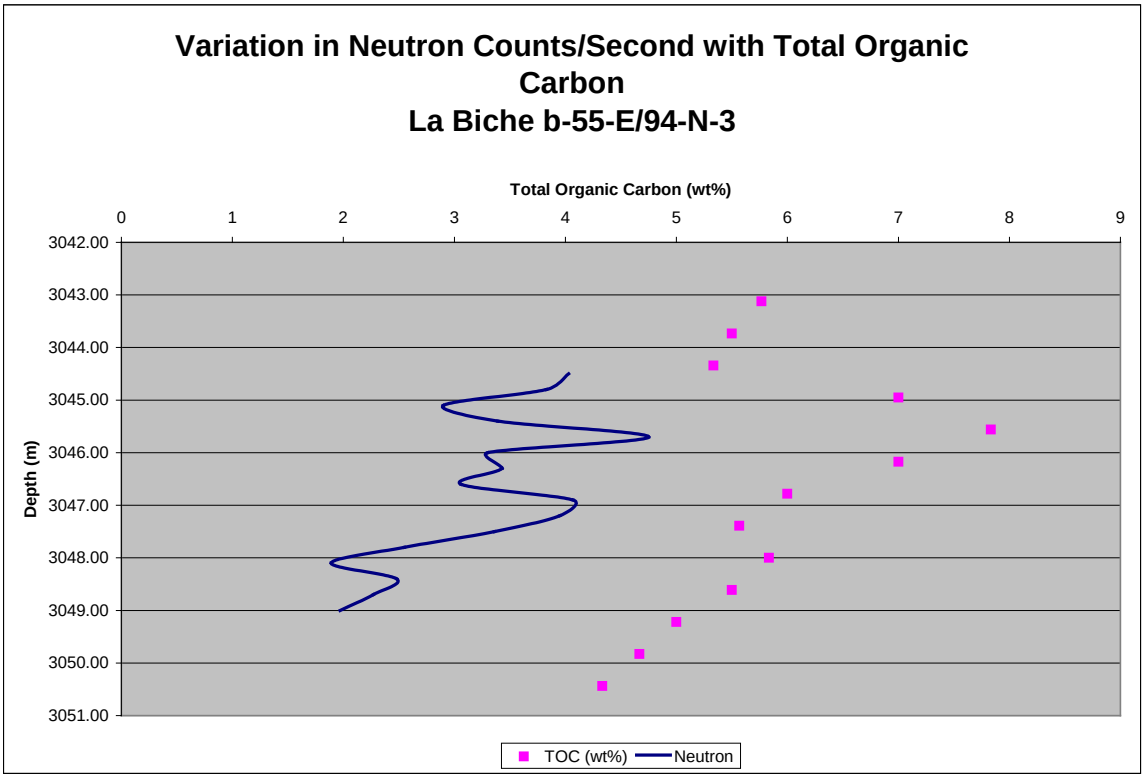

Figure 22. Variation in neutron counts with total organic carbon content for the La Biche b-55-E/94-O-13 core interval.

Thermal Maturity and Organic Matter Type

Select Besa River Formation shale samples were analyzed using Rock-Eval pyrolysis to determine both the thermal maturity and organic matter type. Table 10 shows the Rock-Eval data for twenty analyzed samples from two wells. The low S2 values measured in many of the samples suggest that the shales are very mature. As a result, the Tmax values are suspect and cannot be used reliably to determine an absolute maximum thermal exposure.

All of the analyzed samples plot in the Type II to III organic matter range (Figure 23) but because of the high level of maturity the kerogen typing via the Van Krevelan diagram is not definitive.

Depth	Tmax	S1	S2	S3	PI	S2/S3	PC(%)	TOC(%)	HI	OI
Dunedin d-75-E										
3688.8	604	0.00	0.00	0.47	0.74	0.00	0.00	3.09	0	15
3681.4	288	0.16	0.02	0.65	0.87	0.03	0.02	3.13	1	21
3695.1	327	0.08	0.06	0.63	0.60	0.10	0.02	4.14	1	15
3773.8	395	0.38	1.55	0.38	0.20	4.08	0.16	3.20	48	12
3773.8	381	0.38	1.55	0.58	0.19	2.67	0.16	3.20	48	18
3774.1	486	0.02	0.00	0.48	0.87	0.00	0.01	3.43	0	14
3774.7	327	0.03	0.00	0.33	0.94	0.00	0.01	3.35	0	10
3775.0	423	0.10	0.05	0.46	0.67	0.11	0.01	4.57	1	10
3775.0	387	0.05	0.01	0.48	0.88	0.02	0.01	3.35	0	14
3872.1	-40	0.02	0.00	0.49	1.00	0.00	0.01	5.96	0	8
3890.0	423	0.02	0.00	0.39	0.85	0.00	0.00	4.56	0	9
3890.6	309	0.06	0.00	0.68	0.96	0.00	0.01	4.40	0	15
3891.8	-40	0.03	0.00	0.32	1.00	0.00	0.01	5.73	0	6
3892.1	605	0.31	0.01	0.42	0.97	0.02	0.03	6.04	0	7
3893.0	321	0.01	0.00	0.38	0.88	0.00	0.00	6.27	0	6
3893.5	406	0.02	0.02	0.20	0.48	0.10	0.00	1.76	1	11
3894.5	-40	0.01	0.00	0.40	1.00	0.00	0.01	5.83	0	7
3895.7	369	0.02	0.00	0.35	0.94	0.00	0.01	4.91	0	7
3896.0	490	0.02	0.01	0.59	0.63	0.02	0.01	4.68	0	13
La Biche b-55-E										
3044.8	494	0.16	1.02	0.17	0.13	6.00	0.11	3.86	27	4
3046.15	508	0.04	0.60	0.41	0.07	1.46	0.06	3.24	19	13
3047.2	492	0.04	0.53	0.20	0.07	2.65	0.05	3.34	17	6
3047.2	507	0.02	0.65	0.79	0.03	0.82	0.07	3.78	18	21

Table 10. Rock-Eval data for the Besa River Formation.

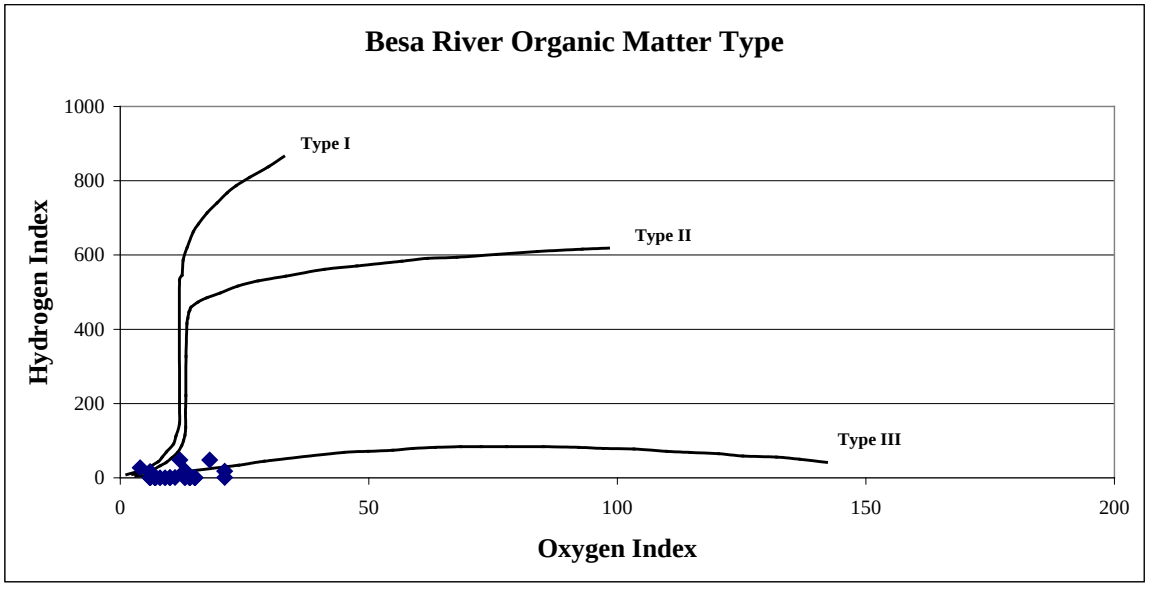

Figure 23. Van Krevelen diagram for the Besa River Formation shales. The level of maturity is so high that it is not possible to type the kerogen based on the Van Krevelen plot.

Porosity

Twenty-three shale samples from the Besa River Formation were analyzed for total porosity (Table 11). The analyzes show that the range of porosity is from 1.3 to 7.2% with an average value of 4.6%. Assuming the formation is saturated, the pore space in the shale provides additional gas storage capacity which may significantly increase the potential gas in place. The effect of porosity on gas capacity in place is shown in the following section.

Sample	Depth (m)	Formation	Hg Bulk Density (cc/g)	He Skeletal Density (cc/g)	Std Dev.	Porosity	
						Fraction	Percent
Dunedin d-75-E/94-N-8	3687.3	Besa River	2.66	2.74	0.010	0.029	2.92
Dunedin d-75-E/94-N-8	3687.6	Besa River	2.55	2.66	0.021	0.040	3.98
Dunedin d-75-E/94-N-8	3688.8	Besa River	2.48	2.62	0.007	0.055	5.47
Dunedin d-75-E/94-N-8	3691.8	Besa River	2.42	2.52	0.013	0.037	3.67
Dunedin d-75-E/94-N-8	3695.1	Besa River	2.47	2.61	0.007	0.055	5.52
Dunedin d-75-E/94-N-8	3698.1	Besa River	2.38	2.49	0.011	0.047	4.73
Dunedin d-75-E/94-N-8	3701.1	Besa River	2.79	2.86	0.005	0.025	2.51
Dunedin d-75-E/94-N-8	3773.5	Besa River	2.44	2.62	0.004	0.070	7.04
Dunedin d-75-E/94-N-8	3773.8	Besa River	2.41	2.57	0.008	0.063	6.26
Dunedin d-75-E/94-N-8	3774.1	Besa River	2.51	2.55	0.007	0.015	1.55
Dunedin d-75-E/94-N-8	3774.7	Besa River	2.44	2.61	0.007	0.065	6.51
Dunedin d-75-E/94-N-8	3775.0	Besa River	2.37	2.53	0.009	0.063	6.27
Dunedin d-75-E/94-N-8	3890.0	Besa River	2.46	2.59	0.003	0.051	5.05
Dunedin d-75-E/94-N-8	3890.6	Besa River	2.80	2.93	0.011	0.044	4.42
Dunedin d-75-E/94-N-8	3891.8	Besa River	2.45	2.57	0.005	0.045	4.50
Dunedin d-75-E/94-N-8	3892.1	Besa River	2.07	2.64	0.017	0.072	7.19
Dunedin d-75-E/94-N-8	3893.0	Besa River	2.41	2.57	0.012	0.062	6.24
Dunedin d-75-E/94-N-8	3894.5	Besa River	2.48	2.57	0.003	0.037	3.74
Dunedin d-75-E/94-N-8	3895.7	Besa River	2.43	2.57	0.003	0.054	5.37
Dunedin d-75-E/94-N-8	3896.0	Besa River	2.53	2.64	0.026	0.041	4.05
La Biche b-55-E/94-O-13	3044.8	Besa River	2.52	2.66	0.022	0.053	5.33
La Biche b-55-E/94-O-13	3046.2	Besa River	2.61	2.65	0.016	0.013	1.33
La Biche b-55-E/94-O-13	3047.3	Besa River	2.55	2.63	0.009	0.029	2.94

Table 11. Porosity values for select Besa River shale samples.

Sorption Capacity

In order to quantify the sorbed gas capacity in place, adsorption isotherms were completed on 13 samples from 2 wells in northeastern British Columbia. Base on drilling depths, intersections of the Besa River Formation range from approximately 1000 to 3700 m. Using the drill depth range of 1000 to 3700 m, the calculated reservoir pressures range from 11100 to 41100 kPa (1600 to 6000 psi). The TOC contents of the samples

ranges from 3.1% to 6.3%. The average TOC measured for all of the Besa River Formation samples collected for this study is approximately 4%.

All adsorption data (gas capacity data) is presented at reservoir pressure and an average pressure of 11 MPa (1600 psi). The average gas capacity (at reservoir pressures) measured for the Besa River samples is 1.4 cc/g (44 scf/ton) not accounting for free gas porosity. At a standard pressure of 11 MPa, the gas capacity is 1.0 cc/g (32 scf/ton) Sample 3044.8 from La Biche b-55-E/94-O-13 (3044.8 m) provides a characteristic sorption profile for a Besa River shale with 3.9% TOC (Figure 24). Table 12 provides the gas capacity data for each Besa River Formation sample at reservoir pressure and a standard pressure of 11 MPa.

Because there is significant porosity in the Besa River Formation samples, the gas capacity increases significantly if free gas capacity is considered. In figure 25, the gas capacities have been calculated to show the effect of porosity on gas capacity. End members of 2% and 7% porosity have been used to calculate the gas capacity in a 3.9% TOC sample. At 11 MPa pressure, the sorbed gas capacity is 0.85 cc/g (27 scf/ton). At 11 MPa pressure, the gas capacity with 2% porosity is 1.8 cc/g (57 scf/ton) which is a 112% increase over the sorbed gas capacity. With 7% porosity, the gas capacity is 4.6 cc/g (147 scf/ton) which is a 440% increase over the sorbed gas capacity.

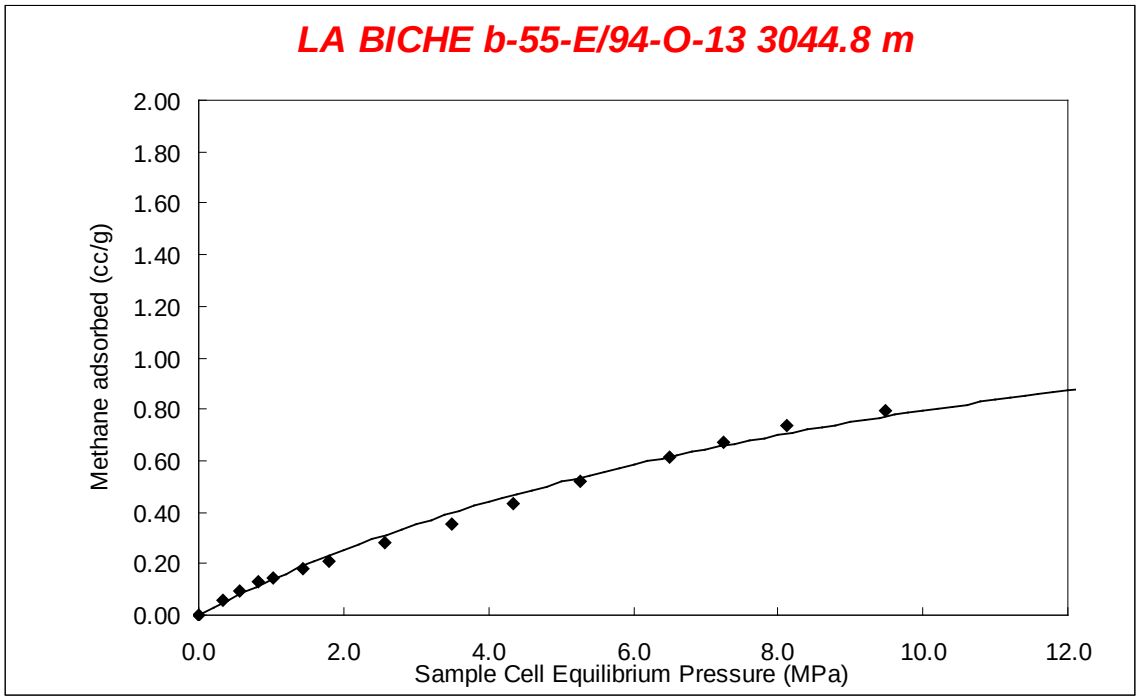

Figure 24. Adsorption isotherm for a shale sample from the Besa River Formation. Sample has a TOC content of 3.9%. Gas capacity for pressures greater than 10 MPa is extrapolated using the Langmuir equation.

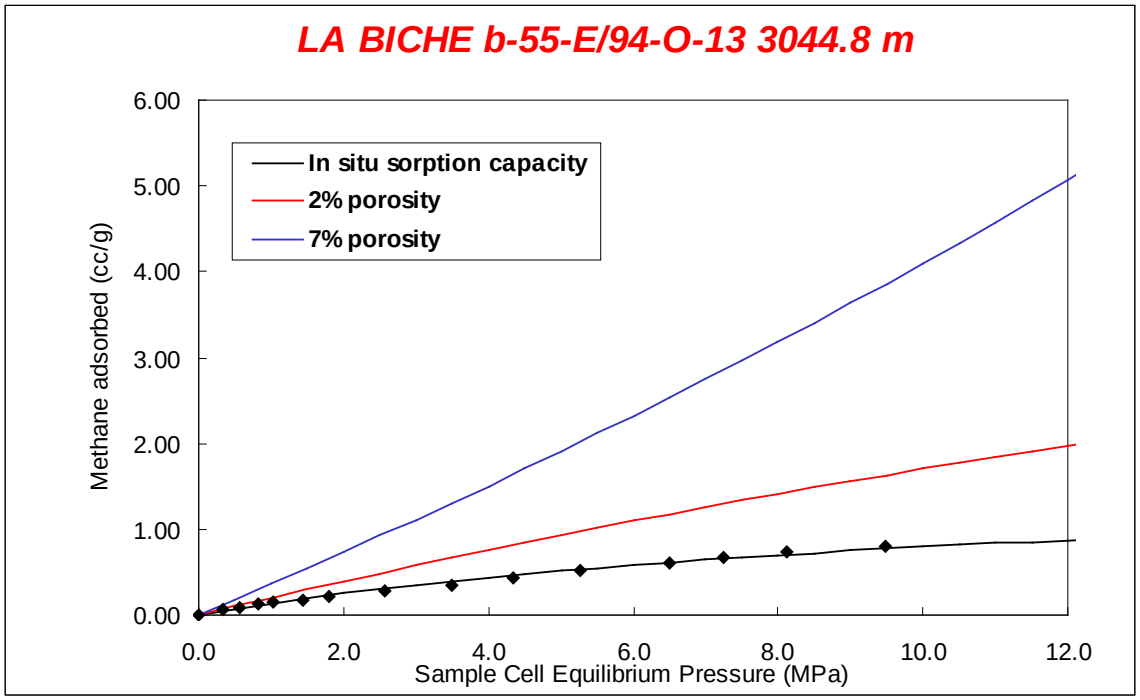

Figure 25. Sorbed plus free gas capacity in a 5% TOC sample.

Well Name	Location	Depth (m)	Reservoir Pressure (psi)	Reservoir Pressure (kPa)	Gas Capacity (cc/g)	Gas Capacity @ 11 Mpa (cc/g)	TOC
Besa River							
La Biche	b-55-E/94-O-13	3044.80	4295	29616	1.2	0.83	3.86
		3046.15	4297	29629	0.8	0.68	3.24
		3047.20	4299	29640	0.9	0.77	3.56
Dunedin	d-75-E/94-N-8	3688.80	5204	35880	1.7	1.46	3.09
		3695.10	5213	35942	0.6	0.5	4.14
		3773.80	5324	36707	0.4	0.39	3.20
		3775.00	5326	36719	1.5	0.85	4.57
		3890.60	5489	37843	0.4	0.35	4.40
		3892.10	5491	37858	2.4	1.66	6.04
		3893.00	5492	37867	1.7	1.31	6.27
		3894.50	5494	37881	3.0	1.95	5.83
		3895.70	5496	37893	1.6	1.14	4.91
		3896.00	5496	37896	0.8	0.65	4.68

Table 12. Variation in sorption capacity with total organic carbon content for Besa River Formation shale samples. Capacities are given at reservoir pressure and a standard pressure of 11 MPa.

Clay Mineralogy

X-ray diffraction analyzes was completed on 17 samples from the Besa River Formation in order to determine the mineralogy of the shale samples. Samples are limited to two core wells, La Biche b-55-E/94-O-13 and Dunedin d-75-E/94-N-8. Several of the samples from the Dunedin d-75-E/94-N-8 were collected within the overlying Mattson Formation which consists of shale interbedded with sandstone and siltstone (Figure 20).

Table 13 shows a summary of the x-ray diffraction data. X-ray diffraction traces for each sample are shown Appendix B.

All of the analyzed Besa River samples are comprised of quartz, illite and kaolinite with minor pyrite. Samples 3046.15 m (b-55-E) and sample 3773.8 m (d-75-E) contain significant dolomite.

The variation in the mineralogy of the Besa River data set reflects the different facies in the formation. From TOC analyzes, the Besa River samples are organic-rich (> 2wt%

TOC). Albeit a small data set, a relationship can be seen between the grey, silty shales versus the darker black shales. In general, the soft, black shale samples from Dunedin d-75-E/94-N-8, core 17, contain the highest organic carbon contents. These samples have low quartz contents (~40%) and high clay contents (~ 50% illite and kaolinite). The remaining Besa River samples excluding the dolomite-rich samples, have quartz contents ranging from 70-90% and clay contents less than 30%. The TOC content in Dunedin d-75-E/94-N-8, core 15 is variable as the samples represent the transition from the Besa River Formation into the Mattson Formation which consists of interbedded shale, sandstone and siltstone.

BESA RIVER XRD				Mineralogy (% Relative)					
Name	Location	Core	Depth (m)	Illite/Mica (d=10.00)	Kaolinite (d=7.10)	Quartz (d=4.23	Calcite (d=3.03)	Pyrite (d=2.71)	Dolomite (d=2.89)
La Biche	b-55-E/94-O-13	16	3044.8	4	9	87	0	0	0
			3046.15	4	0	6	0	0	90
			3047.2	11	8	81	0	0	0
Dunedin	d-75-E/94-N-8	15	3687.3	2	8	86	0	3	0
			3687.6	16	0	84	0	0	0
			3688.8	15	2	80	0	3	0
			3695.1	8	18	66	0	9	0
			3701.1	22	0	78	0	0	0
		16	3773.8	21	5	36	0	0	38
		17	3891.8	25	26	42	0	7	0
			3896.0	22	36	35	0	7	0

Table 13. Relative mineralogy percentages determined from XRD analyzes. "d" refers to the d-spacing of the principal plane of each mineral that was used to (semi-) quantify the relative abundances.

Gas Capacity in Place

Because gas capacities are highly variable due to changing organic contents, reservoir pressures, formation thicknesses and porosity, gas in place numbers can be calculated based on a range of reservoir properties. Table 14 provides gas capacity in place numbers for an average TOC content of 4% and varying reservoir pressures and

porosities. The gas in place values are calculated using an average density of 2.49 g/cc which is measured using mercury submersion.

Porosity (%)	TOC (%)	Shale Thickness (m)	Pressure (MPa)	Resources (cc/cm2)	Resources (bcf/section)	Average Gas Content (scf/ton)	Average Gas Content (cc/g)	Density (g/cc)
0.0	3.9	100.0	34.0	31872	29	41	1.3	2.49
0.0	3.9	500.0	34.0	159360	146	41	1.3	2.49
0.0	3.9	1000.0	34.0	318720	292	41	1.3	2.49
2.0	3.9	100.0	34.0	102588	94	132	4.1	2.49
2.0	3.9	500.0	34.0	512940	469	132	4.1	2.49
2.0	3.9	1000.0	34.0	1025880	938	132	4.1	2.49
7.0	3.9	100.0	34.0	540579	494	696	21.7	2.49
7.0	3.9	500.0	34.0	2702895	2472	696	21.7	2.49
7.0	3.9	1000.0	34.0	5405790	4944	696	21.7	2.49
0.0	3.9	100.0	11.0	20667	19	27	0.8	2.49
0.0	3.9	500.0	11.0	99600	91	26	0.8	2.49
0.0	3.9	1000.0	11.0	199200	182	26	0.8	2.49
2.0	3.9	100.0	11.0	45816	42	59	1.8	2.49
2.0	3.9	500.0	11.0	229080	210	59	1.8	2.49
2.0	3.9	1000.0	11.0	458160	419	59	1.8	2.49
7.0	3.9	100.0	11.0	114042	104	147	4.6	2.49
7.0	3.9	500.0	11.0	570210	522	147	4.6	2.49
7.0	3.9	1000.0	11.0	1140420	1043	147	4.6	2.49

Table 14. Gas capacity in place based on an average of 3.9% TOC content at two different pressures. Also shown is the variation in gas capacity with increasing porosity.

Conclusions

The Besa River Formation is a carbonaceous shale interval which is widely distributed throughout northeastern British Columbia. Maximum thickness of the Besa River Formation in northeastern British Columbia is reported to reach thickness up to 1600 m. Individual organic rich sections (characterized by high gamma ray response) reach thickness of up 25 to 30 m and occur throughout the formation. The maximum total organic carbon (TOC) content measured in this study is 8.8% with an average of 4.3%. Low TOC values measured are characteristic of lithological variations within the formation. Due to the high organic contents, the Besa River shales have potential for high sorbed gas capacity. A sample with 4% TOC can hold 1.3 cc/g at a typical reservoir pressure of 34 MPa. With porosity in the range of 2% to 7%, the free gas potential,

assuming saturation, can increase the gas capacity by 100% to 400% over the sorbed gas capacity.

Fort Simpson Formation

Lithology and Stratigraphy

The Fort Simpson Formation is a thick green to gray fissile marine shale (Gray and Kassube, 1963; Torrie, 1973) which is variably calcareous and carbonaceous. Fine grained sandstone and siltstone beds are present throughout, increasing the potential for permeability pathways. The Fort Simpson Formation is a marine shale deposited on the continental shelf. Following a period of low sedimentation rates and black shale deposition (Muskwa Formation), an increase in sediment influx from the north and northwest resulted in the thick deposits of the Fort Simpson Formation (Morrow and Geldsetezer, 1988). Local features within the Fort Simpson Formation include pyrite bands and nodules and organic-rich sections.

Within the study area, the Fort Simpson conformably overlies the Muskwa Formation. From east to west, the top of the Fort Simpson Formation has been defined as the base of the Jean Marie Member, Kakisa, Trout River or Tetcho formations (Torrie, 1973). The Woodbend Group in Alberta is the stratigraphic equivalent of the Fort Simpson and Muskwa formations to the east in Alberta. In the Yukon and Northwest Territories, the Fort Simpson and Horn River formations grade together into an undifferentiated unit consisting of siltstone, limestone and shales (Douglas and Norris, 1961).

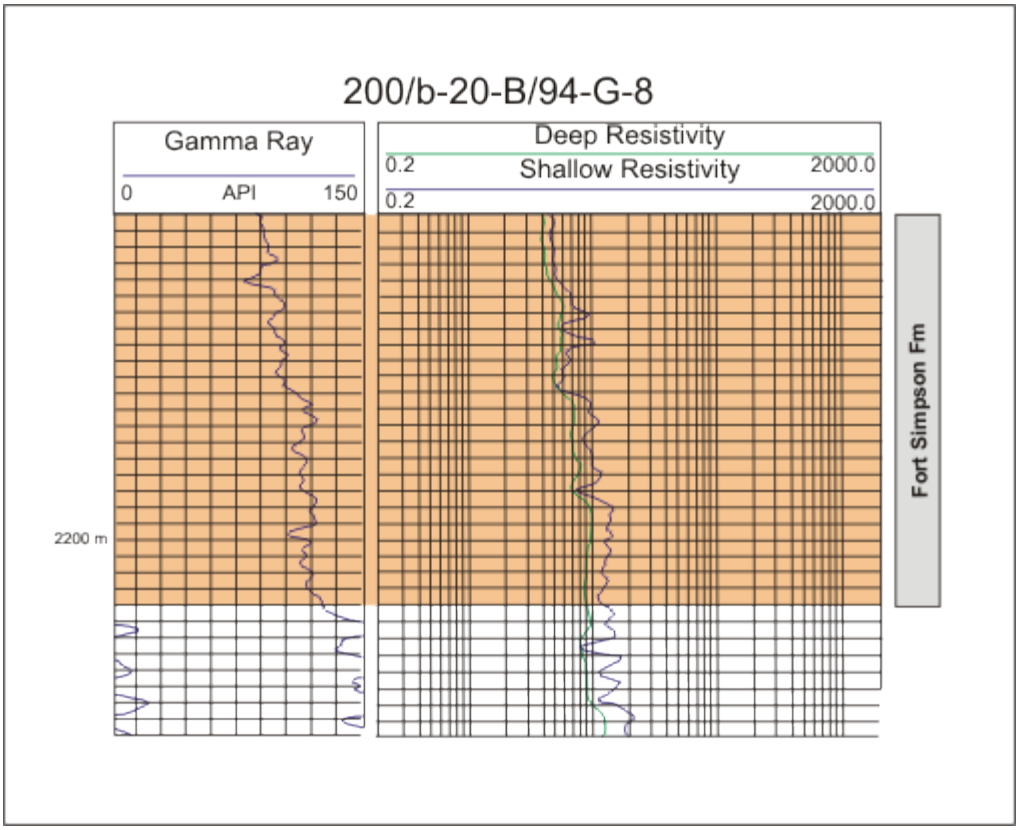

Figure 26. Typical log signature of the transition from the Muskwa Formation into the overlying Fort Simpson Formation.

Lateral Extent and Thickness

Within the study area, the Fort Simpson reaches thicknesses of up to 800 m and extends throughout northeastern British Columbia (north of the Peace River Arch), northwestern Alberta and the Northwest Territories (Figure 27). The thickest accumulations occur in the northwest and thin towards the southeast in the township and range block of the Peace River Arch (Figure 30). Hadley and Jones (1990) noted that occasional thinning of the Fort Simpson Formation occurs due to localized thickened sections of the underlying Slave Point and Muskwa formations.

Structurally, the Fort Simpson Formation dips from north to south (Figure 31). The deepest intersections of the Fort Simpson Formation occur in the Peace River Arch block and reach depths of 3000 m below surface. The shallowest intersections recorded in the study area are approximately 1200 m below surface and occur primarily in the northeast.

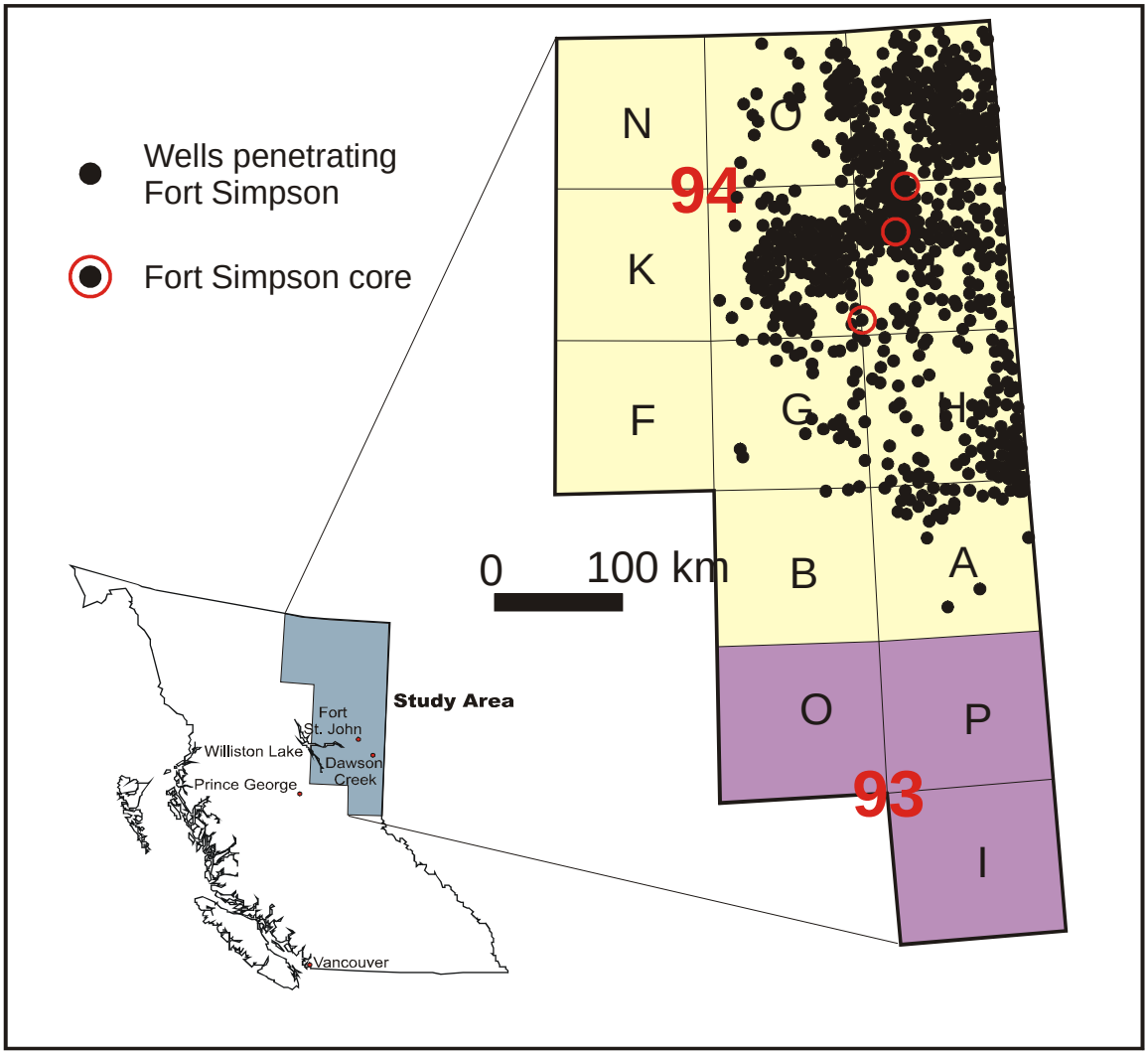

Figure 27. Distribution of wells penetrating the Fort Simpson Formation. Red circles indicate wells with core.

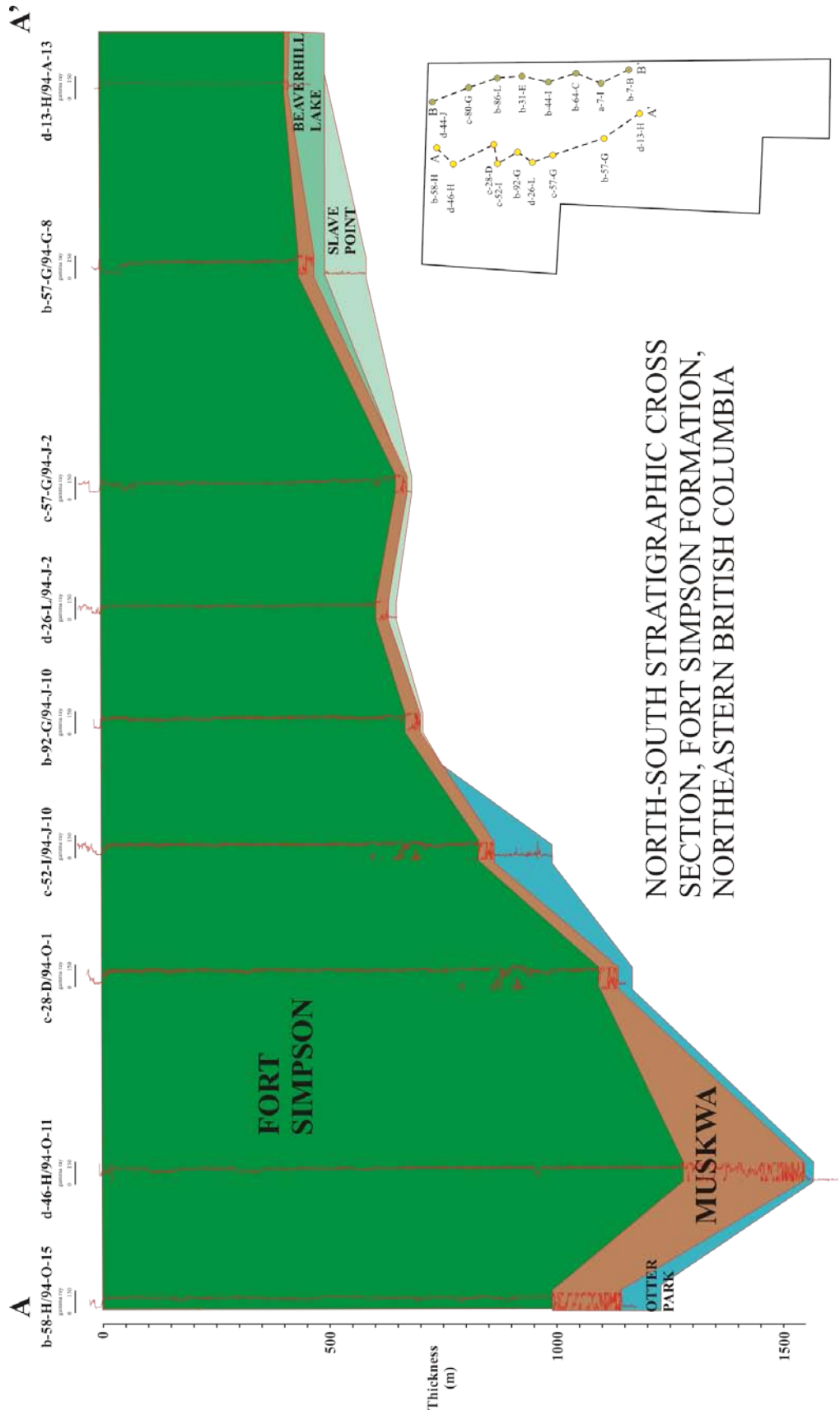

Figure 28. North to south stratigraphic cross section of the Fort Simpson Formation in the western portion of the study area (A – A').

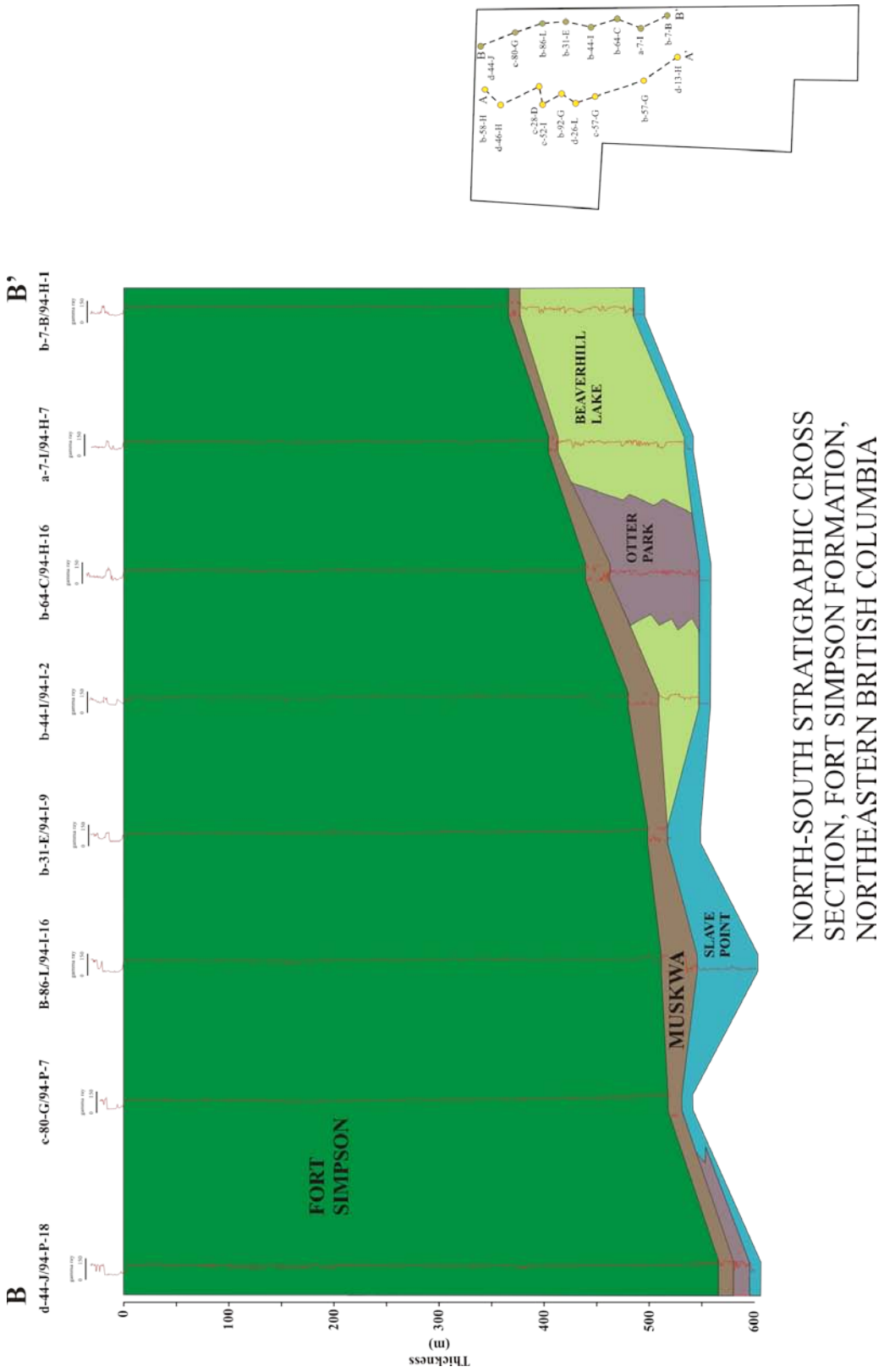

Figure 29. North to south stratigraphic cross section of the Fort Simpson Formation in the eastern portion of the study area (B – B').

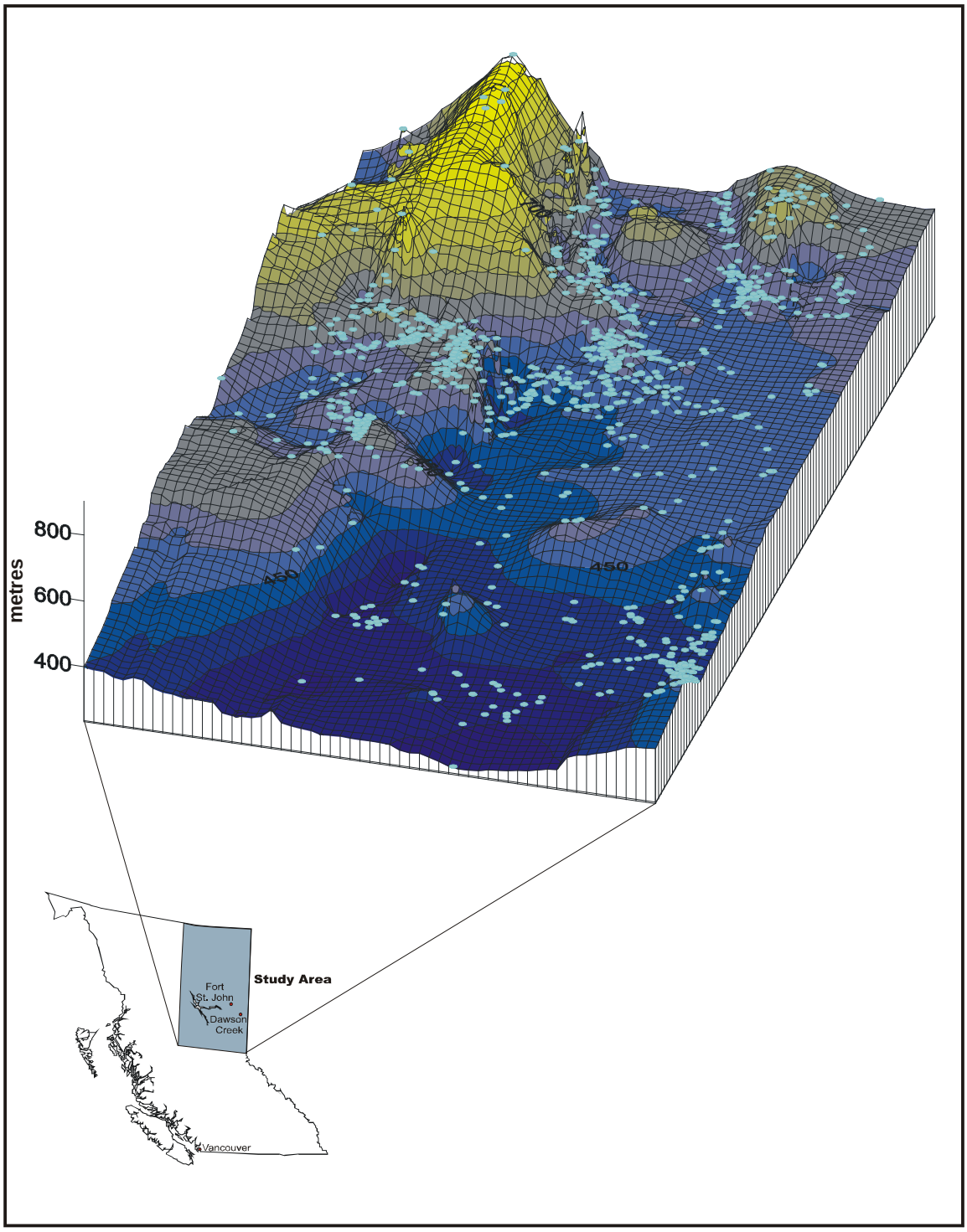

Figure 30. Isopach map of the Fort Simpson Formation shows a thickening trend from east to west.

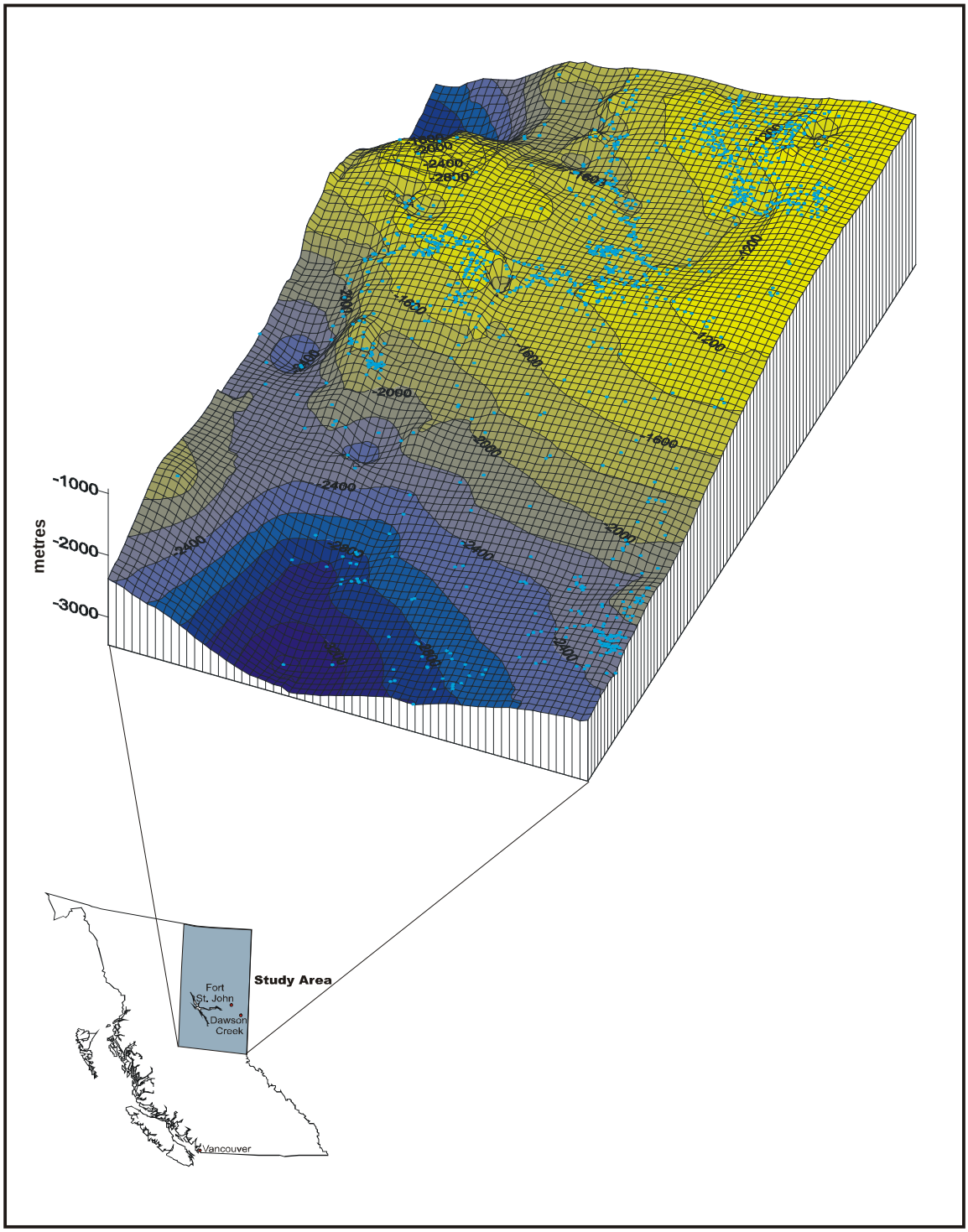

Figure 31. Upper surface of the Fort Simpson Formation showing the drill depths from surface.

Total Organic Carbon

For the Fort Simpson Formation, a total of 41 samples from two cored wells were run for TOC (Table 15). The Fort Simpson Formation is characterized by low total organic carbon contents (Table 15) with an average value 0.4% and a maximum value of 1.3%.

For the two core wells sampled, Sikanni Chief b-92-D/94-I-4 and Junior c-60-E/94-I-11 the TOC contents are relatively consistent throughout. The log signatures for the Fort Simpson in both wells also shows very little variability. The Sikanni Chief well b-92-D/94-I-4 has three cores at different intervals within the Fort Simpson Formation: core 13 is from 1953.16 – 1959.25 m, core 14 is from 2103.12 – 2109.22 m and core 15 is from 2215.90 – 2221.99 m. Because there is very little variation in the geophysical logs, a correlation between TOC content and log signature cannot be made. Junior c-60-E/94-I-11 has two cores that penetrate through the bottom of the Fort Simpson Formation where it begins to transition into the Muskwa Formation (Figure 32). Within the transition zone, the gamma ray intensity increases slightly which is reflected with slightly higher TOC values in this interval.

Well	Depth m	Total Carbon %	Inorganic Carbon %	Organic Carbon %
Junior c-60E/94-I-11	1857.10	0.55	0.28	0.27
	1858.00	0.70	0.38	0.32
	1858.90	0.66	0.40	0.26
	1860.10	0.71	0.39	0.32
	1861.00	0.81	0.40	0.41
	1861.90	0.54	0.08	0.46
	1863.10	0.50	0.26	0.24
	1864.00	0.68	0.50	0.18
	1864.90	0.62	0.36	0.26
	1866.10	0.49	0.21	0.28
	1867.00	0.52	0.26	0.26
	1867.30	0.45	0.30	0.15
	1867.90	1.12	0.70	0.42
	1869.10	0.93	0.71	0.22
	1870.00	1.11	0.46	0.65
	1870.90	0.83	0.51	0.32
	1872.40	0.70	0.27	0.43
	1873.00	0.32	0.08	0.24
	1875.10	0.58	0.29	0.29
	1876.00	1.40	0.29	1.11
	1878.10	1.18	0.33	0.85
	1879.90	1.98	0.70	1.28

Well	Depth m	Total Carbon %	Inorganic Carbon %	Organic Carbon %
Sikanni Chief b-92-D/94-I-4	1954.10	0.50	0.18	0.32
	1955.00	1.06	0.76	0.30
	1956.10	0.64	0.28	0.36
	1957.00	0.72	0.36	0.36
	1957.90	0.52	0.26	0.26
	1959.10	0.68	0.43	0.25
	2103.40	0.40	0.16	0.24
	2104.00	0.57	0.34	0.23
	2104.90	0.69	0.54	0.15
	2105.80	0.47	0.18	0.29
	2107.10	0.48	0.17	0.31
	2108.00	0.55	0.20	0.35
	2216.20	1.17	0.44	0.73
	2217.20	0.41	0.12	0.29
	2218.10	0.52	0.26	0.26
	2218.70	0.39	0.30	0.09
	2219.00	0.39	0.14	0.25
	2219.90	1.03	0.79	0.24
	2221.10	0.39	0.17	0.22

Table 15. TOC data for Fort Simpson Formation shales.

Figure 32. Gamma ray and sonic log signatures and TOC data for Junior c-60-E/94-I-11 showing the core interval from 1857.10 – 1882.75 m. "C" indicates core intervals.

Thermal Maturity and Organic Matter Type

Select Fort Simpson shale samples were analyzed using Rock-Eval pyrolysis to determine both the thermal maturity and organic matter type. Table 16 shows the Rock-Eval data for twenty-three analyzed samples from four wells. The low S2 values measured in all of the samples suggest that the shales are very mature. As a result, the Tmax values are suspect and cannot be used reliably to determine an absolute maximum thermal exposure. All of the analyzed samples plot in the Type III organic matter range (Figure 33) however the low organic carbon content and the high level of the maturity of the samples makes kerogen typing using the Van Krevelan diagram suspect.

Depth	Tmax	S1	S2	S3	PI	S2/S3	PC(%)	TOC(%)	HI	OI
Sikahni Chief b-92-D										
1953.8	500	0.00	0.04	0.20	0.05	0.20	0.00	0.23	17	87
1957.5	504	0.01	0.05	0.13	0.10	0.38	0.00	0.22	23	59
2106.7	494	0.01	0.05	0.20	0.11	0.25	0.01	0.28	18	71
2216.6	504	0.00	0.02	0.16	0.12	0.13	0.00	0.19	11	84
2217.2	423	0.00	0.05	0.23	0.09	0.22	0.01	0.29	17	79
2221.7	474	0.00	0.01	0.16	0.12	0.06	0.00	0.20	5	80
Kotcho c-32-K										
1979.0	385	0.00	0.03	0.15	0.07	0.20	0.00	0.24	13	63
1979.2	371	0.00	0.01	0.07	0.21	0.14	0.00	0.21	5	33
1982.2	360	0.01	0.04	0.07	0.16	0.57	0.00	0.23	17	30
1982.2	344	0.03	0.05	0.15	0.38	0.33	0.01	1.65	3	9
1988.1	387	0.01	0.02	0.12	0.30	0.17	0.01	0.26	8	46
1988.8	426	0.00	0.03	0.42	0.11	0.07	0.01	0.13	23	323
Helmet b-49-G										
1810.9	575	0.01	0.05	0.11	0.12	0.45	0.01	0.77	6	14
1812.3	585	0.01	0.06	0.15	0.12	0.40	0.01	1.09	6	14
1813.6	588	0.01	0.06	0.13	0.13	0.46	0.01	1.32	5	10
1815.1	591	0.01	0.08	0.12	0.11	0.67	0.01	1.41	6	9
1816.5	594	0.01	0.05	0.16	0.14	0.31	0.00	1.32	4	12
1816.5	595	0.01	0.10	0.26	0.11	0.38	0.01	1.37	8	19
Junior c-60-E										
1857.7	432	0.00	0.06	0.27	0.02	0.22	0.01	0.24	25	113
1869.7	331	0.00	0.00	0.09	0.83	0.00	0.00	0.21	0	43
1873.9	344	0.01	0.02	0.09	0.35	0.22	0.01	0.22	9	41
1876.9	606	0.00	0.01	0.09	0.06	0.11	0.00	1.32	1	7
1879.0	593	0.01	0.02	0.09	0.27	0.22	0.00	1.25	2	7
1879.6	440	0.01	0.04	0.18	0.14	0.22	0.02	0.90	4	20
1880.3	606	0.02	0.12	0.25	0.10	0.48	0.02	2.46	5	10
1880.3	443	0.01	0.07	0.63	0.12	0.11	0.01	2.33	3	27

Table 16. Rock-Eval data for select Fort Simpson Formation shale samples.

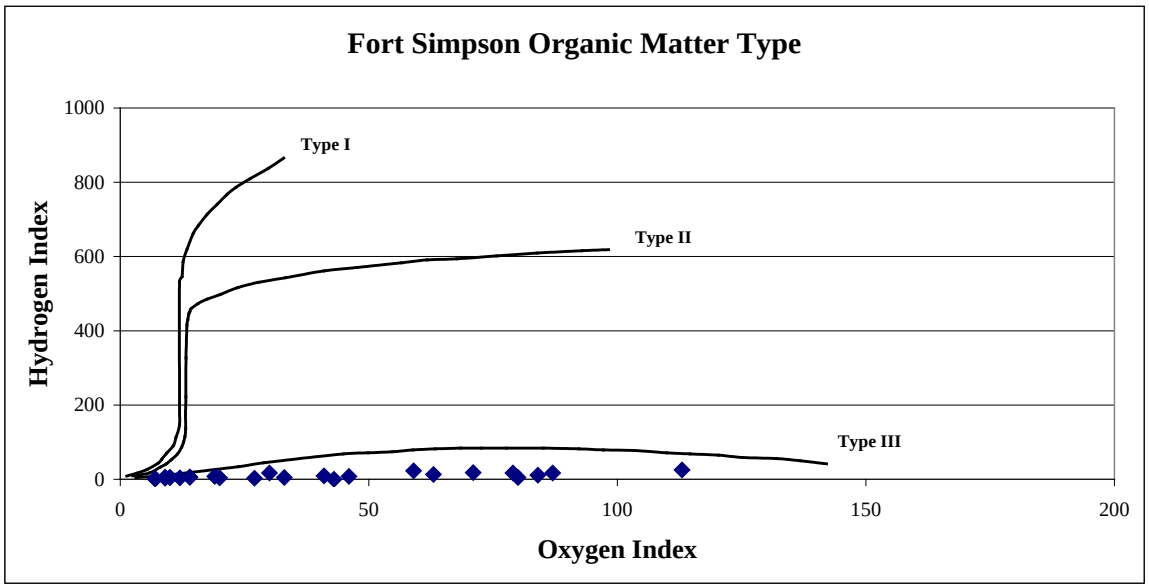

Figure 33. Van Krevelen diagram for the Fort Simpson Formation. The level of maturity is so high that it is not possible to type the kerogen based on the Van Krevelen plot.

Porosity

Seventeen shale samples from the Fort Simpson Formation were analyzed for total porosity (Table 17). The analyzes show that the range of porosity is from 1.5 to 9.7% with an average value of 3.3%. Assuming the formation is saturated, the pore space in the shale provides additional gas storage capacity which may significantly increase the potential gas in place. The effect of porosity on gas capacity in place is shown in the following section.

Sample	Depth (m)	Formation	Hg Bulk Density (cc/g)	He Skeletal Density (cc/g)	Std Dev.	Porosity	
						Fraction	Percent
Sikanni Chief b-92-D/94-I-4	1953.8	Ft Simpson	2.60	2.74	0.002	0.049	4.92
Sikanni Chief b-92-D/94-I-4	1957.5	Ft Simpson	2.64	2.71	2.720	0.026	2.58
Sikanni Chief b-92-D/94-I-4	2106.7	Ft Simpson	2.61	2.89	0.007	0.097	9.73
Sikanni Chief b-92-D/94-I-4	2216.6	Ft Simpson	2.64	2.70	0.003	0.022	2.18
Sikanni Chief b-92-D/94-I-4	2219.6	Ft Simpson	2.65	2.73	0.003	0.030	2.96
Sikanni Chief b-92-D/94-I-4	2221.7	Ft Simpson	2.63	2.71	0.012	0.032	3.16
Junior c-60-E/94-I-11	1858.3	Ft Simpson	2.67	2.75	0.005	0.031	3.14
Junior c-60-E/94-I-11	1861.3	Ft Simpson	2.67	2.73	0.006	0.020	2.03
Junior c-60-E/94-I-11	1864.3	Ft Simpson	2.67	2.77	0.014	0.033	3.34
Junior c-60-E/94-I-11	1867.6	Ft Simpson	2.64	2.77	0.012	0.049	4.85
Junior c-60-E/94-I-11	1869.7	Ft Simpson	2.66	2.74	0.010	0.031	3.15
Junior c-60-E/94-I-11	1873.9	Ft Simpson	2.73	2.77	0.009	0.016	1.56
Junior c-60-E/94-I-11	1876.3	Ft Simpson	2.66	2.72	0.008	0.022	2.24
Junior c-60-E/94-I-11	1876.9	Ft Simpson	2.60	2.67	0.002	0.024	2.45
Junior c-60-E/94-I-11	1878.1	Ft Simpson	2.66	2.74	0.021	0.028	2.84
Junior c-60-E/94-I-11	1879.0	Ft Simpson	2.63	2.70	0.008	0.025	2.49
Junior c-60-E/94-I-11	1879.6	Ft Simpson	2.62	2.70	0.008	0.031	3.11

Table 17. Porosity data for select Fort Simpson shale samples.

Sorption Capacity

Sorption capacity for the Fort Simpson Formation was measured on nine samples. Based on drilling depths, intersections of the Fort Simpson Formation range from approximately 1200 m in the northern portion of the study area to approximately 3000 m in the southern portion of the study area (Peace River Arch block). Using the drill depth range of 1200 to 3000 m, the calculated reservoir pressures range from 13300 to 33200 kPa (1900 to 4800 psi). For all of the samples collected in the Fort Simpson Formation, the average TOC value is 0.4%. Because of the low organic content, the sorbed gas capacity of the Fort Simpson Formation is low.

All adsorption data (gas capacity data) is presented at reservoir pressure and a standard pressure of 11 MPa (1600 psi). The standard pressure allows for direct comparison of all the samples analyzed. The range of TOC contents measured within the Fort Simpson Formation is from 0.1 to 1.3%. The low end member for TOC is characterized at a depth of 2216.6 m (TOC = 0.20%) in the Sikanni Chief b-92-D/94-I-4 well. At the reservoir pressure of 21.6 MPa (3100 psi), the gas capacity (not accounting for porosity) is 0.31 cc/g (9.9 scf/ton). At a standard pressure of 11 MPa, the gas capacity is 0.24 cc/g (7.7 scf/ton; Figure 34). The high end member for TOC is characterized at a depth of 1876.9

m (TOC = 1.32%) in the Junior c-60-E/94-I-11 well. At the reservoir pressure of 18.3 MPa (1650 psi), the gas capacity (not accounting for porosity) is 0.67 cc/g (21.5 scf/ton). At a standard pressure of 11 MPa, the gas capacity is 0.53 cc/g (17 scf/ton) (Figure 35). Table 18 provides the gas capacity data for each Fort Simpson Formation sample at both reservoir pressure and a standard pressure of 11 MPa.

Because there is significant porosity in the Fort Simpson Formation samples, the gas capacity increases considerably if free gas capacity is factored in. In figure 36, the gas capacities have been calculated to show the effect of porosity on gas capacity. End members of 2% and 5% porosity have been used to calculate the gas capacity in a 0.90% TOC sample. At 11 MPa pressure, the gas capacity with 2% porosity is 1.35 cc/g (43.2 scf/ton) which is a 214% increase of the sorbed gas capacity of 0.43 cc/g (13.8 scf/ton). With 5% porosity, the gas capacity is 2.87 cc/g (91.9 scf/ton) which is a 567% increase over the sorbed gas capacity.

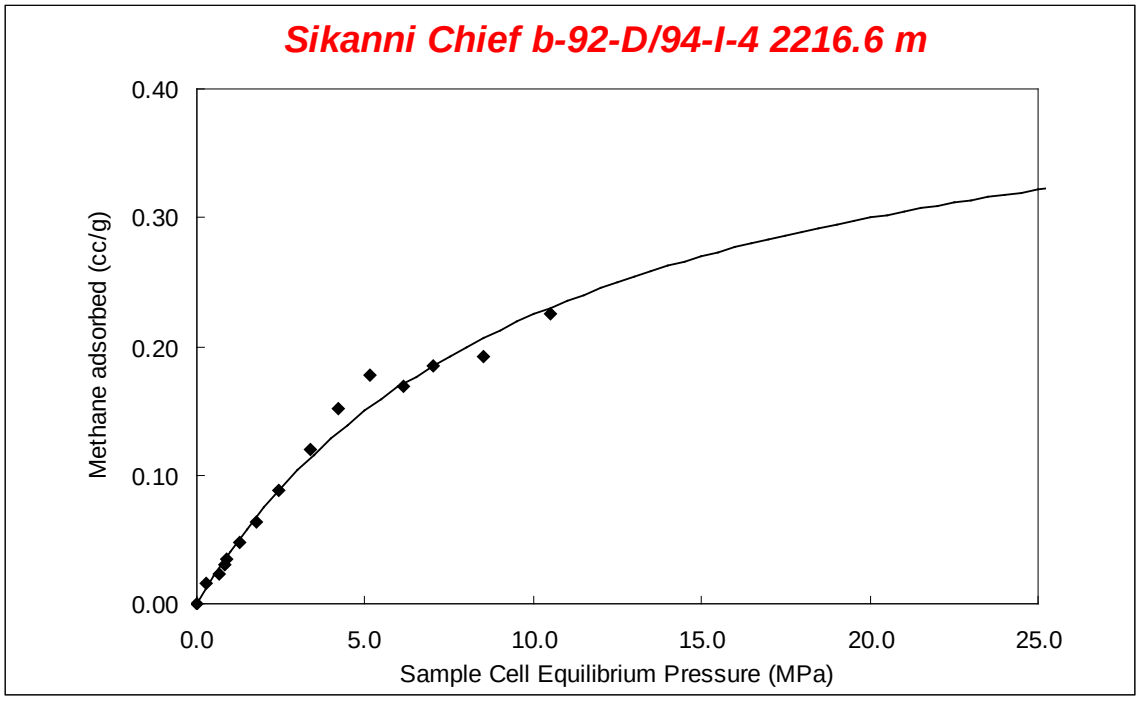

Figure 34. Adsorption isotherm for a shale sample from the Fort Simpson Formation. Sample has a TOC content of 0.2%. Gas capacity for pressures greater than 10 MPa is extrapolated using the Langmuir equation. The poor data quality is a product of the low sorption capacity.

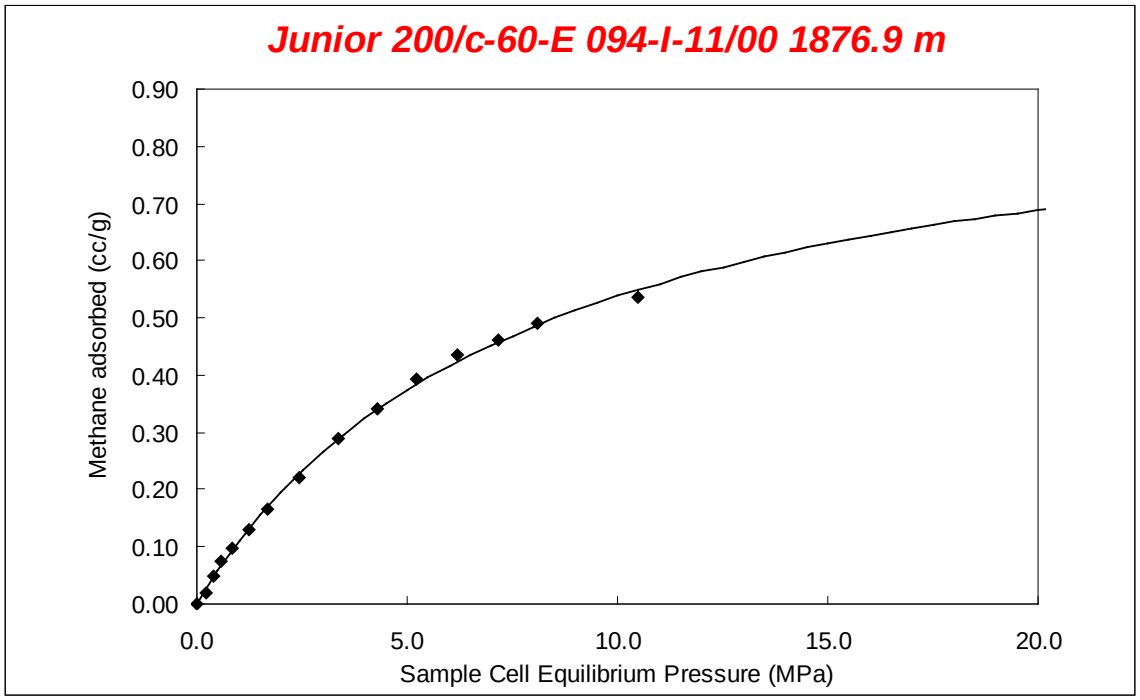

Figure 35. Adsorption isotherm for a shale sample from the Fort Simpson Formation. Sample has a TOC content of 1.32%. Gas capacity for pressures greater than 10 MPa is extrapolated using the Langmuir equation.

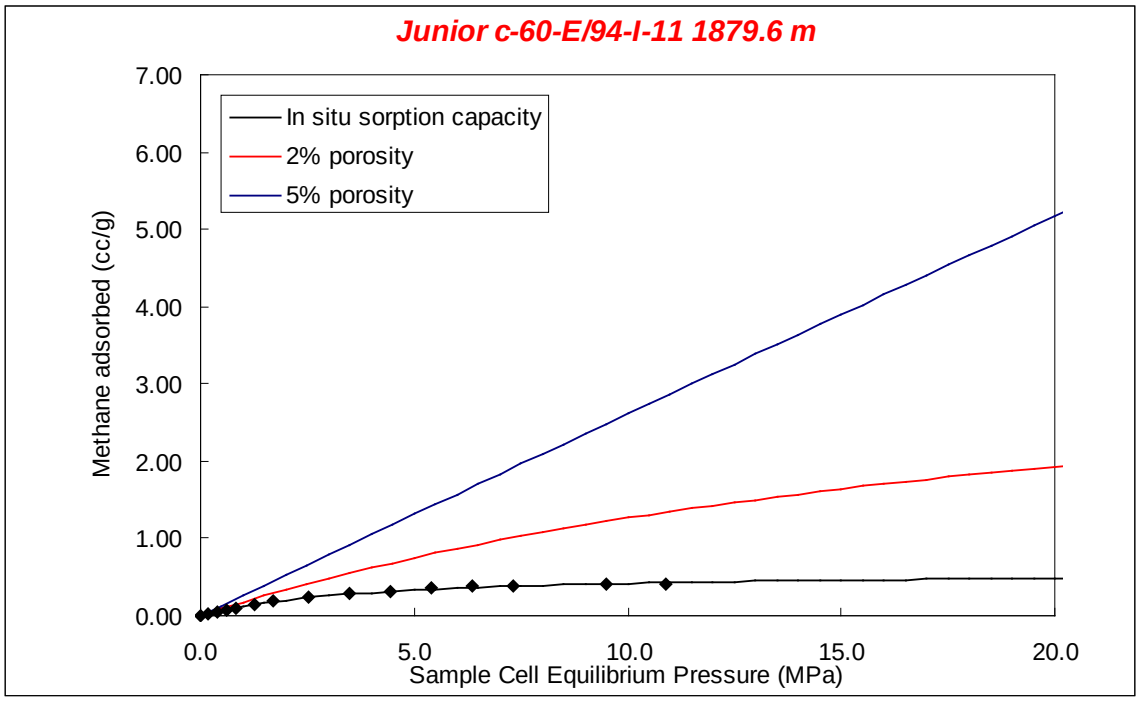

Figure 36. Sorbed plus free gas capacity in a 0.9% TOC sample.

Well Name	Location	Depth (m)	Reservoir Pressure (psi)	Reservoir Pressure (kPa)	Gas Capacity (cc/g)	Gas Capacity @ 11 Mpa (cc/g)	TOC
Fort Simpson							
Junior	c-60-E/94-I-11	1869.70	2638	18186	0.32	0.32	0.21
		1873.90	2644	18227	0.46	0.46	0.22
		1876.90	2648	18256	0.67	0.53	1.32
		1879.00	2651	18277	0.38	0.35	1.25
		1879.60	2652	18283	0.48	0.43	0.90
Sikanni Chief	b-92-D/94-I-4	1953.80	2756	19004	0.44	0.44	0.23
		1957.50	2762	19040	0.39	0.39	0.22
		2106.70	2972	20492	0.26	0.24	0.28
		2216.60	3127	21561	0.31	0.24	0.19

Table 18. Variation in sorption capacity with total organic carbon content for Fort Simpson Formation shale samples. Capacities are given at reservoir pressure and a standard pressure of 11 MPa.

Clay Mineralogy

X-ray diffraction analyzes was completed on 5 samples from the Fort Simpson Formation in order to determine the mineralogy of the shale samples. Table 19 shows a summary of the x-ray diffraction data. The x-ray diffraction traces for each sample are provided in Appendix B. The analyzed Fort Simpson Formation samples (Junior c-60-E/94-I-11 and Sikanni Chief b-92-D/94-I-4) are comprised mainly of quartz, kaolinite and illite with one sample (1879.6 m Sikanni Chief) having minor pyrite and dolomite. Four of the analyzed samples have degraded illite in the range of 9% to 16%. Degraded illite is water sensitive and may be affected (swell) by water based fluids during drilling and completion.

Ft. Simpson			Mineralogy (% Relative)					
Name	Location	Depth (m)	Illite/Mica (d=10.00)	Kaolinite (d=7.10)	Quartz (d=4.23)	Calcite (d=3.03)	Pyrite (d=2.71)	Dolomite (d=2.89)
Junior	c-60-E/94-I-11	1858.30	16	23	56	0	0	0
		1879.60	9	2	75	0	2	12
Sikanni Chief	b-92-D/94-I-4	1957.50	14	23	58	0	0	0
		2106.70	15	25	53	0	0	0
		2216.60	11	16	34	0	0	0

Table 19. Relative mineralogy percentages determined from XRD analyzes. "d" refers to the d-spacing of the principal plane of each mineral that was used to (semi-) quantify the relative abundances. Shaded regions show degraded illite which has a range of d spacings.

Gas Capacity in Place

Because gas capacities are highly variable due to changing organic contents, reservoir pressures, formation thickness and porosity, gas in place numbers can be calculated based on a range of reservoir properties. Tables 20 and 21 provide gas capacity in place numbers for varying TOC contents, reservoir pressures, porosities and thickness. The gas capacity in place values are calculated using an average density of 2.65 cc/g which is measured using mercury immersion.

Porosity (%)	TOC (%)	Shale Thickness (m)	Pressure (MPa)	Resources (cc/cm2)	Resources (bcf/section)	Average Gas Content (scf/ton)	Average Gas Content (cc/g)	Density (g/cc)
0.0	0.2	200.0	11.0	12720	**12**	8	0.2	2.65
0.0	0.2	500.0	11.0	31800	**29**	8	0.2	2.65
0.0	0.2	900.0	11.0	57240	**52**	8	0.2	2.65
2.0	0.2	200.0	11.0	63070	**58**	38	1.2	2.65
2.0	0.2	500.0	11.0	157675	**144**	38	1.2	2.65
2.0	0.2	900.0	11.0	283815	**260**	38	1.2	2.65
5.0	0.2	200.0	11.0	142040	**130**	86	2.7	2.65
5.0	0.2	500.0	11.0	355100	**325**	86	2.7	2.65
5.0	0.2	900.0	11.0	639180	**585**	86	2.7	2.65
0.0	0.9	200.0	11.0	22790	**21**	14	0.4	2.65
0.0	0.9	500.0	11.0	56975	**52**	14	0.4	2.65
0.0	0.9	900.0	11.0	102555	**94**	14	0.4	2.65
2.0	0.9	200.0	11.0	71550	**65**	43	1.4	2.65
2.0	0.9	500.0	11.0	178875	**164**	43	1.4	2.65
2.0	0.9	900.0	11.0	321975	**294**	43	1.4	2.65
5.0	0.9	200.0	11.0	152110	**139**	92	2.9	2.65
5.0	0.9	500.0	11.0	380275	**348**	92	2.9	2.65
5.0	0.9	900.0	11.0	684495	**626**	92	2.9	2.65
0.0	1.3	200.0	11.0	29680	**27**	18	0.6	2.65
0.0	1.3	500.0	11.0	74200	**68**	18	0.6	2.65
0.0	1.3	900.0	11.0	133560	**122**	18	0.6	2.65
2.0	1.3	200.0	11.0	84270	**77**	51	1.6	2.65
2.0	1.3	500.0	11.0	210675	**193**	51	1.6	2.65
2.0	1.3	900.0	11.0	379215	**347**	51	1.6	2.65
5.0	1.3	200.0	11.0	181260	**166**	110	3.4	2.65
5.0	1.3	500.0	11.0	453150	**414**	110	3.4	2.65
5.0	1.3	900.0	11.0	815670	**746**	110	3.4	2.65

Table 20. Variations of gas capacity in place based on varying thickness, porosity and TOC content. Values are calculated at a standard pressure of 11 MPa.

Porosity (%)	TOC (%)	Shale Thickness (m)	Pressure (MPa)	Resources (cc/cm2)	Resources (bcf/section)	Average Gas Content (scf/ton)	Average Gas Content (cc/g)	Density (g/cc)
0.0	0.2	200.0	19.0	15370	**14**	9	0.3	2.65
0.0	0.2	500.0	19.0	38425	**35**	9	0.3	2.65
0.0	0.2	900.0	19.0	69165	**63**	9	0.3	2.65
2.0	0.2	200.0	19.0	111300	**102**	67	2.1	2.65
2.0	0.2	500.0	19.0	278250	**254**	67	2.1	2.65
2.0	0.2	900.0	19.0	500850	**458**	67	2.1	2.65
5.0	0.2	200.0	19.0	280900	**257**	170	5.3	2.65
5.0	0.2	500.0	19.0	702250	**642**	170	5.3	2.65
5.0	0.2	900.0	19.0	1264050	**1156**	170	5.3	2.65
0.0	0.9	200.0	19.0	25440	**23**	15	0.5	2.65
0.0	0.9	500.0	19.0	63600	**58**	15	0.5	2.65
0.0	0.9	900.0	19.0	114480	**105**	15	0.5	2.65
2.0	0.9	200.0	19.0	99640	**91**	60	1.9	2.65
2.0	0.9	500.0	19.0	249100	**228**	60	1.9	2.65
2.0	0.9	900.0	19.0	448380	**410**	60	1.9	2.65
5.0	0.9	200.0	19.0	260760	**238**	158	4.9	2.65
5.0	0.9	500.0	19.0	651900	**596**	158	4.9	2.65
5.0	0.9	900.0	19.0	1173420	**1073**	158	4.9	2.65
0.0	1.3	200.0	19.0	36040	**33**	22	0.7	2.65
0.0	1.3	500.0	19.0	90100	**82**	22	0.7	2.65
0.0	1.3	900.0	19.0	162180	**148**	22	0.7	2.65
2.0	1.3	200.0	19.0	133560	**122**	81	2.5	2.65
2.0	1.3	500.0	19.0	333900	**305**	81	2.5	2.65
2.0	1.3	900.0	19.0	601020	**550**	81	2.5	2.65
5.0	1.3	200.0	19.0	404920	**370**	245	7.6	2.65
5.0	1.3	500.0	19.0	1012300	**926**	245	7.6	2.65
5.0	1.3	900.0	19.0	1822140	**1667**	245	7.6	2.65

Table 21. Variations of gas capacity in place based on varying thickness, porosity and TOC content. Values are calculated at an average reservoir pressure of 19 MPa.

Conclusions

The Fort Simpson Formation is a thick marine shale unit that is pervasive throughout the study area. Maximum thickness reaches approximately 800 m in the northwest portion of the study area. The overall organic content of the Fort Simpson Formation is extremely low, averaging 0.4%, resulting in low sorbed gas capacities. However, due to large vertical thickness and lateral extent as well as high shale porosities (potential free gas porosity), the Fort Simpson shale section has potential for extensive gas in place.

Flow pathways within the Fort Simpson are limited to thin siltstone interbeds. No fracturing is evident in the examined cores within the study area.

Muskwa Formation

Lithology and Stratigraphy

The Muskwa Formation is a dark gray to black, organic shale interval which is variably calcareous and pyritic. Originally, the radioactive shales of the Muskwa were assigned as a member of the upper Horn River Formation (Gray and Kassube, 1963). Griffin, in 1965, suggested the stratigraphic differentiation of the Muskwa into a separate formation. The Muskwa Formation was deposited on the continental shelf during a period of rapid sea level rise (Torrie, 1973; Savoy and Mountjoy, 1995). Low sedimentation rates and increased subsidence resulted in a starved, anoxic basin creating favourable conditions for preserving the organic rich sediments of the Muskwa Formation (Morrow and Geldsetzer, 1988). To the north of the Peace River Arch the Muskwa Formations depositionally very basinal and is generally isolated from possible reservoirs (i.e., time-synchronous reefs or underlying platforms). This results in very minor oil reserves attributable to this source north of the Peace River Arch.

Within the study area, the Muskwa Formation overlies the Slave Point Formation with an erosional contact (Griffin, 1967). In localized regions of the western portion of the study area, the Muskwa Formation overlies the Otter Park Formation. The Muskwa Formation is conformably overlain by the Fort Simpson Formation. On geophysical logs, the Muskwa Formation has a characteristically high gamma ray response which decreases as the organic rich shales grade into organic poor gray shales of the overlying Fort Simpson Formation (Figure 37). In Alberta, interbedded limestones and organic rich shales of the Duvernay Formation, part of the Woodbend Group (Upper Devonian) are laterally equivalent to the Muskwa Formation.

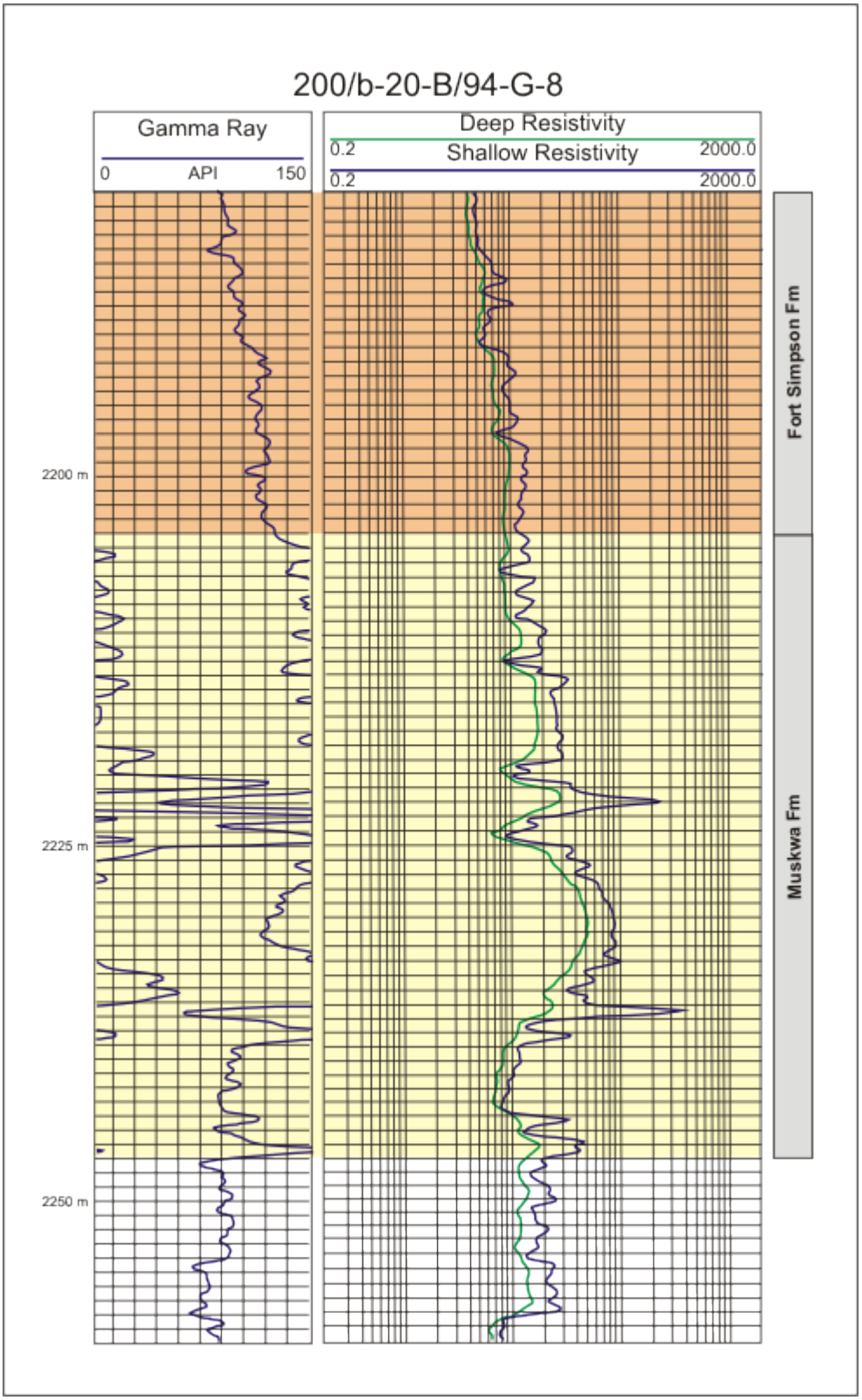

Figure 37. Typical log signature of the Muskwa Formation.

Lateral Extent and Thickness

Within the study area, the Muskwa reaches thicknesses of up to 60 m and extends throughout northeastern British Columbia (north of the Peace River Arch), northwestern Alberta and the Northwest Territories (Figures 38). The thickest accumulations occur in the northwest and thin towards the southeast in the township and range block of the Peace River Arch (Figure 41).

Structurally, the Muskwa Formation dips from north to south (Figure 42). The deepest intersections of the Fort Simpson Formation occur in the Peace River Arch block and reach depths of 3000 m. The shallowest intersections recorded in the study area are at depths of approximately 200 m and occur primarily in the northeast.

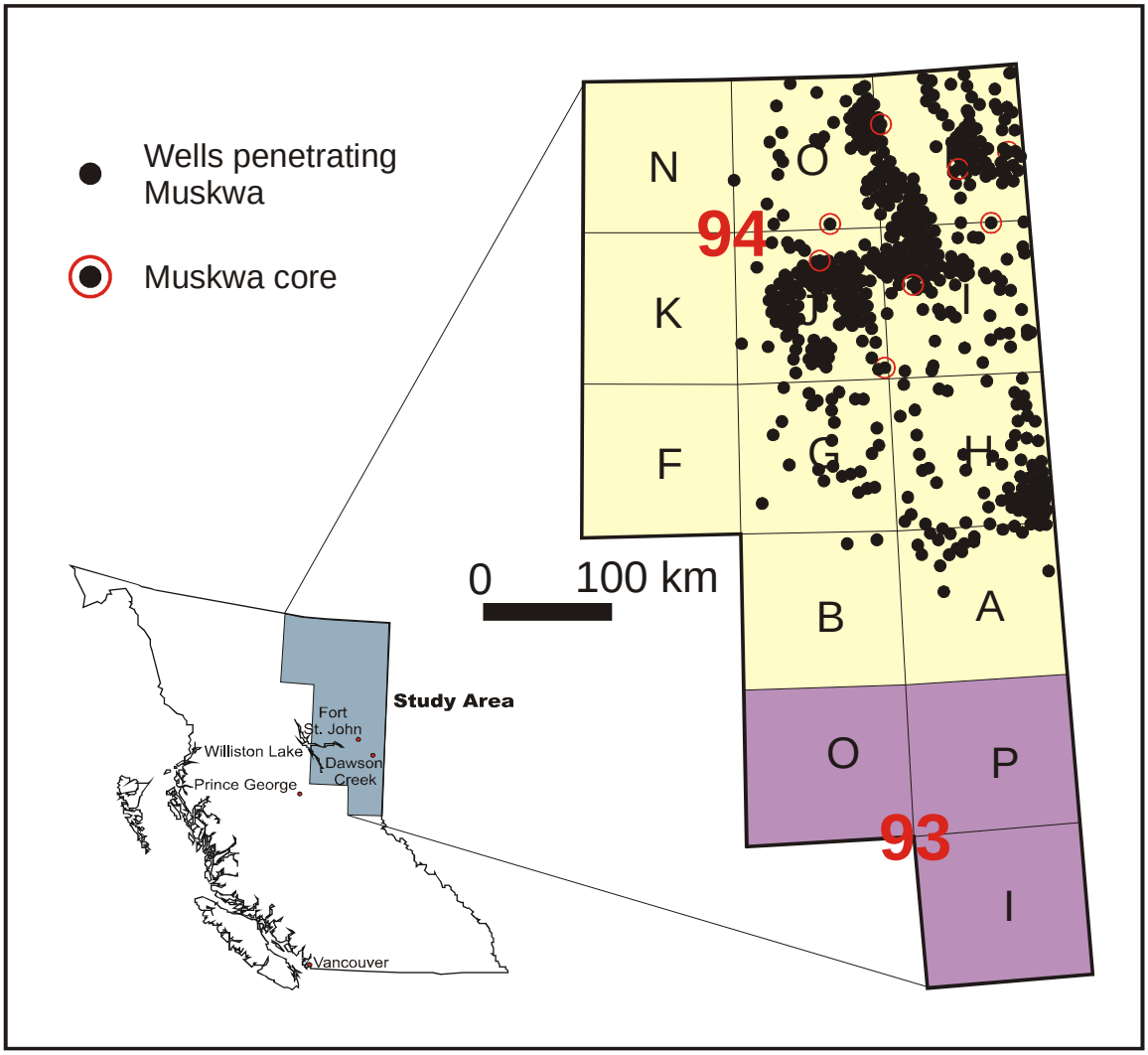

Figure 38. Distribution of wells penetrating the Muskwa Formation. Red circles indicate wells with core.

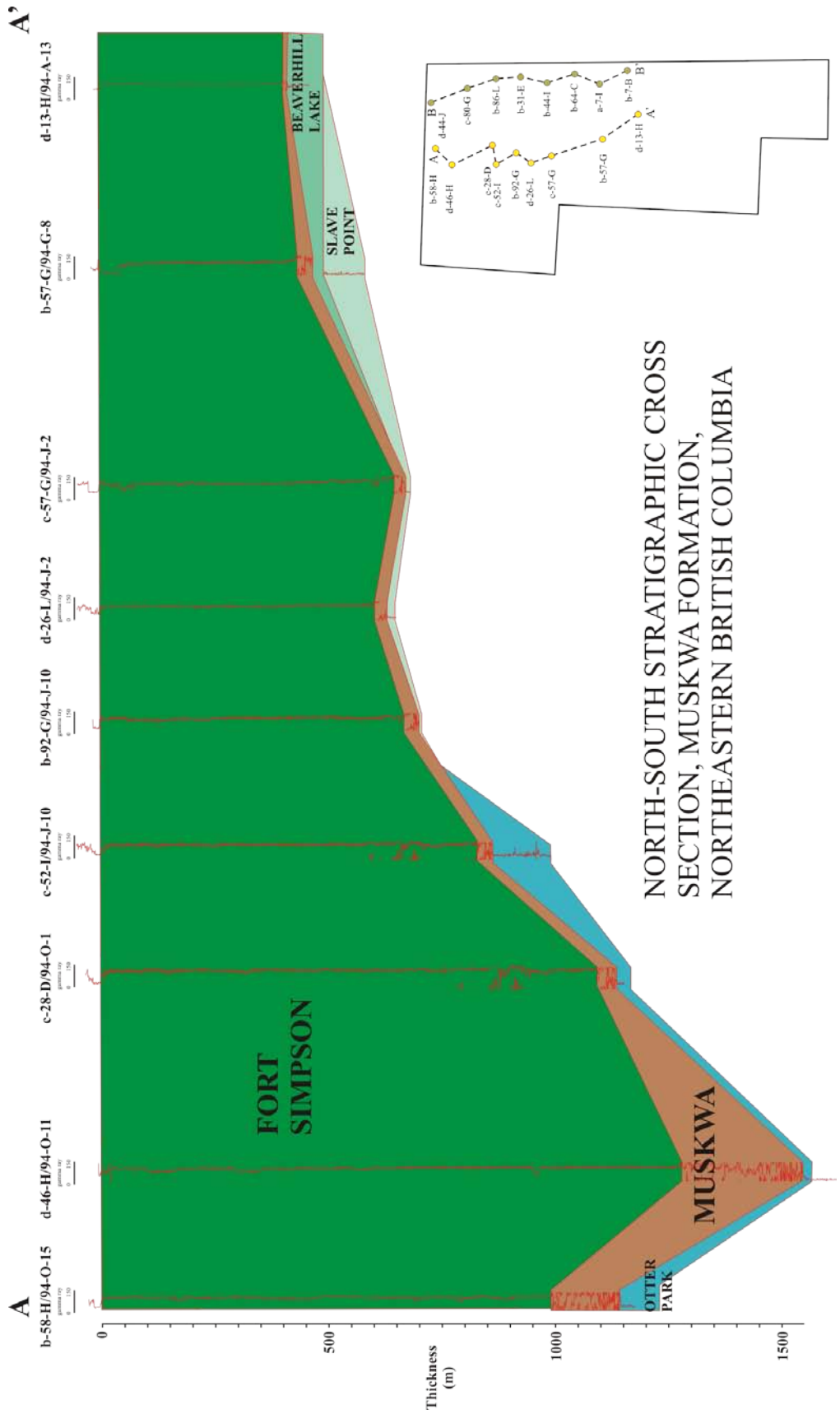

Figure 39. North to south stratigraphic cross section of the Muskwa Formation in the western portion of the study area (A – A').

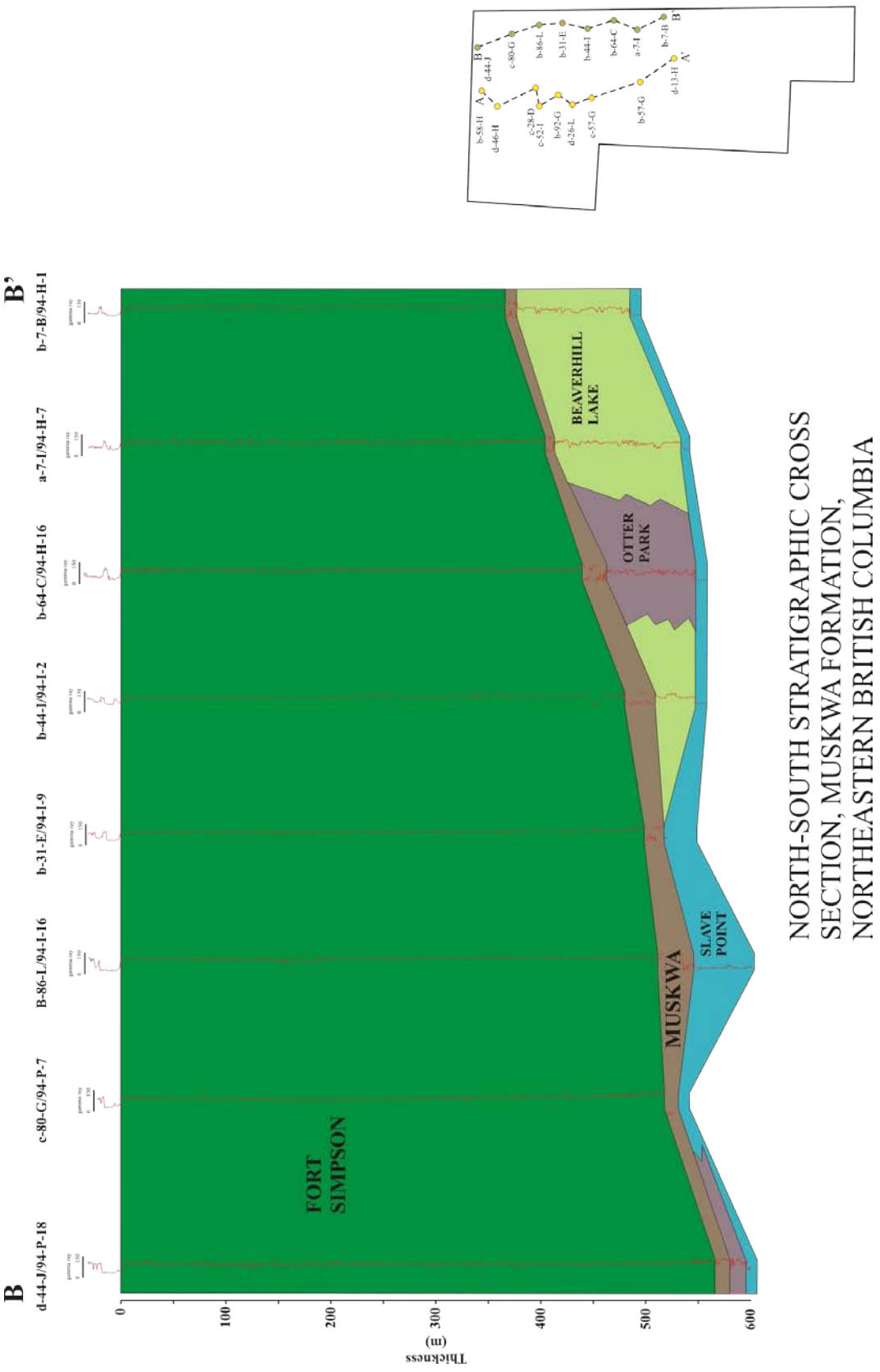

Figure 40. North to south stratigraphic cross section of the Muskwa Formation in the eastern portion of the study area (B – B').

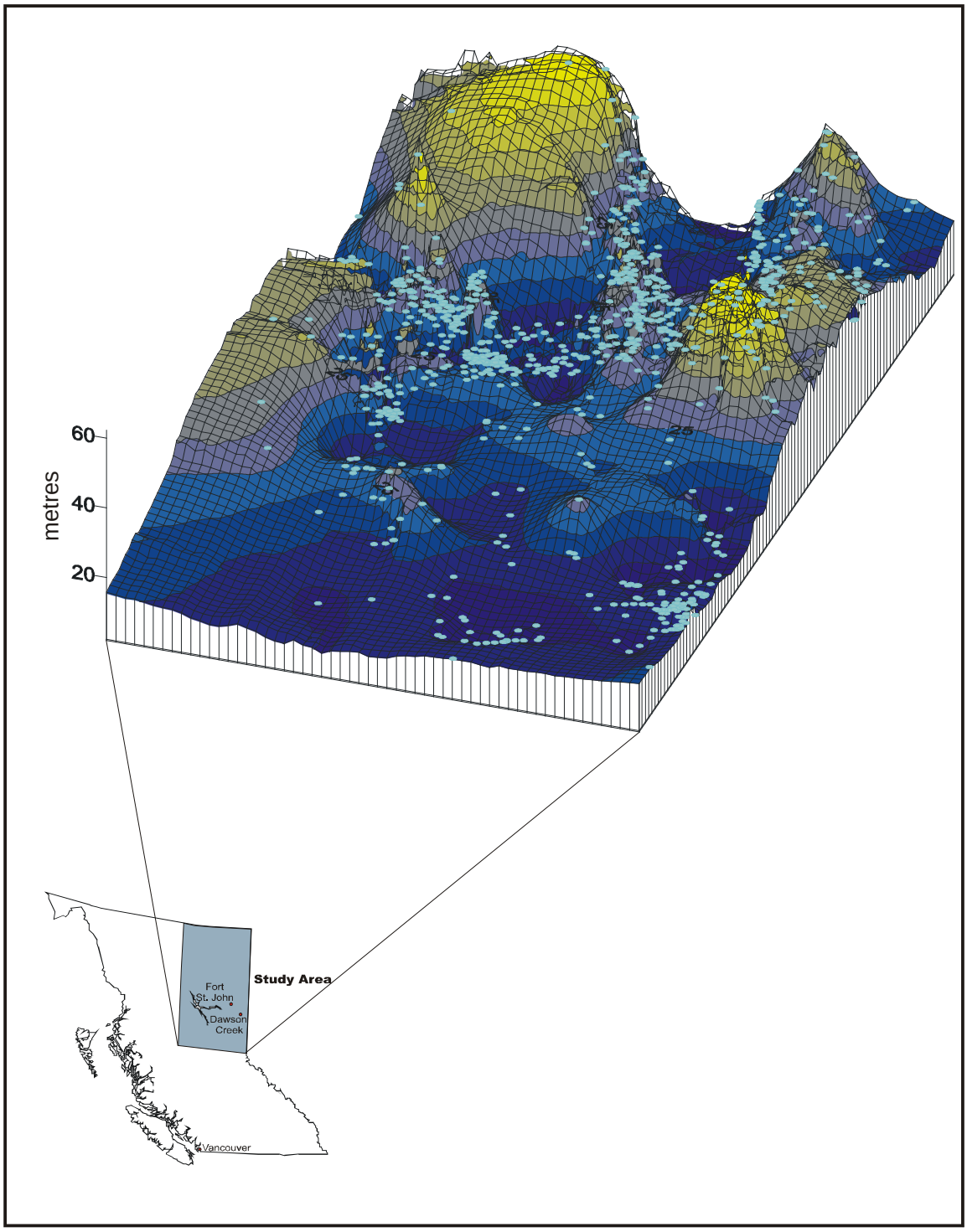

Figure 41. Isopach map of the Muskwa Formation shows a thickening trend from east to west.

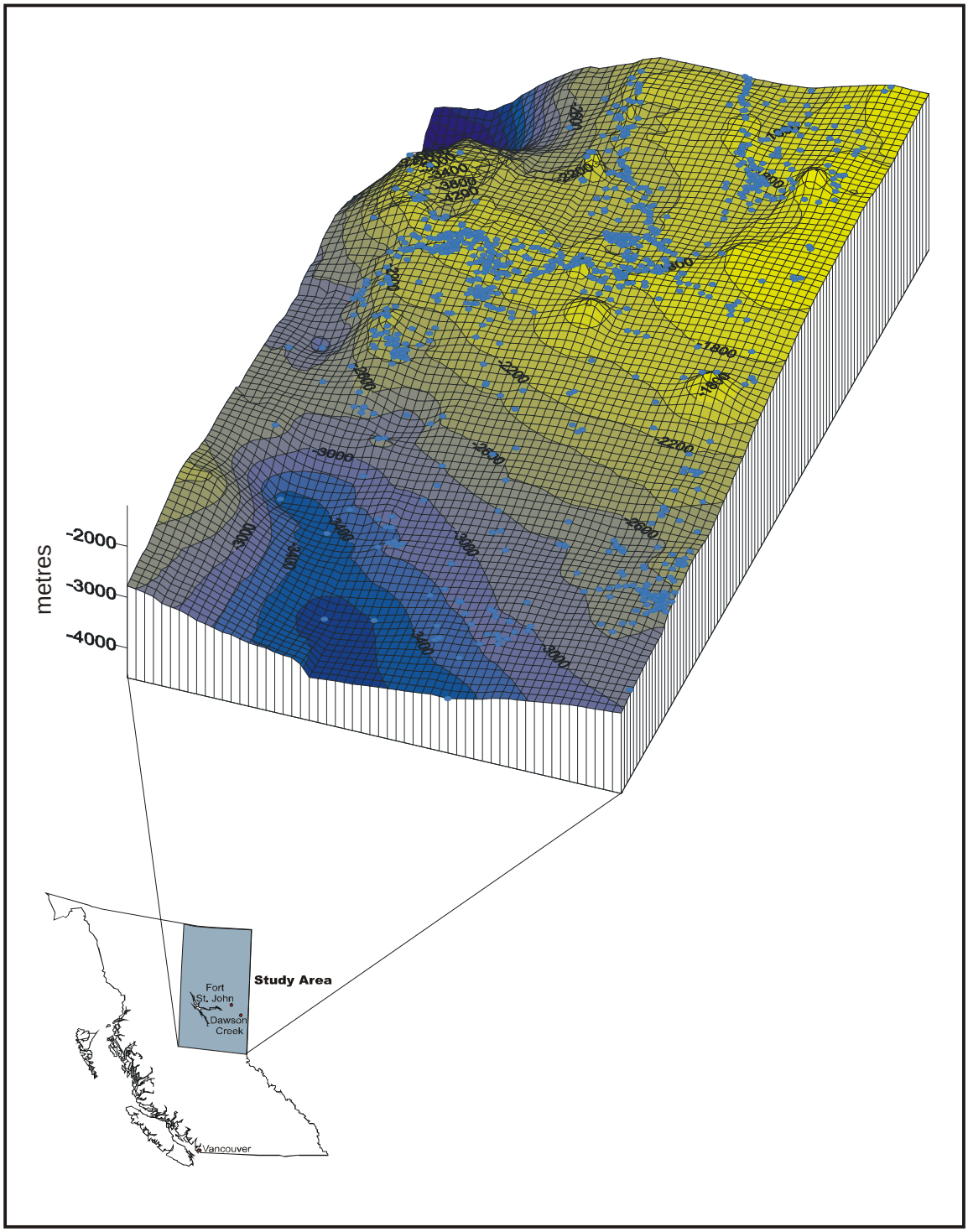

Figure 42. Upper surface of the Muskwa Formation showing the drill depths from surface.

Total Organic Carbon

The Muskwa Formation is typically organic rich, with an average total organic carbon content of 3.1% (Table 22). The transitional strata from the underlying Otter Park and Slave Point formations to the Muskwa Formation generally show very low TOC contents (<1%).

Samples from two wells, Helmet b-49-G/94-P-7 and Kotcho c-32-K/94-I-14, were collected to measure the TOC content within the transition from the Muskwa Formation into the Fort Simpson Formation. The samples collected within the transition zone are grey shales with low organic content. The Helmet b-49-G sample measured 1.1% TOC and the Kotcho c-32-K measured 0.7%.

Samples from Shekilie a-94-G/94-P-8 and Snake River c-28-D/94-O-1 were collected within the Muskwa Formation. The samples collected within the Muskwa are visibly dark grey to black which is reflected in the high TOC contents measured. The average TOC for the Shekilie a-94-G/94-P-8 core (1539.40 – 1554.48 m) is 2.7%. The TOC correlates well with gamma ray intensities (Figure 43). The one Muskwa sample collected from the Snake River c-28-D/94-O-1 core 1 (1949.20 – 1953.16 m) is 6.0% TOC.

Within the transition zones from the underlying Slave Point and Otter Park formations, the TOC values are low. Samples collected in Fort Nelson c-70-I/94-J-10 (1966.26 – 1969.31 m) represent the basal Muskwa/Slave Point and have an average TOC content of 0.2%. Samples collected in Dilly a-88-F/94-P-12 (2168.00 – 2179.20 m) represent the basal Muskwa/Slave Point and have an average TOC content of <0.1 wt%. The sample analyzed in Walrus b-86-L/94-I-16 (1761.44 – 1764.18 m) sample contains 0.16% TOC and is from the top of the Slave Point Formation. Kotcho c-98-G/94-I-14 (1999.40 – 2000.70 m) is from the Otter Park Formation, underlying the Muskwa (in the NW quadrant of the study area). TOC contents in the Kotcho well average 0.4% (Table 23).

Well	Depth m	Total Carbon %	Inorganic Carbon %	Organic Carbon %
Shekilie a-94-G/94-P-8	1539.24	2.39	0.23	2.16
	1539.30	3.67	0.30	3.37
	1539.60	2.67	0.26	2.41
	1539.90	3.36	0.52	2.84
	1540.20	2.93	0.24	2.69
	1540.50	3.40	0.53	2.87
	1540.80	3.21	0.56	2.65
	1541.10	1.25	0.07	1.18
	1541.40	2.99	0.41	2.58
	1541.70	3.61	0.78	2.83
	1542.00	2.63	0.46	2.17
	1542.30	2.54	0.43	2.11
	1542.60	3.40	1.18	2.22
	1542.90	3.11	0.39	2.72
	1543.20	2.28	0.24	2.04
	1543.50	2.77	0.47	2.30
	1543.70	0.89	0.17	0.72
	1543.80	3.35	0.36	2.99
	1544.10	4.55	1.63	2.92
	1544.40	5.44	3.70	1.74
	1544.70	5.53	1.09	4.44
	1545.00	5.32	1.64	3.68
	1545.30	2.44	0.22	2.22
	1545.60	2.52	0.20	2.32
	1545.90	6.10	5.68	0.42
	1546.20	3.58	0.85	2.73
	1546.50	5.38	0.31	5.07
	1546.80	5.55	1.73	3.82
	1547.10	4.65	0.47	4.18
	1547.40	7.73	5.38	2.35
	1547.70	4.98	0.15	4.83
	1548.00	5.72	0.11	5.61
	1548.30	6.26	0.34	5.92
	1548.60	3.43	0.41	3.02
	1548.90	4.00	0.29	3.71
	1549.20	4.33	0.16	4.17
	1549.50	4.30	0.20	4.10
	1549.80	4.97	0.15	4.82

Well	Depth m	Total Carbon %	Inorganic Carbon %	Organic Carbon %
Shekilie a-94-G/94-P-8	1550.10	3.77	0.20	3.57
	1550.40	4.25	0.17	4.08
	1550.70	5.03	0.18	4.85
	1551.00	4.29	0.50	3.79
	1551.30	4.45	0.06	4.39
	1551.60	5.59	0.35	5.24
	1551.90	7.29	5.42	1.87
	1552.20	3.92	0.29	3.63
	1552.50	6.31	4.36	1.95
	1552.80	9.04	8.62	0.42
	1553.10	10.05	9.74	0.31
	1553.40	10.30	10.35	0.01
	1553.70	10.15	10.05	0.10
	1554.00	10.05	10.05	0.01
	1554.30	9.36	9.30	0.06
	1554.90	9.92	10.00	0.01
	1555.50	3.92	2.81	1.11
	1555.80	10.10	9.96	0.14
Dilly a-88-F/94-P-12	2168.00	11.70	11.70	<0.05
	2168.90	11.30	11.35	<0.05
	2170.10	11.35	11.30	0.05
	2171.00	11.45	11.40	0.05
	2171.90	10.10	10.15	<0.05
	2173.10	10.55	10.60	<0.05
	2174.00	0.15	0.05	0.10
	2175.00	11.55	11.30	0.25
Snake River c-28-D/94-O-1	1950.40	6.11	0.14	5.97
Junior c-60E/94-I-11	1879.30	1.49	0.19	1.30
Kotcho c-32-K/94-I-14	1980.50	0.84	0.77	0.07
Walrus b-86-L/94-I-16	1762.60	1.56	1.40	0.16
Fort Nelson c-70-I/94-J-10	1966.30	1.79	1.50	0.29
	1966.60	6.01	5.56	0.45
	1967.50	1.76	1.54	0.22
	1968.10	1.97	1.71	0.26
	1968.40	1.90	1.63	0.27
	1969.00	1.80	1.38	0.42
Helmet b-49-G/94-P-7	1814.10	2.19	1.06	1.13

Table 22. TOC data for Muskwa Formation shales.

Well	Depth m	Total Carbon %	Inorganic Carbon %	Organic Carbon %
Kotcho c-98-G/94-I-14	2000.00	2.61	2.29	0.32
	2000.90	3.07	2.81	0.26
	2002.10	3.31	3.15	0.16
	2003.00	2.85	2.27	0.58
	2003.90	3.16	2.67	0.49
	2005.10	2.99	2.72	0.27
	2006.00	3.19	2.91	0.28
	2006.90	3.94	3.39	0.55

Table 23. TOC values for the Otter Park Formation in Kotcho, c-98-G/94-I-14.

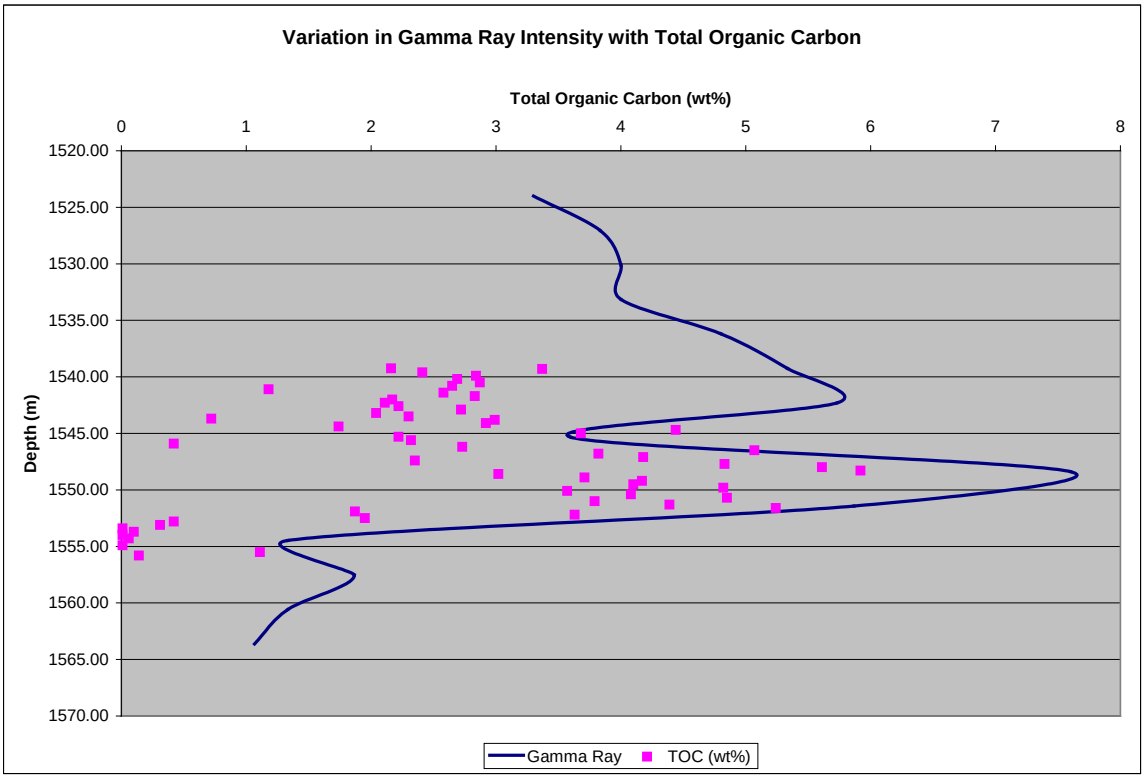

Figure 43. Variation in gamma ray intensity with total organic carbon from Shekilie a-94-G/94-P-8.

Thermal Maturity and Organic Matter Type

Select Muskwa Formation shale samples were analyzed using Rock-Eval pyrolysis to determine both the thermal maturity and organic matter type. Table 24 shows the Rock-

Eval data for twenty analyzed samples from seven wells. The low S2 values measured in all of the samples suggest that the shales are very mature. As a result, the Tmax values are suspect and cannot be used reliably to determine an absolute maximum thermal exposure. Samples from Nelson c-70-I, Dilly a-88-F and Walrus b-86-L were collected within the transitions zone from the Otter Park and Slave Point formations into the Muskwa Formation. The hydrogen and oxygen indices are slightly higher for samples collected in the transition zone. All of the analyzed samples plot in the Type III organic matter range (Figure 44) reflecting the high level of maturity rather than kerogen type.

Depth	Tmax	S1	S2	S3	PI	S2/S3	PC(%)	TOC(%)	HI	OI
Shekilie a-94-G										
1539.6	585	0.02	0.14	0.18	0.14	0.78	0.02	2.31	6	8
1542.0	587	0.05	0.11	0.11	0.30	1.00	0.02	2.63	5	4
1544.1	589	0.04	0.19	0.23	0.17	0.83	0.02	2.75	8	8
1545.6	336	0.07	0.13	0.18	0.34	0.72	0.02	2.23	6	8
1551.6	589	0.05	0.15	0.18	0.21	0.83	0.02	3.88	4	5
Snake River c-28-D										
1951.0	290	0.21	0.01	0.65	0.94	0.02	0.02	3.32	0	20
1951.8	307	0.05	0.05	0.33	0.52	0.15	0.02	1.70	3	19
1952.6	415	0.03	0.01	0.32	0.72	0.03	0.00	1.22	1	26
1990.1	606	0.07	0.04	0.27	0.58	0.15	0.02	4.74	1	6
Kotcho d-12-C										
2065.1	605	0.03	0.08	0.13	0.25	0.62	0.01	4.19	2	3
Helmet b-49-G										
1810.9	575	0.01	0.05	0.11	0.12	0.45	0.01	0.77	6	14
1812.3	585	0.01	0.06	0.15	0.12	0.40	0.01	1.09	6	14
1813.6	588	0.01	0.06	0.13	0.13	0.46	0.01	1.32	5	10
1815.1	591	0.01	0.08	0.12	0.11	0.67	0.01	1.41	6	9
1816.5	594	0.01	0.05	0.16	0.14	0.31	0.00	1.32	4	12
1816.5	595	0.01	0.10	0.26	0.11	0.38	0.01	1.37	8	19
Nelson c-70-I										
1967.4	403	0.00	0.01	0.28	0.19	0.04	0.00	0.10	10	280
1967.5	384	0.00	0.01	0.18	0.48	0.06	0.00	0.22	5	82
1968.9	423	0.01	0.01	0.31	0.31	0.03	0.01	0.20	5	155
Dilly a-88-F										
2168.6	427	0.00	0.03	0.27	0.09	0.11	0.01	0.12	25	225
Walrus b-86-L										
1762.3	426	0.00	0.04	0.38	0.06	0.11	0.00	0.11	36	345

Table 24. Rock-Eval data for select Muskwa Formation shales.

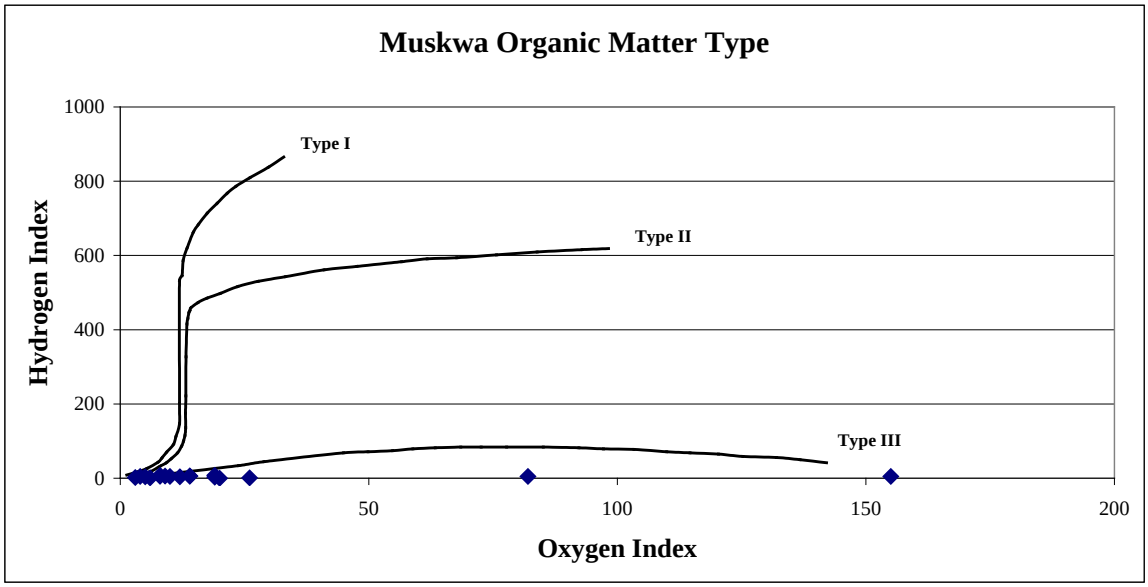

Figure 44. Van Krevelen diagram for the Muskwa Formation. The level of maturity is so high that it is not possible to type the kerogen based on the Van Krevelen plot.

Porosity

Twenty-eight shale samples from the Muskwa Formation were analyzed for total porosity (Table 25). The analyzes show that the range of porosity is from 0.6 to 9.2% with an average value of 3.2%. Assuming the formation is saturated, the pore space in the shale provides additional gas storage capacity which may significantly increase the potential gas in place. The effect of porosity on gas capacity in place is shown in the following section.

Sample	Depth (m)	Formation	Hg Bulk Density (cc/g)	He Skeletal Density (cc/g)	Std Dev.	Porosity	
						Fraction	Percent
Helmet b-49-G/94-P-7	1810.9	Muskwa	2.65	2.68	0.007	0.011	1.07
Helmet b-49-G/94-P-7	1812.3	Muskwa	2.65	2.69	0.004	0.017	1.68
Helmet b-49-G/94-P-7	1813.6	Muskwa	2.64	2.68	0.015	0.014	1.42
Helmet b-49-G/94-P-7	1815.1	Muskwa	2.58	2.66	0.003	0.030	3.02
Helmet b-49-G/94-P-7	1816.5	Muskwa	2.67	2.92	0.010	0.086	8.56
Esso Walrus b-86-L/94-I-16	1761.9	Muskwa	2.71	2.74	0.003	0.009	0.89
Esso Walrus b-86-L/94-I-16	1763.7	Muskwa	2.71	2.75	0.008	0.015	1.49
Shekile a-94-G/94-P-8	1539.6	Muskwa	2.54	2.63	0.007	0.033	3.28
Shekile a-94-G/94-P-8	1542	Muskwa	2.57	2.66	0.008	0.035	3.49
Shekile a-94-G/94-P-8	1544.1	Muskwa	2.59	2.65	0.005	0.023	2.26
Shekile a-94-G/94-P-8	1545.6	Muskwa	2.59	2.61	0.007	0.005	0.55
Shekile a-94-G/94-P-8	1548.6	Muskwa	2.48	2.55	0.016	0.026	2.60
Shekile a-94-G/94-P-8	1551.6	Muskwa	2.54	2.55	0.007	0.007	0.65
Shekilie a-94-G/94-P-8	1553.6	Muskwa	2.66	2.93	0.010	0.092	9.23
Snake River c-28-D/94-O-1	1947.7	Muskwa	2.48	2.57	0.031	0.037	3.70
Snake River c-28-D/94-O-1	1951.1	Muskwa	2.58	2.67	0.003	0.034	3.38
Snake River c-28-D/94-O-1	1952.6	Muskwa	2.64	2.71	0.005	0.027	2.66
Kotcho c-32-K/94-I-14	1979.2	Muskwa	2.63	2.71	0.024	0.033	3.25
Kotcho c-32-K/94-I-14	1981.1	Muskwa	2.61	2.72	0.006	0.040	4.02
Kotcho c-32-K/94-I-14	1982.2	Muskwa	2.63	2.75	0.006	0.044	4.36
Kotcho c-32-K/94-I-14	1984.4	Muskwa	2.59	2.71	0.026	0.042	4.24
Kotcho c-32-K/94-I-14	1985.6	Muskwa	2.62	2.70	0.013	0.027	2.69
Kotcho c-32-K/94-I-14	1988.1	Muskwa	2.66	2.74	0.015	0.032	3.22
Kotcho c-32-K/94-I-14	2000	Muskwa	2.70	2.83	0.002	0.047	4.72
Kotcho c-32-K/94-I-14	2003	Muskwa	2.68	2.79	0.041	0.037	3.66
Kotcho c-32-K/94-I-14	2005.8	Muskwa	2.73	2.81	0.004	0.030	3.04
Ft Nelson c-70-I/94-J-10	1967.4	Muskwa	2.67	2.77	2.926	0.035	3.51
Ft Nelson c-70-I/94-J-10	1968.9	Muskwa	2.72	2.78	2.637	0.021	2.07

Table 25. Porosity data for select Muskwa shale samples.

Sorption Capacity

In order to quantify the sorbed gas capacity in place, adsorption isotherms were completed on 19 samples from 6 wells in northeastern British Columbia. The TOC contents of the isotherm samples ranges from 0.1% to 4.7%. The lower TOC samples are representative of the transitions from and into underlying and overlying formations. The average TOC measured for all of the true Muskwa Formation samples is 3.1%.

All adsorption data (gas capacity data) is presented at reservoir pressure and a standard pressure of 11 MPa (1600 psi) (Table 26). The average TOC value of 3% is represented at a depth of 1544.1 m in the Shekilie a-94-G/94-P-8 well. At the reservoir pressure of 15 MPa (2180 psi), the gas capacity (not accounting for porosity) is 0.73 cc/g (23.4 scf/ton) (Figure 45). At a standard pressure of 11 MPa, the gas capacity is 0.69 cc/g (22.1 scf/ton). Samples with TOC values around 1% represent the lower end members of the Muskwa Formation. A sample with 1.2% TOC was measured at a depth of 1952.6 m in the Snake River c-28-D/94-O-1 well (Figure 46). At the reservoir pressure of 19 MPa (2760 psi), the gas capacity (not accounting for porosity) is 0.35 cc/g (11.2 scf/ton). At a standard pressure of 11 MPa, the gas capacity is 0.31 cc/g (9.9 scf/ton). Table 24 provides the gas capacity data for each Muskwa Formation sample at both reservoir pressure and a standard pressure of 11 MPa.

Because there is significant porosity in the Muskwa Formation samples, the gas capacity may increase considerably if free gas capacity is factored in. In figure 47, the gas capacities have been calculated to show the effect of porosity on gas capacity. End members of 2% and 4.5% porosity have been used to calculate the gas capacity in a 3% TOC sample. At 11 MPa pressure, the gas capacity with 2% porosity is 1.56 cc/g (50.0 scf/ton) which is a 126% increase over the sorbed gas capacity of 0.69 cc/g (22.1 scf/ton). With 4.5% porosity, the gas capacity is 2.79 cc/g (89.4 scf/ton) which is a 304% increase over the sorbed gas capacity.

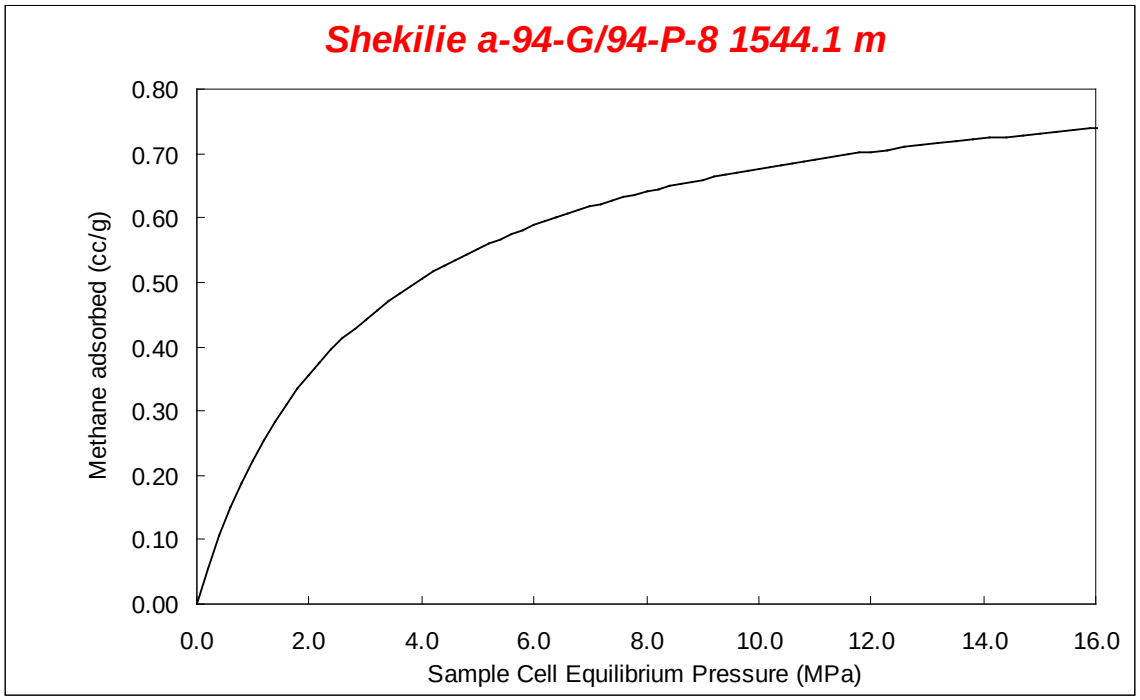

Figure 45. Adsorption isotherm for a shale sample from the Muskwa Formation. Sample has a TOC content of 2.8%. Gas capacity for pressures greater than 10 MPa is extrapolated using the Langmuir equation.

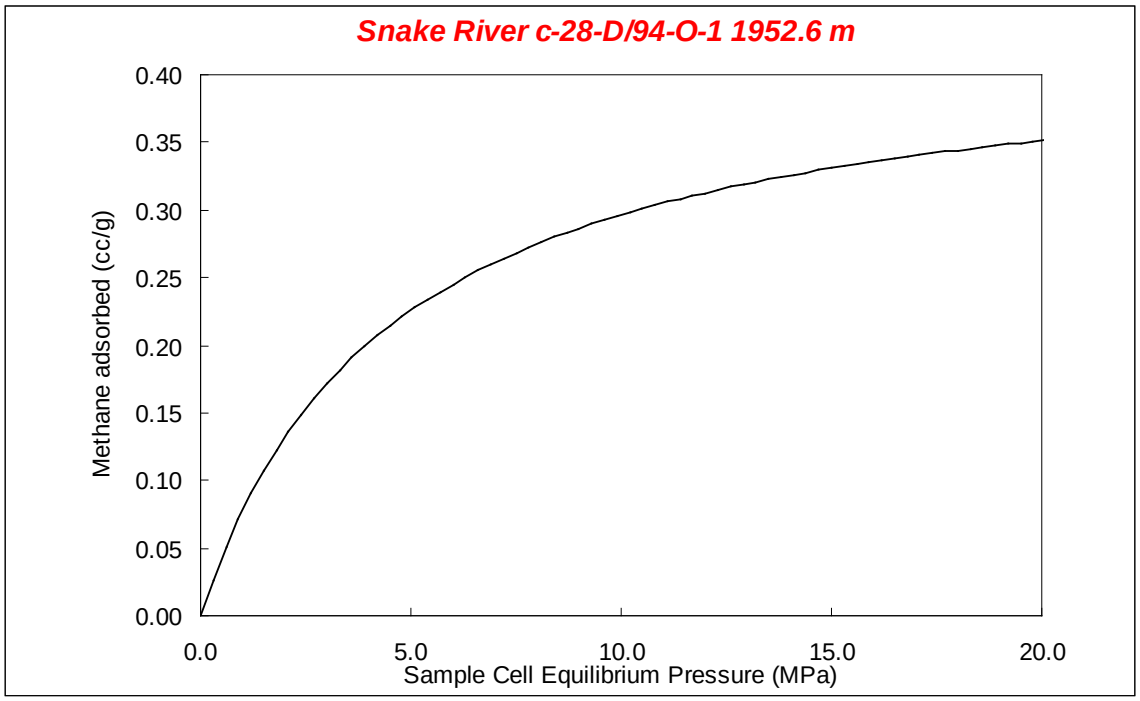

Figure 46. Adsorption isotherm for a shale sample from the Muskwa Formation. Sample has a TOC content of 1.2%. Gas capacity for pressures greater than 10 MPa is extrapolated using the Langmuir equation.

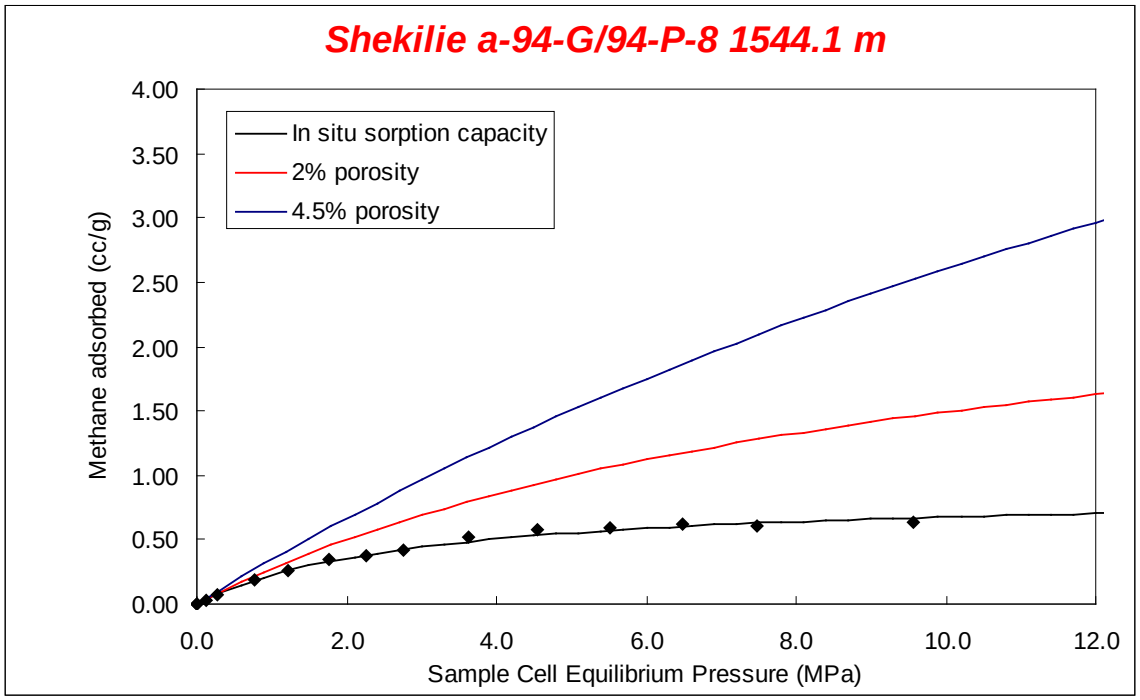

Figure 47. Sorbed plus free gas capacity in a 3% TOC sample.

Well Name	Location	Depth (m)	Reservoir Pressure (psi)	Reservoir Pressure (kPa)	Gas Capacity (cc/g)	Gas Capacity @ 11 Mpa (cc/g)	TOC
			Muskwa				
Snake River	c-28-D/94-O-1	1951.10	2753	18978	0.44	0.41	3.32
		1952.60	2755	18993	0.35	0.31	1.22
		1990.10	2808	19357	1.40	1.22	4.74
Shekilie	a-94-G/94-P-8	1539.60	2172	14975	0.93	0.91	2.31
		1544.10	2178	15019	0.73	0.69	2.75
		1545.60	2180	15034	0.91	0.81	2.23
		1551.60	2189	15092	1.32	1.27	3.88
Kotcho	c-32-K/94-I-14	1981.10	2795	19270	0.17	0.17	0.28
		1982.20	2796	19281	0.29	0.28	1.65
		1984.40	2800	19302	0.01	0.01	0.10
		1988.10	2805	19338	0.17	0.16	0.26
Fort Nelson	c-70-I/94-J-10	1967.40	2776	19137	0.30	0.28	0.10
		1968.90	2778	19151	0.38	0.38	0.20
Helmet	b-49-G/94-P-7	1810.9	2555	17614	0.30	0.29	0.77
		1812.30	2557	17628	0.34	0.34	1.09
		1813.60	2559	17641	0.48	0.47	1.32
		1815.10	2561	17655	0.75	0.69	1.41
		1816.30	2562	17667	0.67	0.62	1.32

Table 26. Variation in sorption capacity with total organic carbon content for Muskwa Formation shale samples. Capacities are given at reservoir pressure and a standard pressure of 11 MPa.

Clay Mineralogy

X-ray diffraction analyzes were completed on 28 samples from the Muskwa Formation in order to determine the mineralogy of the shale samples. Table 27 shows a summary of the x-ray diffraction data. The x-ray diffraction traces for each sample are provided in Appendix B. The sampling program employed for the Muskwa Formation allows for the examination in variations in mineralogy within the transition from the lower Fort Simpson Formation into the Muskwa Formation as well as the transition from the Muskwa Formation into the underlying Otter Park Formation and Slave Point Formation.

Wells sampled within the transition from the Muskwa Formation into the Fort Simpson Formation consist of grey shales which have TOC contents less than or ~ 1.0 wt%. These shales contain quartz, illite and variable amounts of kaolinite, pyrite and dolomite. Samples from the Kotcho c-32-K/94-I-14 well have high illite contents (30 – 50%) and no kaolinite. Samples from the Helmet b-49-G/94-P-7 well contain 10-40% illite and 0-5% kaolinite. In general, TOC contents are less in the clay-rich Kotcho well than the silt--rich shales of the Helmet well.

The Snake River c-28-D/94-O-1 and Shekilie a-94-G/94-P-8 wells penetrate into the black shales of the Muskwa Formation (Figure 48). The samples are comprised mainly of quartz, and illite (1-22%) with some samples having minor kaolinite, pyrite, calcite and dolomite. Sample 1553.6 m from the Shekilie a-94-G/94-P-8 is a carbonate (comprised of 99% calcite) in the upper portion of the Slave Point Formation.

In the Kotcho c-98-G/94-I-14 well (Figure 49) the Otter Park Formation (underlying the Muskwa in the NW quadrant of the study area) was sampled for mineralogy. The shale sampled in the Otter Park Formation are TOC-lean and consist of quartz, illite (~30%), with minor amounts of kaolinite and dolomite. The transition from the Muskwa Formation to Otter Park Formation is characterized by a decrease in gamma ray signature (due to a decrease in TOC content) and an increase in density (as indicated from sonic logs).

Muskwa XRD			Mineralogy (% Relative)					
Name	Location	Depth (m)	Illite/Mica (d=10.00)	Kaolinite (d=7.10)	Quartz (d=4.23)	Calcite (d=3.03)	Pyrite (d=2.71)	Dolomite (d=2.89)
Snake River	c-28-D/94-O-1	1949.70	17	4	77	0	0	0
		1951.10	10	3	84	0	3	0
		1952.60	19	0	64	13	0	4
Shekilie	a-94-G/94-P-8	1539.60	16	1	79	0	2	2
		1542.00	22	2	76	0	0	0
		1545.60	18	0	82	0	0	0
		1548.60	8	3	88	0	2	0
		1551.50	11	2	87	0	0	0
		1553.60	1	0	0	99	0	0
Kotcho	c-32-K/94-I-14	1979.20	31	0	63	0	3	2
		1981.10	35	0	46	0	4	14
		1982.20	51	0	49	0	0	0
		1984.40	46	0	54	0	0	0
		1985.60	31	0	69	0	0	0
		1988.10	37	0	52	0	2	8
Walrus	b-86-L/94-I-16	1761.90	19	7	59	0	5	8
		1763.70	29	9	58	0	0	0
Fort Nelson	c-70-I/94-J-10	1967.40	22	15	54	0	0	5
		1968.90	20	17	51	0	2	6
Helmet	b-49-G/94-P-7	1810.90	10	5	81	0	3	1
		1812.30	37	4	59	0	0	0
		1813.60	10	2	83	0	3	2
		1815.10	10	1	84	0	2	2
		1816.50	12	0	78	0	3	7
Kotcho	c-98-G/94-I-14	2000.00	37	4	59	0	0	0
		2005.80	30	0	56	0	0	14

Table 27. Relative mineralogy percentages determined from XRD analyzes. "d" refers to the d-spacing of the principal plane of each mineral that was used to (semi-) quantify the relative abundances. Shaded regions show degraded illite which has a range of d spacings.

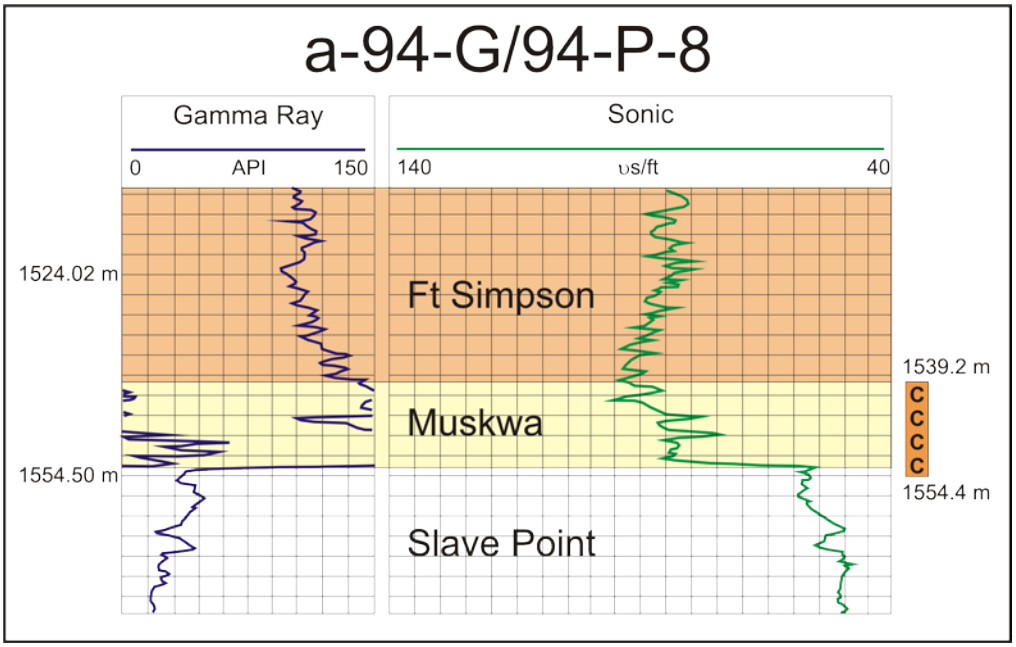

Figure 48. Geophysical log for a-94-G/94-P-8 showing the core interval 1539.2 - 1554.4 m within the Muskwa and upper Slave Point formations. "C" indicates core interval.

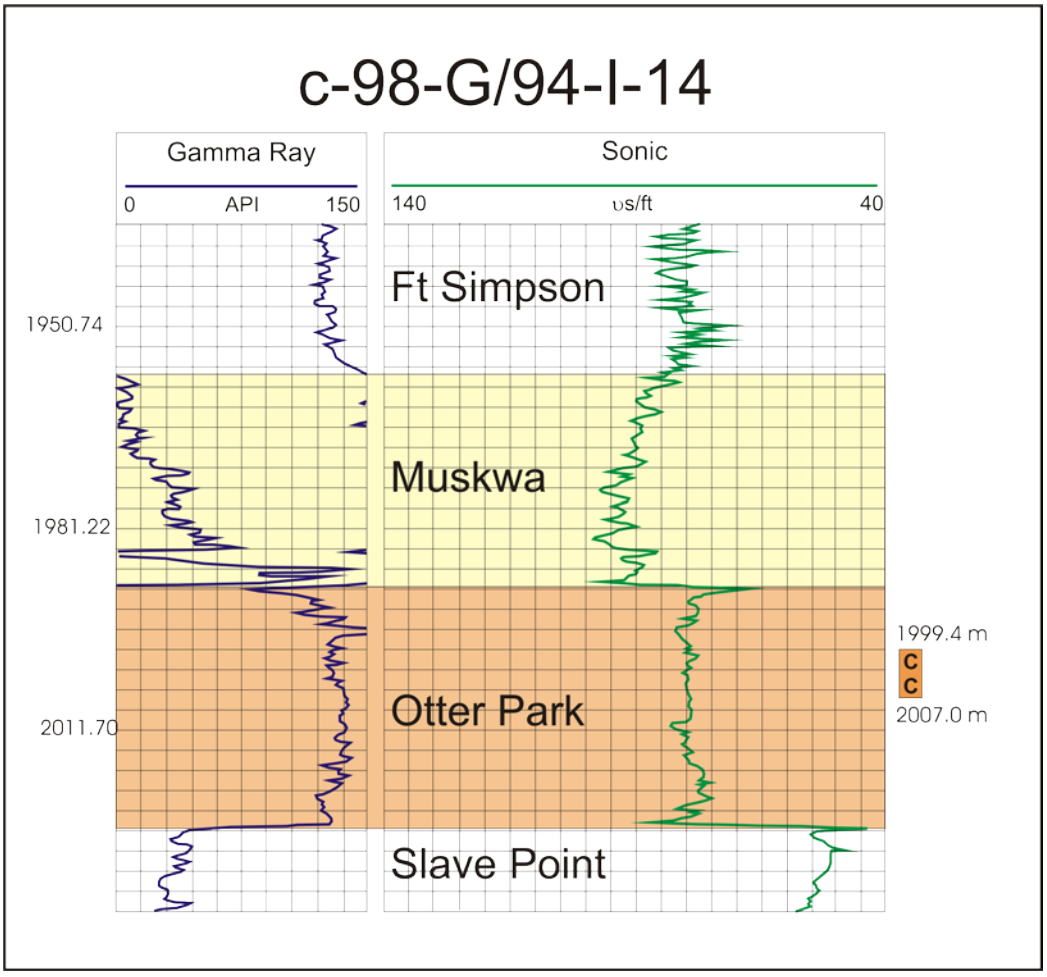

Figure 49. Geophysical log for c-98-G/94-I-14 showing the core interval 1999.4 – 2007.0 m within the Otter Park Formation. "C" indicates core interval.

Gas Capacity in Place

Because gas capacities are highly variable due to changing organic contents, reservoir pressures, formation thickness and porosity, gas in place numbers can be calculated based on a range of reservoir properties. Tables 28 and 29 provide gas capacity in place numbers for varying TOC contents, reservoir pressures, porosities and thickness. The gas capacity in place values are calculated using an average density of 2.63 cc/g which is measured using mercury submersion.

Porosity (%)	TOC (%)	Shale Thickness (m)	Pressure (MPa)	Resources (cc/cm2)	Resources (bcf/section)	Average Gas Content (scf/ton)	Average Gas Content (cc/g)	Density (g/cc)
0.0	1.2	10.0	11.0	815	1	10	0.3	2.63
0.0	1.2	30.0	11.0	2446	2	10	0.3	2.63
0.0	1.2	70.0	11.0	5707	5	10	0.3	2.63
2.0	1.2	10.0	11.0	3945	4	48	1.5	2.63
2.0	1.2	30.0	11.0	11835	11	48	1.5	2.63
2.0	1.2	70.0	11.0	27615	25	48	1.5	2.63
4.5	1.2	10.0	11.0	8442	8	103	3.2	2.63
4.5	1.2	30.0	11.0	25327	23	103	3.2	2.63
4.5	1.2	70.0	11.0	59096	54	103	3.2	2.63
0.0	2.8	10.0	11.0	1815	2	22	0.7	2.63
0.0	2.8	30.0	11.0	5444	5	22	0.7	2.63
0.0	2.8	70.0	11.0	12703	12	22	0.7	2.63
2.0	2.8	10.0	11.0	4103	4	50	1.6	2.63
2.0	2.8	30.0	11.0	12308	11	50	1.6	2.63
2.0	2.8	70.0	11.0	28720	26	50	1.6	2.63
4.5	2.8	10.0	11.0	7338	7	89	2.8	2.63
4.5	2.8	30.0	11.0	22013	20	89	2.8	2.63
4.5	2.8	70.0	11.0	51364	47	89	2.8	2.63

Table 28. Variations of gas capacity in place based on varying thickness, porosity and TOC content. Values are calculated at a standard pressure of 11 MPa.

Porosity (%)	TOC (%)	Shale Thickness (m)	Pressure (MPa)	Resources (cc/cm2)	Resources (bcf/section)	Average Gas Content (scf/ton)	Average Gas Content (cc/g)	Density (g/cc)
0.0	1.2	10.0	17.8	894	1	11	0.3	2.63
0.0	1.2	30.0	17.8	2683	2	11	0.3	2.63
0.0	1.2	70.0	17.8	6259	6	11	0.3	2.63
2.0	1.2	10.0	17.8	6207	6	76	2.4	2.63
2.0	1.2	30.0	17.8	18620	17	76	2.4	2.63
2.0	1.2	70.0	17.8	43448	40	76	2.4	2.63
4.5	1.2	10.0	17.8	17279	16	210	6.6	2.63
4.5	1.2	30.0	17.8	51837	47	210	6.6	2.63
4.5	1.2	70.0	17.8	120954	111	210	6.6	2.63
0.0	2.8	10.0	17.8	1973	2	24	0.8	2.63
0.0	2.8	30.0	17.8	5918	5	24	0.8	2.63
0.0	2.8	70.0	17.8	13808	13	24	0.8	2.63
2.0	2.8	10.0	17.8	4997	5	61	1.9	2.63
2.0	2.8	30.0	17.8	14991	14	61	1.9	2.63
2.0	2.8	70.0	17.8	34979	32	61	1.9	2.63
4.5	2.8	10.0	17.8	10047	9	122	3.8	2.63
4.5	2.8	30.0	17.8	30140	28	122	3.8	2.63
4.5	2.8	70.0	17.8	70326	64	122	3.8	2.63

Table 29. Variations of gas capacity in place based on varying thickness, porosity and TOC content. Values are calculated at an average reservoir pressure of 17.8 MPa.

Conclusions

The Muskwa Formation is an organic rich shale interval that is widely distributed throughout northeastern British Columbia. Maximum thickness of the Muskwa Formation is 75 m. The Muskwa Formation is characterized on geophysical logs by a consistently high gamma ray response which corresponds to high organic content. The maximum total organic carbon content measured in this study is 5.9% with an average of 3.1%. Low TOC values measured are characteristic of the transition zone from the underlying Otter Park and Slave Point formations and into the overlying Fort Simpson Formation. Due to the high organic contents, the Muskwa Formation shales have potential for high sorbed gas capacity. A sample with 2.8% TOC can hold 0.8 cc/g at a typical reservoir pressure of 17.8 MPa. With porosity in the range of 2% to 4.5%, the free gas potential, assuming saturation, can increase the gas capacity by 120% to 300% over the sorbed gas capacity.

REFERENCES

Allan, J. and Creaney, S. 1991. Oil families of the Western Canada Basin. Bulletin of Canadian Petroleum Geology, v. 39, p. 107-122.

Bustin, R.M. 2003. Geology and some engineering aspects of coalbed methane and gas shales. Unpublished short course notes, pp 325.

Bond, G.C. and Kominz, M.A. 1991. Disentangling middle Paleozoic sea level and tectonic events in cratonic margins and cratonic basins of North America. In: Cloetingh, S. (Ed.) Special Section on Long-Term Sea Level Changes, Journal of Geophysical Research, B, Solid Earth and Planets, v. 96, p. 6619-6639

Caplan, M.L. and Bustin, R.M. Palaeoenvironmental and palaeoceanographic controls on black, laminated mudrock deposition: example from Devonian-Carboniferous strata, Alberta, Canada. Sedimentary Geology, v. 145, p. 45-72.

Churcher, P.L. and Majid, A.H. 1989. Similarities between the Tangent-Wabamun type play of the Alberta Basin and the Albion-Scipio type play of the Michigan Basin. Bulletin of Canadian Petroleum Geology, v. 37, p. 241-245.

Core Labs, 2001. Stratigraphic Correlation Chart.

Douglas, R.J.W. and Norris, D.K. 1961. Camsell Bend and Root River map-areas, Northwest Territories. Geological Survey of Canada, Paper 61-13.

Eaton, David W; Ross, Gerald M; Hope, Jacqueline, 1999. The rise and fall of a cratonic arch; a regional seismic perspective on the Peace River Arch, Alberta. Bulletin of Canadian Petroleum Geology, v. 47, p. 346-361.

Fitzgerald, E.L. and Braun, L.T. 1965. Disharmonic folds in Besa River Formation northeastern British Columbia, Canada. Bulletin of the American Association of Petroleum Geologists. V. 49, p. 418-432.

Geldsetzer, H.H.J. 1982. Depositional history of the Devonian succession in the Rocky Mountains, southwest of the Peace River Arch. Geological Survey of Canada Paper 82-1C, Current Research Part C, p. 55-64.

Geldsetzer, H.H.J. and Morrow, D.W., 1991. Upper Devonian carbonate strata in the Foreland belt. *In:* Geology of the Cordilleran Orogen in Canada, DNAG v.G2, Chapter 8, p.222-230.

Gordey, S.P., 1991. Devonian and Mississippian clastics of the Foreland and Omineca Belts. *In:* Geology of the Cordilleran Orogen in Canada, DNAG v.G2, Chapter 8, p.230-242.

Gordey, S.P., Abbott, J.G., Tempelman-Kluit, D.L. and Gabrielse, H. 1987. "Antler" clastics in the Canadian Cordillera. Geology, v. 15, p. 103-107.

Gordey, S.P. Devono-Mississippian clastic sedimentation and tectonism in the Canadian Cordilleran miogeocline. *In:* Devonian of the World. Canadian Society of Petroleum Geology, Memoir 14, v.2, p. 1-14.

Gray, F.F. and Kassube, J.R. 1963. Geology and stratigraphy of Clarke Lake gas field, British Columbia. Bulletin of the American Association of Petroleum Geologists. V. 47, p. 467-483.

Griffin, D.L. 1965. The facies front of the Devonian Slave Point-Elk Point sequence in northeastern British Columbia and the Northwest Territories. Journal of Canadian Petroleum Technology, v. 4, p. 13-22.

Griffin, D.L. 1967. Devonian of northeastern British Columbia. *In:* Oswald, D.H. (Ed.) International Symposium on the Devonian System. Alberta Society of Petroleum Geology, v. 1, p. 803-826.

Hadley, M.G. and Jones, B. 1990. Lithostratigraphy and nomenclature of Devonian strata in the Hay River area, Northwest Territories. Bulletin of Canadian Petroleum Geology, v. 38, p. 332-356.

Halbertsma, H.L. 1994. Devonian Wabamun Group, Geological atlas of the Western Canada Sedimentary Basin. Canadian Society of Petroleum Geologists.

Harker, P. and McLaren, D.J. 1958. The Devonian-Mississippian boundary in the Alberta Rocky Mountains. *In:* Jurassic and Carboniferous of Western Canada, p. 244-253.

Johnson, J.G., Klapper, G. and Sandberg, C.A. 1985. Devonian eustatic fluctuations in Euramerica. Geological Society of America Bulletin. v. 96, p. 567-587.

Kidd, F.A. 1963. The Besa River Formation. Bulletin of Canadian Petroleum Geology, v. 11, p. 369-372

Langmuir, I. 1916. The constitution and fundamental properties of solids and liquids. Journal of the American Society, v. 38, p. 2221-2295.

Lowey, G.W. 1990. Occurrence of turbidites in the Besa River Formation (Devonian-Mississippian), Northwest Territories. Bulletin of Canadian Petroleum Geology, v. 38, p. 426-428.

McClay, K.R., Insley, M.W. and Anderton, R. 1989. Inversions of the Kechika Trough, northeastern British Columbia, Canada. *In:* Cooper, M.A. and Williams, G.D.

(Eds.) Inversion Tectonics Meeting, Geological Society Special Publication 44, p. 235-257.

McMechan, M.E. 2002. Structural geometry in the Carbon Creek area of the Rocky Mountain Fold and Thrust Belt, northeastern British Columbia. Bulletin of Canadian Petroleum Geology, v. 50, p. 407-418.

Macqueen, R.W. and Sandberg, C.A. 1970. Stratigraphy, age, and interregional correlation of the Exshaw Formation, Alberta Rocky Mountains. Bulletin of Canadian Petroleum Geology, v. 18, p. 32-66.

Morrow, D.W. and Geldsetzer, H.H.J., 1988. Devonian of the eastern Canadian cordillera. *In:* Devonian of the World. Canadian Society of Petroleum Geology, Memoir 14, v.1, p. 85-121.

Nadjiwon, L.N., Morrow, D.W. and Coniglio, M. 2000. Stratigraphy of Lower and Middle Devonian carbonate rocks of northeastern British Columbia. *In:* Current Research 2000, Geological Survey of Canada 9 p.

Pelzer, E.E. 1966. Mineralogy, geochemistry and stratigraphy of the Besa River Shale, British Columbia. Bulletin of Canadian Petroleum Geology, v. 14, p. 273-321.

Peters, K.E. 1986. Guidelines for evaluating petroleum source rock using programmed pyrolysis. Bulletin of the American Association of Petroleum Geologists, v. 70, p. 318-329.

Poole, F.G. 1974. Flysch deposits of the Antler Foreland Basin, western United States. In: Dickinson, W.R. (Ed.), Tectonics and Sedimentation. Society of Economic Paleontologists and Mineralogists, Special Publication No. 22, p. 58-82.

Richards, B.C. 1989. Upper Kaskaskia Sequence: uppermost Devonian and Lower Carboniferous, Chapter 9. *In:* Western Canada Sedimentary Basin, a Case History. B.D. Ricketts (ed.). Canadian Society of Petroleum Geologists, p. 165-201.

Richards, B.C. and Higgins, A.C. 1988. Devonian-Carboniferous boundary beds of the Palliser and Exshaw formations at Jura Creek, Rocky Mountains, southwestern Alberta. *In:* Devonian of the World. N.J. McMillan, A.F. Embry and D.J. Glass (eds.). Canadian Society of Petroleum Geologists, Memoir 14, v. 2, p. 399-412.

Richards, B.C., Henderson, C.M., Higgins, A.C., Johnston, D.I., Mamet, B.L. and Meijer Drees, N.C. 1991. The Upper Devonian (Famennian) and Lower Carboniferous (Tournaisian) at Jura Creek, southwestern Alberta. *In:* A field guide to the paleontology of southwestern Canada, P. Smith (ed.), Geological Association of Canada, Paleontology Division, Vancouver, p. 35-76.

Richards, B.C., Bamber, E.W., Henderson, C.M., Higgins, A.C., Johnston, D.I., Mamet, B. and Meijer Drees, N.C. 1993. Uppermost Devonian (Famennian) and Lower Carboniferous (Tournaisian) at Jura Creek, and Mount Rundle, Southwestern Alberta. Carboniferous to Jurassic Pangea Field Trip #7, 1993, Calgary, Alberta. 79 p.

Richards, B.C., Barclay, J.E., Bryan, D., Hartling, A., Henderson, C.M. and Hinds, R.C., 1994, Carboniferous strata of the Western Canada Sedimentary Basin. *In:* Geological Atlas of the Western Canada Sedimentary Basin, G.D. Mossop and I Shetsen, eds., Canadian Society of Petroleum Geologists, p.221-249.

Ross, G. and Stephenson, R.A. 1989. Crystalline basement; the foundation of the Western Canada Sedimentary Basin. In: Ricketts, B.D. (Ed.), Western Canada Sedimentary Basin; a case history, p. 33-45.

Sandberg, C.A., Poole, F.G., Johnson, J.G. 1988. Upper Devonian of Western United States. *In:* Devonian of the World. N.J. McMillan, A.F. Embrey and D.J. Glass (Eds.), Proceedings of the Canadian Society of Petroleum Geologists International Symposium, Devonian System I. p.183-220.

Savoy, L. 1992. Environmental record of Devonian-Mississippian carbonate and low-oxygen facies transitions, southernmost Canadian Rocky Mountains and northwesternmost Montana. Geological Society of America Bulletin, v. 104, p. 1412-1432.

Savoy, L.E. and Mountjoy, E.W. 1995. Cratonic-margin and Antler-age foreland basin strata (Middle Devonian to Lower Carboniferous) of the southern Canadian Rocky Mountains and adjacent Plains. *In:* Stratigraphic Evolution of Foreland Basins. Society of Economic Paleontologists and Mineralogists Special Publication, No. 52, p. 213-231.

Savoy, L.E., Stevenson, R.K. and Mountjoy, E.W. 2000. Provenance of Upper Devonian-Lower Carboniferous miogeoclinal strata, southeastern Canadian Cordillera: link between tectonics and sedimentation. Journal of Sedimentary Research, v. 70, p. 181-193.

Sikabonyi, L.A. and Rodgers, W.J. 1959. Paleozoic tectonics and sedimentation in the northern half of the Western Canada Sedimentary Basin. Journal of the Alberta Society of Petroleum Geology, v. 7, p. 193-216.

Smith, M.T., Dickinson, W.R. and Gehrels, G.E. 1993. Contractional nature of Devonian-Mississippian Antler tectonism along the North American continental margin. Geology, v. 21, p. 21-24.

Stoakes, F.A. 1992. Wabamun megasequence. In: Wendte, J., Stoakes, F.A., Campbell, C.V. (Eds.), Devonian-Early Mississippian carbonates of the Western Canada

sedimentary basin; a sequence stratigraphic framework. SEPM Short Course Notes, v. 28, p. 225-239.

Tissot, B.P. and Welte, D.H., 1984. Petroleum formation and occurrence, 2nd edition. Springer, Berlin. 699 p.

Thompson, R.I. 1982. The nature and significance of large 'blind' thrusts within the northern Rocky Mountains of Canada. *In:* Geologic Studies of the Cordilleran Thrust Belt, volume 1, Rocky Mountain Association of Geologists, p.47-59.

Torrie, J.E. 1973. Northeastern British Columbia. In: Future petroleum provinces of Canada, Canadian Society of Petroleum Geology, Memoir 1, p. 151-186.

Wissner, U.F.G. and Norris, A.W. 1991. Middle Devonian goniatites from the Dunedin and Besa River formations on northeastern British Columbia. *In:* Contributions to Canadian Paleontology, Geological Survey of Canada, Bulletin 412, p. 45-79.

APPENIDIX A – CORE DESCRIPTIONS

APPENIDIX B – X-RAY DIFFRACTION TRACES

BESA RIVER SAMPLES

Well	Location	Depth (m)
Dunedin	d-75-E/94-N-8	3373.80
		3687.30
		3687.60
		3688.80
		3695.10
		3701.10
		3775.00
		3890.60
		3891.80
		3892.10
		3893.00
		3894.50
		3895.70
		3896.00
La Biche	b-55-E/94-O-13	3044.80
		3046.15
		3047.20

Dunedin d-75-E/94-N-8 3373.8 m

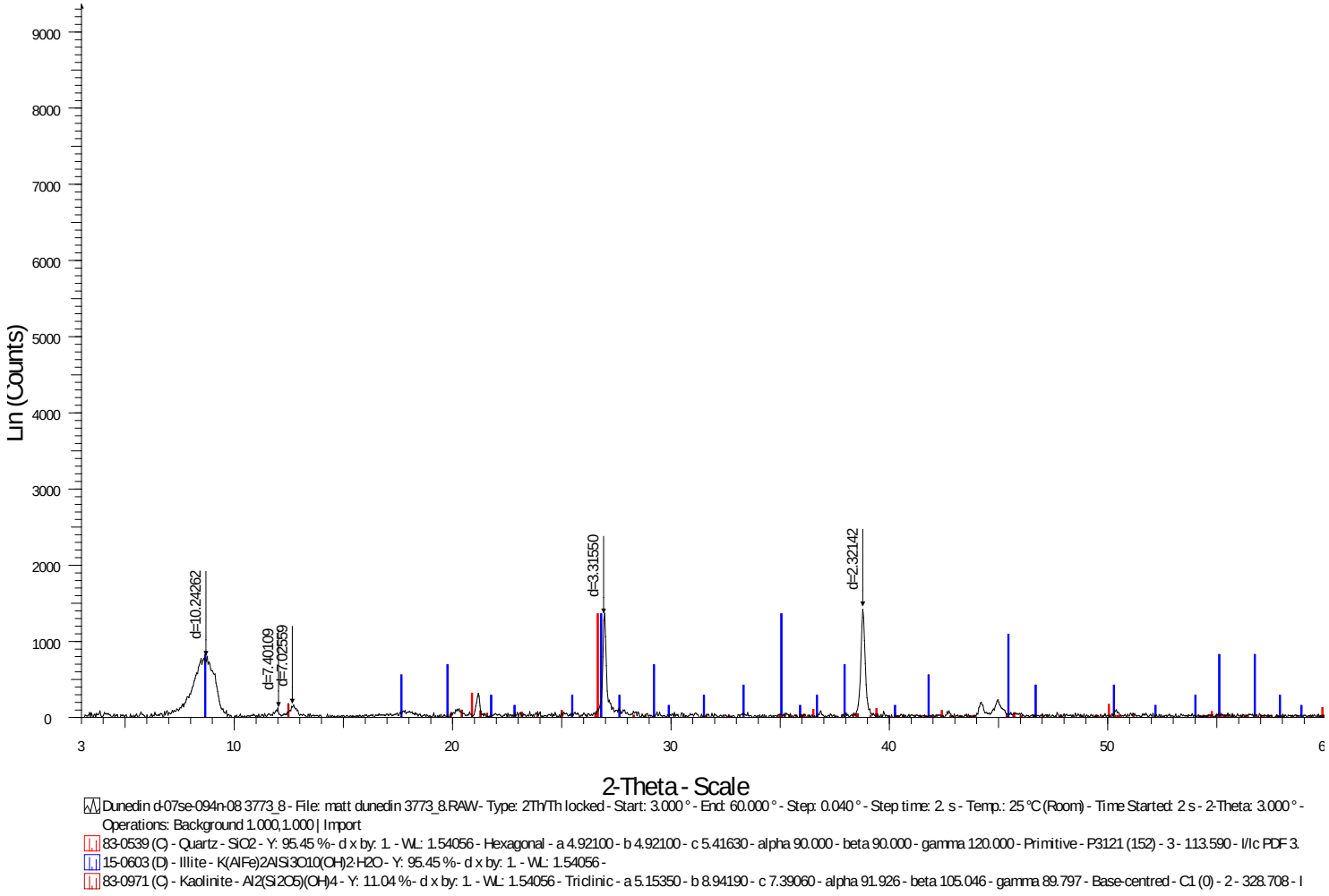

Dunedin d-07se-094n-08 3773_8 - File: matt dunedin 3773_8.RAW - Type: 2Th/Th locked - Start: 3.000 ° - End: 60.000 ° - Step: 0.040 ° - Step time: 2. s - Temp.: 25 °C (Room) - Time Started: 2 s - 2-Theta: 3.000 ° - Operations: Background 1.000,1.000 | Import

83-0539 (C) - Quartz - SiO2 - Y: 95.45 % - d x by: 1. - WL: 1.54056 - Hexagonal - a 4.92100 - b 4.92100 - c 5.41630 - alpha 90.000 - beta 90.000 - gamma 120.000 - Primitive - P3121 (152) - 3 - 113.590 - I/Ic PDF 3.

15-0603 (D) - Illite - K(AlFe)2AlSi3O10(OH)2·H2O - Y: 95.45 % - d x by: 1. - WL: 1.54056 -

83-0971 (C) - Kaolinite - Al2(Si2O5)(OH)4 - Y: 11.04 % - d x by: 1. - WL: 1.54056 - Triclinic - a 5.15350 - b 8.94190 - c 7.39060 - alpha 91.926 - beta 105.046 - gamma 89.797 - Base-centred - C1 (0) - 2 - 328.708 - I

Dunedin d-75-E/94-N-8 3687.3 m

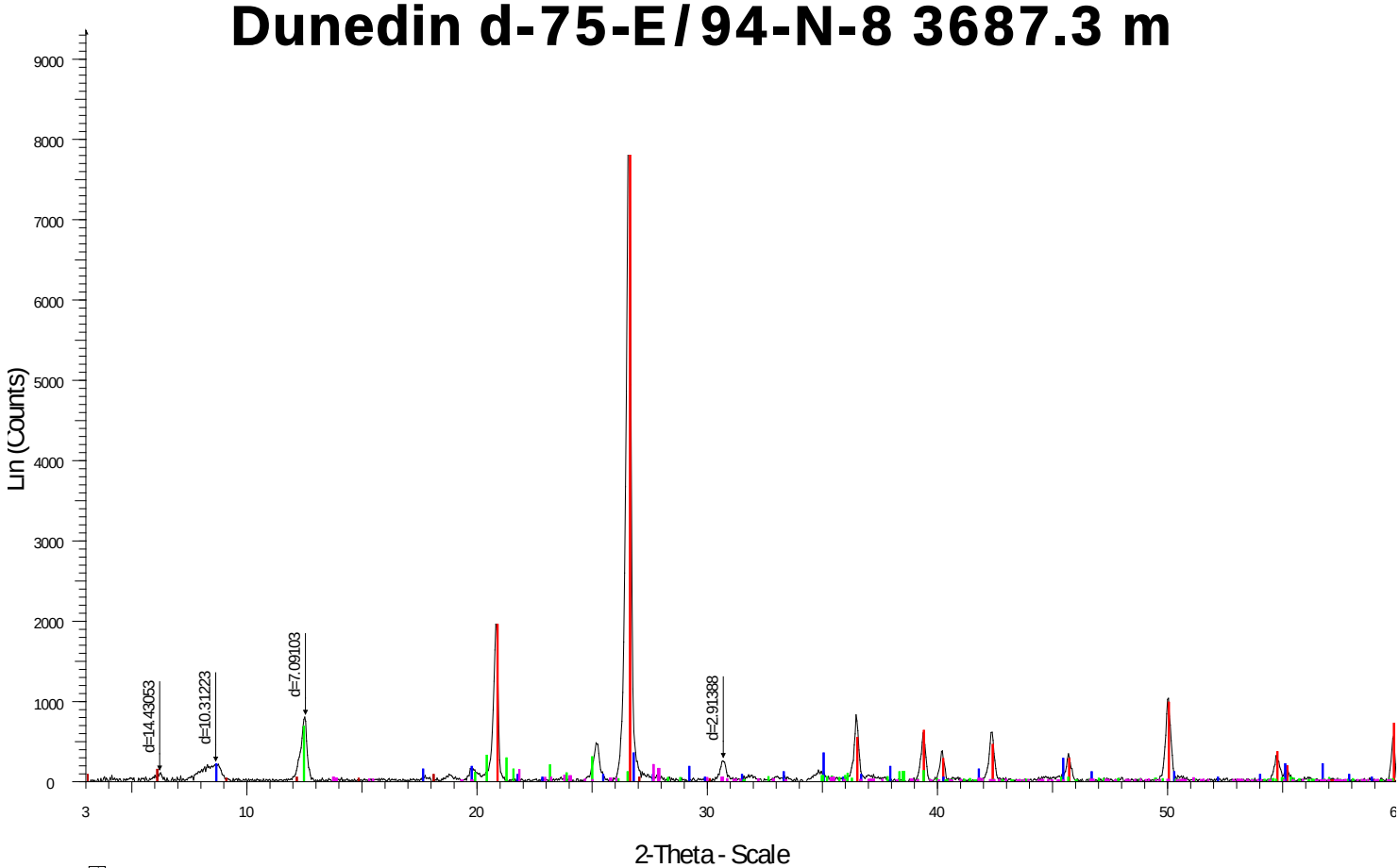

Dunedin d-07SE/094-N-8 3687.3 - File: matt dunedin 3687_3.RAW - Type: 2Th/Th locked - Start: 3.000 ° - End: 60.000 ° - Step: 0.040 ° - Step time: 2. s - Temp.: 25 °C (Room) - Time Started: 2 s - 2-Theta: 3.000 ° - Operations: Background 1.000,1.000 | Import

83-0539 (C) - Quartz - SiO2 - Y: 95.96 % - d x by: 1. - WL: 1.54056 - Hexagonal - a 4.92100 - b 4.92100 - c 5.41630 - alpha 90.000 - beta 90.000 - gamma 120.000 - Primitive - P3121 (152) - 3 - 113.590 - I/Ic PDF 3.

15-0603 (D) - Illite - K(AlFe)2AlSi3O10(OH)2·H2O - Y: 3.64 % - d x by: 1. - WL: 1.54056 -

83-0971 (C) - Kaolinite - Al2(Si2O5)(OH)4 - Y: 7.27 % - d x by: 1. - WL: 1.54056 - Triclinic - a 5.15350 - b 8.94190 - c 7.39060 - alpha 91.926 - beta 105.046 - gamma 89.797 - Base-centred - C1 (0) - 2 - 328.708 - I/I

07-0051 (D) - Montmorillonite - (Na,Ca)0.3(Al,Mg)2Si2O10(OH)2·nH2O - Y: 1.43 % - d x by: 1. - WL: 1.54056 -

71-1154 (C) - Albite high - Na(AlSi3O8) - Y: 2.08 % - d x by: 1. - WL: 1.54056 - Triclinic - a 8.25080 - b 12.94890 - c 7.14310 - alpha 91.161 - beta 116.169 - gamma 90.030 - Base-centred - C-1 (0) - 4 - 684.755 - I/I

Dunedin d-75-E/94-N-8 3687.3 m

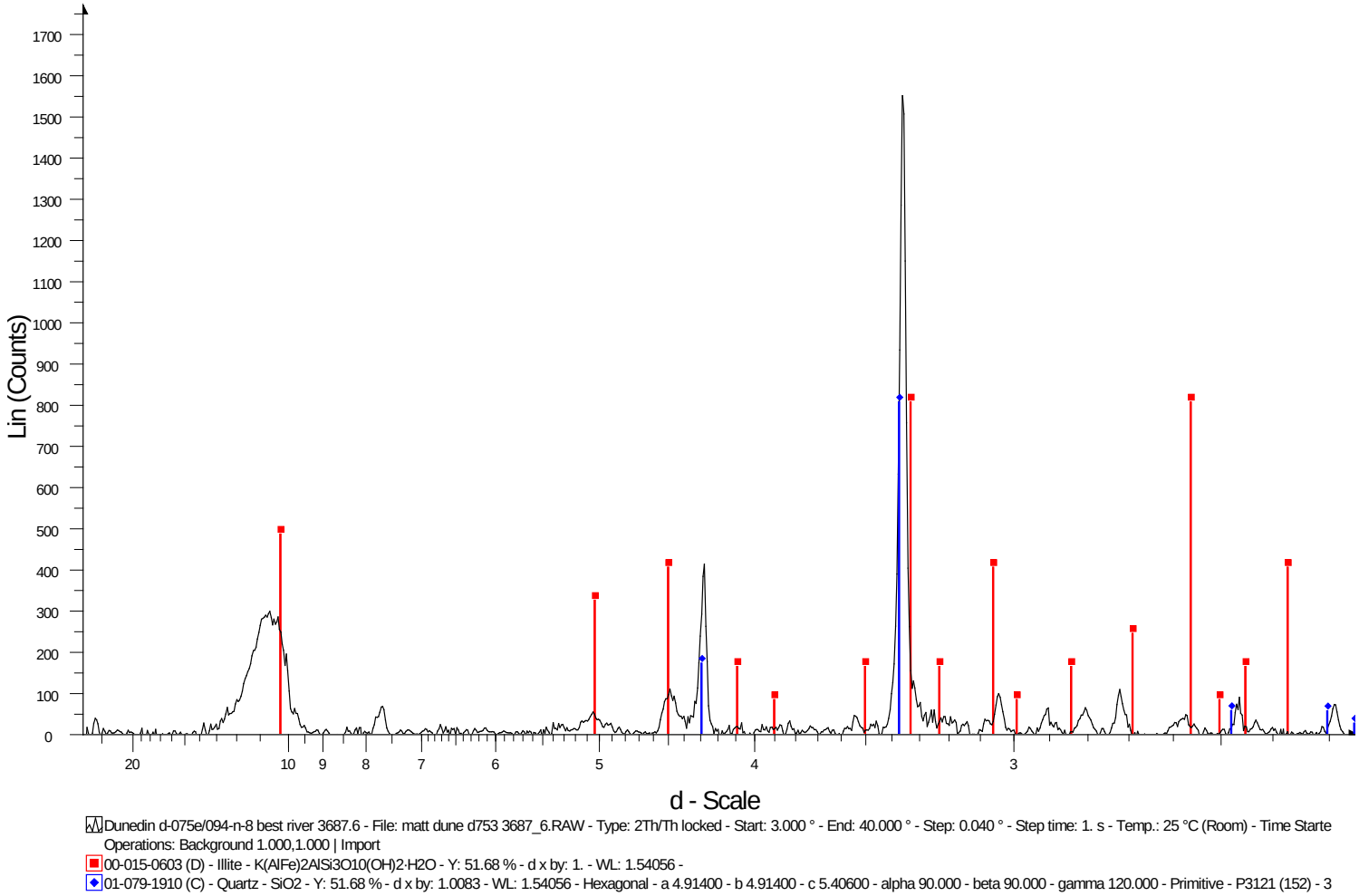

Dunedin d-75-E/94-N-8 3688.8 m

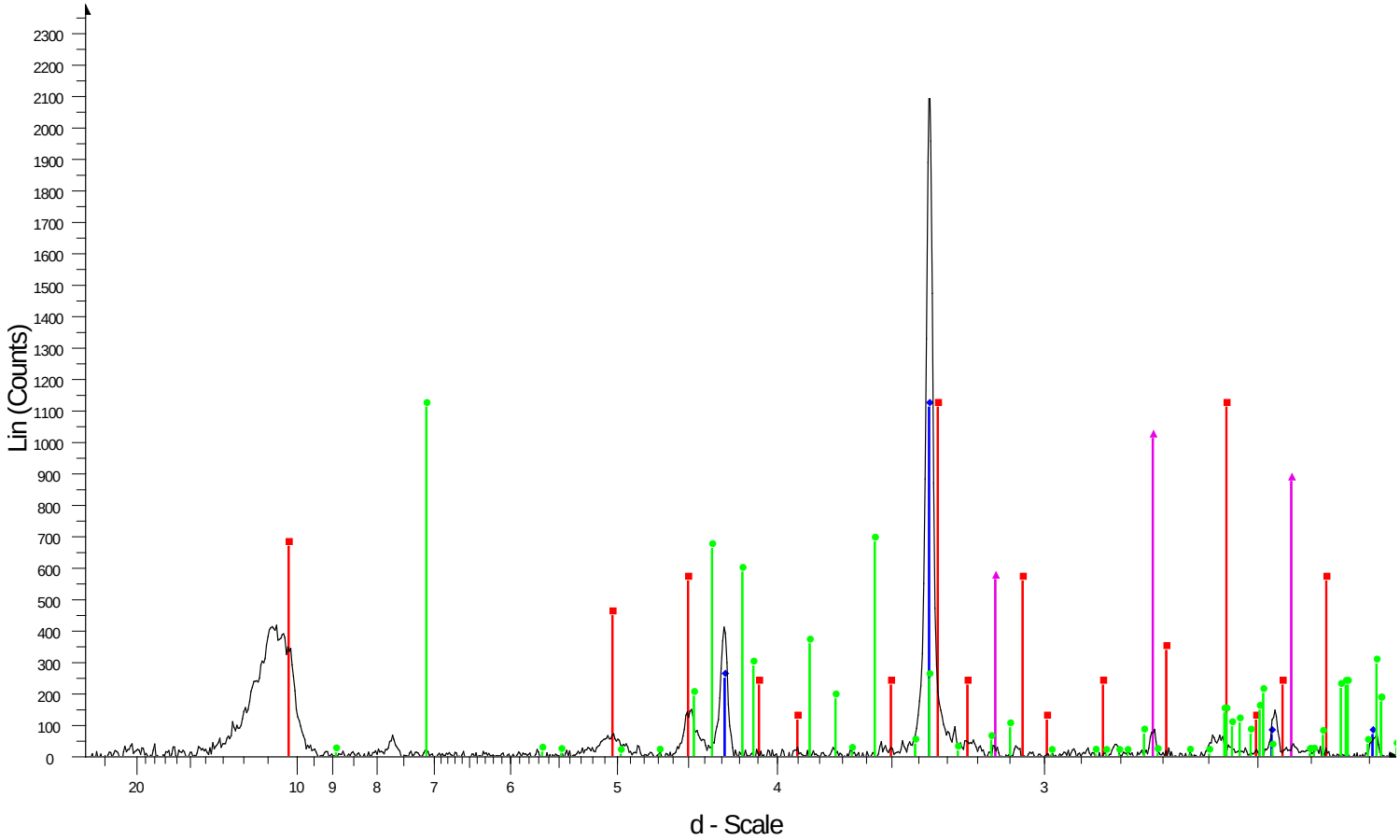

Dunedin d-075e/094n-8 best river 3688.8 - File: mattdunedind75e 3688_8.RAW - Type: 2Th/Th locked - Start: 3.000 ° - End: 40.000 ° - Step: 0.040 ° - Step time: 1. s - Temp.: 25 °C (Room) - Time Start
Operations: Background 1.000,1.000 | Import

00-015-0603 (D) - Illite - K(AlFe)2AlSi3O10(OH)2·H2O - Y: 50.54 % - d x by: 1. - WL: 1.54056 -

01-078-1252 (A) - Quartz low, syn - SiO2 - Y: 50.54 % - d x by: 1.0042 - WL: 1.54056 - Hexagonal - a 4.91920 - b 4.91920 - c 5.40500 - alpha 90.000 - beta 90.000 - gamma 120.000 - Primitive - P3221

01-078-2110 (C) - Kaolinite - Al4(OH)8(Si4O10) - Y: 50.54 % - d x by: 1. - WL: 1.54056 - Triclinic - a 5.14971 - b 8.93507 - c 7.38549 - alpha 91.928 - beta 105.042 - gamma 89.791 - Primitive - P1 (1) -

01-079-0617 (A) - Pyrite - FeS2 - Y: 50.00 % - d x by: 1. - WL: 1.54056 - Cubic - a 5.44100 - b 5.44100 - c 5.44100 - alpha 90.000 - beta 90.000 - gamma 90.000 - Primitive - Pa-3 (205) - 4 - 161.078 - I/I

Dunedin d-75-E/94-N-8 3695.1 m

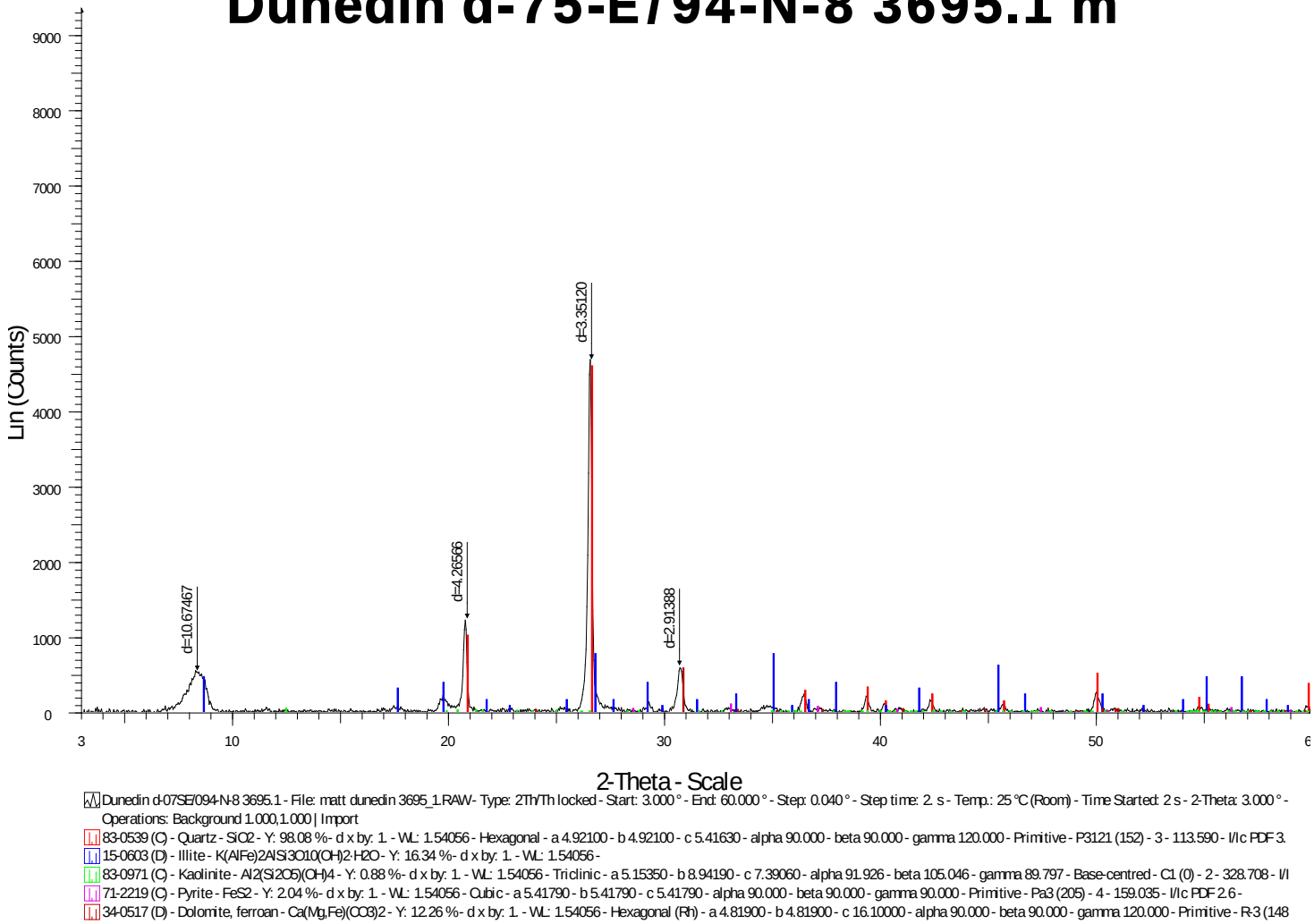

Dunedin d-07SE/094-N-8 3695.1 - File: matt dunedin 3695_1.RAW - Type: 2Th/Th locked - Start: 3.000 ° - End: 60.000 ° - Step: 0.040 ° - Step time: 2. s - Temp.: 25 °C (Room) - Time Started: 2 s - 2-Theta: 3.000 ° - Operations: Background 1.000,1.000 | Import

83-0539 (C) - Quartz - SiO2 - Y: 98.08 % - d x by: 1. - WL: 1.54056 - Hexagonal - a 4.92100 - b 4.92100 - c 5.41630 - alpha 90.000 - beta 90.000 - gamma 120.000 - Primitive - P3121 (152) - 3 - 113.590 - I/Ic PDF 3.

15-0603 (D) - Illite - K(AlFe)2AlSi3O10(OH)2-H2O - Y: 16.34 % - d x by: 1. - WL: 1.54056 -

83-0971 (C) - Kaolinite - Al2(Si2O5)(OH)4 - Y: 0.88 % - d x by: 1. - WL: 1.54056 - Triclinic - a 5.15350 - b 8.94190 - c 7.39060 - alpha 91.926 - beta 105.046 - gamma 89.797 - Base-centred - C1 (0) - 2 - 328.708 - I/I

71-2219 (C) - Pyrite - FeS2 - Y: 2.04 % - d x by: 1. - WL: 1.54056 - Cubic - a 5.41790 - b 5.41790 - c 5.41790 - alpha 90.000 - beta 90.000 - gamma 90.000 - Primitive - Pa3 (205) - 4 - 159.035 - I/Ic PDF 2.6 -

34-0517 (D) - Dolomite, ferroan - Ca(Mg,Fe)(CO3)2 - Y: 12.26 % - d x by: 1. - WL: 1.54056 - Hexagonal (Rh) - a 4.81900 - b 4.81900 - c 16.10000 - alpha 90.000 - beta 90.000 - gamma 120.000 - Primitive - R-3 (148

[Dunedin d-75-E/94-N-8 3707.1 m

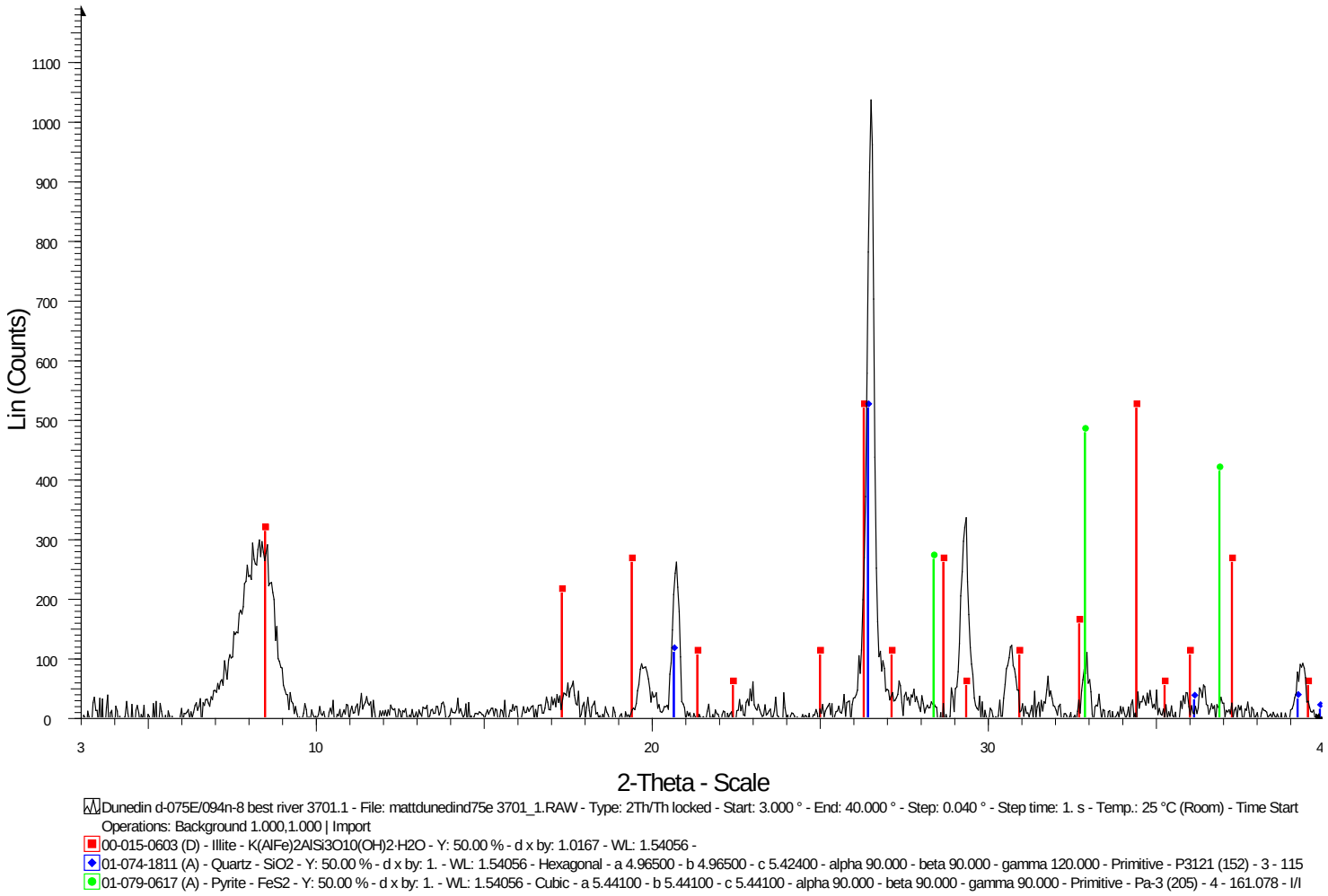

Dunedin d-75-E/94-N-8 3775.0 m

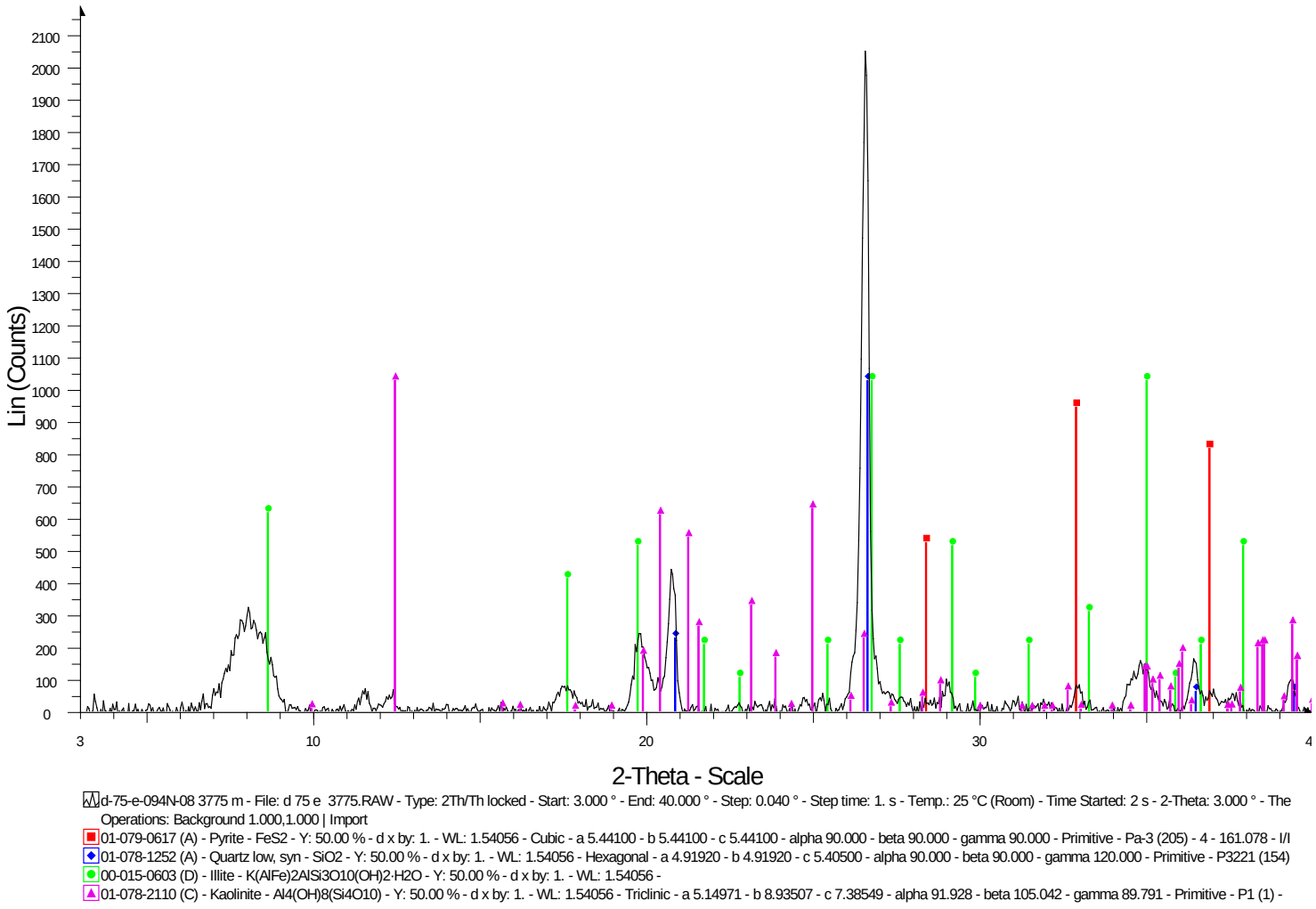

d-75-e-094N-08 3775 m - File: d 75 e 3775.RAW - Type: 2Th/Th locked - Start: 3.000 ° - End: 40.000 ° - Step: 0.040 ° - Step time: 1. s - Temp.: 25 °C (Room) - Time Started: 2 s - 2-Theta: 3.000 ° - The Operations: Background 1.000,1.000 | Import

01-079-0617 (A) - Pyrite - FeS2 - Y: 50.00 % - d x by: 1. - WL: 1.54056 - Cubic - a 5.44100 - b 5.44100 - c 5.44100 - alpha 90.000 - beta 90.000 - gamma 90.000 - Primitive - Pa-3 (205) - 4 - 161.078 - I/I

01-078-1252 (A) - Quartz low, syn - SiO2 - Y: 50.00 % - d x by: 1. - WL: 1.54056 - Hexagonal - a 4.91920 - b 4.91920 - c 5.40500 - alpha 90.000 - beta 90.000 - gamma 120.000 - Primitive - P3221 (154)

00-015-0603 (D) - Illite - K(AlFe)2AlSi3O10(OH)2·H2O - Y: 50.00 % - d x by: 1. - WL: 1.54056 -

01-078-2110 (C) - Kaolinite - Al4(OH)8(Si4O10) - Y: 50.00 % - d x by: 1. - WL: 1.54056 - Triclinic - a 5.14971 - b 8.93507 - c 7.38549 - alpha 91.928 - beta 105.042 - gamma 89.791 - Primitive - P1 (1) -

Dunedin d-75-E/94-N-8 3891.8 m

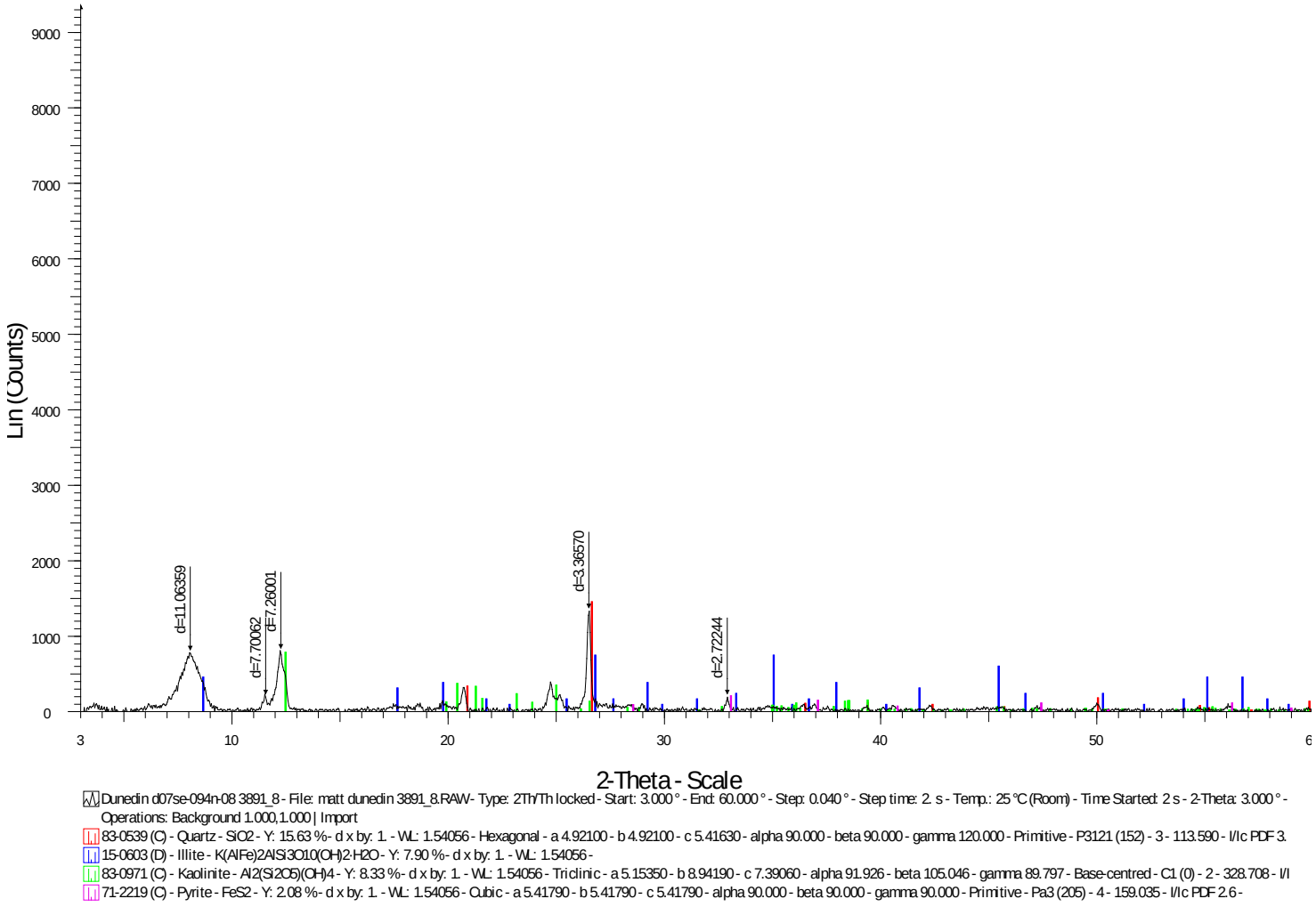

Dunedin d07se-094n-08 3891_8 - File: matt dunedin 3891_8.RAW- Type: 2Th/Th locked - Start: 3.000 ° - End: 60.000 ° - Step: 0.040 ° - Step time: 2. s - Temp.: 25 °C (Room) - Time Started: 2 s - 2-Theta: 3.000 ° - Operations: Background 1.000,1.000 | Import

83-0539 (C) - Quartz - SiO2 - Y: 15.63 %- d x by: 1. - WL: 1.54056 - Hexagonal - a 4.92100 - b 4.92100 - c 5.41630 - alpha 90.000 - beta 90.000 - gamma 120.000 - Primitive - P3121 (152) - 3 - 113.590 - I/Ic PDF 3.

15-0603 (D) - Illite - K(AlFe)2AlSi3O10(OH)2-H2O - Y: 7.90 %- d x by: 1. - WL: 1.54056 -

83-0971 (C) - Kaolinite - Al2(Si2O5)(OH)4 - Y: 8.33 %- d x by: 1. - WL: 1.54056 - Triclinic - a 5.15350 - b 8.94190 - c 7.39060 - alpha 91.926 - beta 105.046 - gamma 89.797 - Base-centred - C1 (0) - 2 - 328.708 - I/I

71-2219 (C) - Pyrite - FeS2 - Y: 2.08 %- d x by: 1. - WL: 1.54056 - Cubic - a 5.41790 - b 5.41790 - c 5.41790 - alpha 90.000 - beta 90.000 - gamma 90.000 - Primitive - Pa3 (205) - 4 - 159.035 - I/Ic PDF 2.6 -

Dunedin d-75-E/94-N-8 3892.1 m

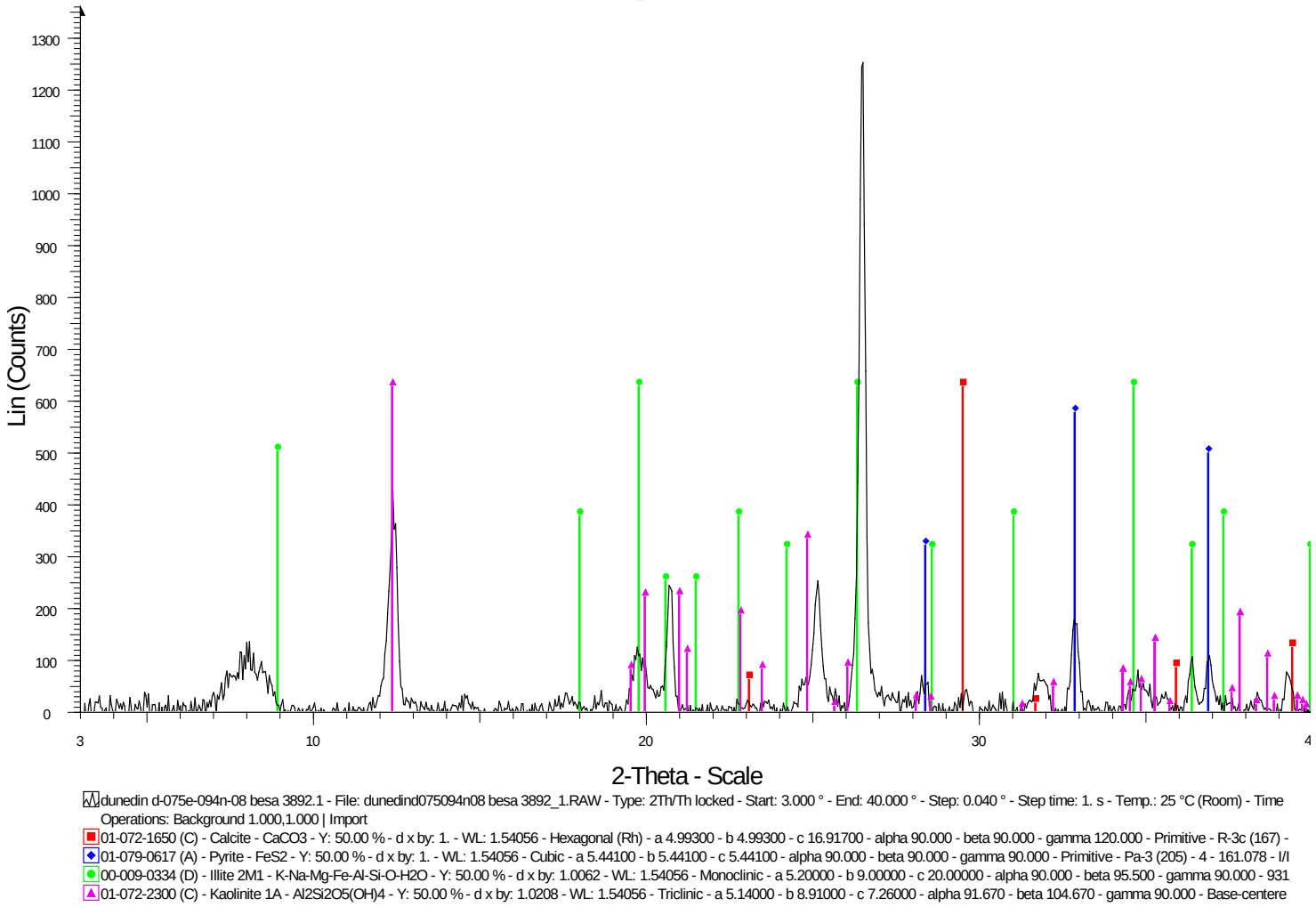

dunedin d-075e-094n-08 besa 3892.1 - File: dunedind075094n08 besa 3892_1.RAW - Type: 2Th/Th locked - Start: 3.000 ° - End: 40.000 ° - Step: 0.040 ° - Step time: 1. s - Temp.: 25 °C (Room) - Time Operations: Background 1.000,1.000 | Import

01-072-1650 (C) - Calcite - CaCO3 - Y: 50.00 % - d x by: 1. - WL: 1.54056 - Hexagonal (Rh) - a 4.99300 - b 4.99300 - c 16.91700 - alpha 90.000 - beta 90.000 - gamma 120.000 - Primitive - R-3c (167) -

01-079-0617 (A) - Pyrite - FeS2 - Y: 50.00 % - d x by: 1. - WL: 1.54056 - Cubic - a 5.44100 - b 5.44100 - c 5.44100 - alpha 90.000 - beta 90.000 - gamma 90.000 - Primitive - Pa-3 (205) - 4 - 161.078 - I/I

00-009-0334 (D) - Illite 2M1 - K-Na-Mg-Fe-Al-Si-O-H2O - Y: 50.00 % - d x by: 1.0062 - WL: 1.54056 - Monoclinic - a 5.20000 - b 9.00000 - c 20.00000 - alpha 90.000 - beta 95.500 - gamma 90.000 - 931

01-072-2300 (C) - Kaolinite 1A - Al2Si2O5(OH)4 - Y: 50.00 % - d x by: 1.0208 - WL: 1.54056 - Triclinic - a 5.14000 - b 8.91000 - c 7.26000 - alpha 91.670 - beta 104.670 - gamma 90.000 - Base-centere

Dunedin d-75-E/94-N-8 3893.0 m

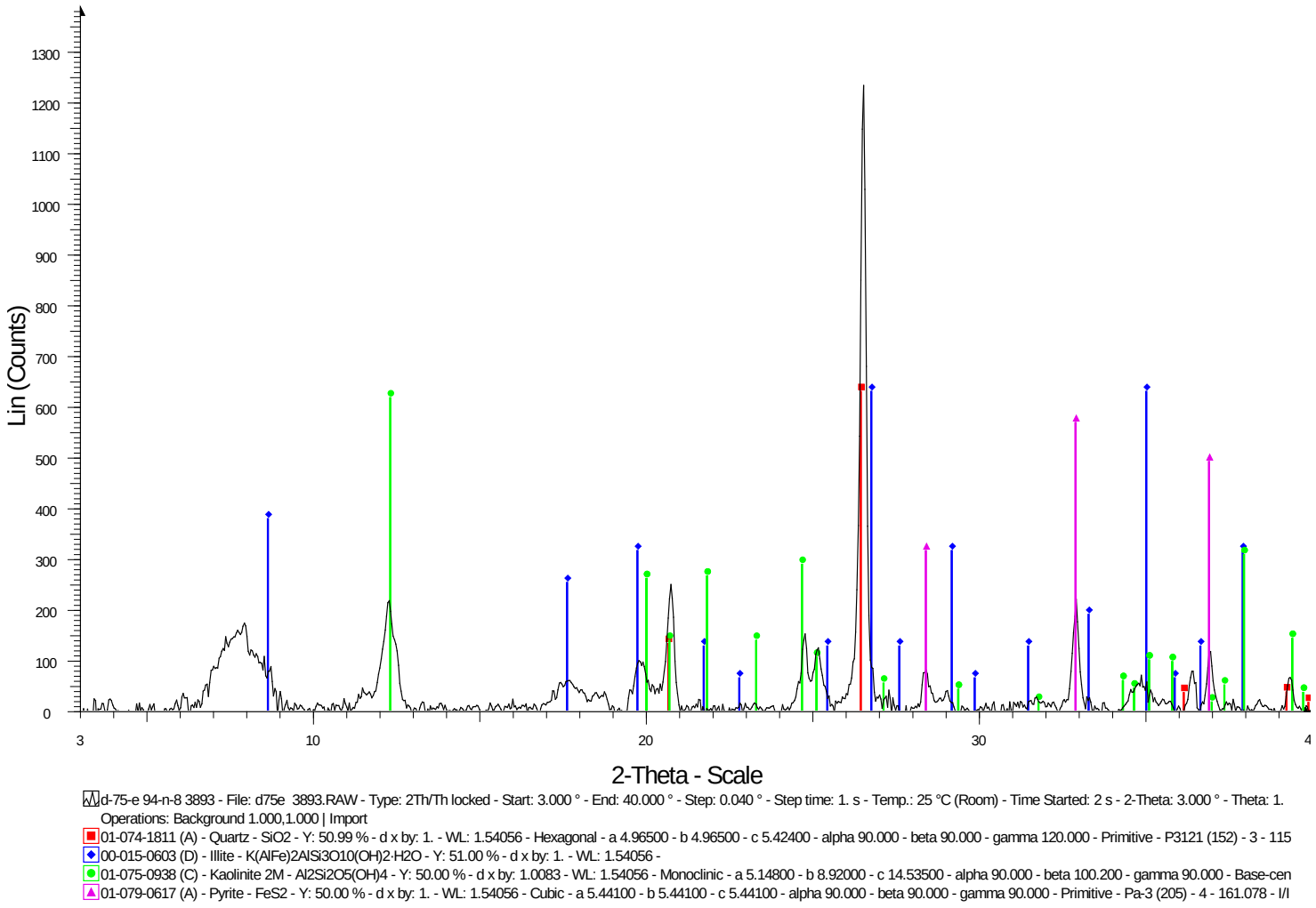

d-75-e 94-n-8 3893 - File: d75e 3893.RAW - Type: 2Th/Th locked - Start: 3.000 ° - End: 40.000 ° - Step: 0.040 ° - Step time: 1. s - Temp.: 25 °C (Room) - Time Started: 2 s - 2-Theta: 3.000 ° - Theta: 1.
Operations: Background 1.000,1.000 | Import

01-074-1811 (A) - Quartz - SiO2 - Y: 50.99 % - d x by: 1. - WL: 1.54056 - Hexagonal - a 4.96500 - b 4.96500 - c 5.42400 - alpha 90.000 - beta 90.000 - gamma 120.000 - Primitive - P3121 (152) - 3 - 115

00-015-0603 (D) - Illite - K(AlFe)2AlSi3O10(OH)2·H2O - Y: 51.00 % - d x by: 1. - WL: 1.54056 -

01-075-0938 (C) - Kaolinite 2M - Al2Si2O5(OH)4 - Y: 50.00 % - d x by: 1.0083 - WL: 1.54056 - Monoclinic - a 5.14800 - b 8.92000 - c 14.53500 - alpha 90.000 - beta 100.200 - gamma 90.000 - Base-cen

01-079-0617 (A) - Pyrite - FeS2 - Y: 50.00 % - d x by: 1. - WL: 1.54056 - Cubic - a 5.44100 - b 5.44100 - c 5.44100 - alpha 90.000 - beta 90.000 - gamma 90.000 - Primitive - Pa-3 (205) - 4 - 161.078 - I/I

Dunedin d-75-E/94-N-8 3894.5 m

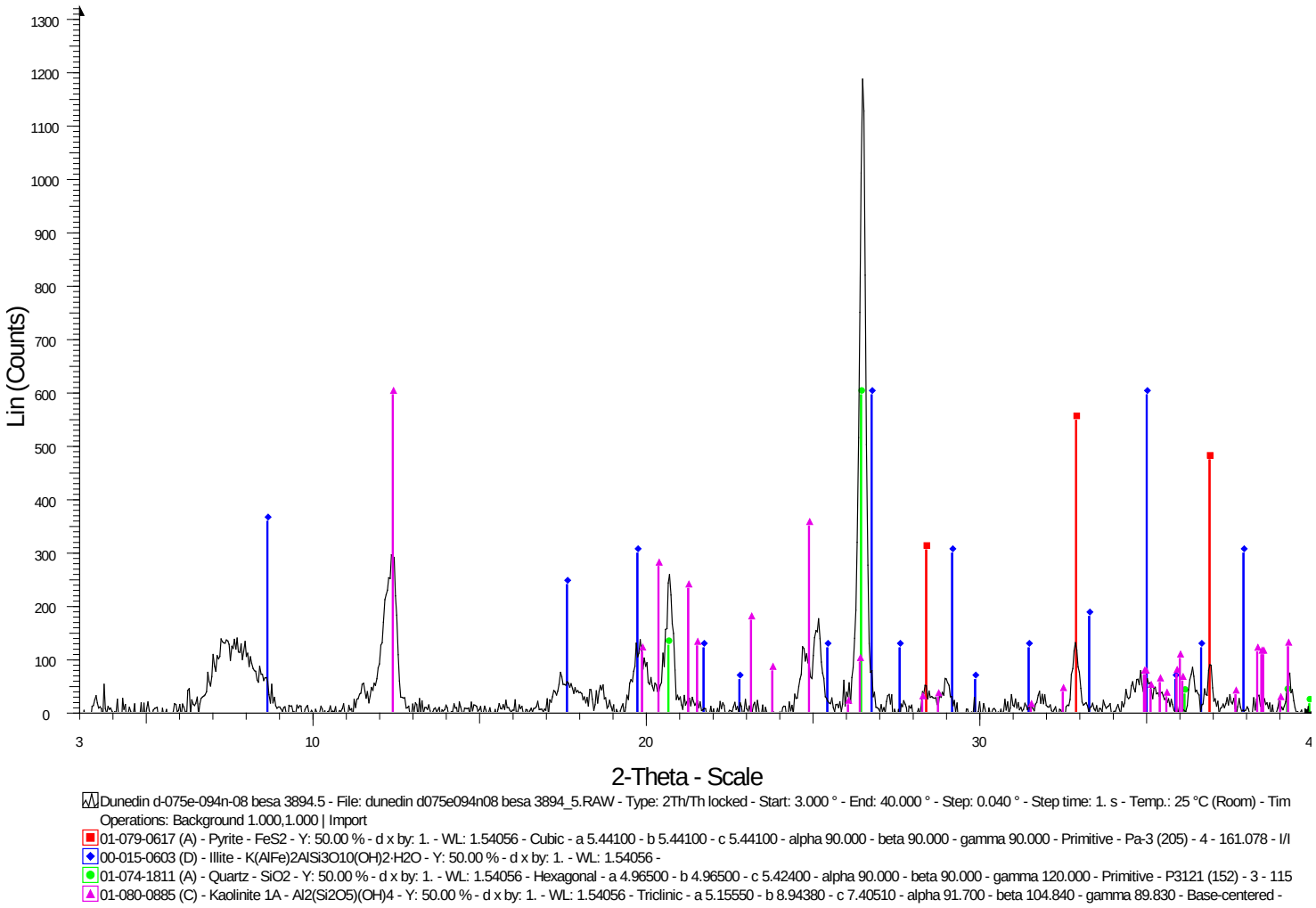

Dunedin d-75-E/94-N-8 3895.7 m

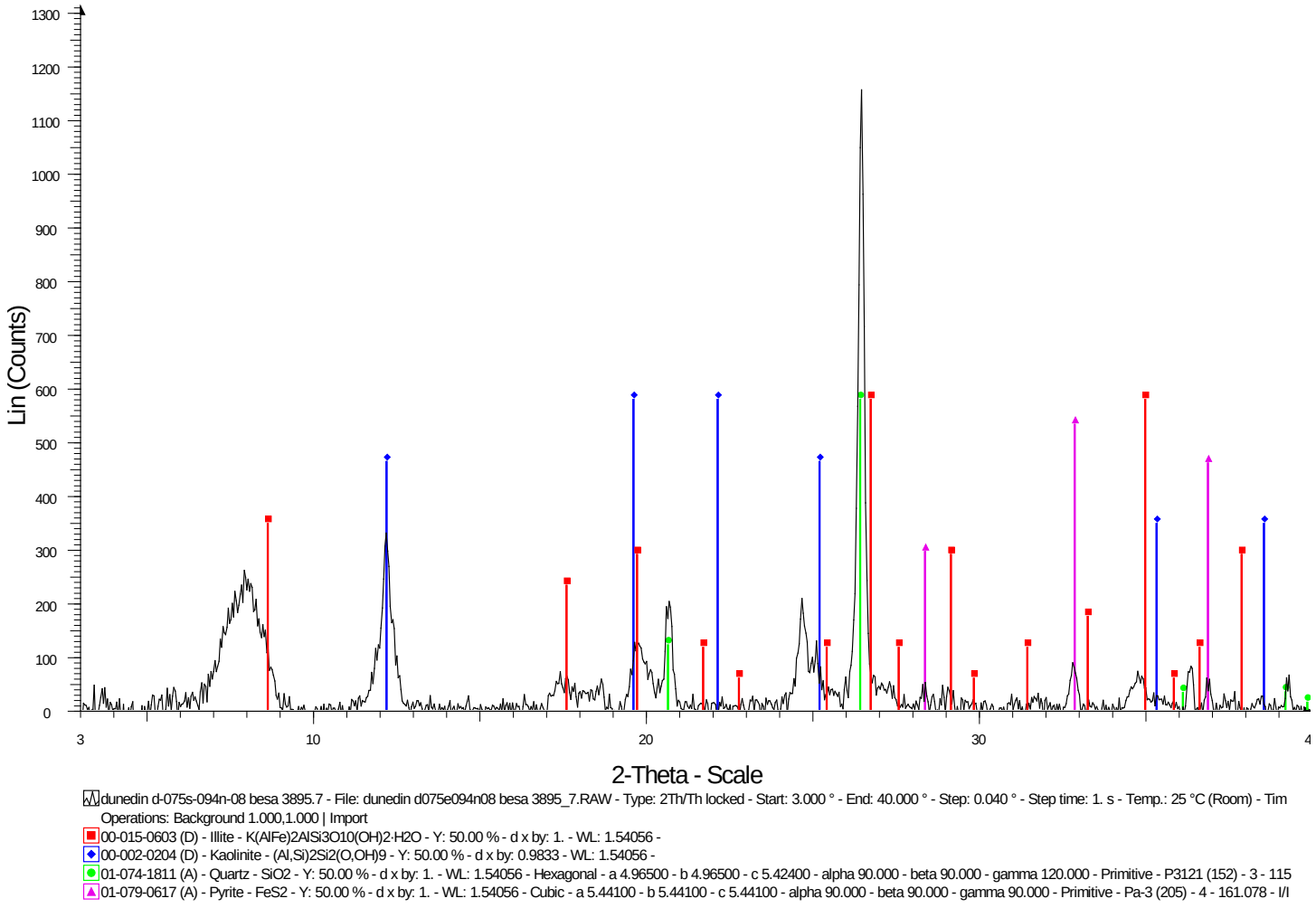

Dunedin d-75-E/94-N-8 3896.0 m

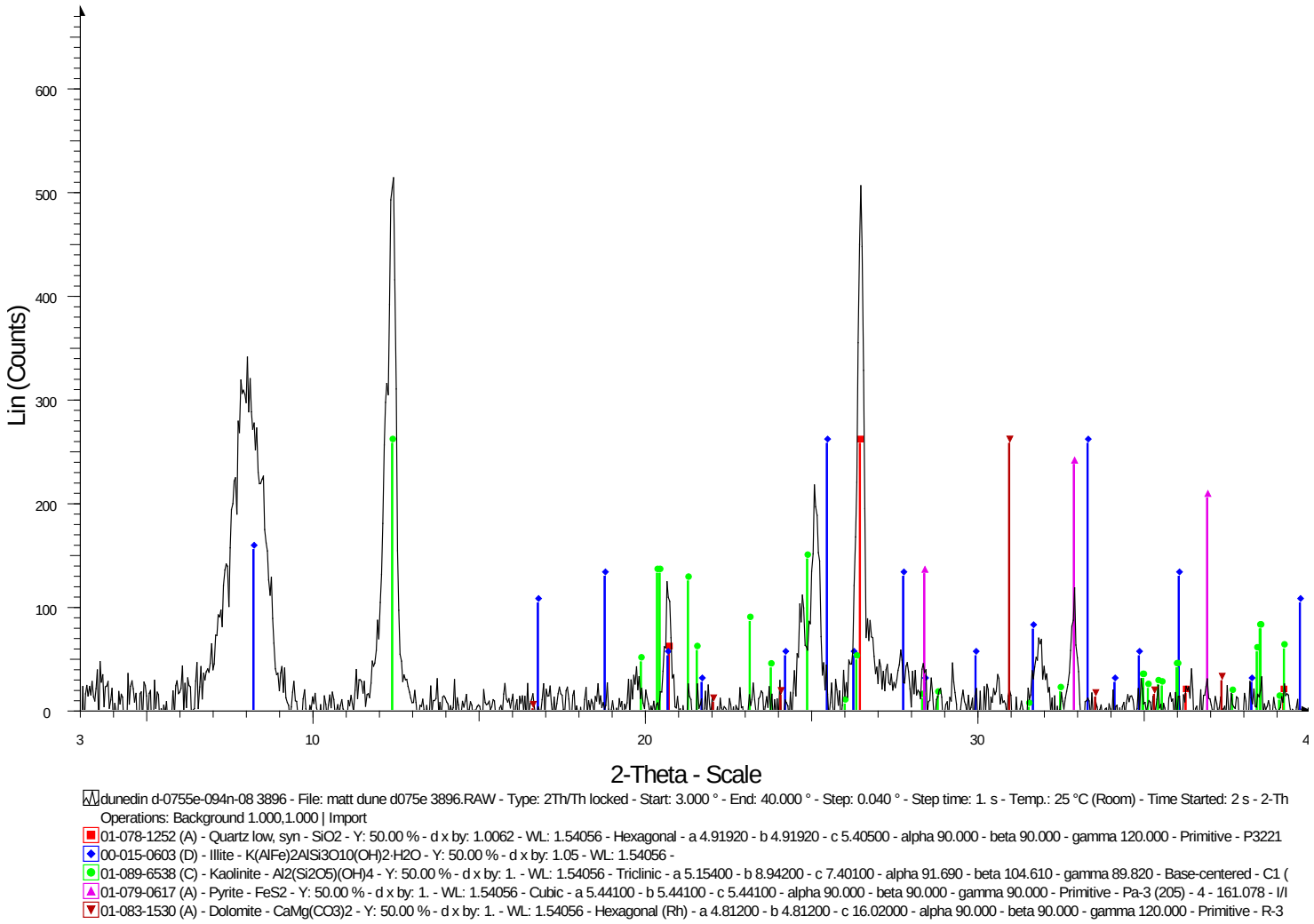

La Biche b-55-E/94-O-13 3044.8 m

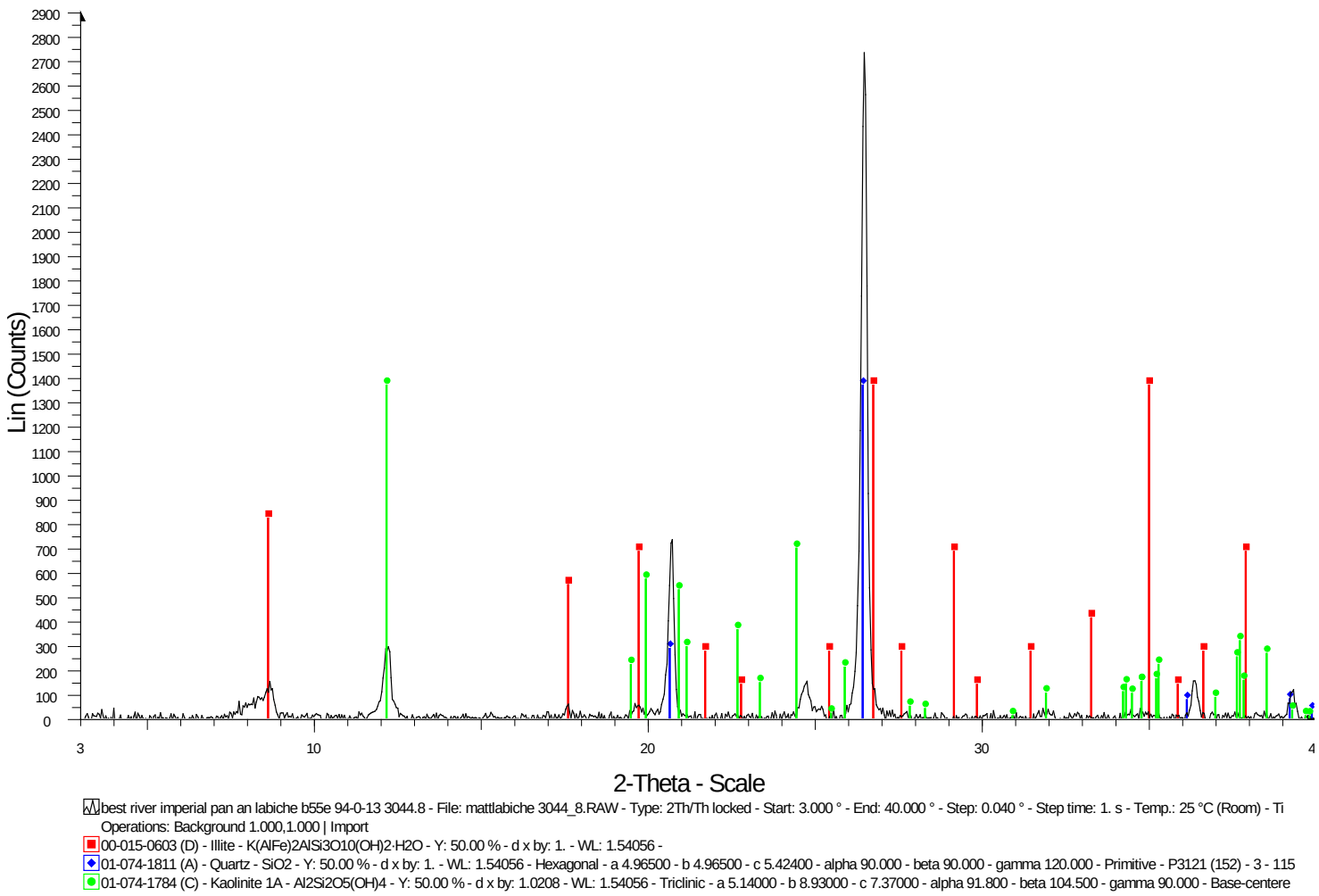

Imperia **La Biche b-55-E/94-O-13 3047.2 m**

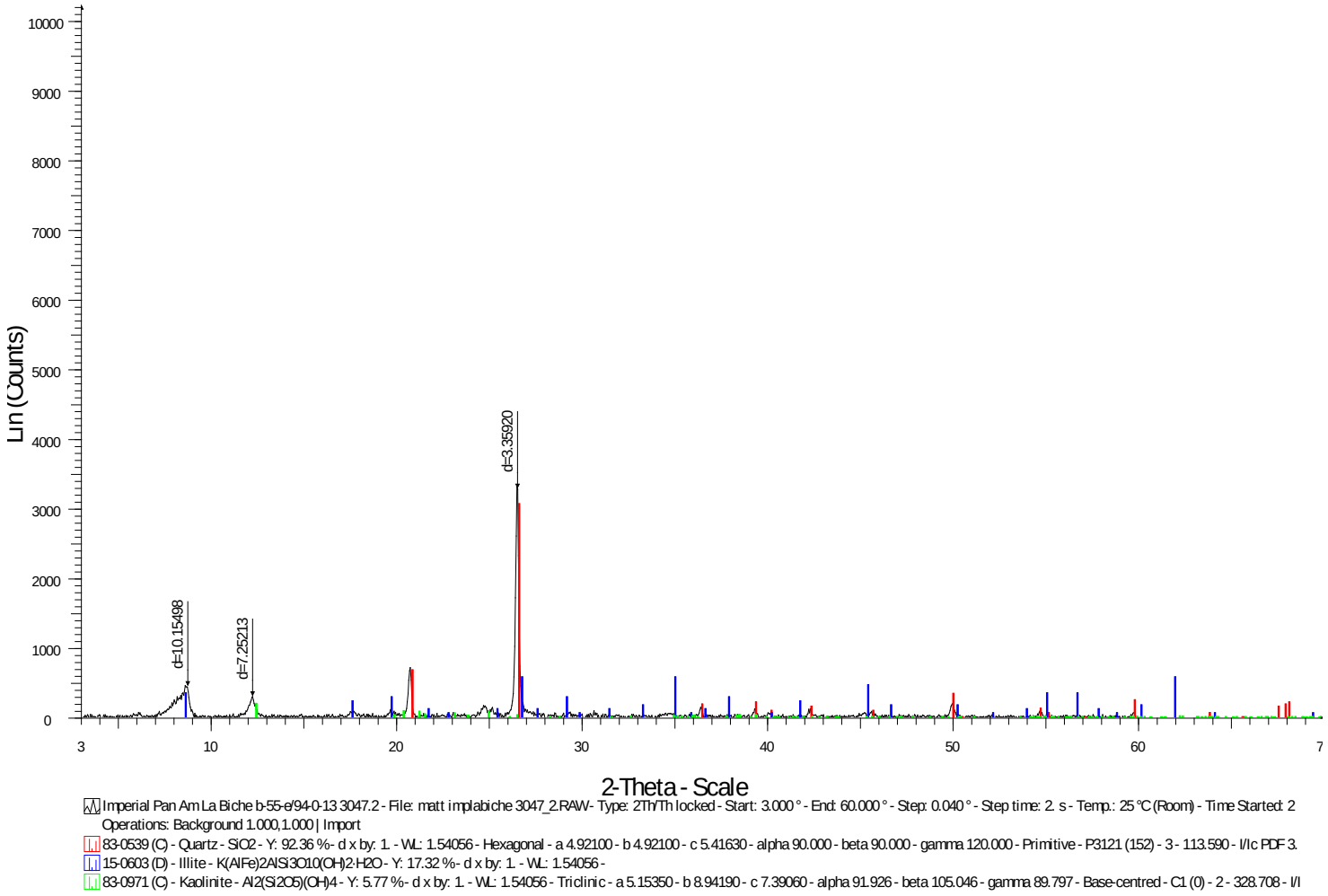

EXSHAW SAMPLES

Well	Location	Depth (m)
Golata	8-29-83-15W6	3386.55
		3390.10
Sikanni Chief	b-92-D/94-I-4	1573.80

Golata 8-29-83-15W6 3386.55 m

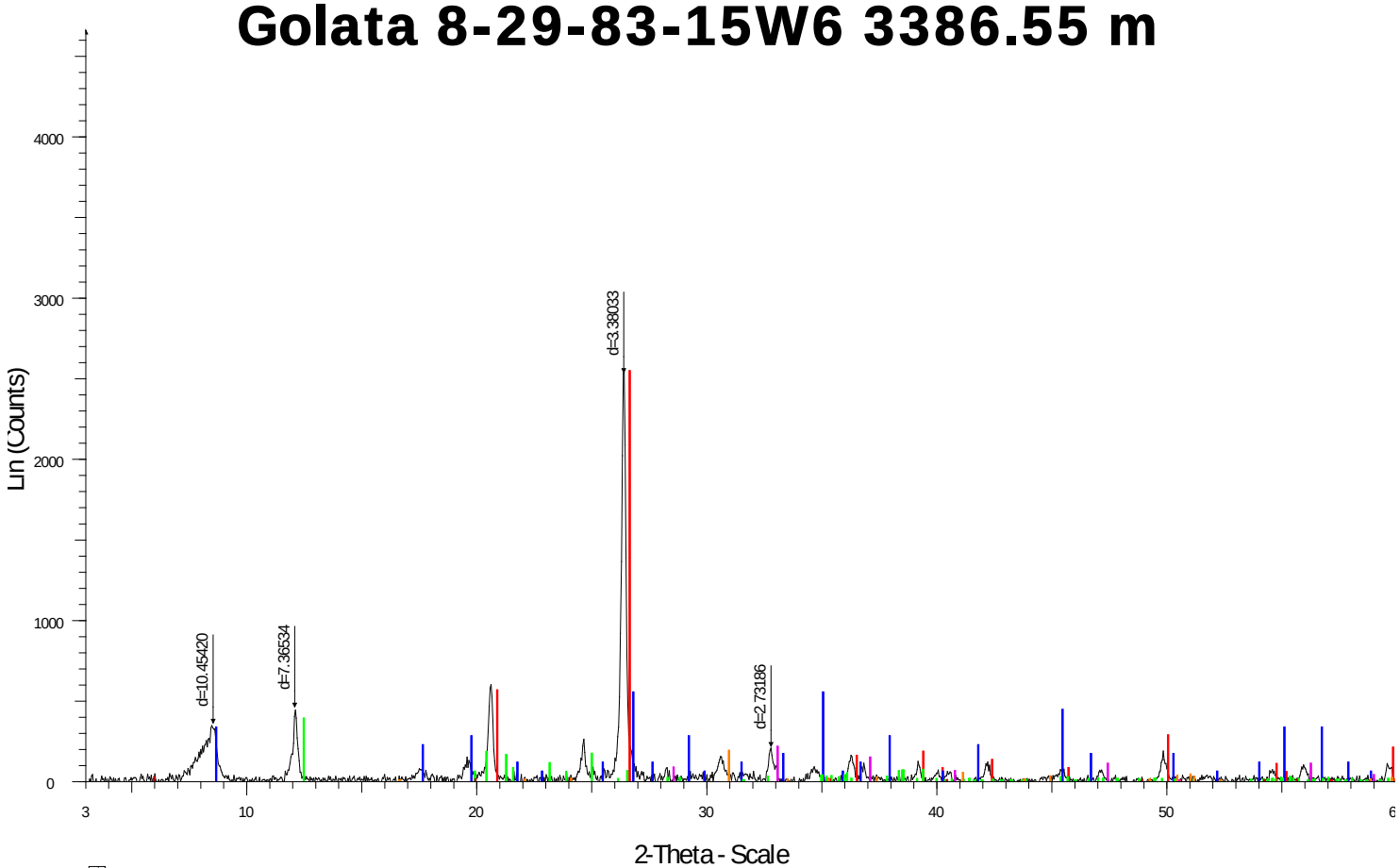

Golata 8-29-85-15W6 3386.55 - File: matt galota 8_29 3386_55.RAW - Type: 2Th/Th locked - Start: 3.000 ° - End: 60.000 ° - Step: 0.040 ° - Step time: 2. s - Temp.: 25 °C (Room) - Time Started: 2 s - 2-Theta: 3.000
Operations: Background 1.000,1.000 | Import

83-0539 (C) - Quartz - SiO2 - Y: 100.19 % - d x by: 1. - WL: 1.54056 - Hexagonal - a 4.92100 - b 4.92100 - c 5.41630 - alpha 90.000 - beta 90.000 - gamma 120.000 - Primitive - P3121 (152) - 3 - 113.590 - I/Ic PDF 3

15-0603 (D) - Illite - K(AlFe)2AlSi3O10(OH)2·H2O - Y: 21.54 % - d x by: 1. - WL: 1.54056 -

83-0971 (C) - Kaolinite - Al2(Si2O5)(OH)4 - Y: 15.10 % - d x by: 1. - WL: 1.54056 - Triclinic - a 5.15350 - b 8.94190 - c 7.39060 - alpha 91.926 - beta 105.046 - gamma 89.797 - Base-centred - C1 (0) - 2 - 328.708 - I

71-2219 (C) - Pyrite - FeS2 - Y: 8.23 % - d x by: 1. - WL: 1.54056 - Cubic - a 5.41790 - b 5.41790 - c 5.41790 - alpha 90.000 - beta 90.000 - gamma 90.000 - Primitive - Pa3 (205) - 4 - 159.035 - I/Ic PDF 2.6 -

03-0015 (D) - Montmorillonite (bentonite) - (Na,Ca)0.3(Al,Mg)2Si4O10(OH)2·xH2O - Y: 0.79 % - d x by: 1. - WL: 1.54056 -

84-1208 (C) - Dolomite - CaMg(CO3)2 - Y: 7.22 % - d x by: 1. - WL: 1.54056 - Hexagonal (Rh) - a 4.81100 - b 4.81100 - c 16.04700 - alpha 90.000 - beta 90.000 - gamma 120.000 - Primitive - R-3 (148) - 3 - 321.659

Golata 8-29-83-15W6 3390.1 m

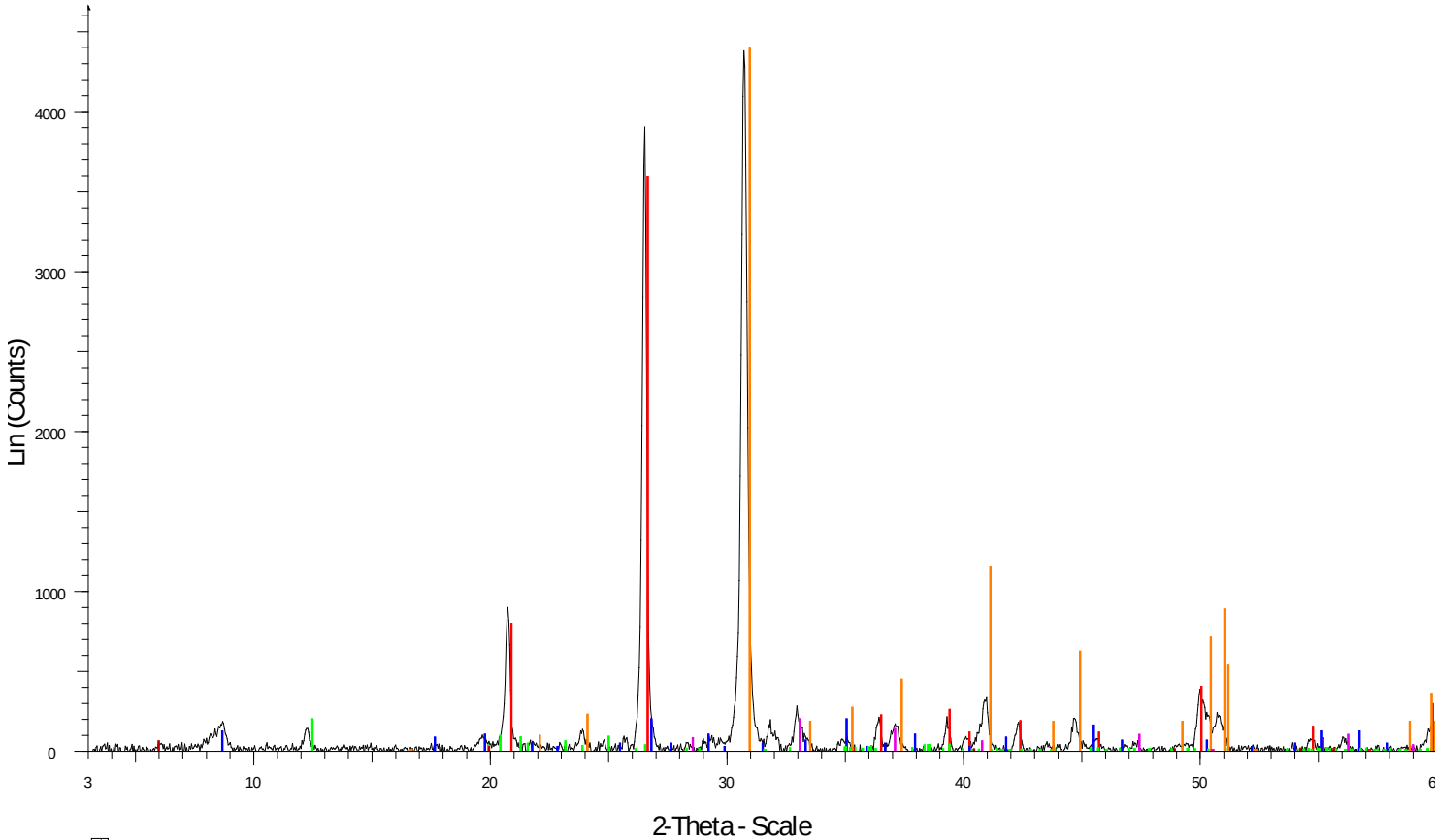

galata 3390.1 - File: matt galata 3390_1.RAW - Type: 2Th/Th locked - Start: 3.000 ° - End: 60.000 ° - Step: 0.040 ° - Step time: 2. s - Temp.: 25 °C (Room) - Time Started: 2 s - 2-Theta: 3.000 ° - Theta: 1.500 ° - Phi
Operations: Background 1.000,1.000 | Import

83-0539 (C) - Quartz - SiO2 - Y: 82.03 % - d x by: 1. - WL: 1.54056 - Hexagonal - a 4.92100 - b 4.92100 - c 5.41630 - alpha 90.000 - beta 90.000 - gamma 120.000 - Primitive - P3121 (152) - 3 - 113.590 - I/Ic PDF 3.

15-0603 (D) - Illite - K(AlFe)2AlSi3O10(OH)2·H2O - Y: 4.37 % - d x by: 1. - WL: 1.54056 -

83-0971 (C) - Kaolinite - Al2(Si2O5)(OH)4 - Y: 4.38 % - d x by: 1. - WL: 1.54056 - Triclinic - a 5.15350 - b 8.94190 - c 7.39060 - alpha 91.926 - beta 105.046 - gamma 89.797 - Base-centred - C1 (0) - 2 - 328.708 - I/I

71-2219 (C) - Pyrite - FeS2 - Y: 4.38 % - d x by: 1. - WL: 1.54056 - Cubic - a 5.41790 - b 5.41790 - c 5.41790 - alpha 90.000 - beta 90.000 - gamma 90.000 - Primitive - Pa3 (205) - 4 - 159.035 - I/Ic PDF 2.6 -

03-0015 (D) - Montmorillonite (bentonite) - (Na,Ca)0.3(Al,Mg)2Si4O10(OH)2·xH2O - Y: 1.23 % - d x by: 1. - WL: 1.54056 -

84-1208 (C) - Dolomite - CaMg(CO3)2 - Y: 100.47 % - d x by: 1. - WL: 1.54056 - Hexagonal (Rh) - a 4.81100 - b 4.81100 - c 16.04700 - alpha 90.000 - beta 90.000 - gamma 120.000 - Primitive - R-3 (148) - 3 - 321.6

Sikanni Chief b-92-D/94-I-4 1573.8 m

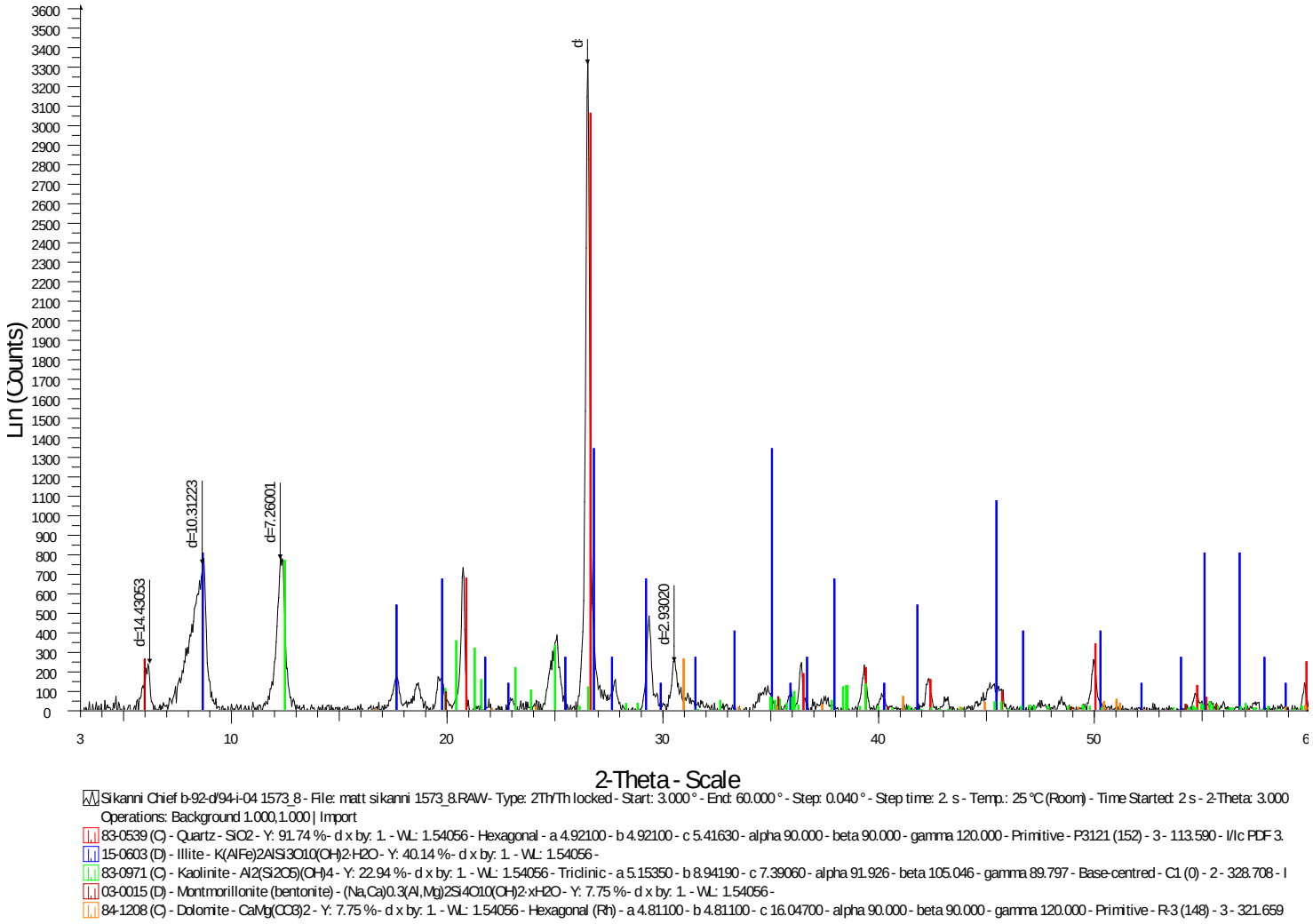

FORT SIMPSON SAMPLES

Well	Location	Depth (m)
Helmet	b-49-G/94-P-7	1810.90
		1812.30
		1813.10
		1815.10
		1816.50
Junior	c-60-E/94-I-11	1858.30
		1879.60
Sikanni Chief	b-92-D/94-I-4	2106.70
		2216.60
Kotcho	c-32-K/94-I-14	1979.20
		1981.10
		1982.20
		1984.40
		1985.60
		1988.10

Helmet b-49-G/94-P-7 1810.9 m

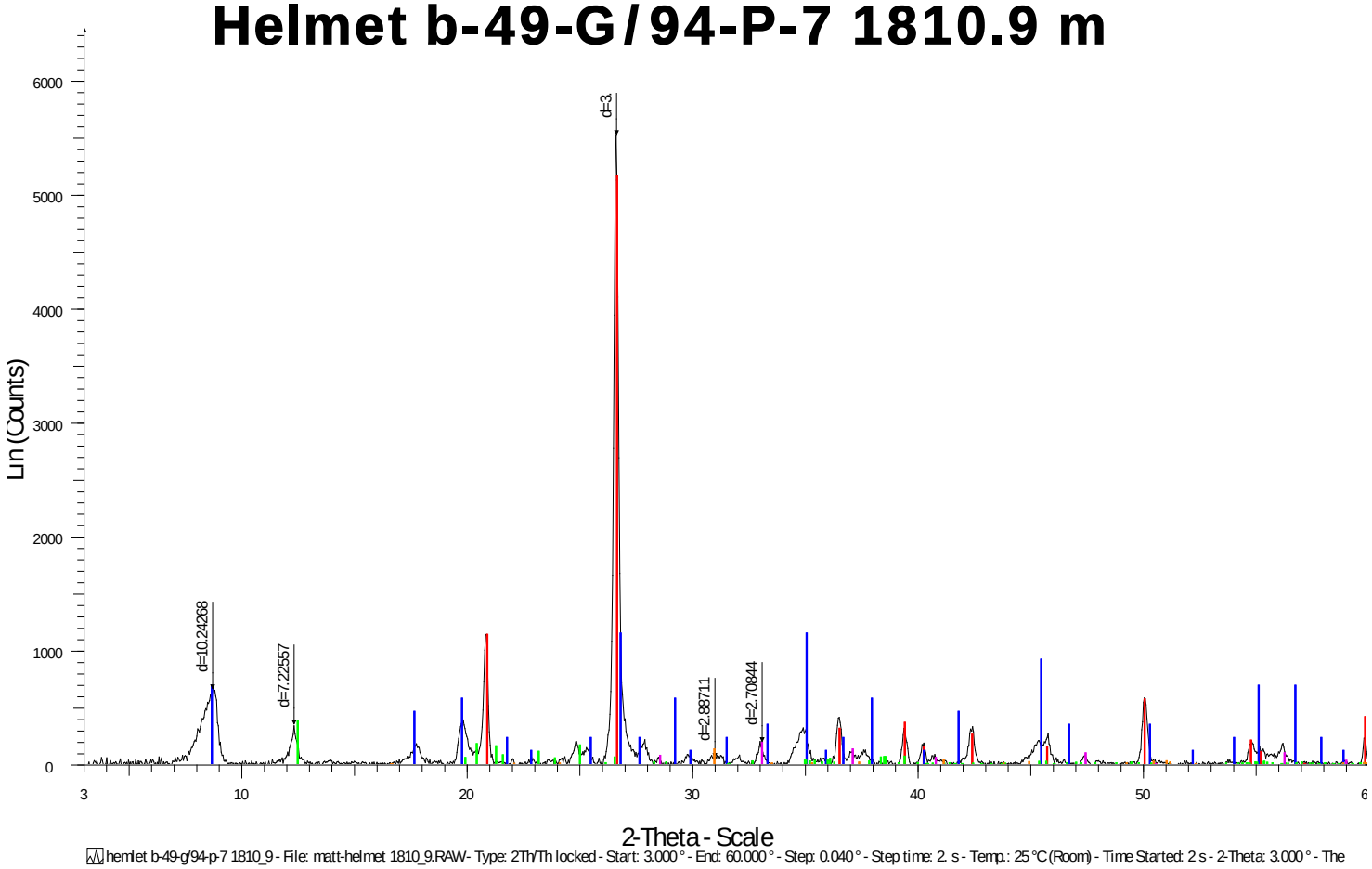

hemlet b-49-g/94-p-7 1810_9 - File: matt-helmet 1810_9.RAW - Type: 2Th/Th locked - Start: 3.000 ° - End: 60.000 ° - Step: 0.040 ° - Step time: 2. s - Temp.: 25 °C (Room) - Time Started: 2 s - 2-Theta: 3.000 ° - The Operations: Background 1.000,1.000 | Import

83-0539 (C) - Quartz - SiO2 - Y: 93.49 % - d x by: 1. - WL: 1.54056 - Hexagonal - a 4.92100 - b 4.92100 - c 5.41630 - alpha 90.000 - beta 90.000 - gamma 120.000 - Primitive - P3121 (152) - 3 - 113.590 - I/Ic PDF 3.

15-0603 (D) - Illite - K(AlFe)2AlSi3O10(OH)2·H2O - Y: 20.77 % - d x by: 1. - WL: 1.54056 -

83-0971 (C) - Kaolinite - Al2(Si2O5)(OH)4 - Y: 6.92 % - d x by: 1. - WL: 1.54056 - Triclinic - a 5.15350 - b 8.94190 - c 7.39060 - alpha 91.926 - beta 105.046 - gamma 89.797 - Base-centred - C1 (0) - 2 - 328.708 - I/I

71-2219 (C) - Pyrite - FeS2 - Y: 3.46 % - d x by: 1. - WL: 1.54056 - Cubic - a 5.41790 - b 5.41790 - c 5.41790 - alpha 90.000 - beta 90.000 - gamma 90.000 - Primitive - Pa3 (205) - 4 - 159.035 - I/Ic PDF 2.6 -

84-1208 (C) - Dolomite - CaMg(CO3)2 - Y: 2.34 % - d x by: 1. - WL: 1.54056 - Hexagonal (Rh) - a 4.81100 - b 4.81100 - c 16.04700 - alpha 90.000 - beta 90.000 - gamma 120.000 - Primitive - R-3 (148) - 3 - 321.659

Helmet b-49-G/94-P-7 1812.3 m

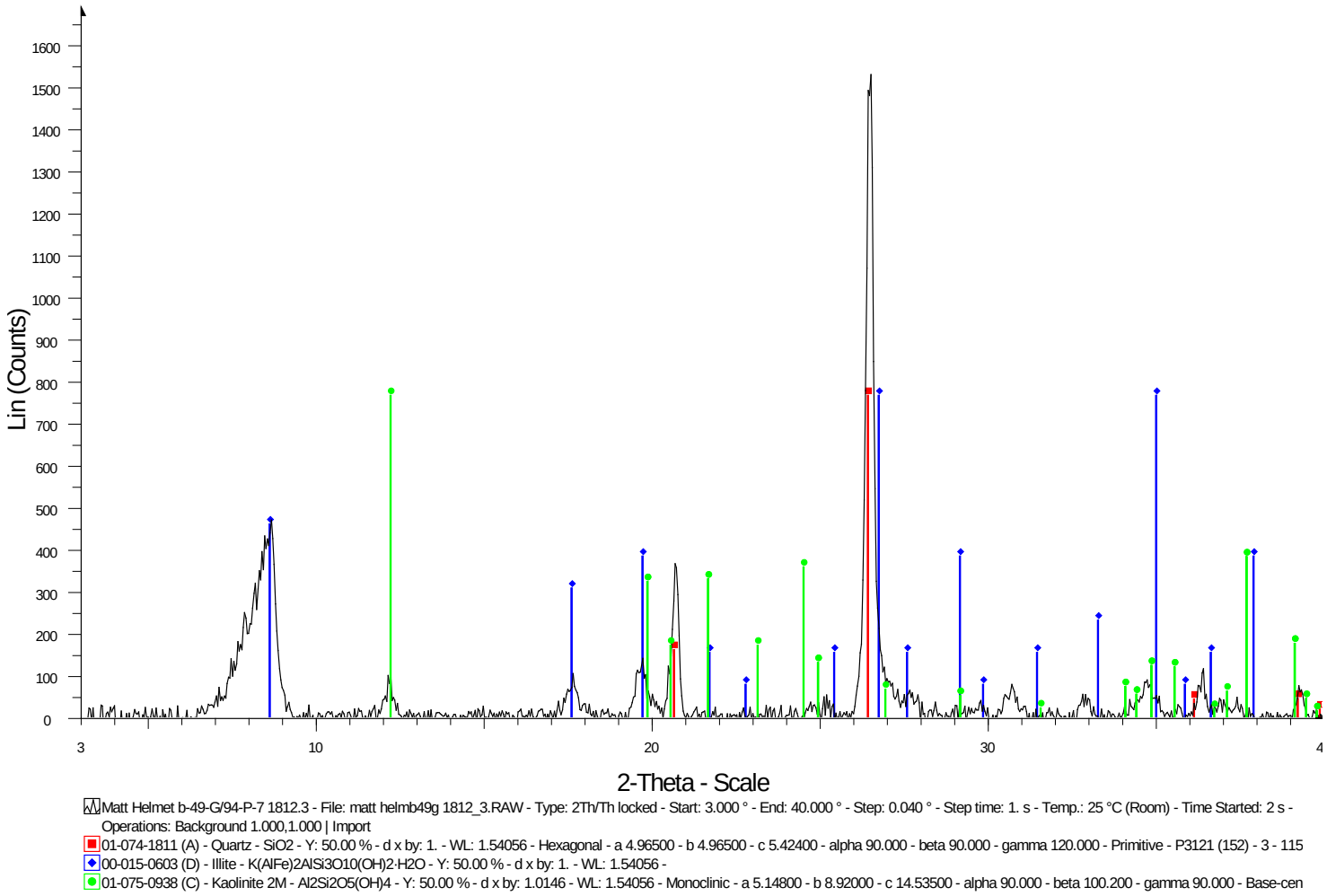

Helmet b-49-G/94-P-7 1813.1 m

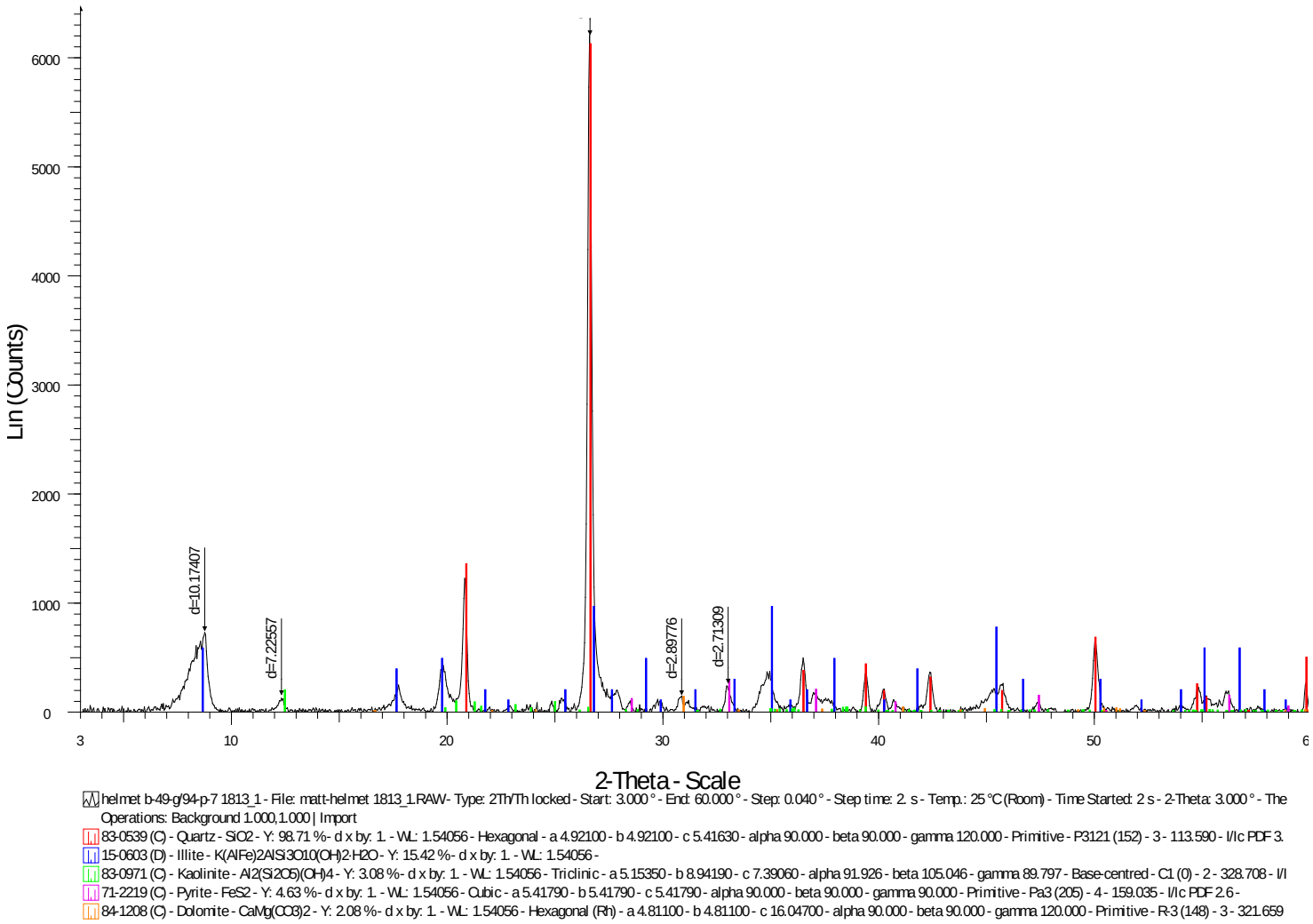

Helmet b-49-G/94-P-7 1815.1 m

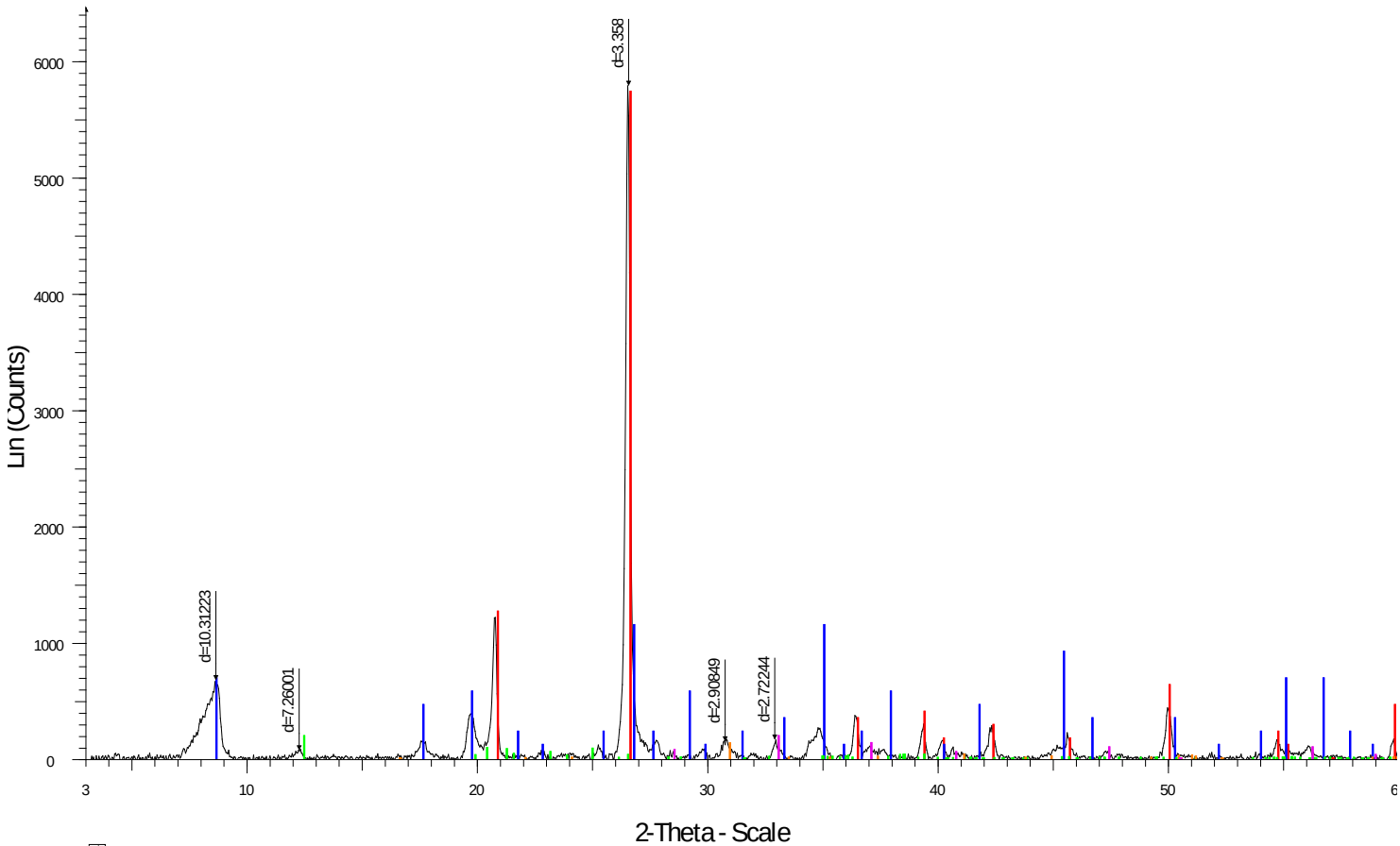

helmet b-49-g/94-p-7 1815_1 - File: matt-helmet 1815_1.RAW - Type: 2Th/Th locked - Start: 3.000 ° - End: 60.000 ° - Step: 0.040 ° - Step time: 2. s - Temp.: 25 °C (Room) - Time Started: 2 s - 2-Theta: 3.000 ° - The Operations: Background 1.000,1.000 | Import

83-0539 (C) - Quartz - SiO2 - Y: 99.15 % - d x by: 1. - WL: 1.54056 - Hexagonal - a 4.92100 - b 4.92100 - c 5.41630 - alpha 90.000 - beta 90.000 - gamma 120.000 - Primitive - P3121 (152) - 3 - 113.590 - I/Ic PDF 3.

15-0603 (D) - Illite - K(AlFe)2AlSi3O10(OH)2·H2O - Y: 19.83 % - d x by: 1. - WL: 1.54056 -

83-0971 (C) - Kaolinite - Al2(Si2O5)(OH)4 - Y: 3.31 % - d x by: 1. - WL: 1.54056 - Triclinic - a 5.15350 - b 8.94190 - c 7.39060 - alpha 91.926 - beta 105.046 - gamma 89.797 - Base-centred - C1 (0) - 2 - 328.708 - I/I

71-2219 (C) - Pyrite - FeS2 - Y: 3.31 % - d x by: 1. - WL: 1.54056 - Cubic - a 5.41790 - b 5.41790 - c 5.41790 - alpha 90.000 - beta 90.000 - gamma 90.000 - Primitive - Pa3 (205) - 4 - 159.035 - I/Ic PDF 2.6 -

84-1208 (C) - Dolomite - CaMg(CO3)2 - Y: 2.23 % - d x by: 1. - WL: 1.54056 - Hexagonal (Rh) - a 4.81100 - b 4.81100 - c 16.04700 - alpha 90.000 - beta 90.000 - gamma 120.000 - Primitive - R-3 (148) - 3 - 321.659

Helmet b-49-G/94-P-7 1816.5 m

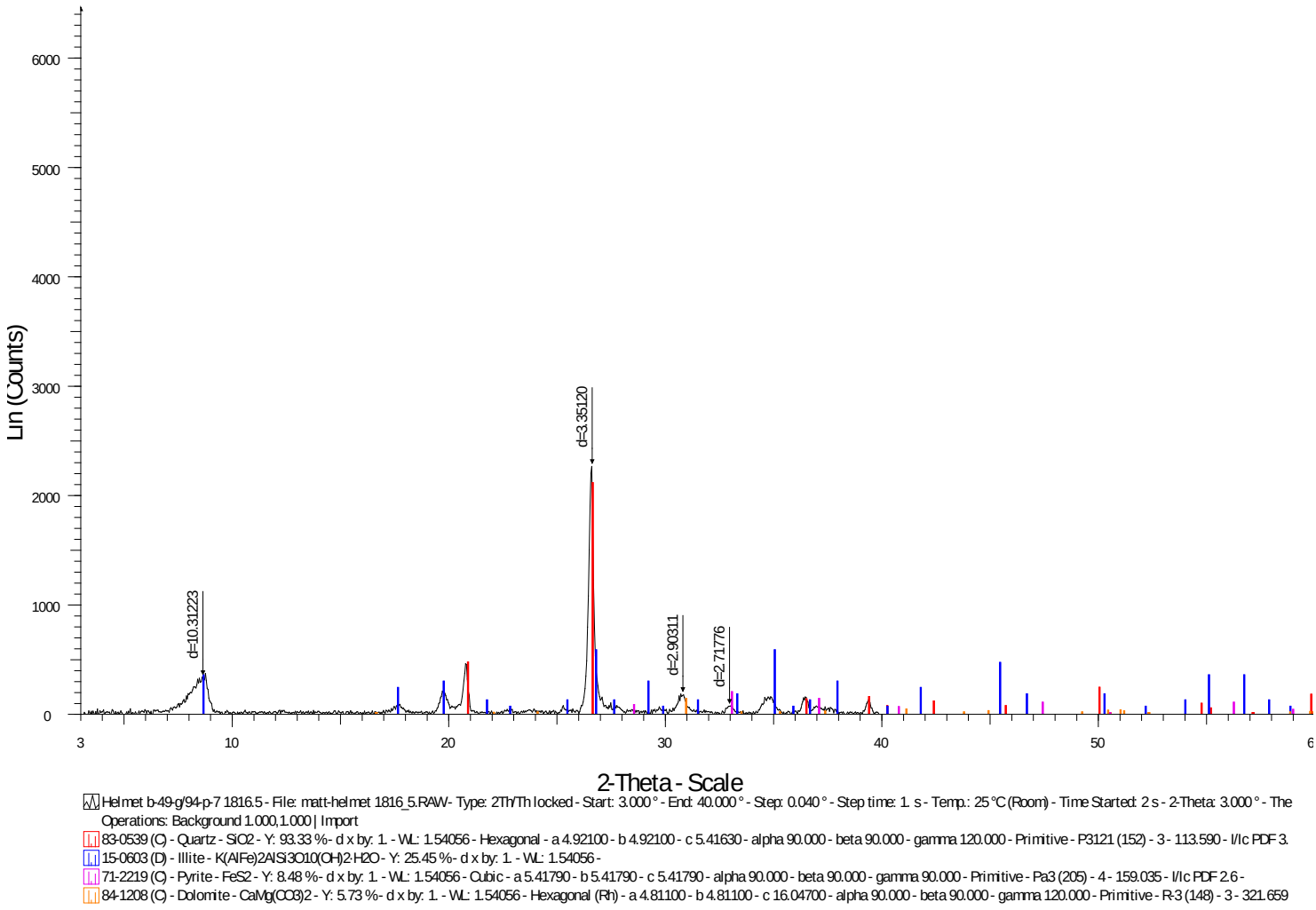

Junior c-60-E/94-I-11 1858.3 m

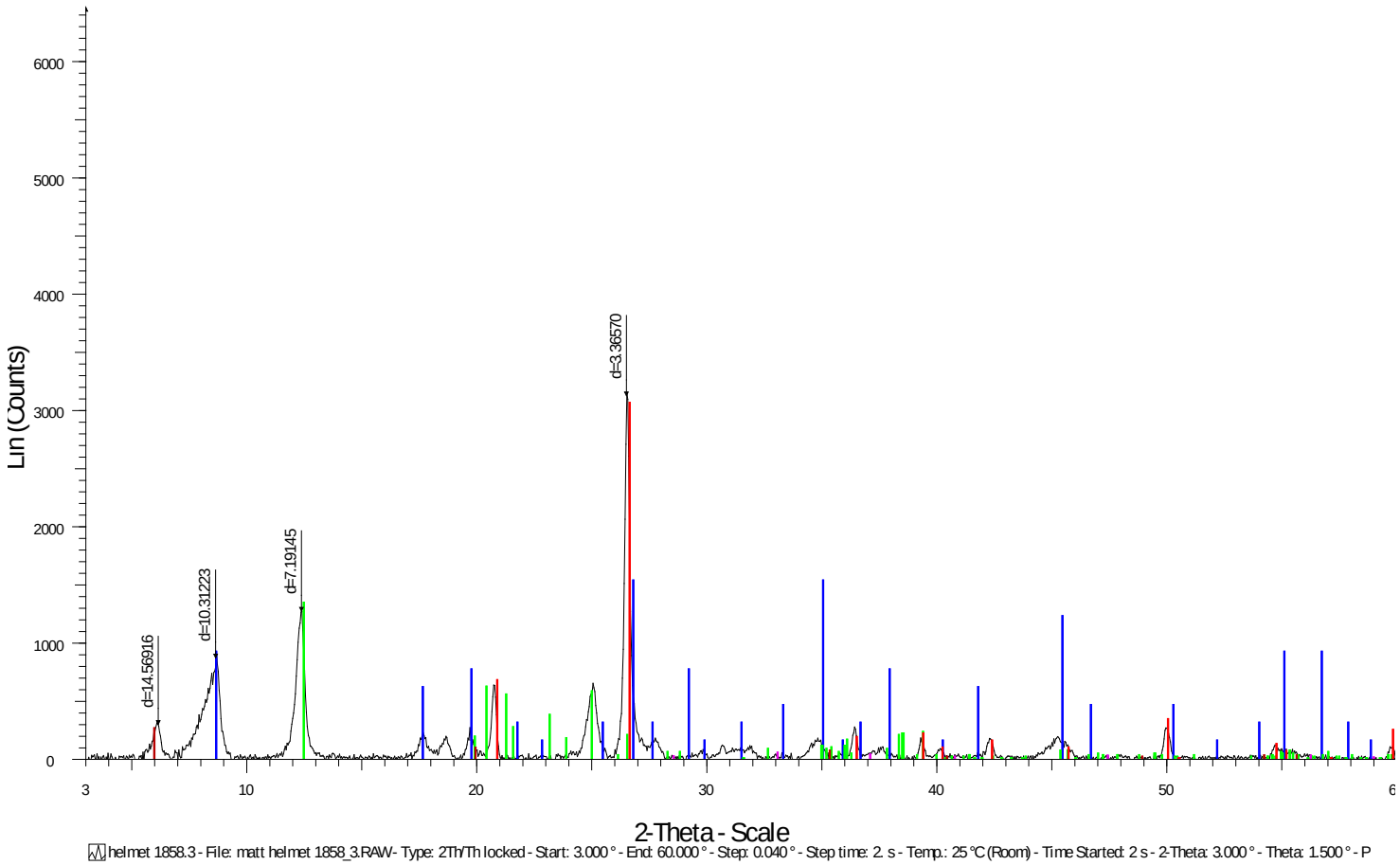

Junior c-60-E/94-I-11 1879.6 m

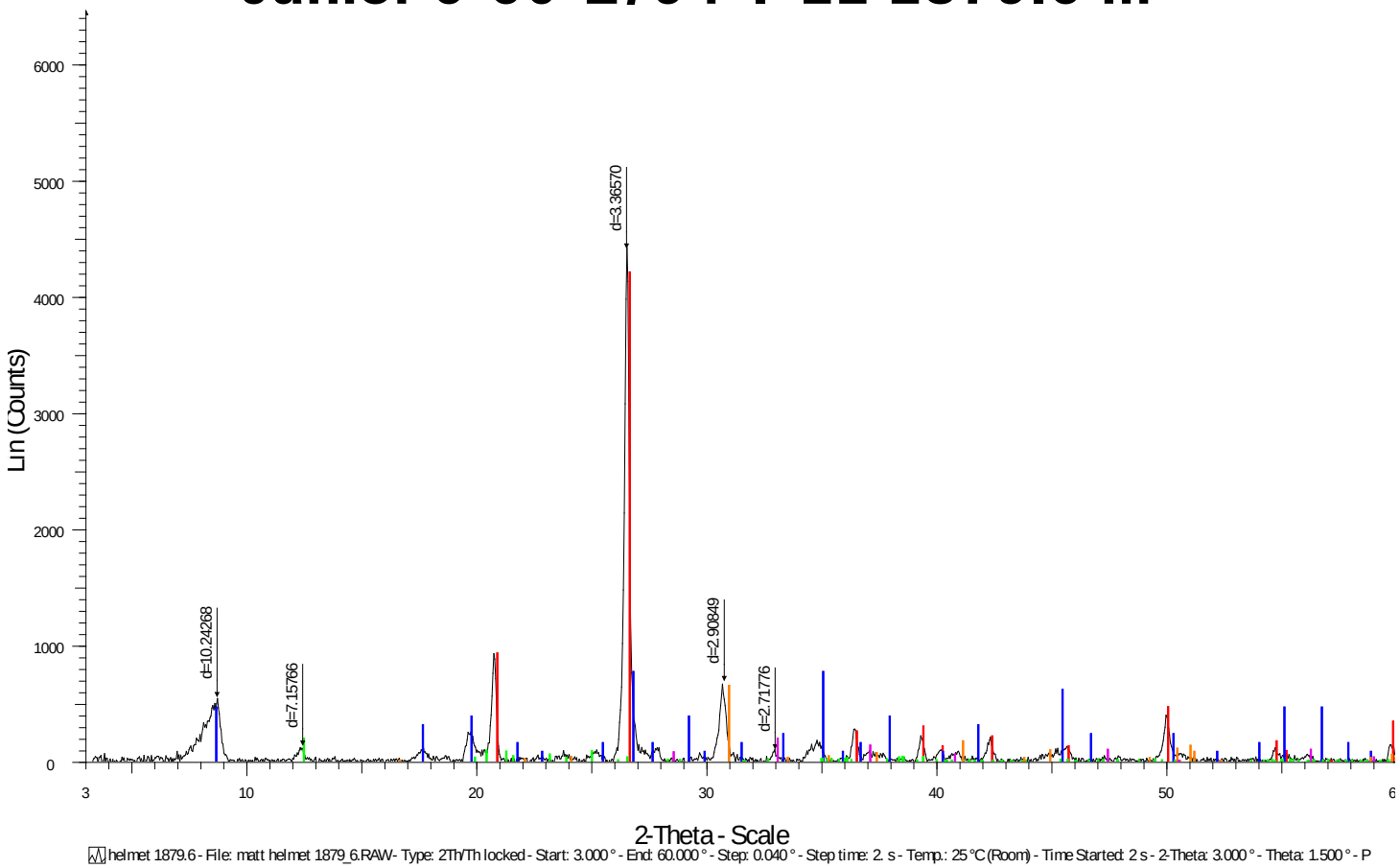

Sikanni Chief b-92-E/94-I-4 2106.7 m

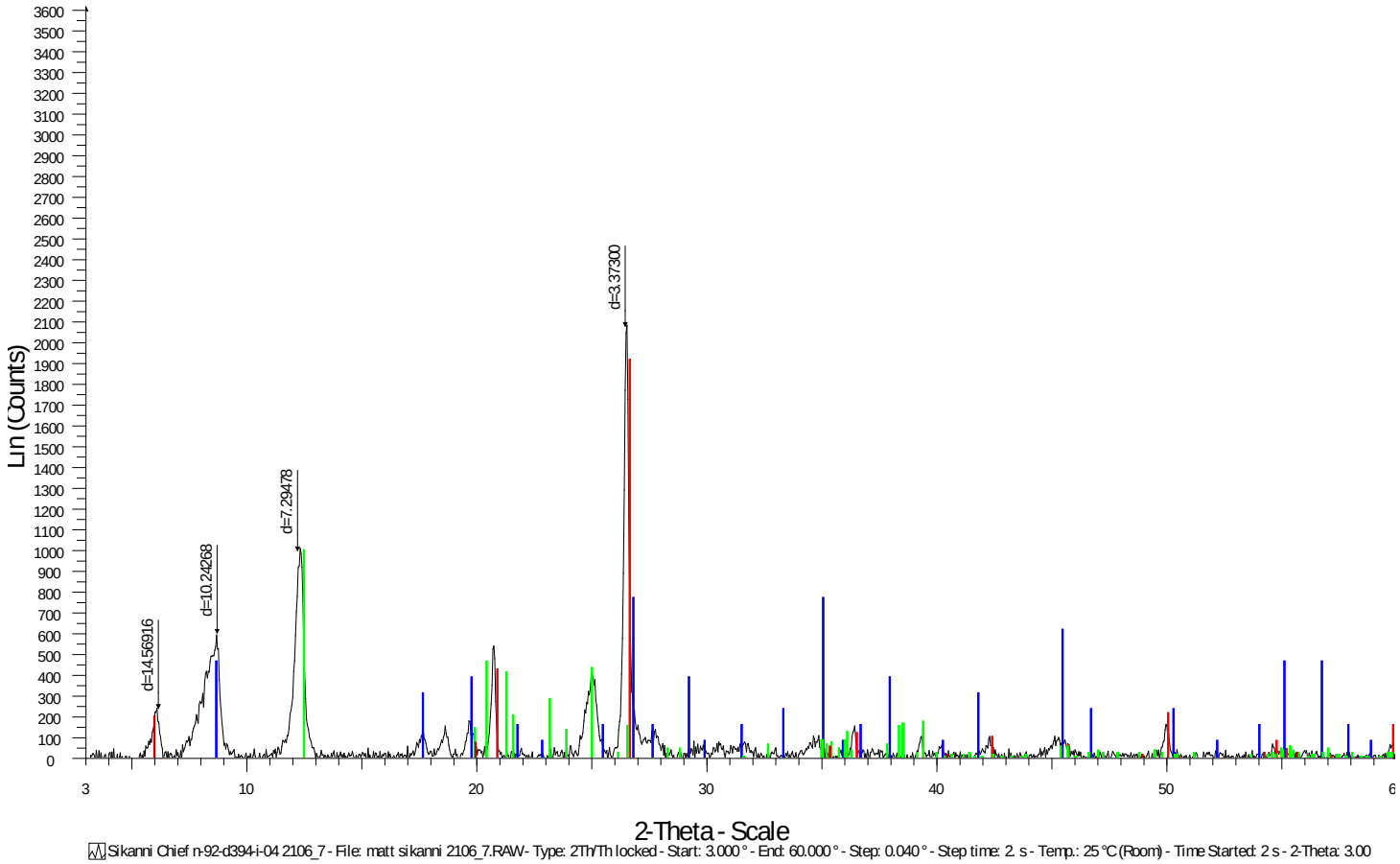

Sikanni Chief b-92-E/94-I-4 2216.6 m

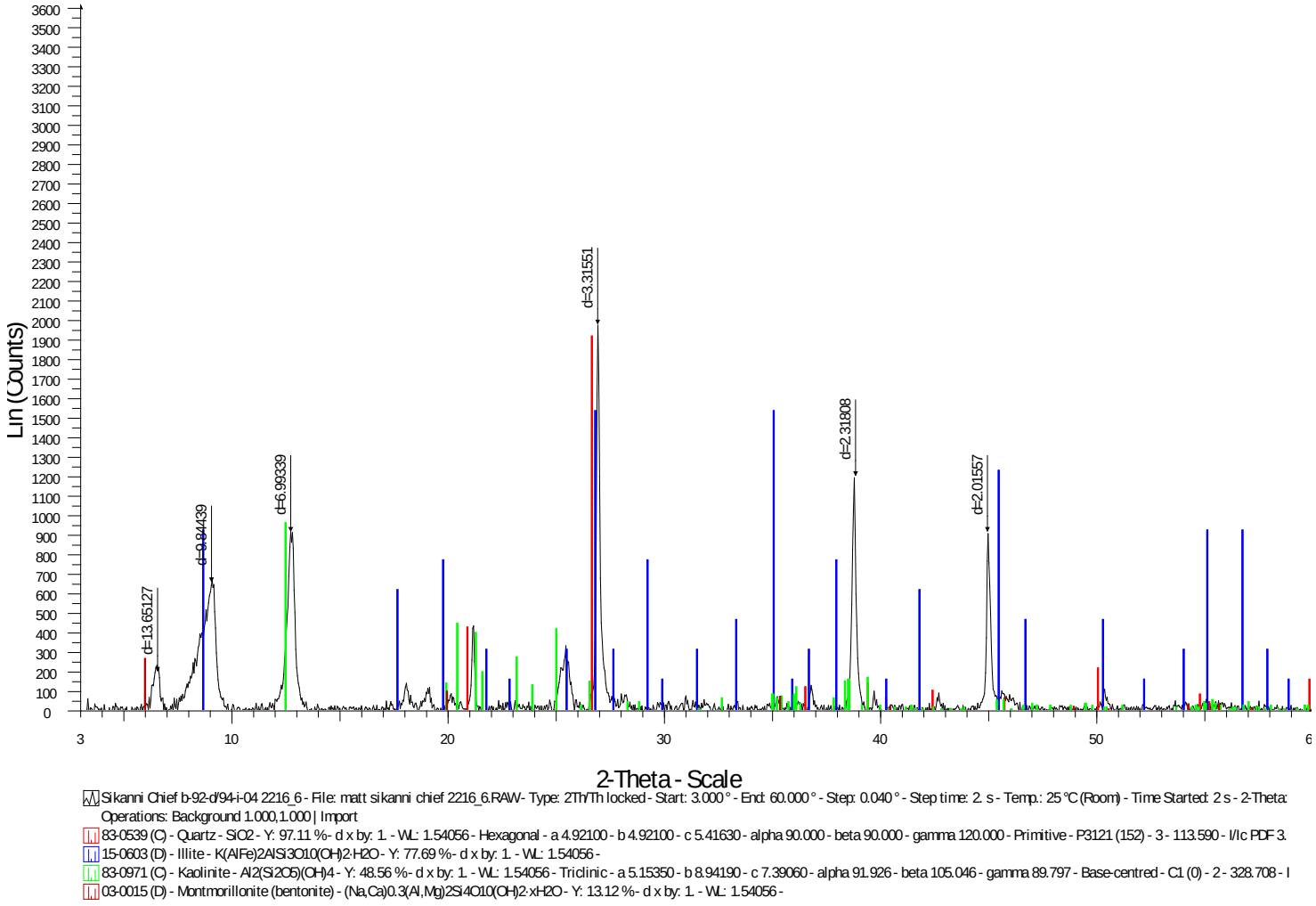

Kotcho c-32-K/94-I-14 1979.2 m

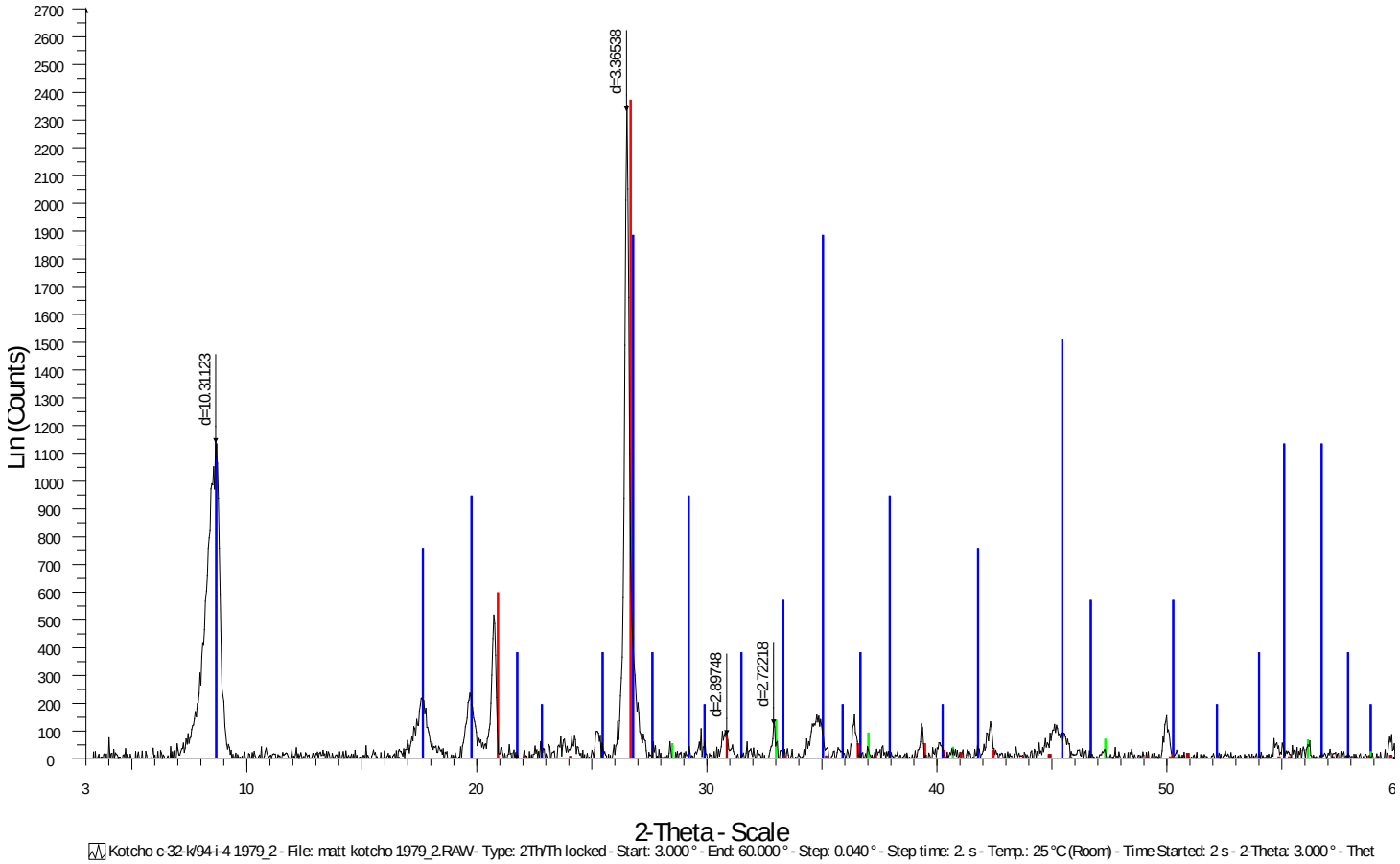

Kotcho c-32-K/94-I-14 1981.1 m

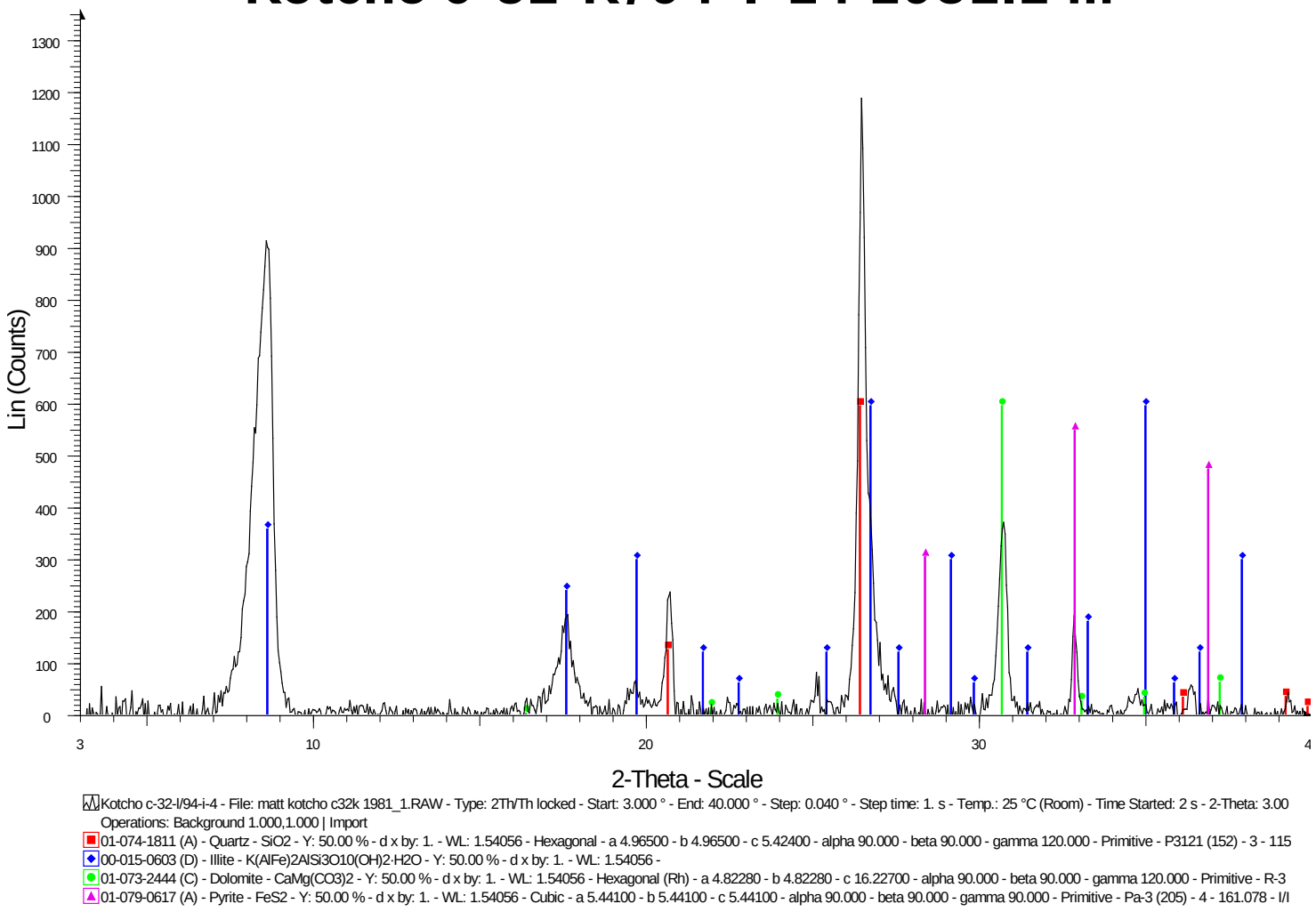

Kotcho c-32-I/94-i-4 - File: matt kotcho c32k 1981_1.RAW - Type: 2Th/Th locked - Start: 3.000 ° - End: 40.000 ° - Step: 0.040 ° - Step time: 1. s - Temp.: 25 °C (Room) - Time Started: 2 s - 2-Theta: 3.00
Operations: Background 1.000,1.000 | Import

01-074-1811 (A) - Quartz - SiO2 - Y: 50.00 % - d x by: 1. - WL: 1.54056 - Hexagonal - a 4.96500 - b 4.96500 - c 5.42400 - alpha 90.000 - beta 90.000 - gamma 120.000 - Primitive - P3121 (152) - 3 - 115

00-015-0603 (D) - Illite - K(AlFe)2AlSi3O10(OH)2·H2O - Y: 50.00 % - d x by: 1. - WL: 1.54056 -

01-073-2444 (C) - Dolomite - CaMg(CO3)2 - Y: 50.00 % - d x by: 1. - WL: 1.54056 - Hexagonal (Rh) - a 4.82280 - b 4.82280 - c 16.22700 - alpha 90.000 - beta 90.000 - gamma 120.000 - Primitive - R-3

01-079-0617 (A) - Pyrite - FeS2 - Y: 50.00 % - d x by: 1. - WL: 1.54056 - Cubic - a 5.44100 - b 5.44100 - c 5.44100 - alpha 90.000 - beta 90.000 - gamma 90.000 - Primitive - Pa-3 (205) - 4 - 161.078 - I/I

Kotcho c-32-K/94-I-14 1982.2 m

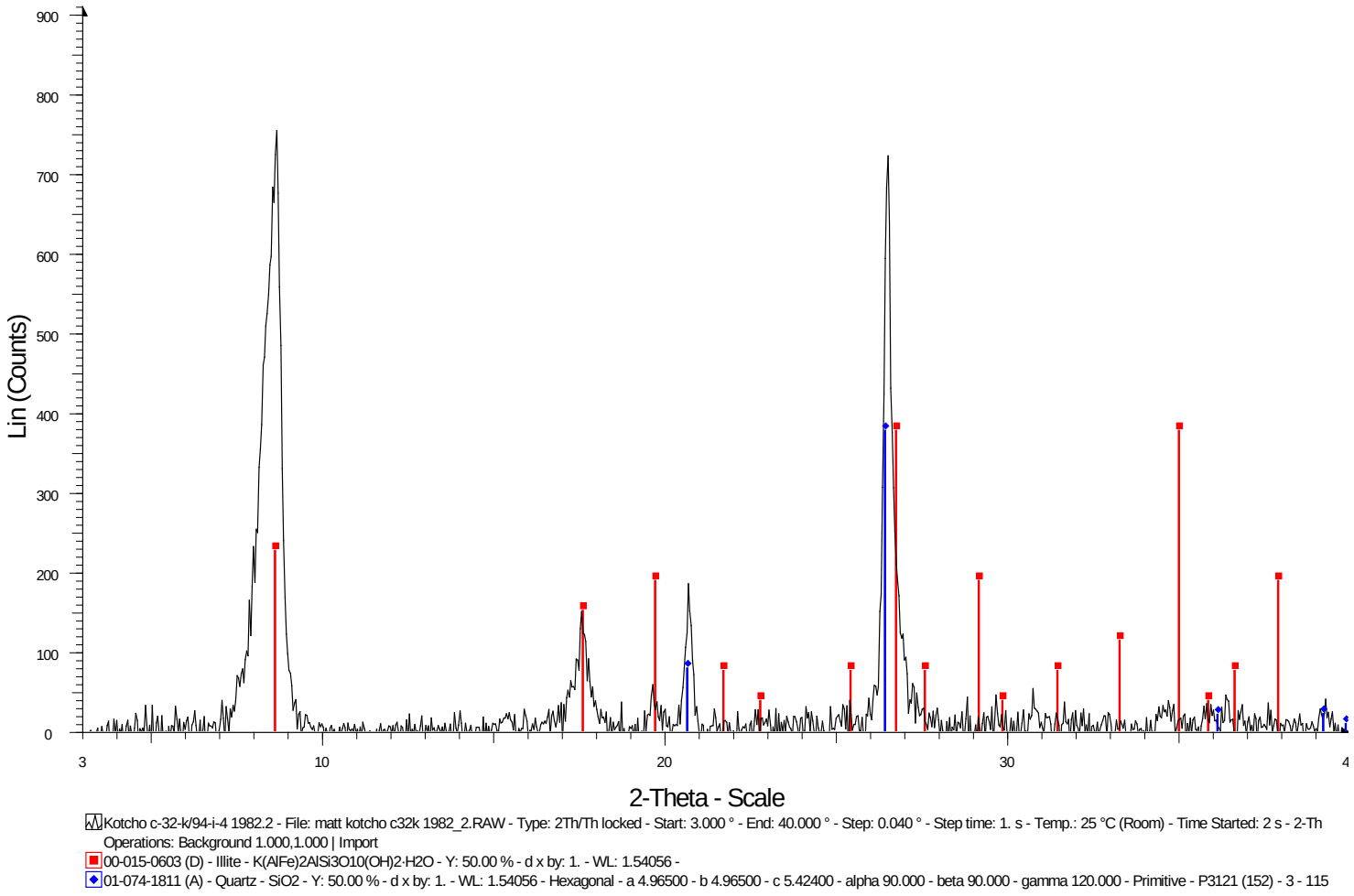

Kotcho c-32-K/94-I-14 1984.4 m

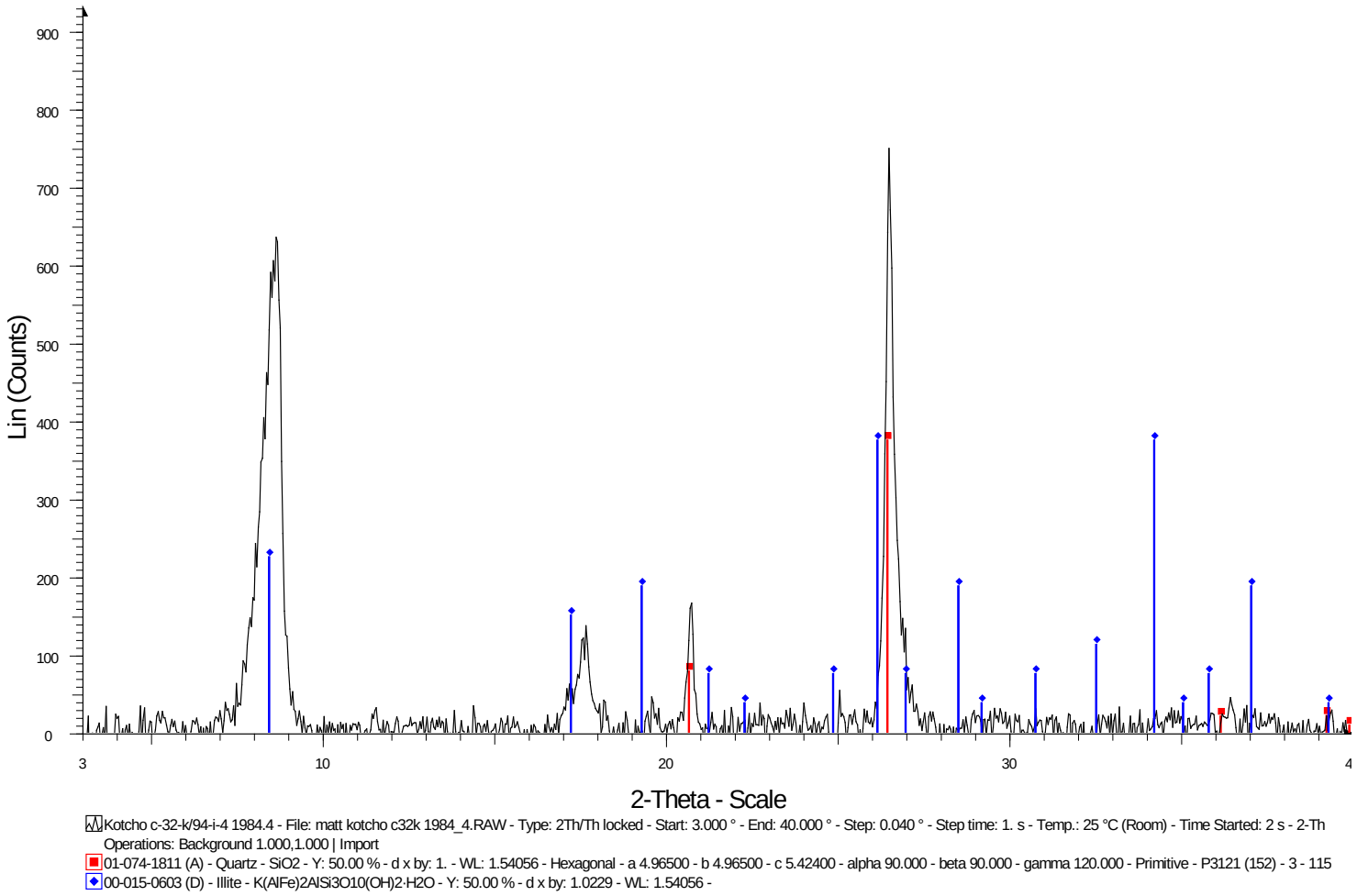

Kotcho c-32-K/94-I-14 1985.6 m

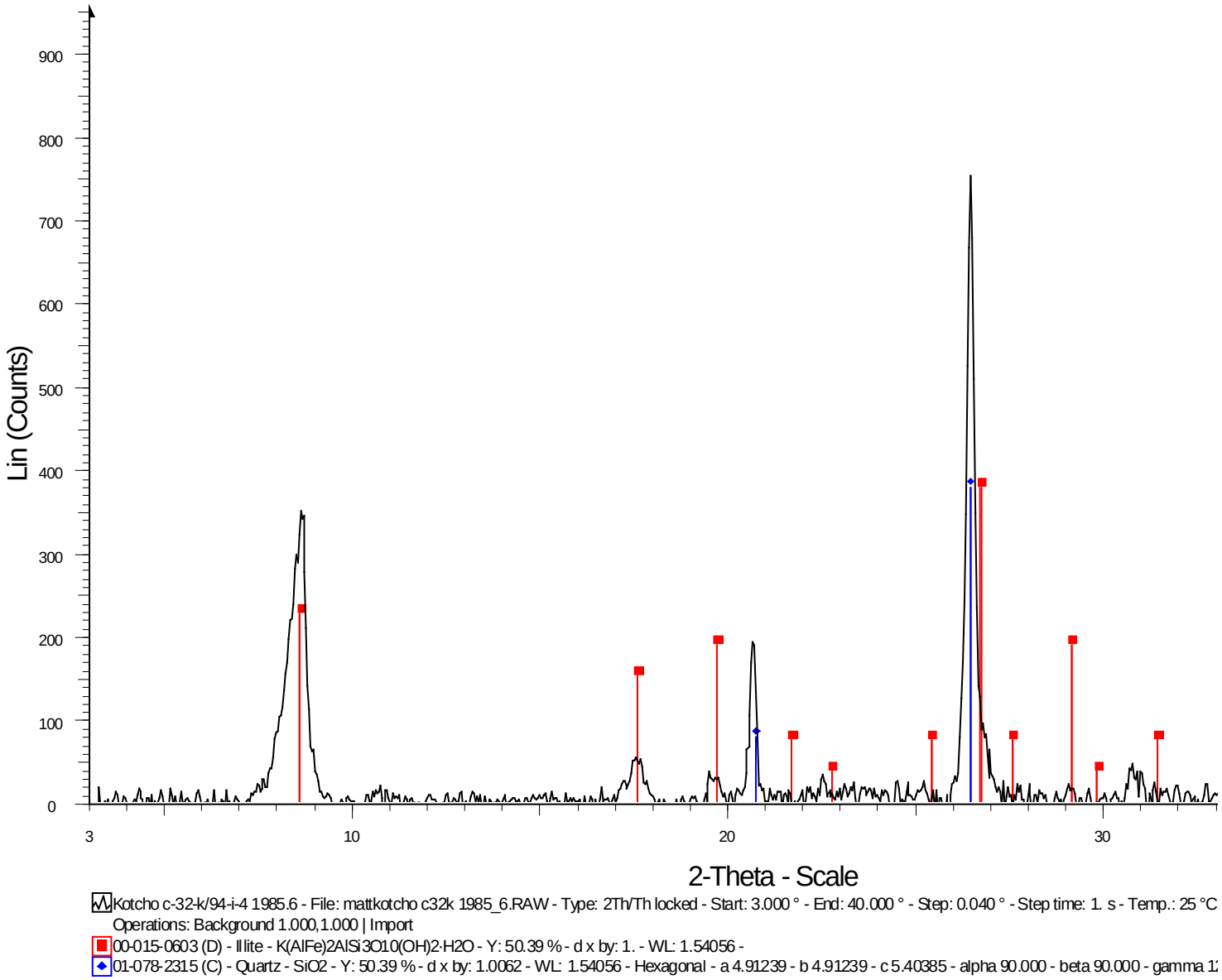

Kotcho c-32-K/94-I-14 1988.1 m

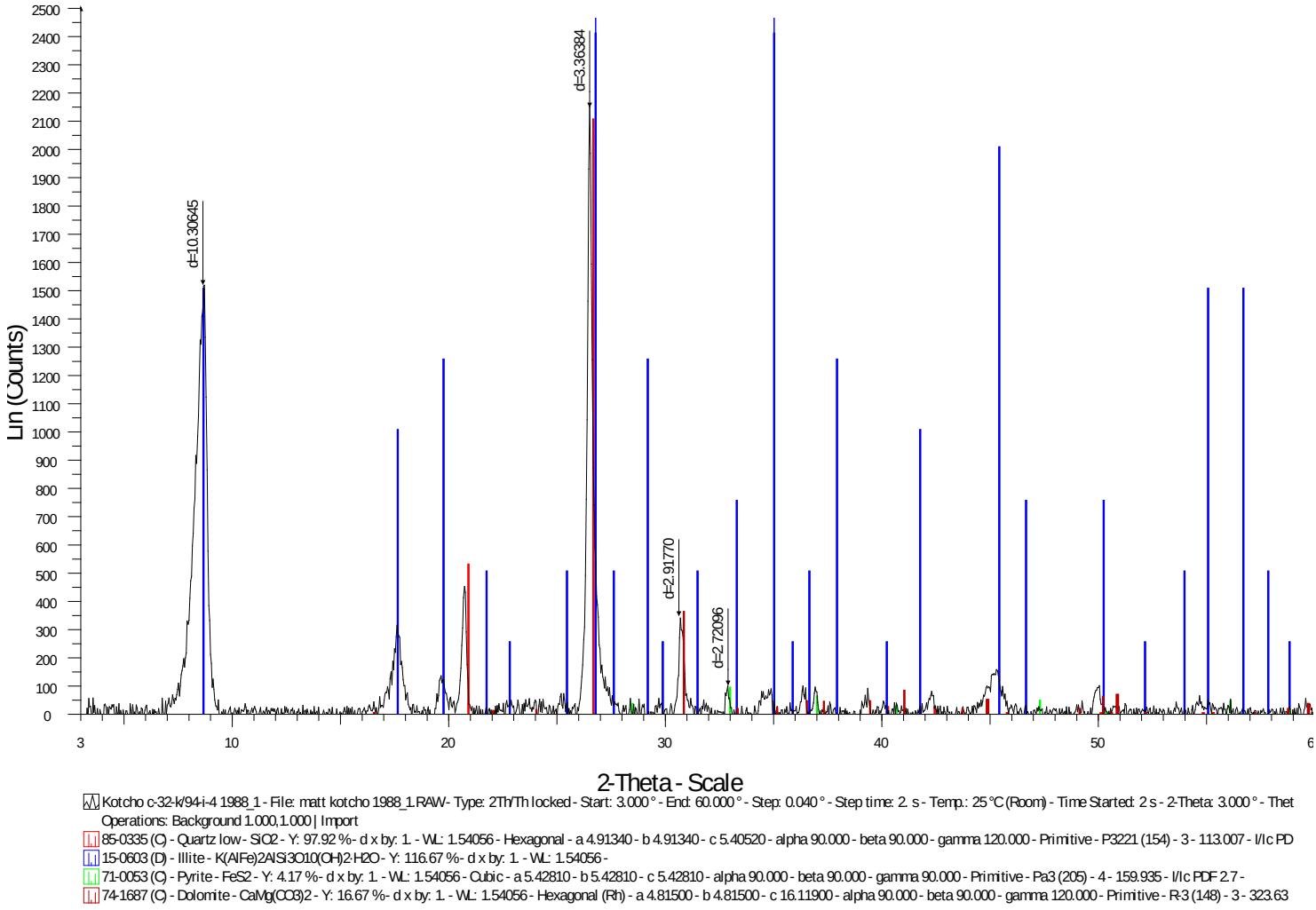

MUSKWA SAMPLES

Well	Location	Depth (m)
Shekilie	a-94-G/94-P-8	1539.60
		1542.00
		1545.60
		1548.60
		1553.60
		1555.50
Walrus	b-86-L/94-I-16	1761.80
		1763.70
Fort Nelson	c-70-I/94-J-10	1967.40
		1968.90
Snake River	c-28-D/94-O-1	1949.70
		1951.50
		1952.60

Shekilie a-94-G/94-P-8 1539.6 m

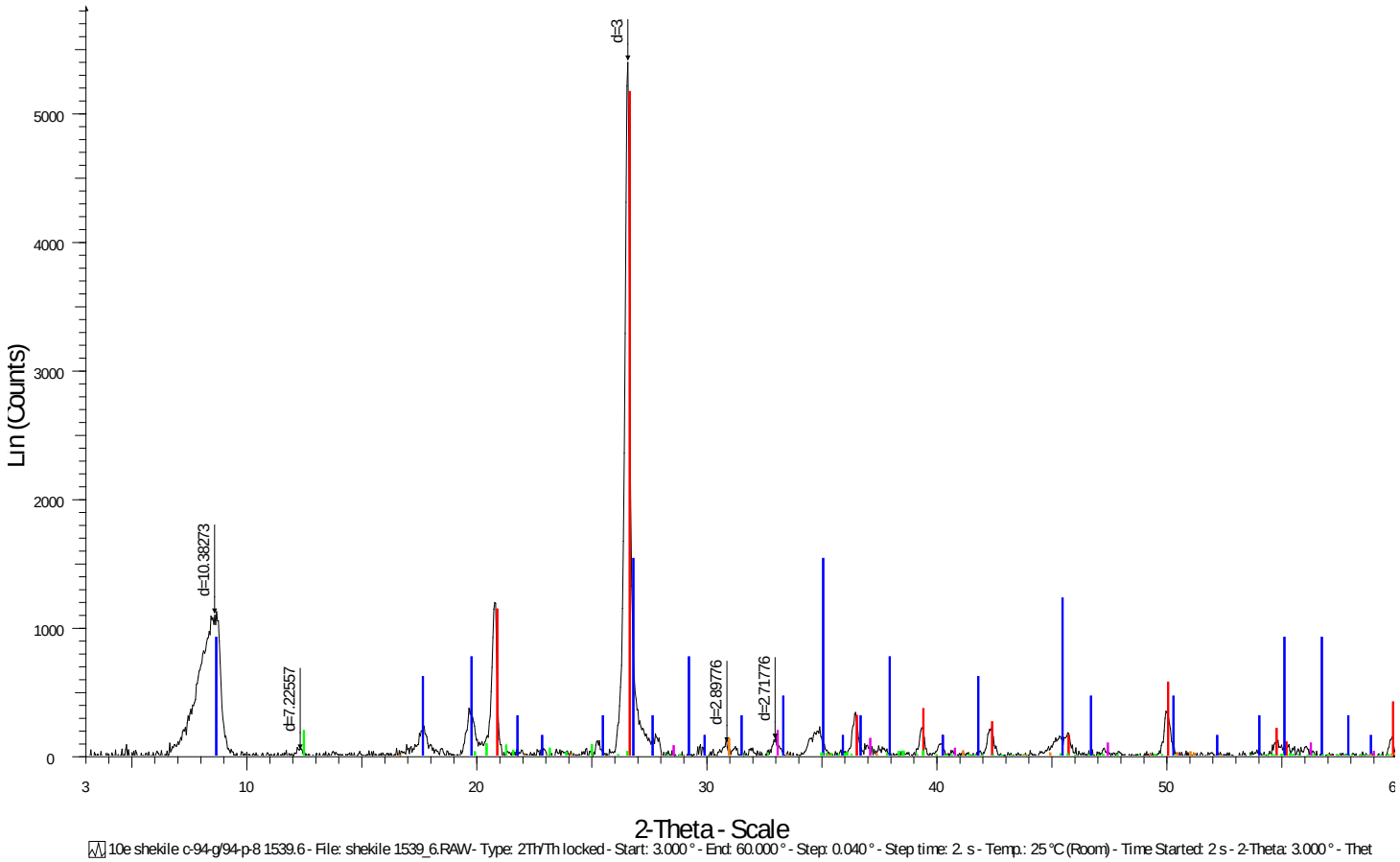

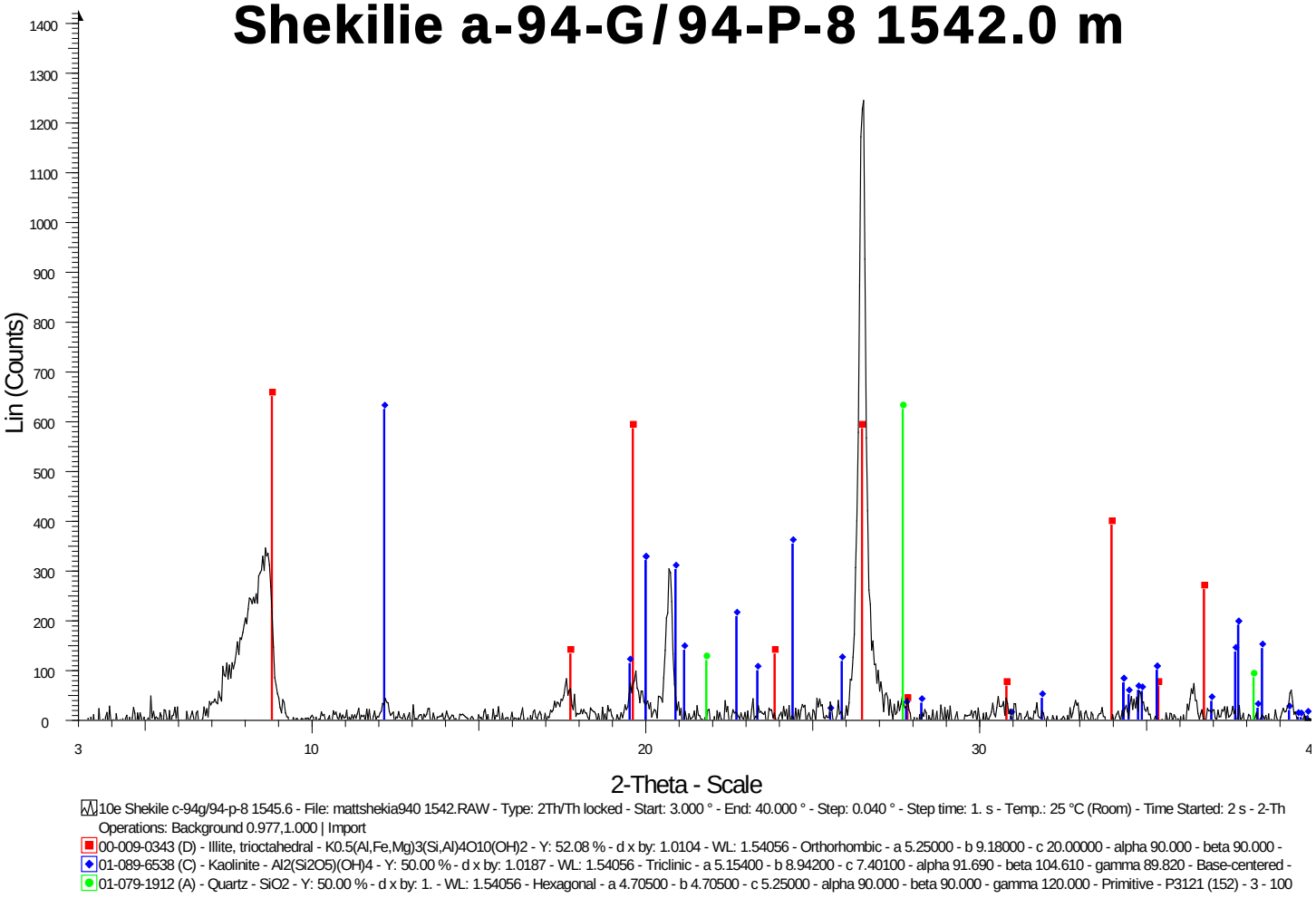
Shekilie a-94-G/94-P-8 1542.0 m
Lin (Counts)
2-Theta - Scale
10e Shekile c-94g/94-p-8 1545.6 - File: mattshekia940 1542.RAW - Type: 2Th/Th locked - Start: 3.000 ° - End: 40.000 ° - Step: 0.040 ° - Step time: 1. s - Temp.: 25 °C (Room) - Time Started: 2 s - 2-Th
Operations: Background 0.977,1.000 | Import
00-009-0343 (D) - Illite, trioctahedral - K0.5(Al,Fe,Mg)3(Si,Al)4O10(OH)2 - Y: 52.08 % - d x by: 1.0104 - WL: 1.54056 - Orthorhombic - a 5.25000 - b 9.18000 - c 20.00000 - alpha 90.000 - beta 90.000 -
01-089-6538 (C) - Kaolinite - Al2(Si2O5)(OH)4 - Y: 50.00 % - d x by: 1.0187 - WL: 1.54056 - Triclinic - a 5.15400 - b 8.94200 - c 7.40100 - alpha 91.690 - beta 104.610 - gamma 89.820 - Base-centered -
01-079-1912 (A) - Quartz - SiO2 - Y: 50.00 % - d x by: 1. - WL: 1.54056 - Hexagonal - a 4.70500 - b 4.70500 - c 5.25000 - alpha 90.000 - beta 90.000 - gamma 120.000 - Primitive - P3121 (152) - 3 - 100

Shekilie a-94-G/94-P-8 1545.6 m

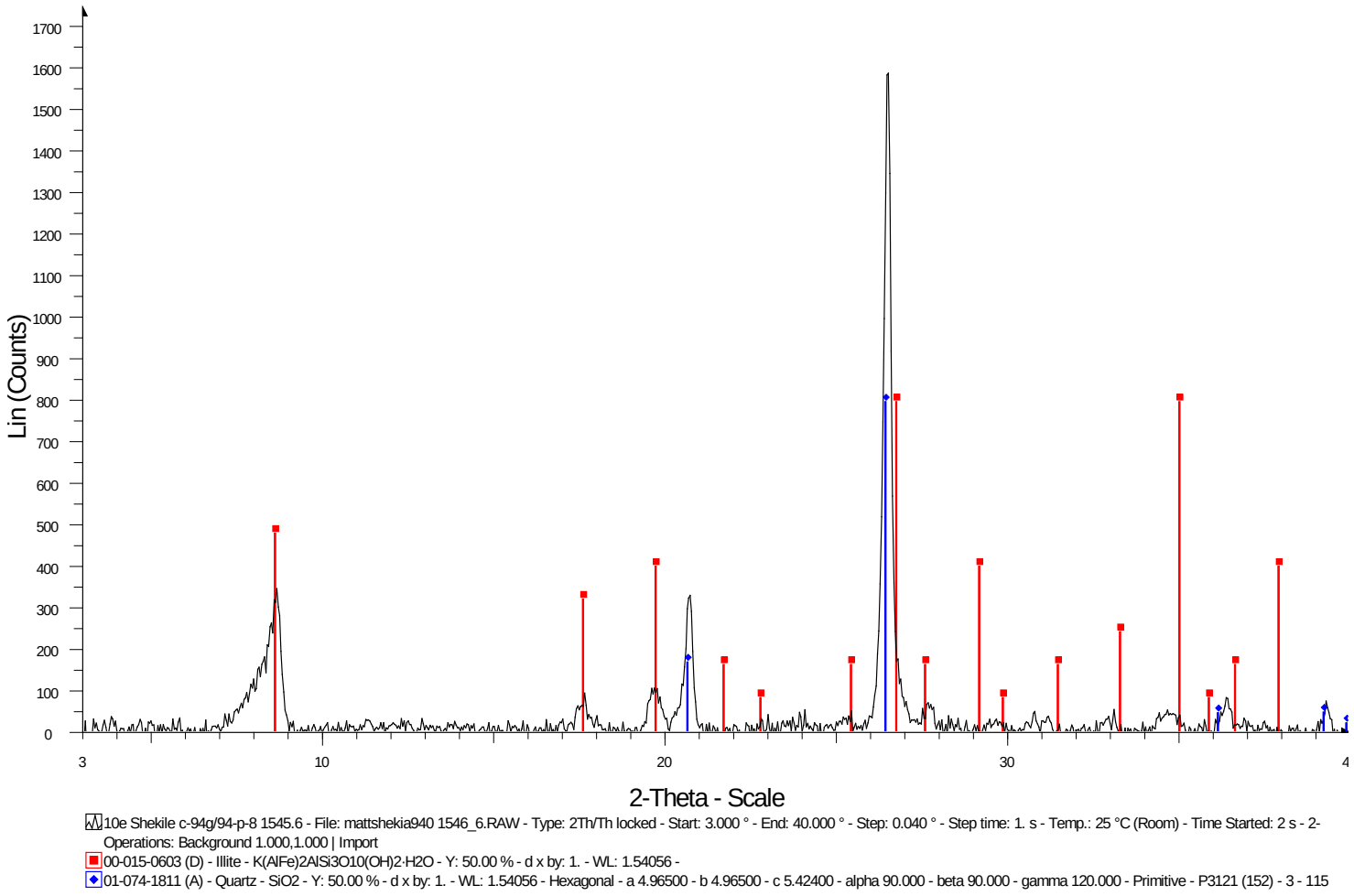

Shekilie a-94-G/94-P-8 1548.6 m

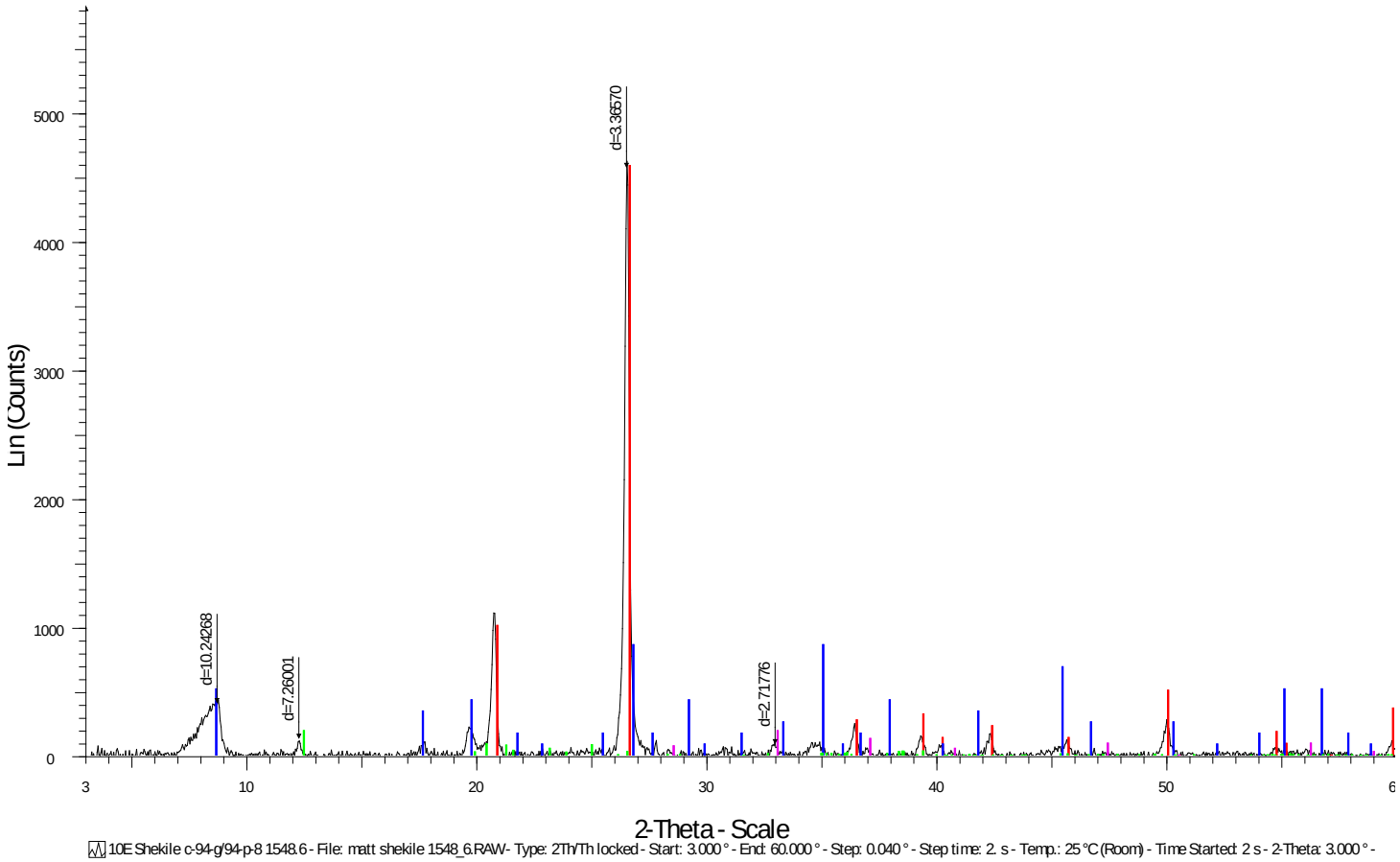

10E Shekile c-94-g/94-p-8 1548.6 - File: matt shekile 1548_6.RAW- Type: 2Th/Th locked - Start: 3.000 ° - End: 60.000 ° - Step: 0.040 ° - Step time: 2. s - Temp.: 25 °C (Room) - Time Started: 2 s - 2-Theta: 3.000 ° - Operations: Background 1.000,1.000 | Import

83-0539 (C) - Quartz - SiO2 - Y: 99.29 % - d x by: 1. - WL: 1.54056 - Hexagonal - a 4.92100 - b 4.92100 - c 5.41630 - alpha 90.000 - beta 90.000 - gamma 120.000 - Primitive - P3121 (152) - 3 - 113.590 - I/Ic PDF 3.

15-0603 (D) - Illite - K(AlFe)2AlSi3O10(OH)2·H2O - Y: 18.62 % - d x by: 1. - WL: 1.54056 -

83-0971 (C) - Kaolinite - Al2(Si2O5)(OH)4 - Y: 4.14 % - d x by: 1. - WL: 1.54056 - Triclinic - a 5.15350 - b 8.94190 - c 7.39060 - alpha 91.926 - beta 105.046 - gamma 89.797 - Base-centred - C1 (0) - 2 - 328.708 - I/I

71-2219 (C) - Pyrite - FeS2 - Y: 4.14 % - d x by: 1. - WL: 1.54056 - Cubic - a 5.41790 - b 5.41790 - c 5.41790 - alpha 90.000 - beta 90.000 - gamma 90.000 - Primitive - Pa3 (205) - 4 - 159.035 - I/Ic PDF 2.6 -

Shekilie a-94-G/94-P-8 1553.6 m

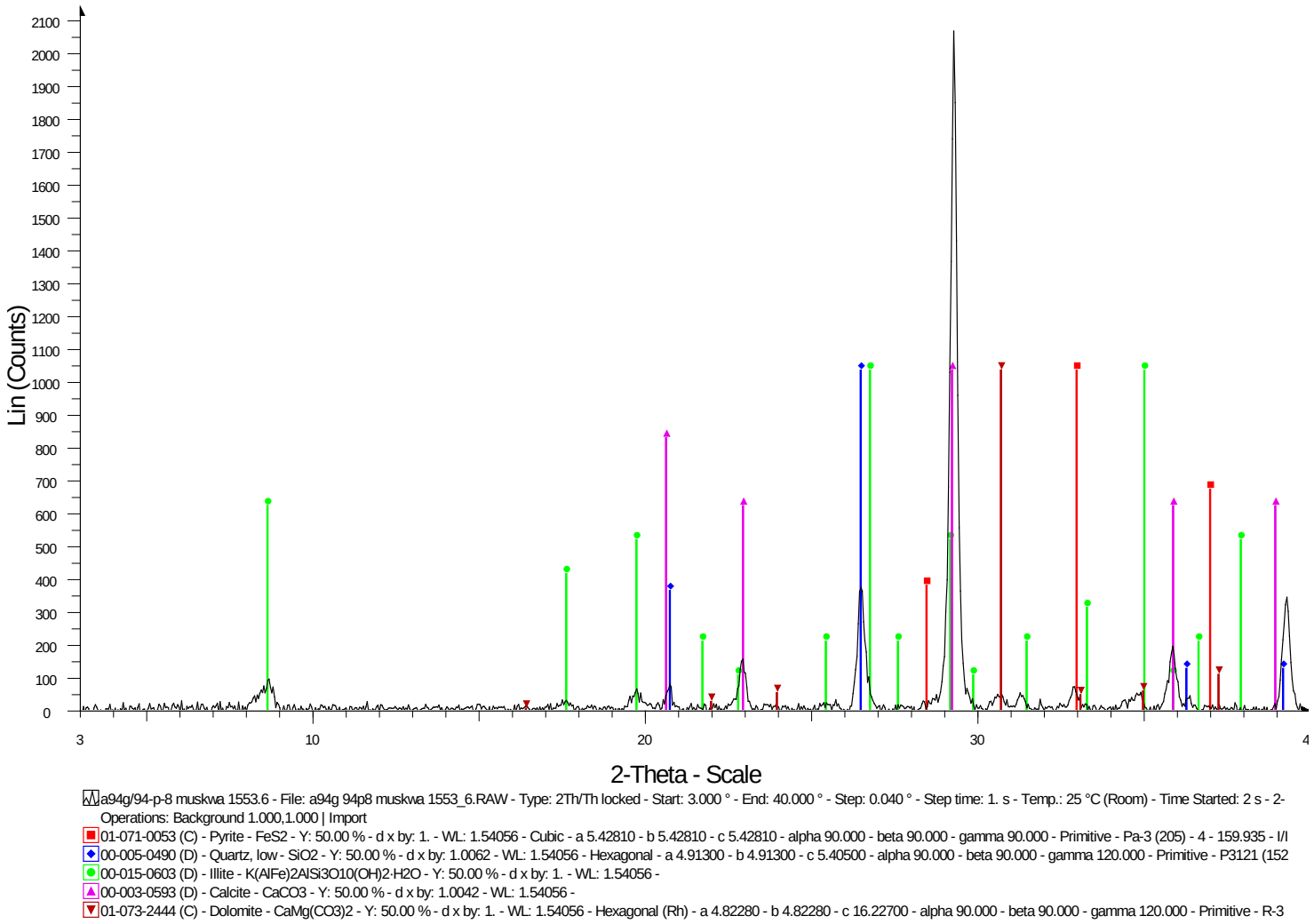

a94g/94-p-8 muskwa 1553.6 - File: a94g 94p8 muskwa 1553_6.RAW - Type: 2Th/Th locked - Start: 3.000 ° - End: 40.000 ° - Step: 0.040 ° - Step time: 1. s - Temp.: 25 °C (Room) - Time Started: 2 s - 2-
Operations: Background 1.000,1.000 | Import

01-071-0053 (C) - Pyrite - FeS2 - Y: 50.00 % - d x by: 1. - WL: 1.54056 - Cubic - a 5.42810 - b 5.42810 - c 5.42810 - alpha 90.000 - beta 90.000 - gamma 90.000 - Primitive - Pa-3 (205) - 4 - 159.935 - I/I

00-005-0490 (D) - Quartz, low - SiO2 - Y: 50.00 % - d x by: 1.0062 - WL: 1.54056 - Hexagonal - a 4.91300 - b 4.91300 - c 5.40500 - alpha 90.000 - beta 90.000 - gamma 120.000 - Primitive - P3121 (152

00-015-0603 (D) - Illite - K(AlFe)2AlSi3O10(OH)2·H2O - Y: 50.00 % - d x by: 1. - WL: 1.54056 -

00-003-0593 (D) - Calcite - CaCO3 - Y: 50.00 % - d x by: 1.0042 - WL: 1.54056 -

01-073-2444 (C) - Dolomite - CaMg(CO3)2 - Y: 50.00 % - d x by: 1. - WL: 1.54056 - Hexagonal (Rh) - a 4.82280 - b 4.82280 - c 16.22700 - alpha 90.000 - beta 90.000 - gamma 120.000 - Primitive - R-3

Shekilie a-94-G/94-P-8 1555.5 m

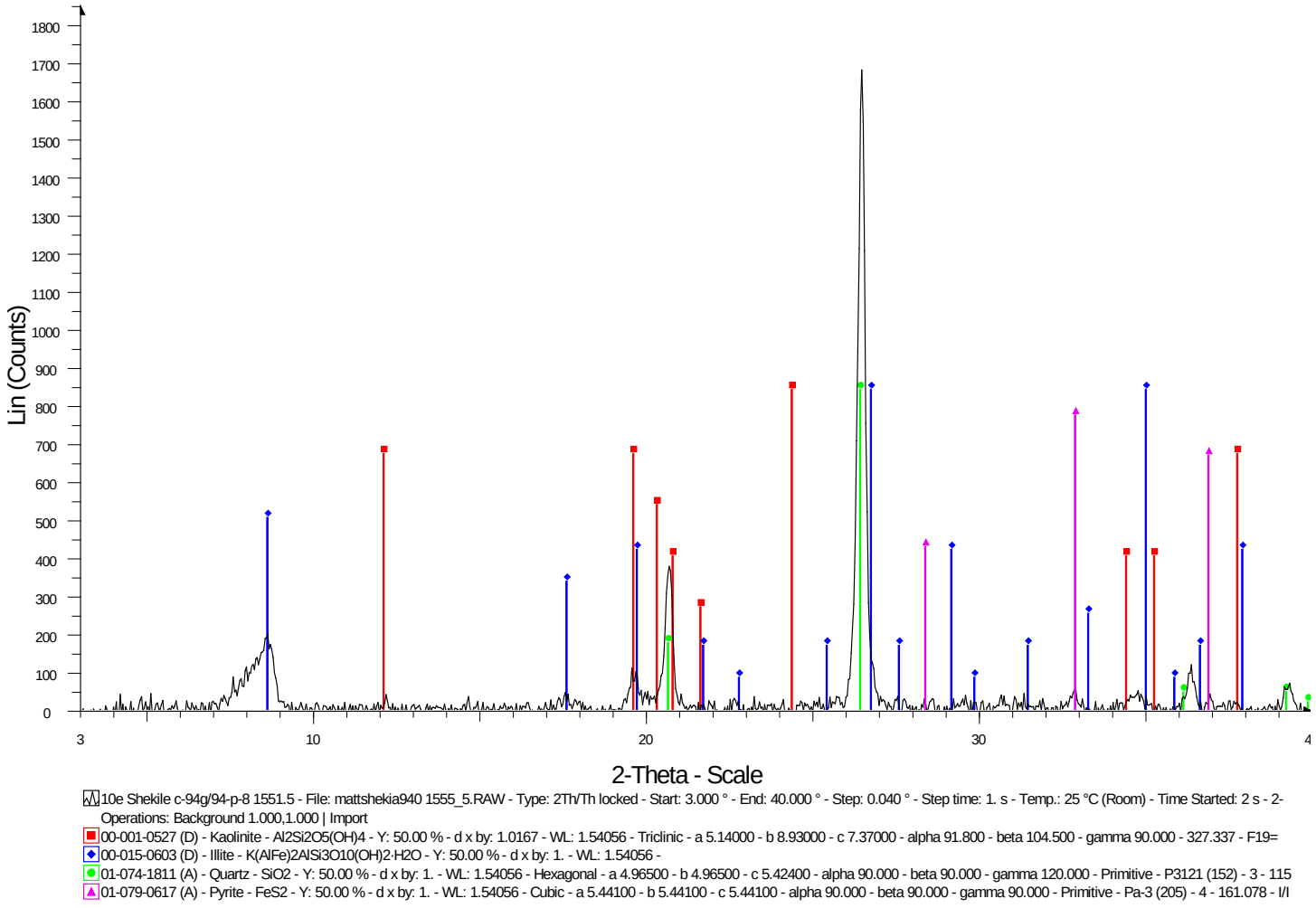

Walrus b-86-L/94-I-16 1761.8 m

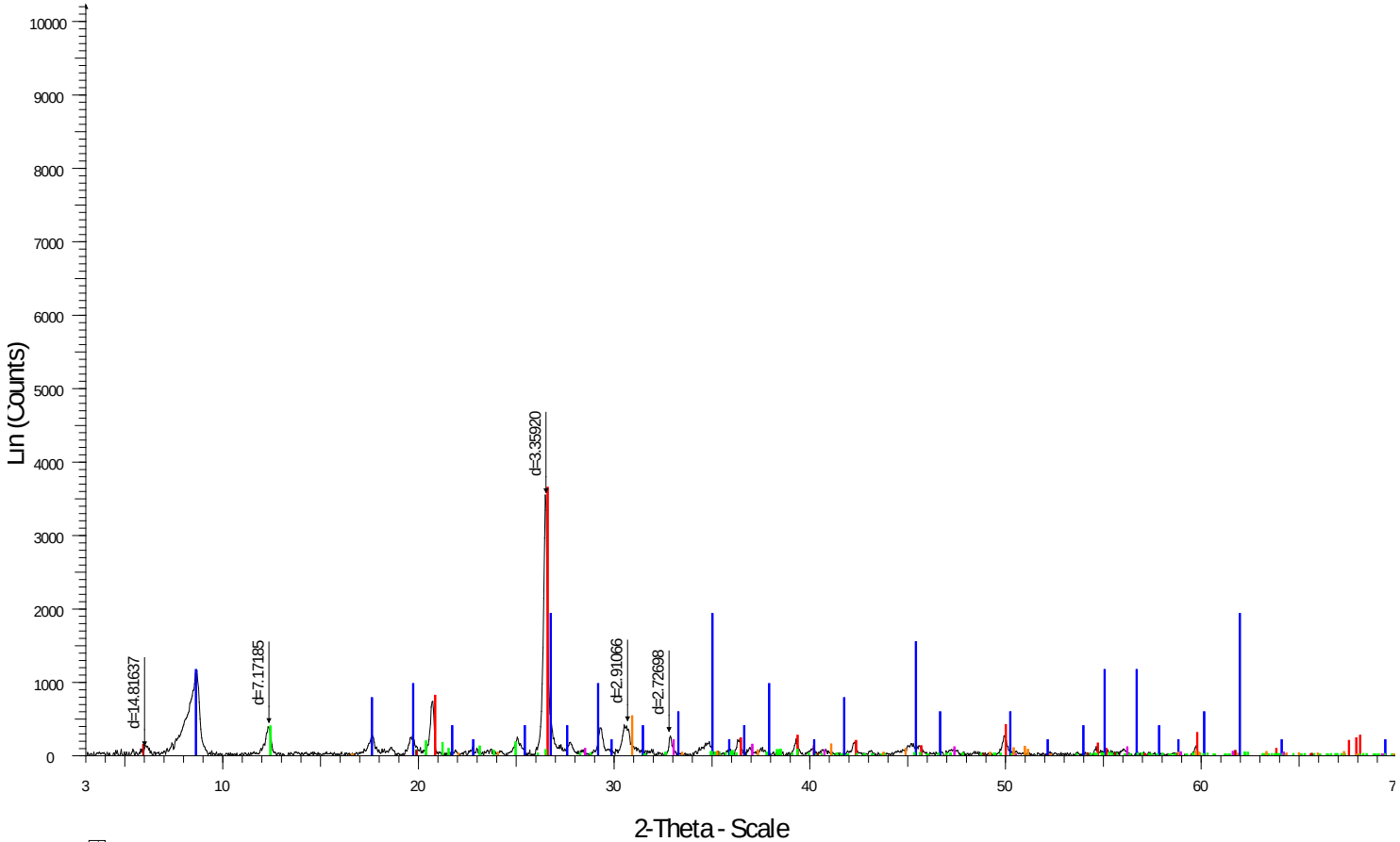

esso walrus b-86-l/94-t-16 1761.8 - File: matt-walrus 1761_8.RAW - Type: 2Th/Th locked - Start: 3.000 ° - End: 60.000 ° - Step: 0.040 ° - Step time: 2. s - Temp.: 25 °C (Room) - Time Started: 2 s - 2-Theta: 3.000 ° - Operations: Background 1.000,1.000 | Import

83-0539 (C) - Quartz - SiO2 - Y: 102.90 % - d x by: 1. - WL: 1.54056 - Hexagonal - a 4.92100 - b 4.92100 - c 5.41630 - alpha 90.000 - beta 90.000 - gamma 120.000 - Primitive - P3121 (152) - 3 - 113.590 - I/Ic PDF 3

15-0603 (D) - Illite - K(AlFe)2AlSi3O10(OH)2·H2O - Y: 54.16 % - d x by: 1. - WL: 1.54056 -

83-0971 (C) - Kaolinite - Al2(Si2O5)(OH)4 - Y: 10.83 % - d x by: 1. - WL: 1.54056 - Triclinic - a 5.15350 - b 8.94190 - c 7.39060 - alpha 91.926 - beta 105.046 - gamma 89.797 - Base-centred - C1 (0) - 2 - 328.708 - I

71-2219 (C) - Pyrite - FeS2 - Y: 5.42 % - d x by: 1. - WL: 1.54056 - Cubic - a 5.41790 - b 5.41790 - c 5.41790 - alpha 90.000 - beta 90.000 - gamma 90.000 - Primitive - Pa3 (205) - 4 - 159.035 - I/Ic PDF 2.6 -

03-0015 (D) - Montmorillonite (bentonite) - (Na,Ca)0.3(Al,Mg)2Si4O10(OH)2·xH2O - Y: 3.66 % - d x by: 1. - WL: 1.54056 -

84-1208 (C) - Dolomite - CaMg(CO3)2 - Y: 14.63 % - d x by: 1. - WL: 1.54056 - Hexagonal (Rh) - a 4.81100 - b 4.81100 - c 16.04700 - alpha 90.000 - beta 90.000 - gamma 120.000 - Primitive - R-3 (148) - 3 - 321.65

Walrus b-86-L/94-I-16 1763.7 m

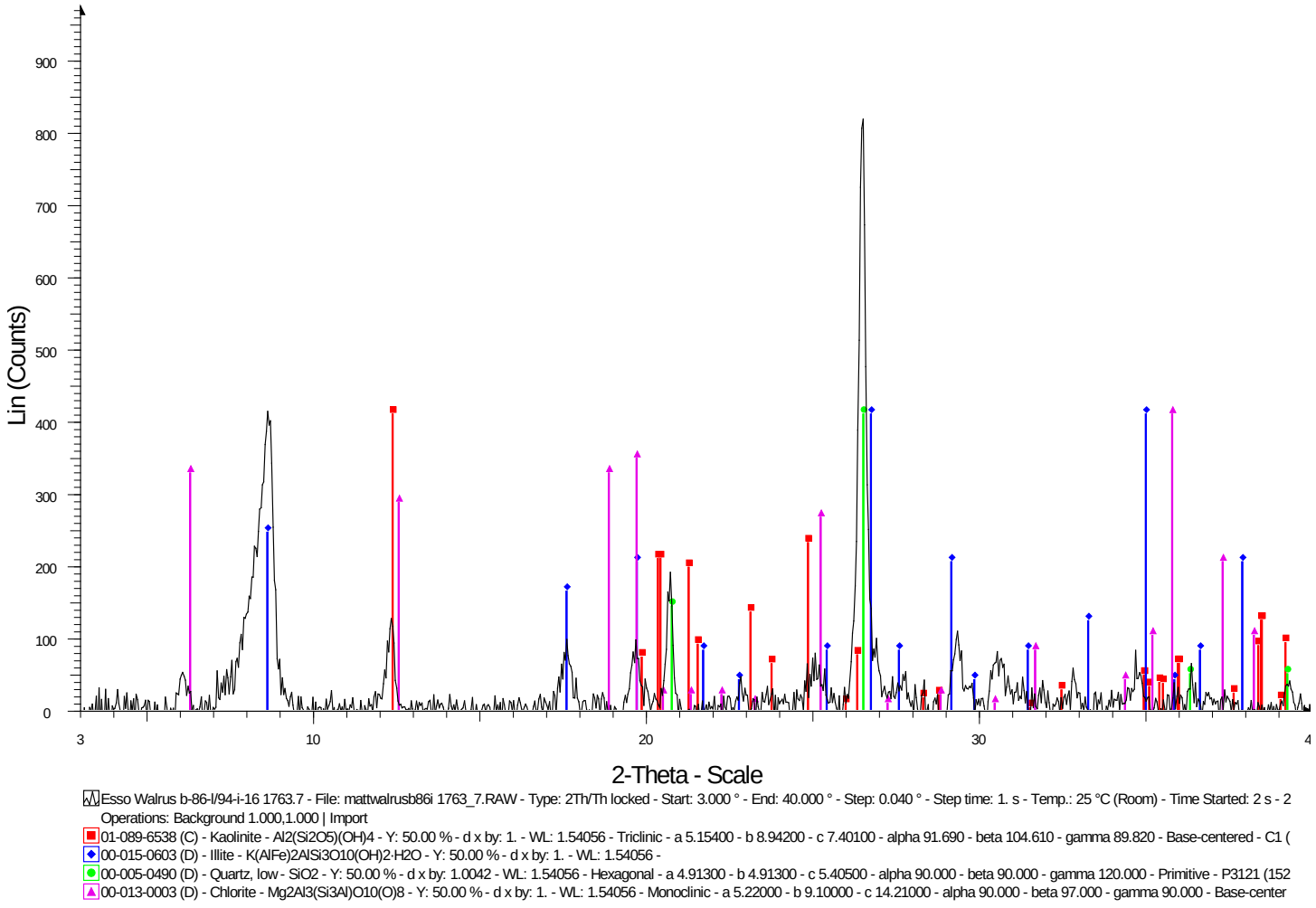

Fort Nelson c-70-I / 94-J-10 1967.4 m

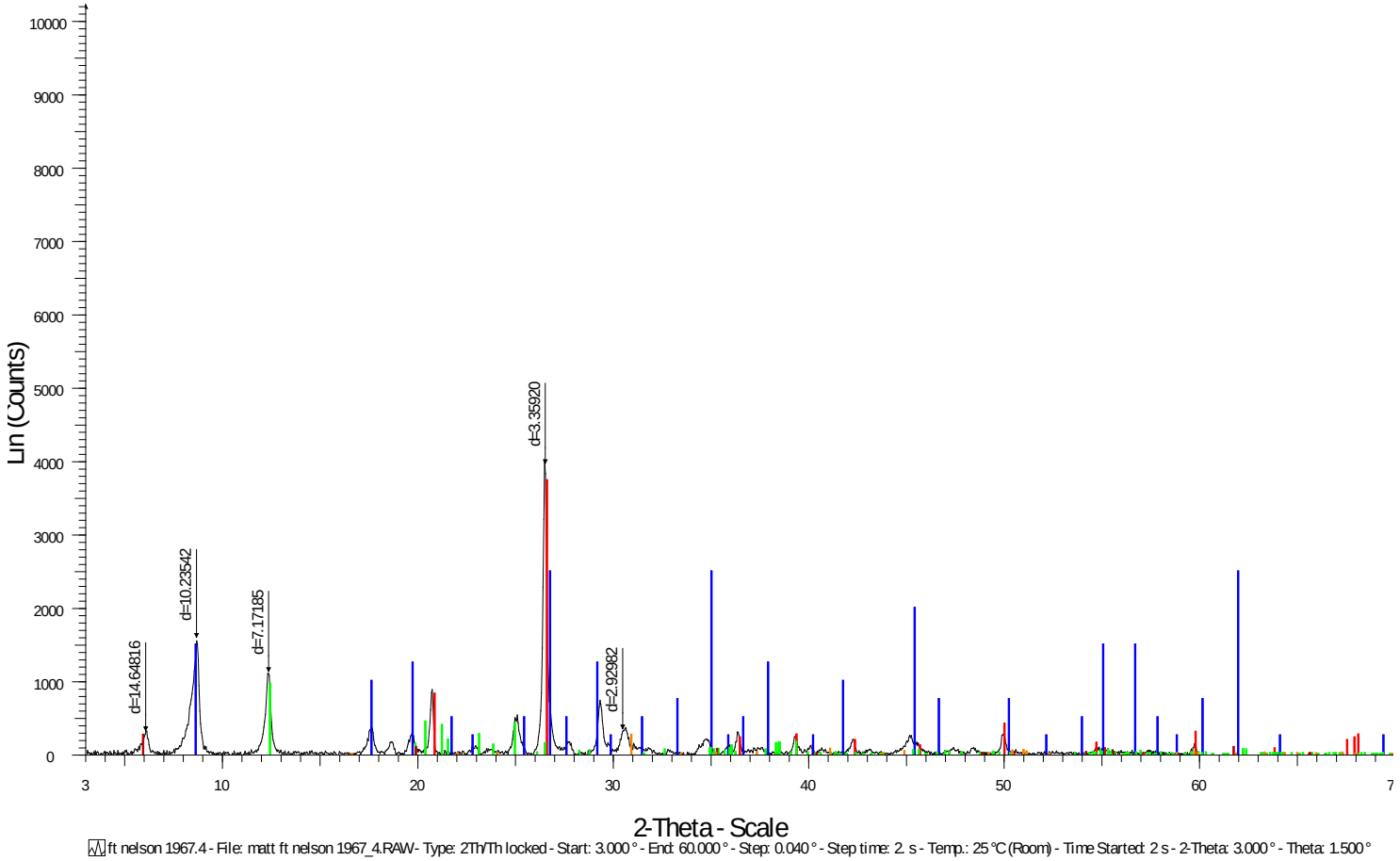

ft nelson 1967.4 - File: matt ft nelson 1967_4.RAW - Type: 2Th/Th locked - Start: 3.000 ° - End: 60.000 ° - Step: 0.040 ° - Step time: 2. s - Temp.: 25 °C (Room) - Time Started: 2 s - 2-Theta: 3.000 ° - Theta: 1.500 °
Operations: Background 1.000,1.000 | Import

83-0539 (C) - Quartz - SiO2 - Y: 93.07 % - d x by: 1. - WL: 1.54056 - Hexagonal - a 4.92100 - b 4.92100 - c 5.41630 - alpha 90.000 - beta 90.000 - gamma 120.000 - Primitive - P3121 (152) - 3 - 113.590 - I/Ic PDF 3.

15-0603 (D) - Illite - K(AlFe)2AlSi3O10(OH)2·H2O - Y: 62.05 % - d x by: 1. - WL: 1.54056 -

83-0971 (C) - Kaolinite - Al2(Si2O5)(OH)4 - Y: 23.86 % - d x by: 1. - WL: 1.54056 - Triclinic - a 5.15350 - b 8.94190 - c 7.39060 - alpha 91.926 - beta 105.046 - gamma 89.797 - Base-centred - C1 (0) - 2 - 328.708 - I

03-0015 (D) - Montmorillonite (bentonite) - (Na,Ca)0.3(Al,Mg)2Si4O10(OH)2·xH2O - Y: 6.45 % - d x by: 1. - WL: 1.54056 -

84-1208 (C) - Dolomite - CaMg(CO3)2 - Y: 6.45 % - d x by: 1. - WL: 1.54056 - Hexagonal (Rh) - a 4.81100 - b 4.81100 - c 16.04700 - alpha 90.000 - beta 90.000 - gamma 120.000 - Primitive - R-3 (148) - 3 - 321.659

Fort Nelson c-70-I/94-J-10 1968.9 m

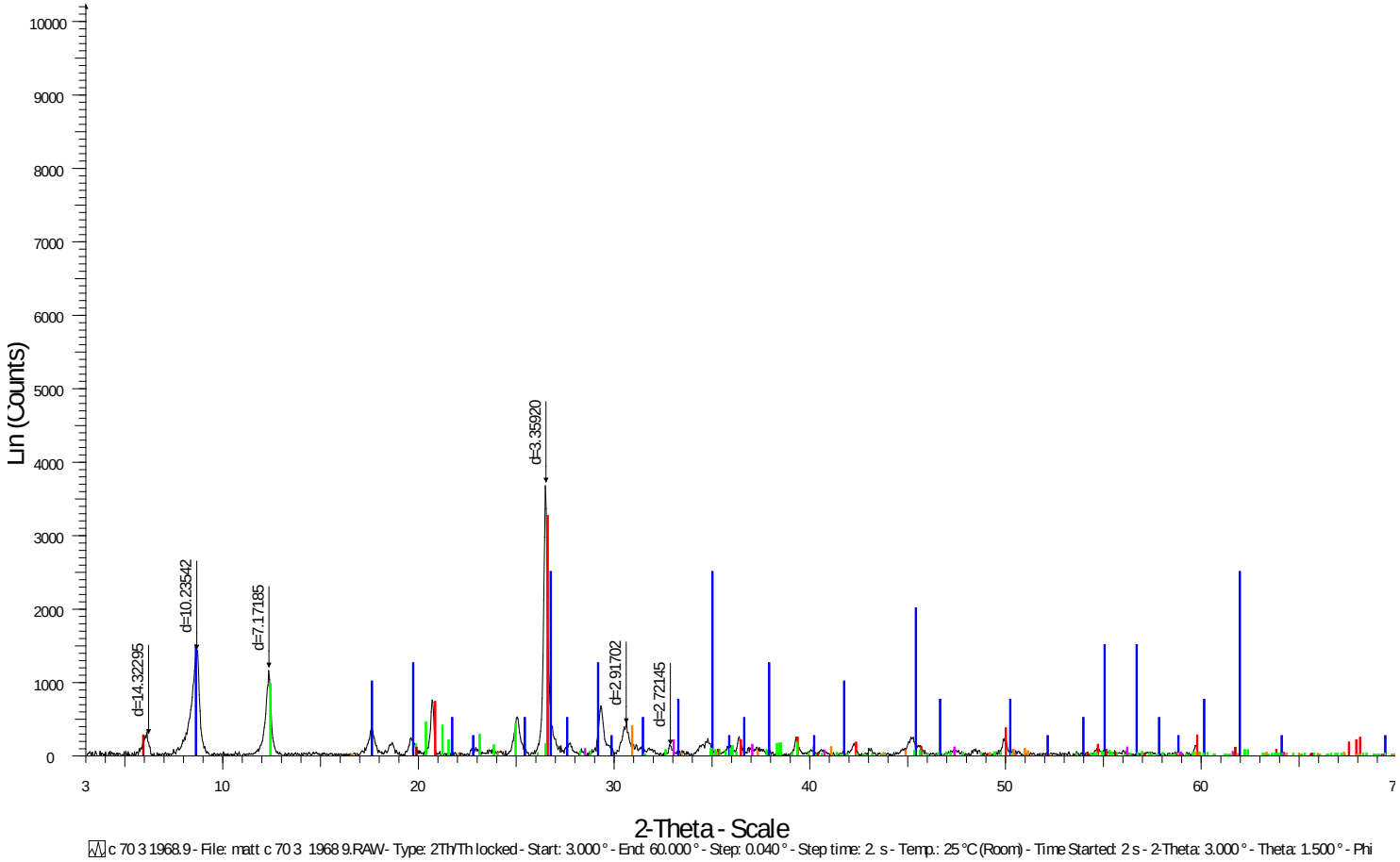

c 70 3 1968.9 - File: matt c 70 3 1968 9.RAW - Type: 2Th/Th locked - Start: 3.000 ° - End: 60.000 ° - Step: 0.040 ° - Step time: 2. s - Temp.: 25 °C (Room) - Time Started: 2 s - 2-Theta: 3.000 ° - Theta: 1.500 ° - Phi
Operations: Background 1.000,1.000 | Import

83-0539 (C) - Quartz - SiO2 - Y: 88.85 % - d x by: 1. - WL: 1.54056 - Hexagonal - a 4.92100 - b 4.92100 - c 5.41630 - alpha 90.000 - beta 90.000 - gamma 120.000 - Primitive - P3121 (152) - 3 - 113.590 - I/Ic PDF 3.

15-0603 (D) - Illite - K(AlFe)2AlSi3O10(OH)2·H2O - Y: 67.95 % - d x by: 1. - WL: 1.54056 -

83-0971 (C) - Kaolinite - Al2(Si2O5)(OH)4 - Y: 26.14 % - d x by: 1. - WL: 1.54056 - Triclinic - a 5.15350 - b 8.94190 - c 7.39060 - alpha 91.926 - beta 105.046 - gamma 89.797 - Base-centred - C1 (0) - 2 - 328.708 - I

71-2219 (C) - Pyrite - FeS2 - Y: 5.23 % - d x by: 1. - WL: 1.54056 - Cubic - a 5.41790 - b 5.41790 - c 5.41790 - alpha 90.000 - beta 90.000 - gamma 90.000 - Primitive - Pa3 (205) - 4 - 159.035 - I/Ic PDF 2.6 -

03-0015 (D) - Montmorillonite (bentonite) - (Na,Ca)0.3(Al,Mg)2Si4O10(OH)2·xH2O - Y: 7.06 % - d x by: 1. - WL: 1.54056 -

84-1208 (C) - Dolomite - CaMg(CO3)2 - Y: 10.59 % - d x by: 1. - WL: 1.54056 - Hexagonal (Rh) - a 4.81100 - b 4.81100 - c 16.04700 - alpha 90.000 - beta 90.000 - gamma 120.000 - Primitive - R-3 (148) - 3 - 321.65

Snake River c-28-D/94-O-1 1949.7 m

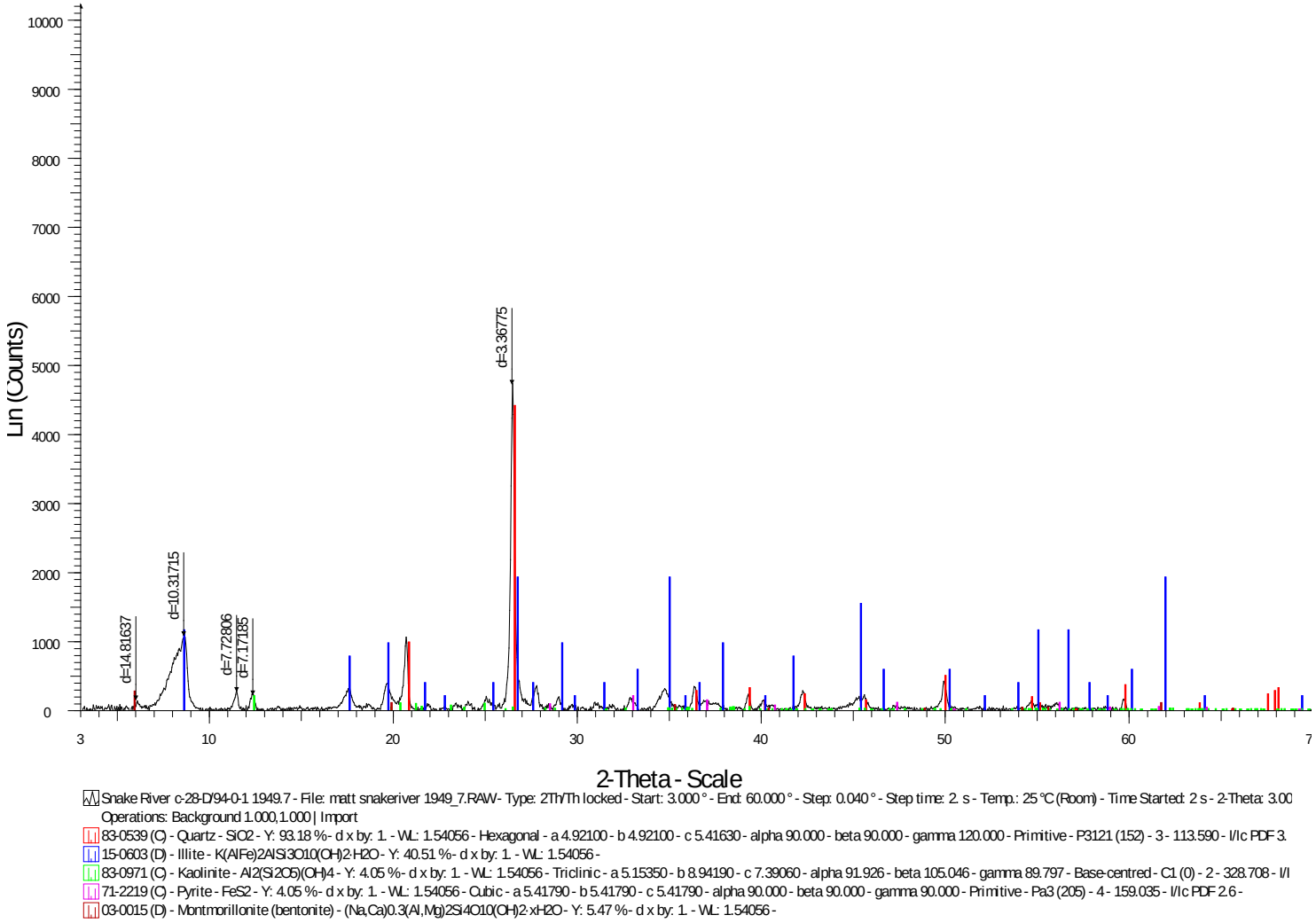

Snake River c-28-D/94-O-1 1951.5 m

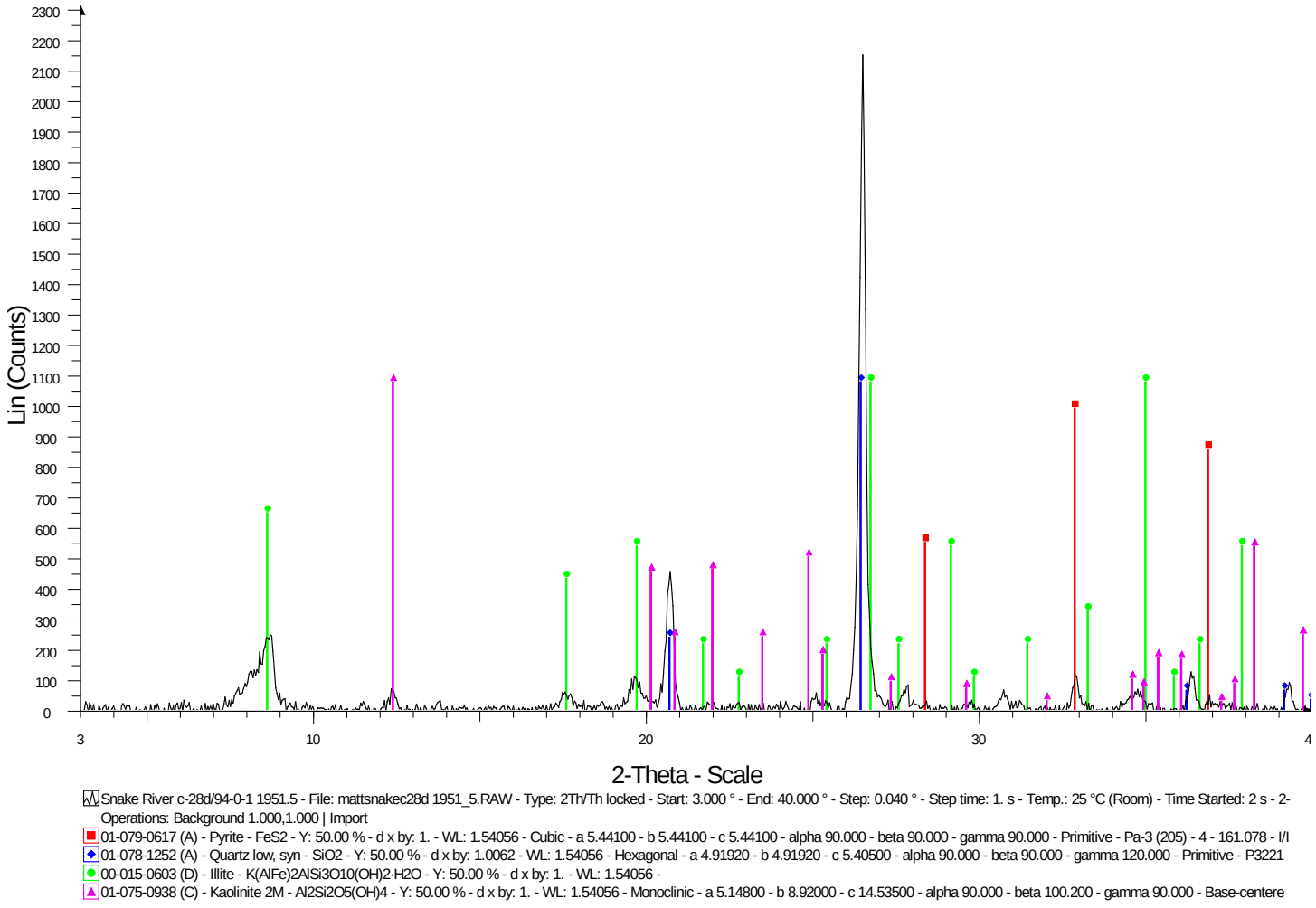

Snake River c-28-D/94-O-1 1952.6 m

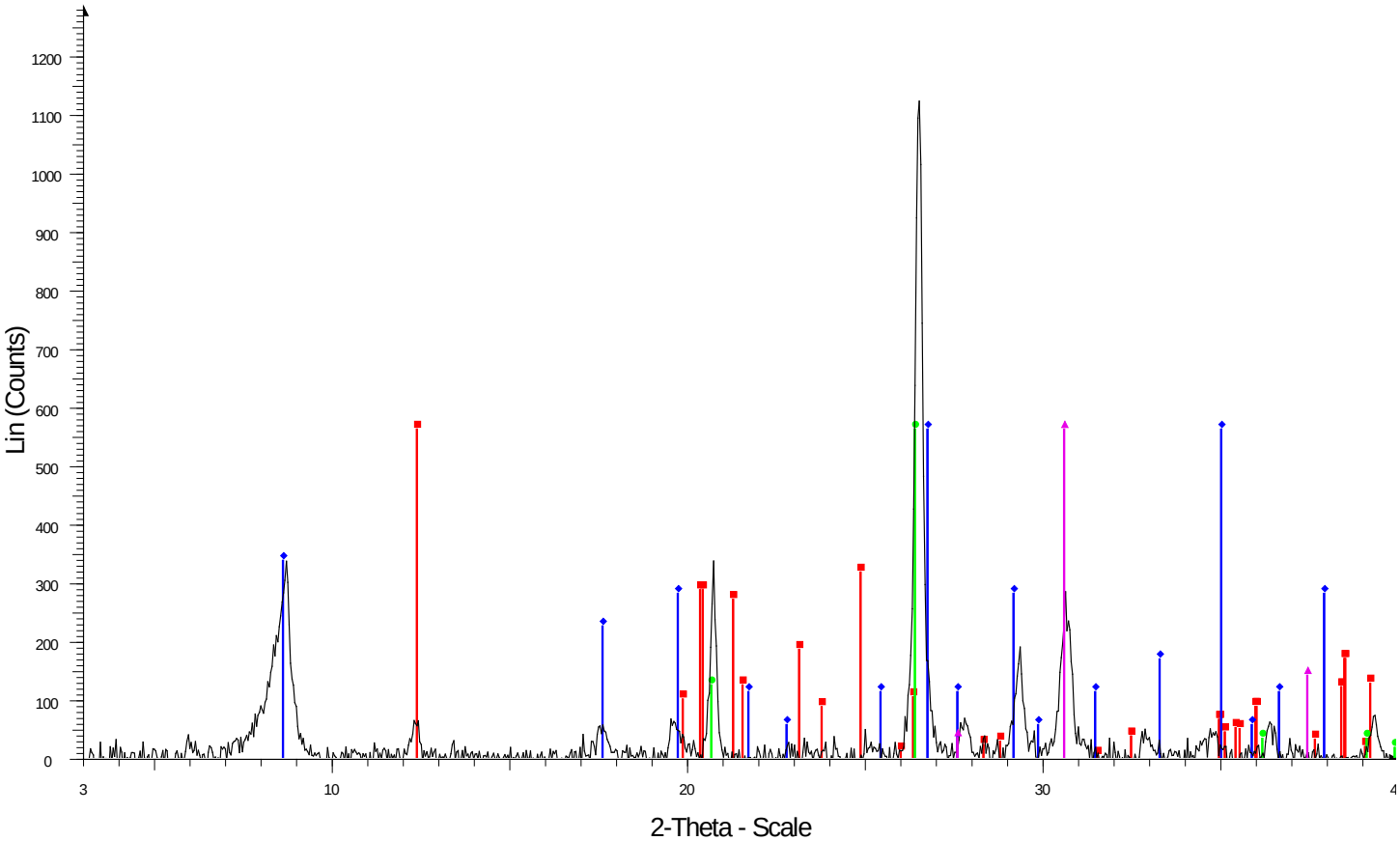

Snake River c-28d/94-0-1 1952.6 - File: mattsnakec28d 1952_6.RAW - Type: 2Th/Th locked - Start: 3.000 ° - End: 40.000 ° - Step: 0.040 ° - Step time: 1. s - Temp.: 25 °C (Room) - Time Started: 2 s - 2-
Operations: Background 1.000,1.000 | Import

01-089-6538 (C) - Kaolinite - Al2(Si2O5)(OH)4 - Y: 50.00 % - d x by: 1. - WL: 1.54056 - Triclinic - a 5.15400 - b 8.94200 - c 7.40100 - alpha 91.690 - beta 104.610 - gamma 89.820 - Base-centered - C1 (

00-015-0603 (D) - Illite - K(AlFe)2AlSi3O10(OH)2·H2O - Y: 50.00 % - d x by: 1. - WL: 1.54056 -

01-078-1252 (A) - Quartz low, syn - SiO2 - Y: 50.00 % - d x by: 1.0083 - WL: 1.54056 - Hexagonal - a 4.91920 - b 4.91920 - c 5.40500 - alpha 90.000 - beta 90.000 - gamma 120.000 - Primitive - P3221

00-003-0670 (D) - Calcite - CaCO3 - Y: 50.00 % - d x by: 1. - WL: 1.54056 - Hexagonal (Rh) - a 4.98300 - b 4.98300 - c 17.02000 - alpha 90.000 - beta 90.000 - gamma 120.000 - Primitive - R-3c (167) -

APPENDIX C – ADSORPTION ISOTHERMS

Exshaw Formation

Well Name	UWI	Depth (m)
Golata	8-29-83-15W6	3388.15
		3390.10
Sikanni Chief	b-92-D/94-I-4	1573.80
		1574.60
Parkland	10-26-081-16W6	3371.95
		3372.40
Kaiser Doe	6-6-81-14W6	3303.80

IMP Pacific Golata 8-29-83-15W6 3388.15 m

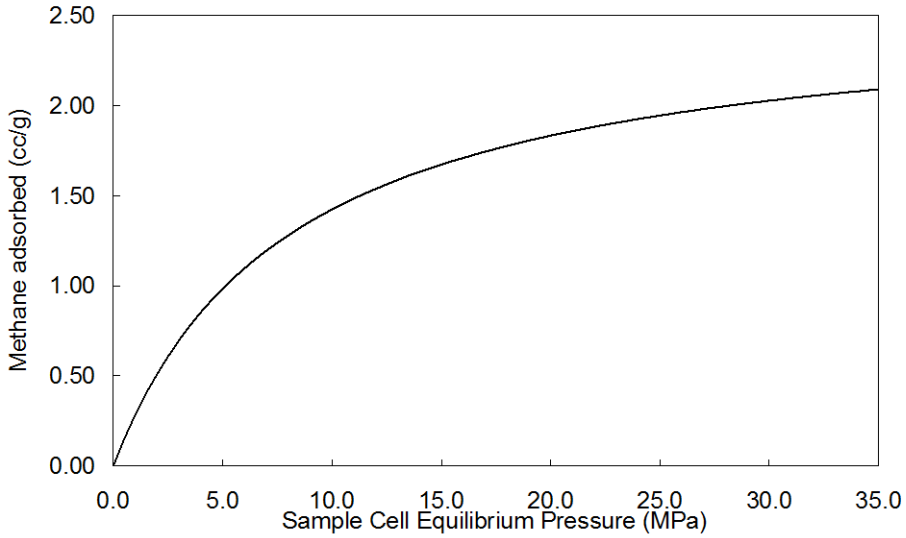

Pressure (MPa)	*Adsorbed gas (cc/g) In-Situ Conditions (Equilbrium Moisture)*
0.303	0.10
0.516	0.17
0.761	0.24
1.068	0.31
1.456	0.39
1.908	0.47
2.772	0.62
3.750	0.75
4.457	0.84
5.290	1.01
6.525	1.07
7.251	1.26
10.809	1.53

Langmuir Parameters

	In-Situ Conditions (Equilbrium Moisture)
Vol. (cc/g)	2.57
Pressure (MPa)	8.06

SUMMARY OF ADSORPTION ANALYSES SI UNITS

Isotherm Temperature: **30.0 ºC**

Goodness of fit of Langmuir regression: **0.95** **Density g/cc**

Moisture % **1.47**

IMP Pacific Golata 8-29-83-15W6 3390.1

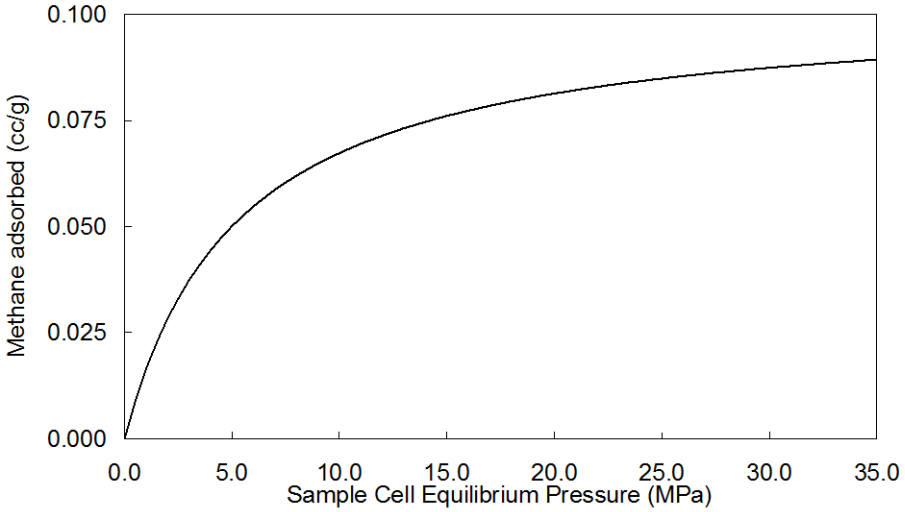

Pressure (MPa)	*Adsorbed gas (cc/g) In-Situ Conditions (Equilbrium Moisture)*
0.311	0.01
0.600	0.02
0.856	0.03
1.101	0.03
1.446	0.04
1.856	0.03
2.558	0.03
3.448	0.03
4.302	0.03
5.241	0.02
6.159	0.07
7.068	0.07
9.493	0.07
10.994	0.09

Langmuir Parameters

	In-Situ Conditions (Equilbrium Moisture)
Vol. (cc/g)	0.10
Pressure (MPa)	5.25

SUMMARY OF ADSORPTION ANALYSES SI UNITS

Isotherm Temperature: **30.0 ºC**

Goodness of fit of Langmuir regression: **0.34** **Density (g/cc)** **2.546**

Moisture% **1.42**

Sikanni Chief b-92-D/94-I-4 1573.8 m

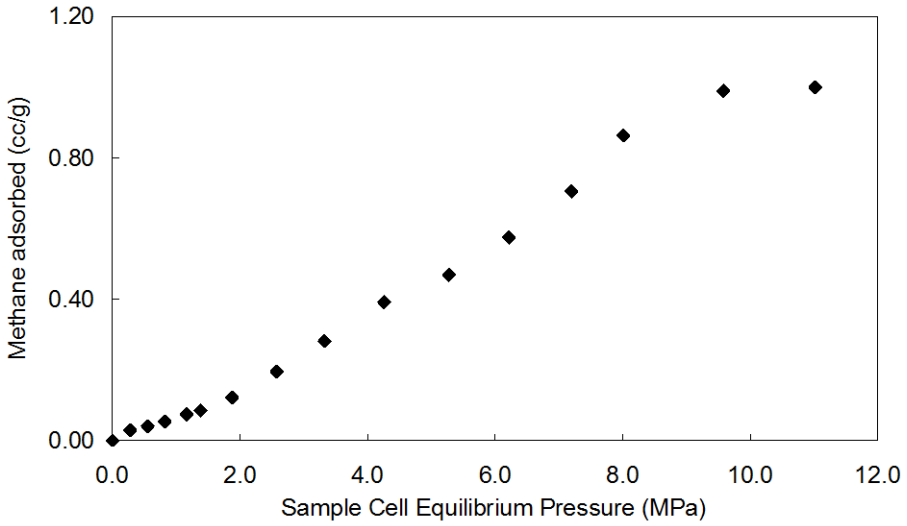

Pressure (MPa)	*Adsorbed gas (cc/g) In-Situ Conditions (Equilbrium Moisture)*
0.279	0.03
0.551	0.04
0.820	0.05
1.162	0.07
1.377	0.09
1.879	0.12
2.575	0.19
3.325	0.28
4.258	0.39
5.275	0.47
6.219	0.57
7.198	0.71
9.580	0.99
11.015	1.00

Langmuir Parameters

	In-Situ Conditions (Equilbrium Moisture)
Vol. (cc/g)	
Pressure (MPa)	

SUMMARY OF ADSORPTION ANALYSES SI UNITS

Isotherm Temperature: **30.0 ºC**

Goodness of fit of Langmuir regression: **0.40** **Density (g/cc)** **2.706**

Moisture% **4.54**

Sikanni Chief b-92-D/94-I-4 1574.6 m

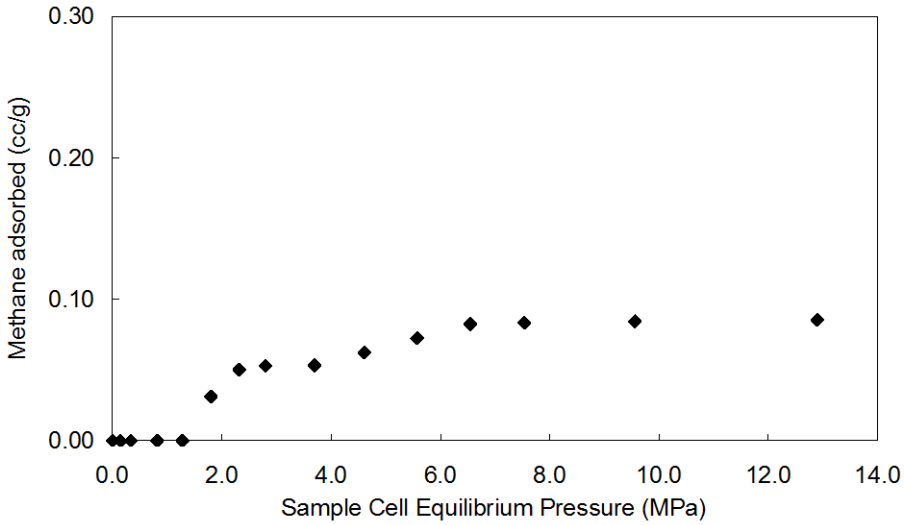

Pressure (MPa)	*Adsorbed gas (cc/g) In-Situ Conditions (Equilbrium Moisture)*
0.149	0.00
0.333	0.00
0.820	0.00
1.281	0.00
1.805	0.03
2.314	0.05
2.799	0.05
3.693	0.05
4.607	0.06
5.569	0.07
6.544	0.08
7.530	0.08
12.888	0.09
16.900	0.09

Langmuir Parameters

	In-Situ Conditions (Equilbrium Moisture)
Vol. (cc/g)	
Pressure (MPa)	

SUMMARY OF ADSORPTION ANALYSES SI UNITS

Isotherm Temperature: 30.0 ºC
Goodness of fit of Langmuir regression: 0.27 **Density (g/cc)** 2.460
Moisture% 3.48

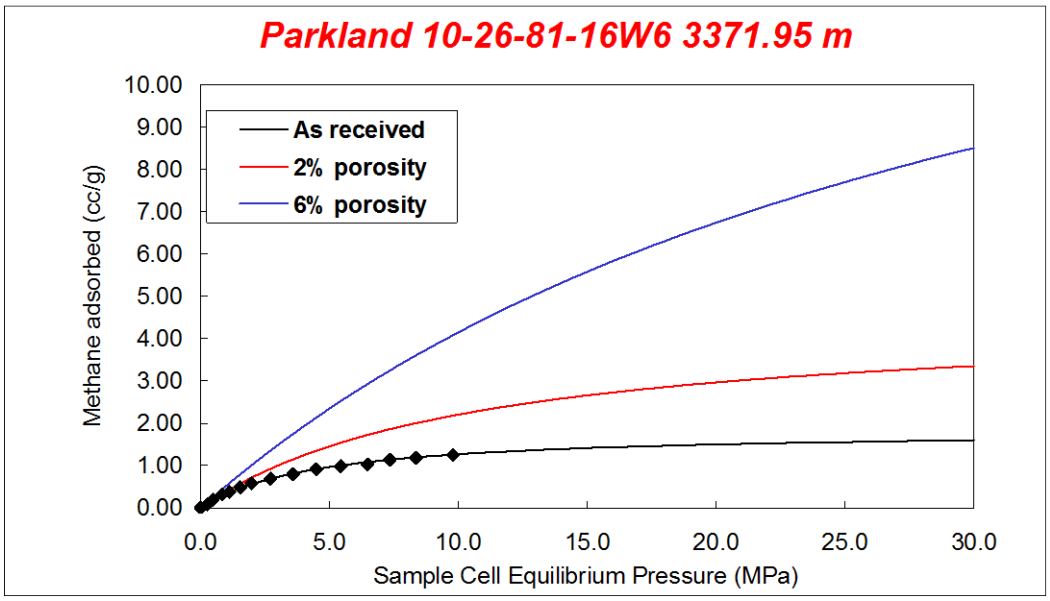

Pressure (MPa)	*Adsorbed gas (cc/g) In-Situ Conditions (Equilbrium Moisture)*
0.259	0.08
0.464	0.19
0.829	0.32
1.109	0.38
1.538	0.49
1.975	0.58
2.710	0.69
3.578	0.80
4.484	0.92
5.439	0.99
6.481	1.03
7.336	1.14
9.791	1.25
10.992	1.35

Langmuir Parameters

	In-Situ Conditions (Equilbrium Moisture)
Vol. (cc/g)	1.84
Pressure (MPa)	4.51

SUMMARY OF ADSORPTION ANALYSES SI UNITS

Isotherm Temperature: **30.0 ºC**

Goodness of fit of Langmuir regression: **0.98** **Density (g/cc)** **2.327**

Moisture% **7.36**

10-26-081-16W6/02 Parkland 3372.4 m

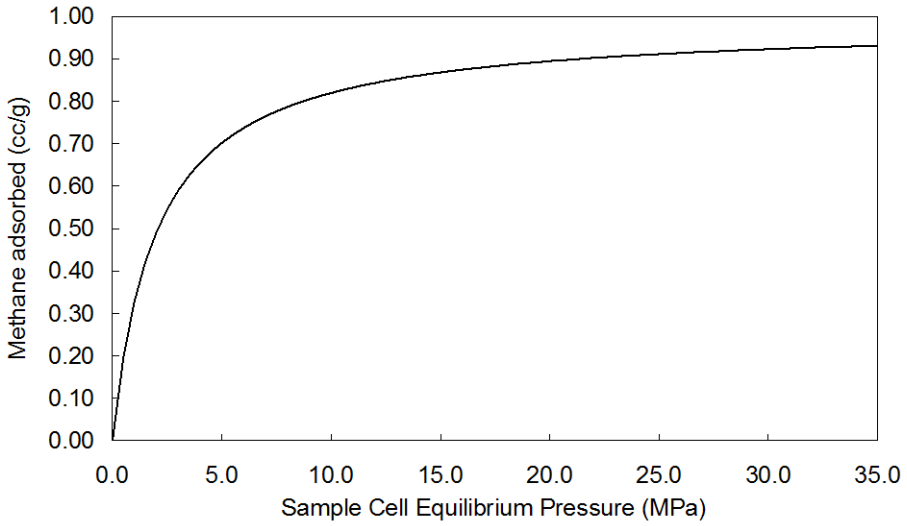

Pressure (MPa)	*Adsorbed gas (cc/g) In-Situ Conditions (Equilbrium Moisture)*
0.278	0.07
0.484	0.17
0.806	0.28
1.161	0.38
1.582	0.47
2.051	0.55
2.918	0.62
3.967	0.72
4.989	0.75
6.005	0.77
8.003	0.80
10.004	0.81

Langmuir Parameters

	In-Situ Conditions (Equilbrium Moisture)
Vol. (cc/g)	0.98
Pressure (MPa)	2.01

SUMMARY OF ADSORPTION ANALYSES SI UNITS

Isotherm Temperature: **30.0 ºC**

Goodness of fit of Langmuir regression: **0.98** **Density (g/cc)** **2.202**

Moisture% **11.88**

Kaiser Doe 6-6-81-14W6 3303.8 m

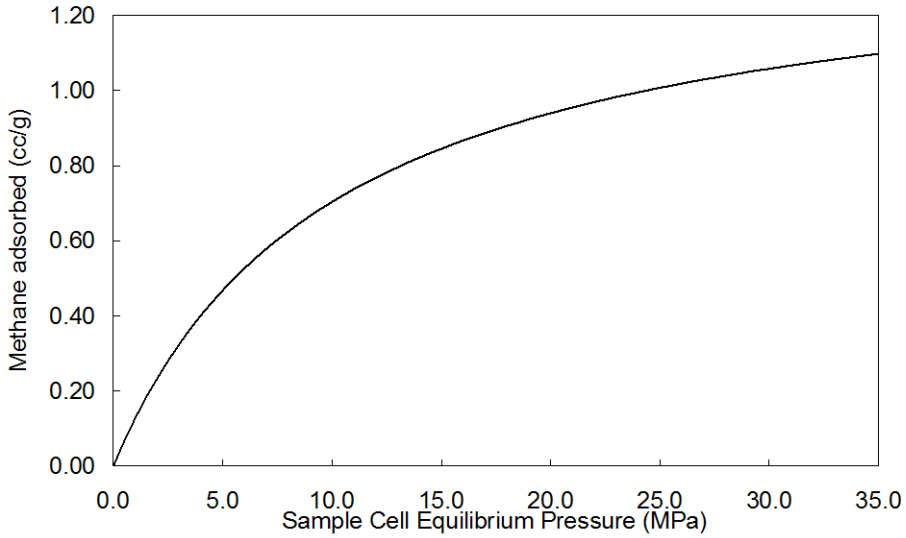

Pressure (MPa)	*Adsorbed gas (cc/g) In-Situ Conditions (Equilbrium Moisture)*
0.237	0.04
0.473	0.07
0.744	0.10
0.927	0.11
1.286	0.14
1.722	0.17
2.500	0.24
3.394	0.34
4.331	0.45
5.295	0.58
6.250	0.62
7.203	0.62
10.000	0.63

Langmuir Parameters

	In-Situ Conditions (Equilbrium Moisture)
Vol. (cc/g)	1.41
Pressure (MPa)	10.11

SUMMARY OF ADSORPTION ANALYSES SI UNITS

Isotherm Temperature: **30.0 ºC**

Goodness of fit of Langmuir regression: **0.76** **2.865**

Besa River

Well Name	UWI	Depth (m)
La Biche	b-55-E/94-O-13	3044.80
		3046.15
		3047.20
Dunedin	d-75-E/94-N-8	3688.80
		3695.10
		3773.80
		3775.00
		3890.60
		3892.10
		3893.00
		3894.50
		3895.70
		3896.00

LA BICHE b-55-E/94-O-13 3044.8 m

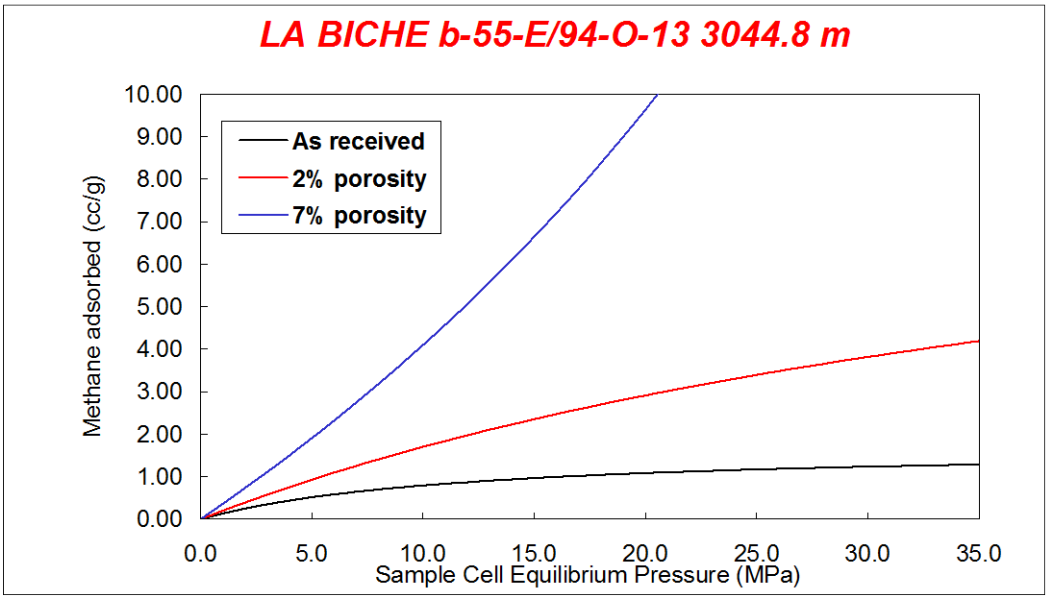

Pressure (MPa)	*Adsorbed gas (cc/g) In-Situ Conditions (Equilbrium Moisture)*
0.329	0.05
0.564	0.09
0.825	0.13
1.028	0.15
1.443	0.18
1.798	0.21
2.560	0.28
3.496	0.35
4.334	0.43
5.265	0.52
6.495	0.61
7.241	0.67
9.493	0.79
10.994	0.85

Langmuir Parameters

	In-Situ Conditions (Equilbrium Moisture)
Vol. (cc/g)	1.72
Pressure (MPa)	11.65

SUMMARY OF ADSORPTION ANALYSES SI UNITS

Isotherm Temperature: **30.0 ºC**

Goodness of fit of Langmuir regression: **0.91** **Density (g/cc)** **2.487**

Moisture% **1.41**

La Biche b-055-E/94-O-13 3046.15 m

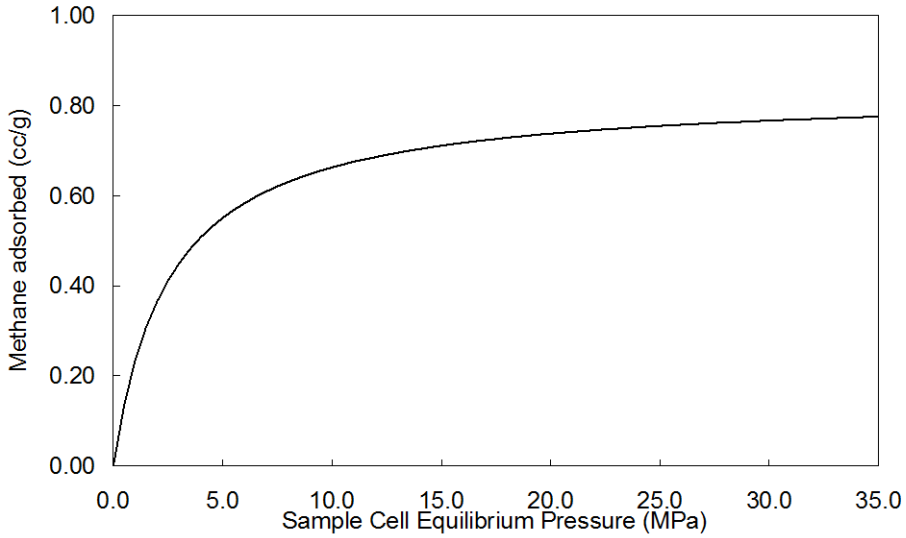

Pressure (MPa)	*Adsorbed gas (cc/g) In-Situ Conditions (Equilbrium Moisture)*
0.186	0.04
0.375	0.11
0.590	0.16
0.831	0.21
1.238	0.27
1.700	0.34
2.504	0.44
3.429	0.50
4.392	0.54
5.358	0.58
6.325	0.61
7.291	0.62
10.500	0.65

Langmuir Parameters

	In-Situ Conditions (Equilbrium Moisture)
Vol. (cc/g)	0.83
Pressure (MPa)	2.55

SUMMARY OF ADSORPTION ANALYSES SI UNITS

Isotherm Temperature: **30.0 ºC**

Goodness of fit of Langmuir regression: **0.99** **2.169**

Moisture % **13.37**

La Biche b-55-E/94-O-13 3047.2 m

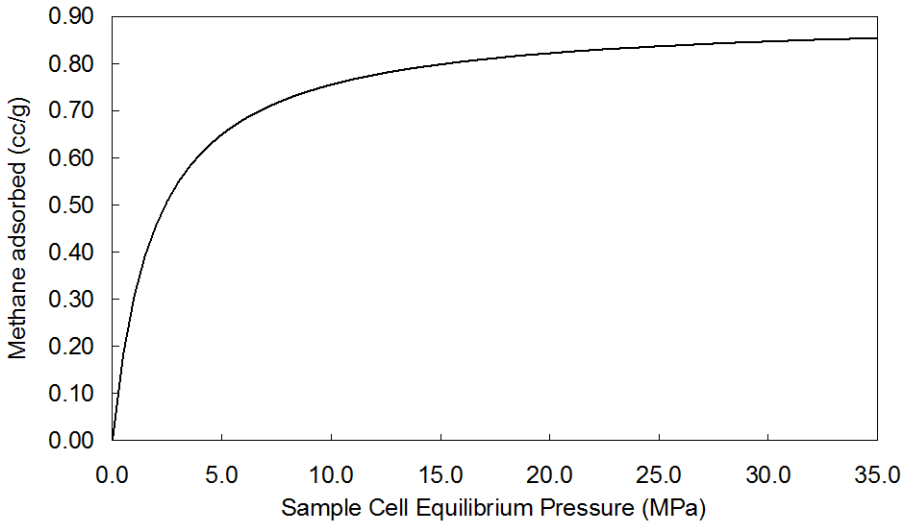

Pressure (MPa)	*Adsorbed gas (cc/g) In-Situ Conditions (Equilbrium Moisture)*
0.170	0.08
0.339	0.15
0.686	0.23
1.074	0.29
1.612	0.39
2.268	0.45
3.167	0.54
3.783	0.60
4.649	0.67
5.624	0.71
6.591	0.72
7.568	0.73

Langmuir Parameters

	In-Situ Conditions (Equilbrium Moisture)
Vol. (cc/g)	0.90
Pressure (MPa)	1.94

SUMMARY OF ADSORPTION ANALYSES SI UNITS

Isotherm Temperature: **30.0 ºC**

Goodness of fit of Langmuir regression: **0.99** **Density (g/cc)** **2.558**

Moisture% **3.09**

DUNEDIN d-75-E/94-N-8 3688.8 m

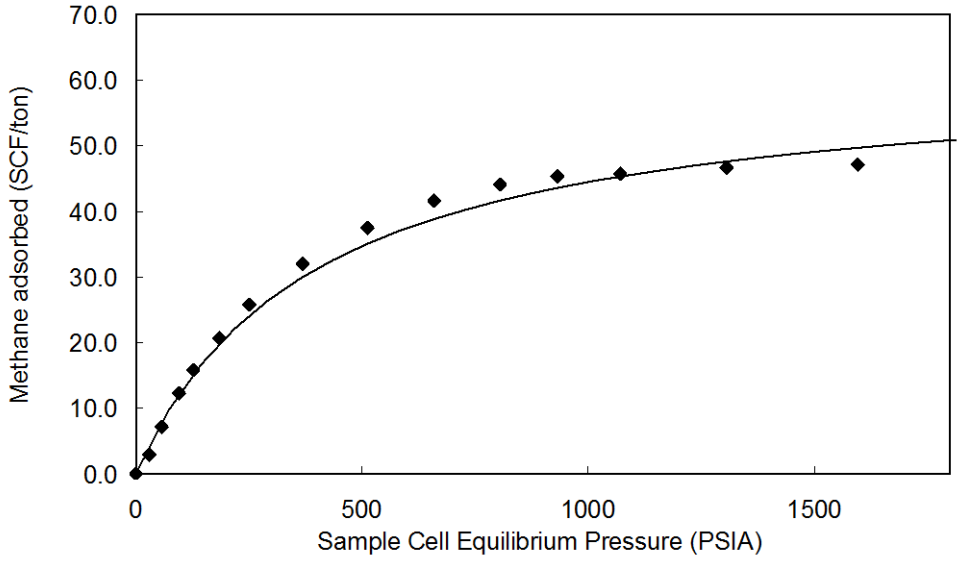

Pressure (PSIA)	*Adsorbed gas (ft^3 /ton) In-Situ Conditions (Equilbrium Moisture)*
30	2.9
57	7.1
95	12.2
127	15.8
184	20.7
251	25.7
369	32.0
512	37.5
659	41.6
805	44.1
931	45.4
1070	45.7
1306	46.7
1596	47.1

Langmuir Parameters

	In-Situ Conditions (Equilbrium Moisture)
Vol. (ft^3 /ton)	61.9
Pressure (PSIA)	392.6

SUMMARY OF ADSORPTION ANALYSES IMP. UNITS

Isotherm Temperature: **86.0 °F**

Goodness of fit of Langmuir regression: **0.98** **2.785**

DUNEDIN d-75-E/94-N-8 3695.1 m

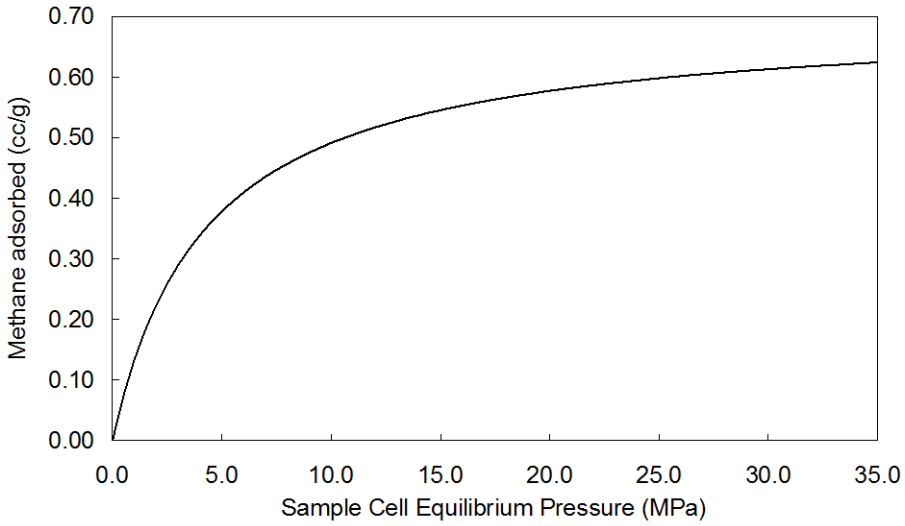

Pressure (MPa)	*Adsorbed gas (cc/g) In-Situ Conditions (Equilbrium Moisture)*
0.215	0.03
0.443	0.07
0.678	0.10
0.906	0.12
1.297	0.16
1.746	0.20
2.495	0.25
3.396	0.31
4.327	0.36
5.295	0.38
6.192	0.43
7.126	0.44
10.940	0.49

Langmuir Parameters

	In-Situ Conditions (Equilbrium Moisture)
Vol. (cc/g)	0.70
Pressure (MPa)	4.25

SUMMARY OF ADSORPTION ANALYSES SI UNITS

Isotherm Temperature: **30.0 ºC**

Goodness of fit of Langmuir regression: **0.99** **Density (g/cc)** **2.490**

Moisture% **5.95**

DUNEDIN d-75-E/94-N-8 3773.8 m

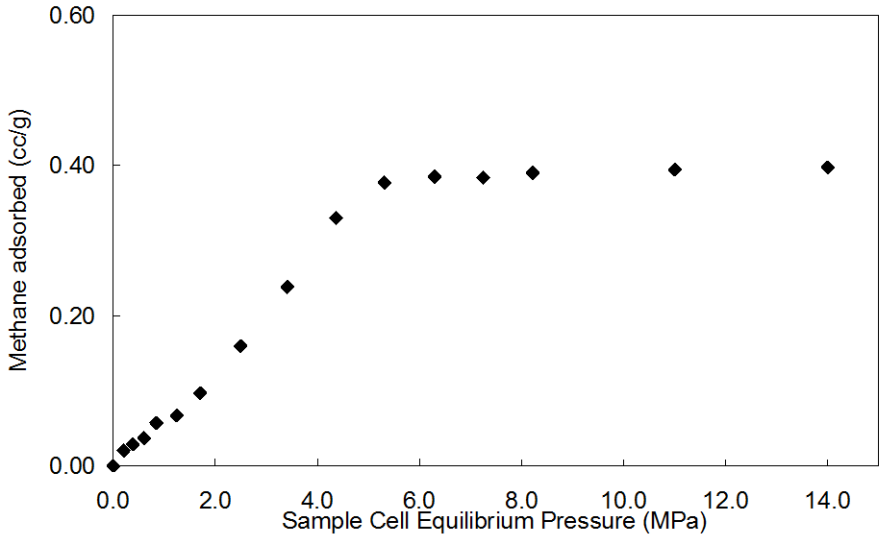

Pressure (MPa)	*Adsorbed gas (cc/g) In-Situ Conditions (Equilbrium Moisture)*
0.204	0.02
0.382	0.03
0.604	0.04
0.841	0.06
1.242	0.07
1.702	0.10
2.496	0.16
3.408	0.24
4.363	0.33
5.313	0.38
6.298	0.38
7.250	0.38
11.000	0.39
14.000	0.40

Langmuir Parameters

	In-Situ Conditions (Equilbrium Moisture)
Vol. (cc/g)	
Pressure (MPa)	

SUMMARY OF ADSORPTION ANALYSES SI UNITS

Isotherm Temperature: **30.0 ºC**

Goodness of fit of Langmuir regression: **0.73** **2.500**

DUNEDIN d-75-E/94-N-08 3775 m

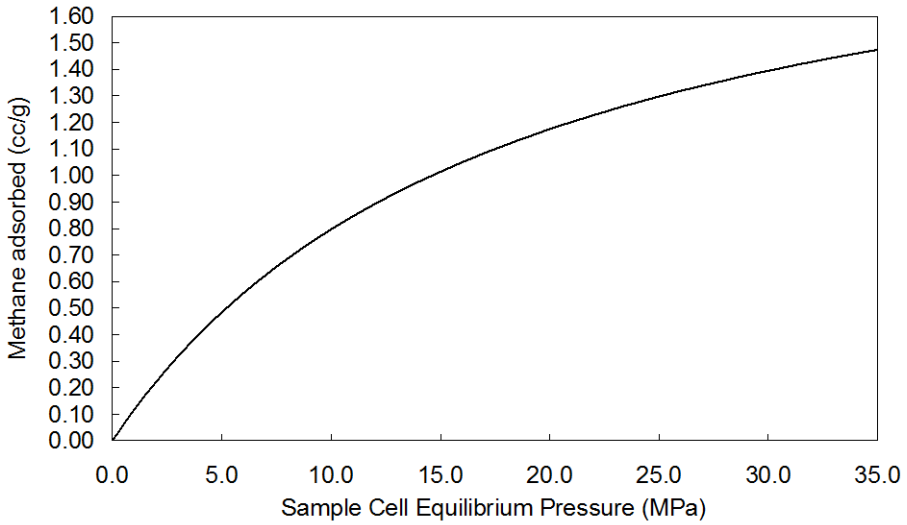

Pressure (MPa)	*Adsorbed gas (cc/g) In-Situ Conditions (Equilbrium Moisture)*
0.435	0.05
0.846	0.10
0.951	0.11
1.200	0.13
1.420	0.15
1.886	0.20
2.634	0.30
3.437	0.38
4.447	0.49
5.321	0.54
6.198	0.60
7.170	0.69
11.600	0.83
13.000	0.88

Langmuir Parameters

	In-Situ Conditions (Equilbrium Moisture)
Vol. (cc/g)	2.23
Pressure (MPa)	18.04

SUMMARY OF ADSORPTION ANALYSES SI UNITS

Isotherm Temperature: **30.0 ºC**
Goodness of fit of Langmuir regression: **0.90** **Density (g/cc)** **2.444**
Moisture% **6.29**

DUNEDIN d-75-E/94-N-08 3890.6 m

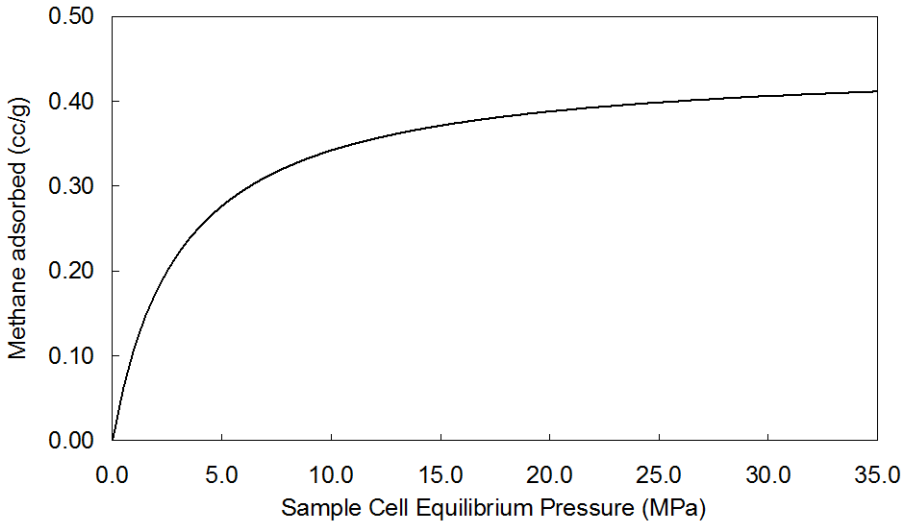

Pressure (MPa)	*Adsorbed gas (cc/g) In-Situ Conditions (Equilbrium Moisture)*
0.225	0.03
0.424	0.06
0.657	0.08
0.893	0.10
1.268	0.13
1.713	0.15
2.502	0.19
3.378	0.25
4.335	0.26
5.279	0.27
6.153	0.30
7.117	0.33
9.551	0.34
11.060	0.35

Langmuir Parameters

	In-Situ Conditions (Equilbrium Moisture)
Vol. (cc/g)	0.45
Pressure (MPa)	3.10

SUMMARY OF ADSORPTION ANALYSES SI UNITS

Isotherm Temperature: **30.0 ºC**

Goodness of fit of Langmuir regression: **1.00** **Density (g/cc)** **2.468**

Moisture% **8.11**

DUNEDIN d-75-E/94-N-08 3892.1 m

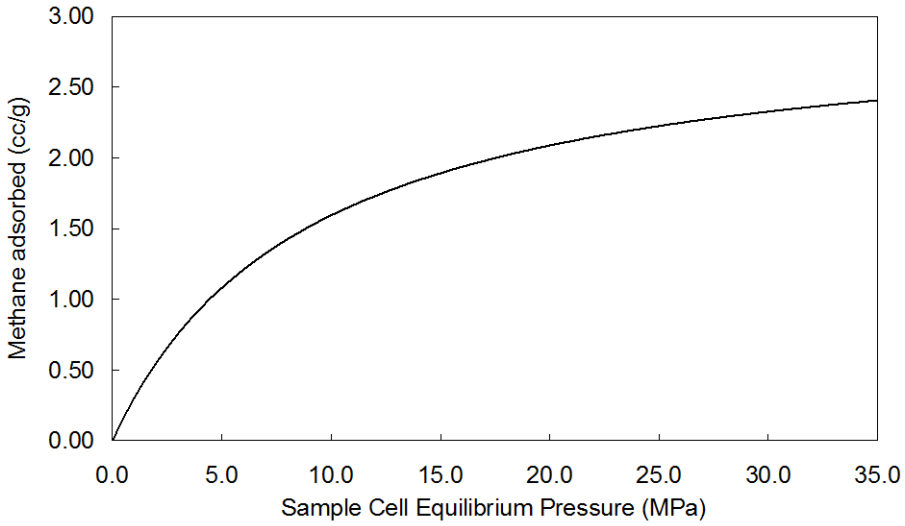

Pressure (MPa)	*Adsorbed gas (cc/g) In-Situ Conditions (Equilbrium Moisture)*
0.257	0.07
0.408	0.13
0.615	0.20
0.842	0.27
1.221	0.37
1.668	0.48
2.437	0.66
3.330	0.83
4.273	0.98
5.214	1.12
6.311	1.26
7.239	1.38
12.000	1.70

Langmuir Parameters

	In-Situ Conditions (Equilbrium Moisture)
Vol. (cc/g)	3.02
Pressure (MPa)	8.97

SUMMARY OF ADSORPTION ANALYSES SI UNITS

Isotherm Temperature: **30.0 ºC**

Goodness of fit of Langmuir regression: **0.98** **Density (g/cc)** **2.597**

Moisture% **5.66**

DUNEDIN d-75-E/94-N-08 3893.0 m

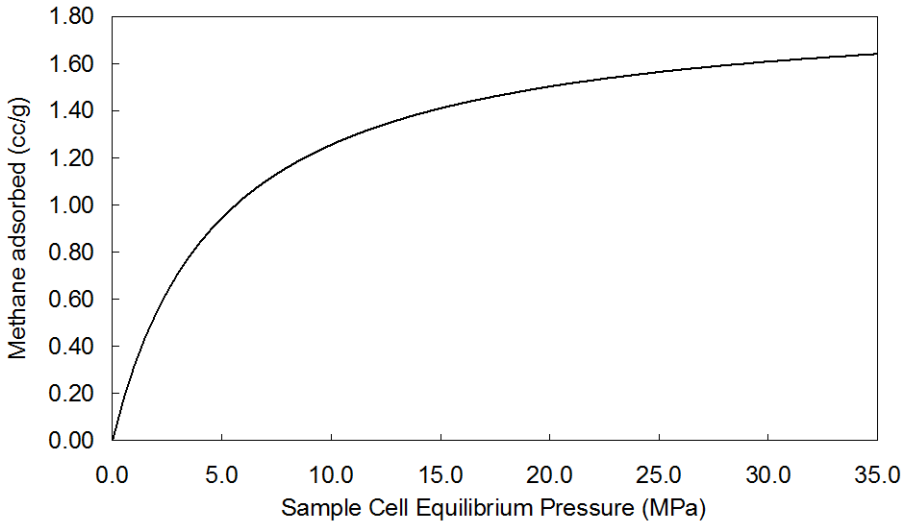

Pressure (MPa)	*Adsorbed gas (cc/g) In-Situ Conditions (Equilbrium Moisture)*
0.126	0.06
0.292	0.12
0.490	0.17
0.721	0.23
1.107	0.32
1.558	0.41
2.331	0.57
3.227	0.72
4.165	0.86
5.200	0.96
6.045	1.03
7.047	1.13
11.000	1.31

Langmuir Parameters

	In-Situ Conditions (Equilbrium Moisture)
Vol. (cc/g)	1.87
Pressure (MPa)	4.90

SUMMARY OF ADSORPTION ANALYSES SI UNITS

Isotherm Temperature: **30.0 ºC**

Goodness of fit of Langmuir regression: **0.98** **Density (g/cc)** **2.614**

Moisture% **5.91**

DUNEDIN d-75-E/94-N-08 3894.5 m

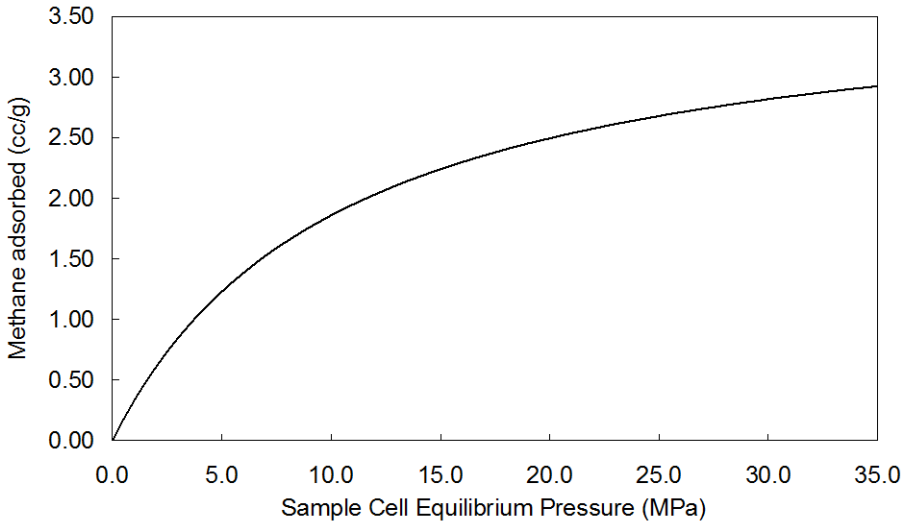

Pressure (MPa)	*Adsorbed gas (cc/g) In-Situ Conditions (Equilbrium Moisture)*
0.217	0.07
0.394	0.15
0.569	0.21
0.786	0.28
1.168	0.39
1.613	0.50
2.377	0.68
3.266	0.89
4.204	1.08
5.163	1.24
6.112	1.38
7.017	1.54
9.500	1.82
11.500	2.01

Langmuir Parameters

	In-Situ Conditions (Equilbrium Moisture)
Vol. (cc/g)	3.79
Pressure (MPa)	10.41

SUMMARY OF ADSORPTION ANALYSES SI UNITS

Isotherm Temperature: **30.0 ºC**

Goodness of fit of Langmuir regression: **0.99** **Density (g/cc)** **2.616**

Moisture% **5.67**

DUNEDIN d-75-E/94-N-08 3895.7 m

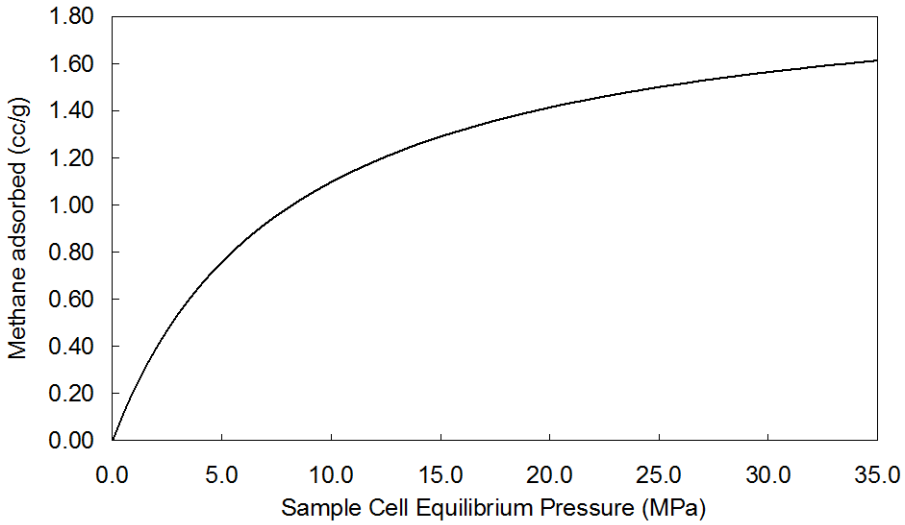

Pressure (MPa)	*Adsorbed gas (cc/g) In-Situ Conditions (Equilbrium Moisture)*
0.224	0.05
0.389	0.09
0.582	0.13
0.806	0.18
1.192	0.25
1.643	0.32
2.418	0.44
3.318	0.58
4.262	0.71
5.224	0.81
6.174	0.89
7.140	0.97
10.500	1.09
12.000	1.14

Langmuir Parameters

	In-Situ Conditions (Equilbrium Moisture)
Vol. (cc/g)	1.99
Pressure (MPa)	8.10

SUMMARY OF ADSORPTION ANALYSES SI UNITS

Isotherm Temperature: **30.0 ºC**
Goodness of fit of Langmuir regression: **0.98** **Density (g/cc)** **2.551**
Moisture% **5.26**

DUNEDIN d-75-E/94-N-08 3896.0 m

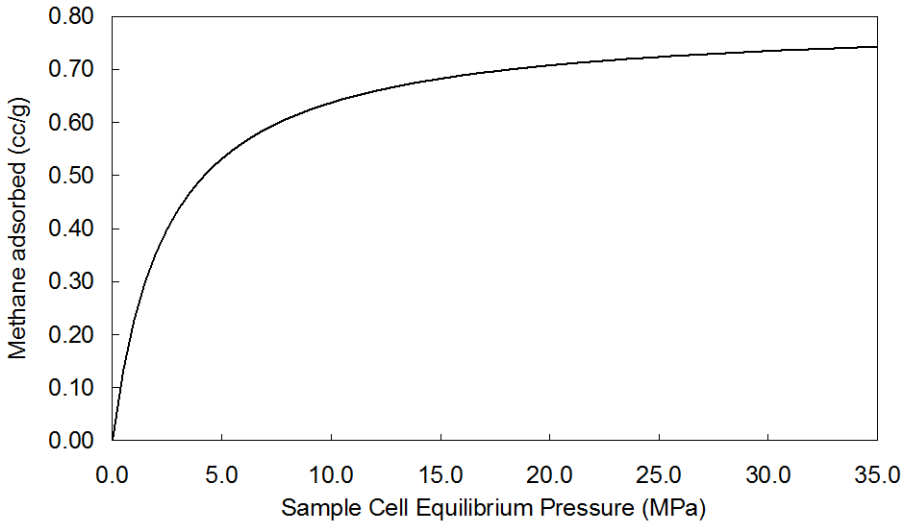

Pressure (MPa)	*Adsorbed gas (cc/g) In-Situ Conditions (Equilbrium Moisture)*
0.220	0.05
0.428	0.11
0.666	0.17
0.886	0.21
1.270	0.27
1.719	0.32
2.491	0.41
3.361	0.47
4.295	0.54
5.272	0.57
6.262	0.58
7.150	0.61
9.475	0.62
10.967	0.62

Langmuir Parameters

	In-Situ Conditions (Equilbrium Moisture)
Vol. (cc/g)	0.80
Pressure (MPa)	2.48

SUMMARY OF ADSORPTION ANALYSES SI UNITS

Isotherm Temperature: **30.0 ºC**

Goodness of fit of Langmuir regression: **0.99** **Density (g/cc)** **2.561**

Moisture% **7.22**

Fort Simpson Formation

Well Name	UWI	Depth (m)
Junior	c-60-E/94-I-11	1869.70
		1873.90
		1876.90
		1879.00
		1879.60
Sikanni Chief	b-92-D/94-I-4	1953.80
		1957.50
		2106.70
		2216.60

Junior 200/c-60-E 094-I-11/00 1869.7 m

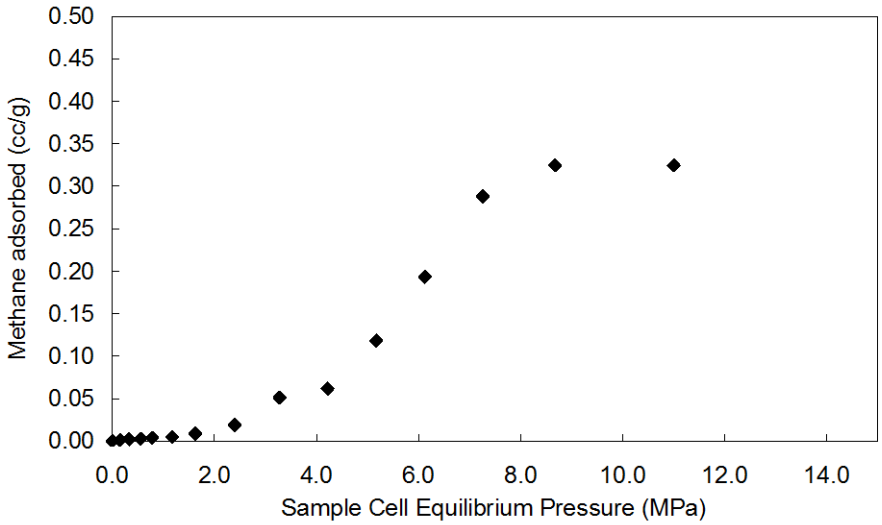

Pressure (MPa)	*Adsorbed gas (cc/g) In-Situ Conditions (Equilbrium Moisture)*
0.148	0.00
0.324	0.00
0.548	0.00
0.780	0.00
1.170	0.00
1.620	0.01
2.393	0.02
3.276	0.05
4.219	0.06
5.169	0.12
6.121	0.19
7.258	0.29
11.000	0.32
14.000	0.32

Langmuir Parameters

	In-Situ Conditions (Equilbrium Moisture)
Vol. (cc/g)	
Pressure (MPa)	

SUMMARY OF ADSORPTION ANALYSES SI UNITS

Isotherm Temperature: **30.0 ºC**

Goodness of fit of Langmuir regression: **0.63** **Density (g/cc)** **2.679**

Moisture% **4.59**

Junior 200/c-60-E 094-I-11/00 1873.9 m

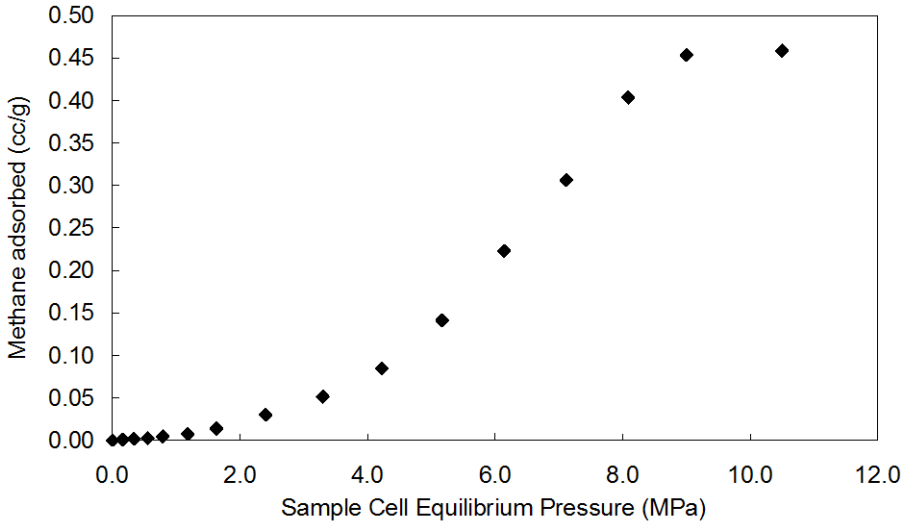

Pressure (MPa)	*Adsorbed gas (cc/g) In-Situ Conditions (Equilbrium Moisture)*
0.158	0.00
0.338	0.00
0.555	0.00
0.792	0.00
1.182	0.01
1.631	0.01
2.404	0.03
3.296	0.05
4.221	0.08
5.165	0.14
6.140	0.22
7.112	0.31
9.000	0.45
10.500	0.46

Langmuir Parameters

	In-Situ Conditions (Equilbrium Moisture)
Vol. (cc/g)	
Pressure (MPa)	

SUMMARY OF ADSORPTION ANALYSES SI UNITS

Isotherm Temperature: **30.0 ºC**

Goodness of fit of Langmuir regression: **0.81** **Density (g/cc)** **2.503**

Moisture% **4.12**

Junior 200/c-60-E 094-I-11/00 1876.9 m

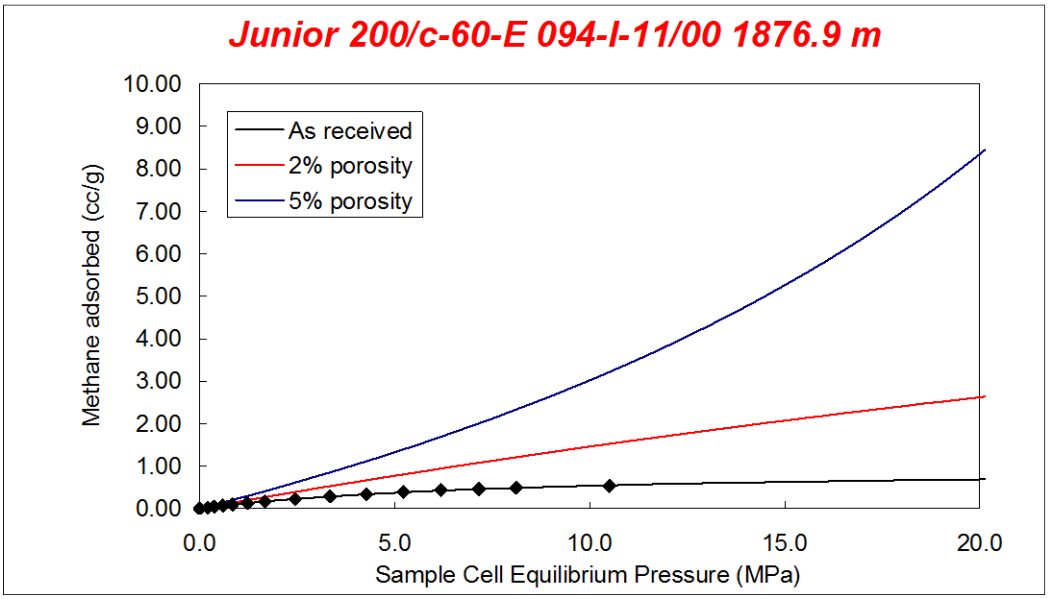

Pressure (MPa)	*Adsorbed gas (cc/g) In-Situ Conditions (Equilbrium Moisture)*
0.203	0.02
0.378	0.05
0.596	0.07
0.835	0.10
1.222	0.13
1.675	0.17
2.450	0.22
3.344	0.29
4.275	0.34
5.224	0.39
6.187	0.44
7.159	0.46
10.500	0.53
	0.00

Langmuir Parameters

	In-Situ Conditions (Equilbrium Moisture)
Vol. (cc/g)	0.96
Pressure (MPa)	7.79

SUMMARY OF ADSORPTION ANALYSES SI UNITS

Isotherm Temperature: **30.0 ºC**

Goodness of fit of Langmuir regression: **0.97** **Density (g/cc)** **2.536**

Moisture% **5.01**

Junior 200/c-60-E 094-I-11/00 1879.0 m

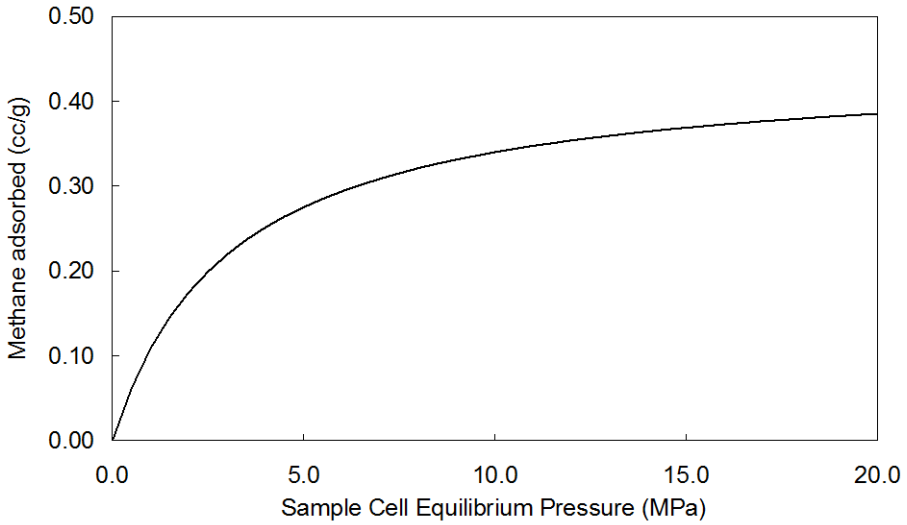

Pressure (MPa)	*Adsorbed gas (cc/g) In-Situ Conditions (Equilbrium Moisture)*
0.078	0.01
0.255	0.04
0.481	0.06
0.720	0.08
1.112	0.11
1.566	0.14
2.351	0.18
3.254	0.23
4.194	0.27
5.159	0.29
6.121	0.30
7.095	0.32
10.500	0.33

Langmuir Parameters

	In-Situ Conditions (Equilbrium Moisture)
Vol. (cc/g)	0.44
Pressure (MPa)	3.07

SUMMARY OF ADSORPTION ANALYSES SI UNITS

Isotherm Temperature: **30.0 ºC**

Goodness of fit of Langmuir regression: **0.99** **Density (g/cc)** **2.561**

Moisture% **4.97**

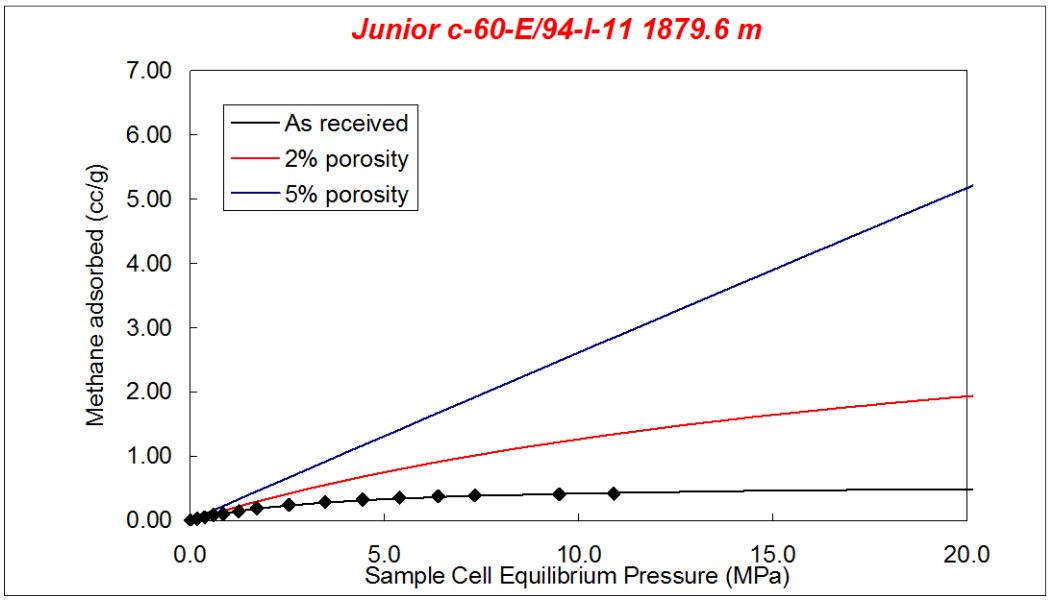

Pressure (MPa)	*Adsorbed gas (cc/g) In-Situ Conditions (Equilbrium Moisture)*
0.176	0.02
0.371	0.05
0.600	0.08
0.839	0.10
1.249	0.14
1.715	0.19
2.536	0.24
3.474	0.28
4.437	0.32
5.392	0.35
6.382	0.37
7.325	0.39
10.902	0.41

Langmuir Parameters

	In-Situ Conditions (Equilbrium Moisture)
Vol. (cc/g)	0.58
Pressure (MPa)	3.78

SUMMARY OF ADSORPTION ANALYSES SI UNITS

Isotherm Temperature: **30.0 ºC**

Goodness of fit of Langmuir regression: **0.99** **2.648**

Sikanni Chief b-92-D/94-I-4 1953.8 m

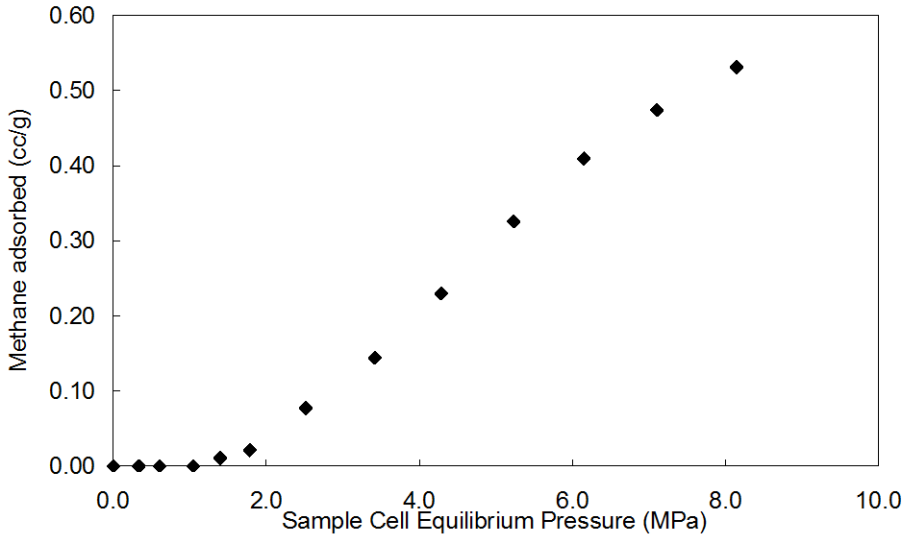

Pressure (MPa)	*Adsorbed gas (cc/g) In-Situ Conditions (Equilbrium Moisture)*
0.335	0.00
0.604	0.00
0.846	0.00
1.045	0.00
1.398	0.01
1.784	0.02
2.516	0.08
3.417	0.14
4.281	0.23
5.230	0.33
6.147	0.41
7.101	0.47

Langmuir Parameters

	In-Situ Conditions (Equilbrium Moisture)
Vol. (cc/g)	
Pressure (MPa)	

SUMMARY OF ADSORPTION ANALYSES SI UNITS

Isotherm Temperature: **30.0 ºC**

Goodness of fit of Langmuir regression: **0.14 Density g/cc**

Moisture % **4.76**

Sikanni Chief b-92-D/94-I-4 1957.5 m

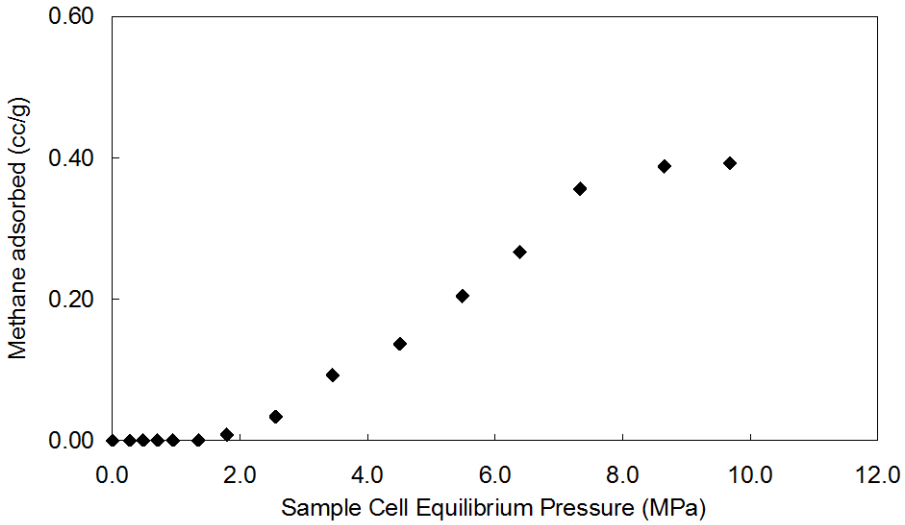

Pressure (MPa)	*Adsorbed gas (cc/g) In-Situ Conditions (Equilbrium Moisture)*
0.272	0.00
0.480	0.00
0.705	0.00
0.949	0.00
1.349	0.00
1.794	0.01
2.561	0.03
3.450	0.09
4.504	0.14
5.486	0.20
6.385	0.27
7.330	0.36
9.681	0.39

Langmuir Parameters

	In-Situ Conditions (Equilbrium Moisture)
Vol. (cc/g)	
Pressure (MPa)	

SUMMARY OF ADSORPTION ANALYSES SI UNITS

Isotherm Temperature: 30.0 ºC

Goodness of fit of Langmuir regression: **Density (g/cc)** 2.529

Moisture% 5.23

Sikanni Chief b-92-D/94-I-4 2106.7 m

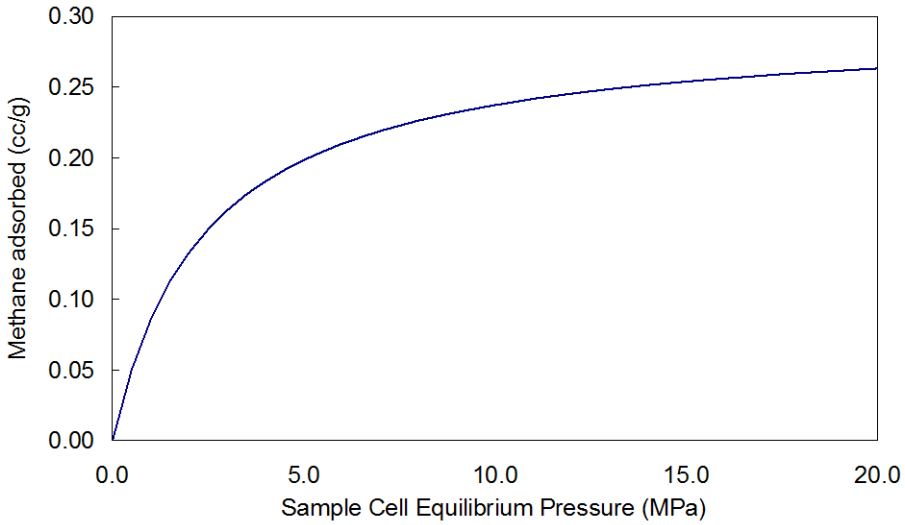

Pressure (MPa)	*Adsorbed gas (cc/g) In-Situ Conditions (Equilbrium Moisture)*
0.258	0.03
0.464	0.05
0.706	0.07
0.962	0.08
1.359	0.10
1.824	0.11
2.635	0.15
3.561	0.18
4.556	0.19
5.420	0.20
6.509	0.21
7.403	0.22
11.038	0.24

Langmuir Parameters

	In-Situ Conditions (Equilbrium Moisture)
Vol. (cc/g)	
Pressure (MPa)	

SUMMARY OF ADSORPTION ANALYSES SI UNITS

Isotherm Temperature: **30.0 ºC**

Goodness of fit of Langmuir regression: **Density (g/cc) 2.489**

Moisture% 5.19

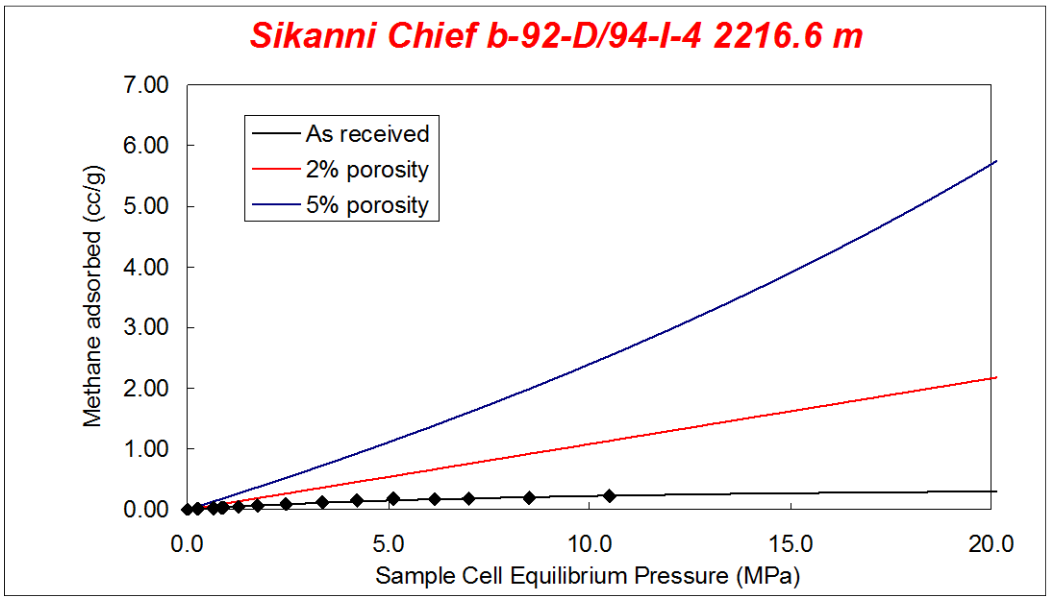

Pressure (MPa)	*Adsorbed gas (cc/g) In-Situ Conditions (Equilbrium Moisture)*
0.250	0.02
0.651	0.02
0.849	0.03
0.896	0.03
1.272	0.05
1.744	0.06
2.452	0.09
3.357	0.12
4.219	0.15
5.123	0.18
6.153	0.17
7.003	0.18
10.500	0.23

Langmuir Parameters

	In-Situ Conditions (Equilbrium Moisture)
Vol. (cc/g)	0.45
Pressure (MPa)	10.09

SUMMARY OF ADSORPTION ANALYSES SI UNITS

Isotherm Temperature: **30.0 ºC**

Goodness of fit of Langmuir regression: **0.83** **Density (g/cc)** **2.690**

Moisture% **4.06**

Muskwa Formation

Well Name	UWI	Depth (m)
Snake River	c-28-D/94-O-1	1951.10 1952.60 1990.10
Shekilie	a-94-G/94-P-8	1539.60 1544.10 1545.60 1551.60
Kotcho	c-32-K/94-I-14	1981.10 1982.20 1984.40 1988.10
Fort Nelson	c-70-I/94-J-10	1967.40 1968.90
Helmet	b-49-G/94-P-7	1810.9 1812.30 1813.60 1815.10 1816.30

Snake River c-28-D/94-O-1 1951.1 m

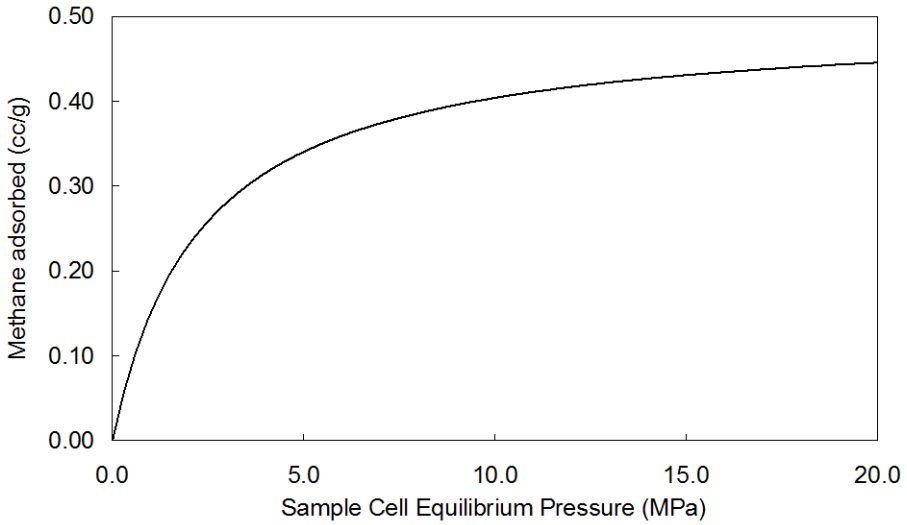

Pressure (MPa)	*Adsorbed gas (cc/g) In-Situ Conditions (Equilbrium Moisture)*
0.121	0.05
0.306	0.07
0.799	0.09
1.276	0.15
1.805	0.22
2.310	0.24
2.814	0.26
3.644	0.29
4.586	0.34
5.554	0.38
6.535	0.38
7.519	0.39

Langmuir Parameters

	In-Situ Conditions (Equilbrium Moisture)
Vol. (cc/g)	0.50
Pressure (MPa)	2.29

SUMMARY OF ADSORPTION ANALYSES SI UNITS

Isotherm Temperature: **30.0 ºC**

Goodness of fit of Langmuir regression: **0.96** **Density (g/cc)** **n/a**

Moisture% **2.84**

Snake River c-28-D/94-O-1 1952.6 m

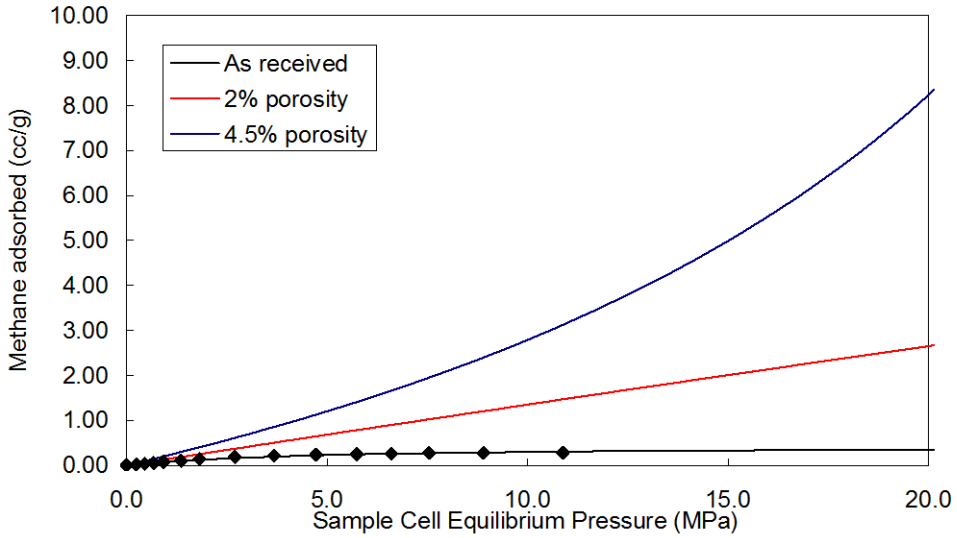

Pressure (MPa)	*Adsorbed gas (cc/g) In-Situ Conditions (Equilbrium Moisture)*
0.242	0.02
0.448	0.03
0.678	0.05
0.924	0.07
1.356	0.10
1.820	0.14
2.700	0.18
3.679	0.22
4.721	0.24
5.734	0.25
6.605	0.26
7.543	0.28
10.880	0.28

Langmuir Parameters

	In-Situ Conditions (Equilbrium Moisture)
Vol. (cc/g)	0.43
Pressure (MPa)	4.55

SUMMARY OF ADSORPTION ANALYSES SI UNITS

Isotherm Temperature: **30.0 ºC**

Goodness of fit of Langmuir regression: **0.95** **2.244**

Moisture % **11.94**

Snake River c-28-D/94-O-1 1990.1 m

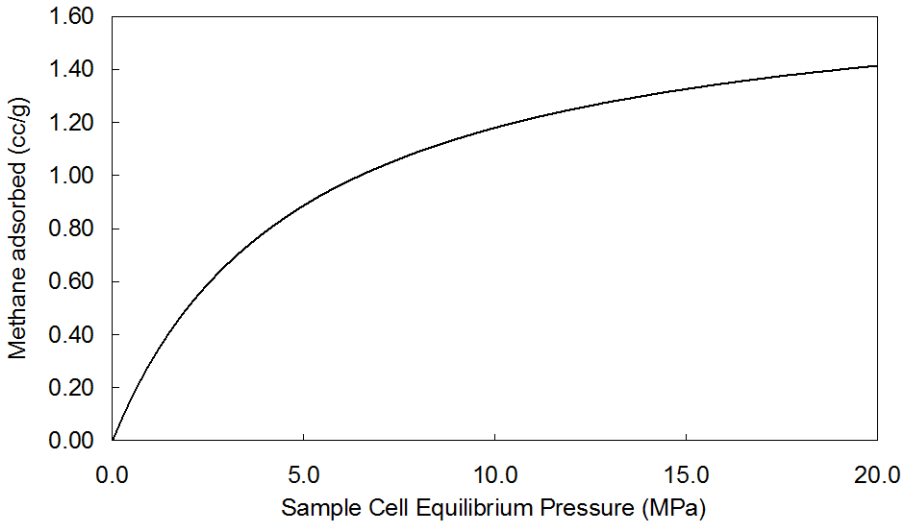

Pressure (MPa)	*Adsorbed gas (cc/g) In-Situ Conditions (Equilbrium Moisture)*
0.157	0.08
0.326	0.12
0.672	0.22
1.051	0.30
1.579	0.40
2.252	0.49
3.176	0.62
3.773	0.71
4.612	0.82
5.563	0.94
6.528	1.04
7.508	1.10

Langmuir Parameters

	In-Situ Conditions (Equilbrium Moisture)
Vol. (cc/g)	1.76
Pressure (MPa)	4.94

SUMMARY OF ADSORPTION ANALYSES SI UNITS

Isotherm Temperature: **30.0 ºC**

Goodness of fit of Langmuir regression: **0.95** **Density (g/cc)** **n/a**

Moisture% **3.48**

Shekilie a-94-G/94-P-8 1539.6 m

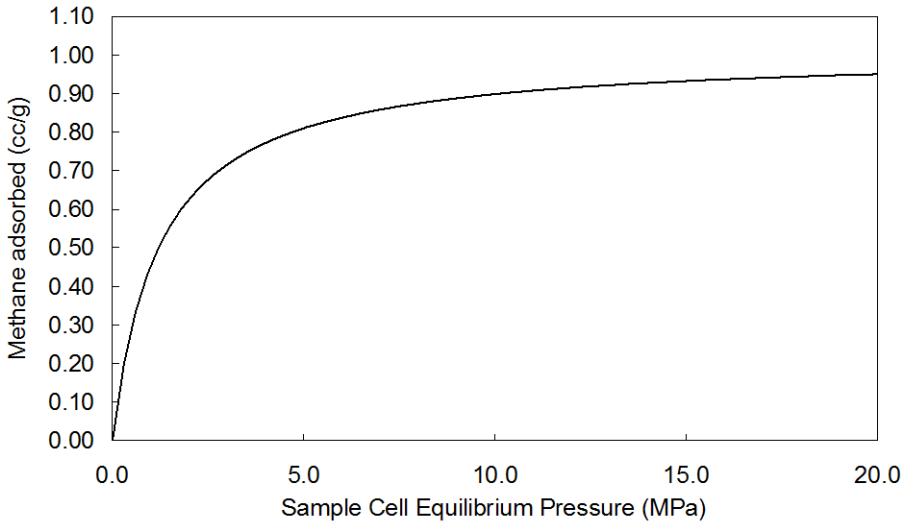

Pressure (MPa)	*Adsorbed gas (cc/g) In-Situ Conditions (Equilbrium Moisture)*
0.118	0.20
0.291	0.27
0.622	0.38
1.008	0.43
1.553	0.52
2.194	0.57
3.085	0.65
4.038	0.71
5.007	0.77
5.973	0.82
6.945	0.88
7.930	0.90

Langmuir Parameters

	In-Situ Conditions (Equilbrium Moisture)
Vol. (cc/g)	1.01
Pressure (MPa)	1.22

SUMMARY OF ADSORPTION ANALYSES SI UNITS

Isotherm Temperature: **30.0 ºC**

Goodness of fit of Langmuir regression: **0.98** **Density (g/cc)** **3.218**

Moisture% **4.40**

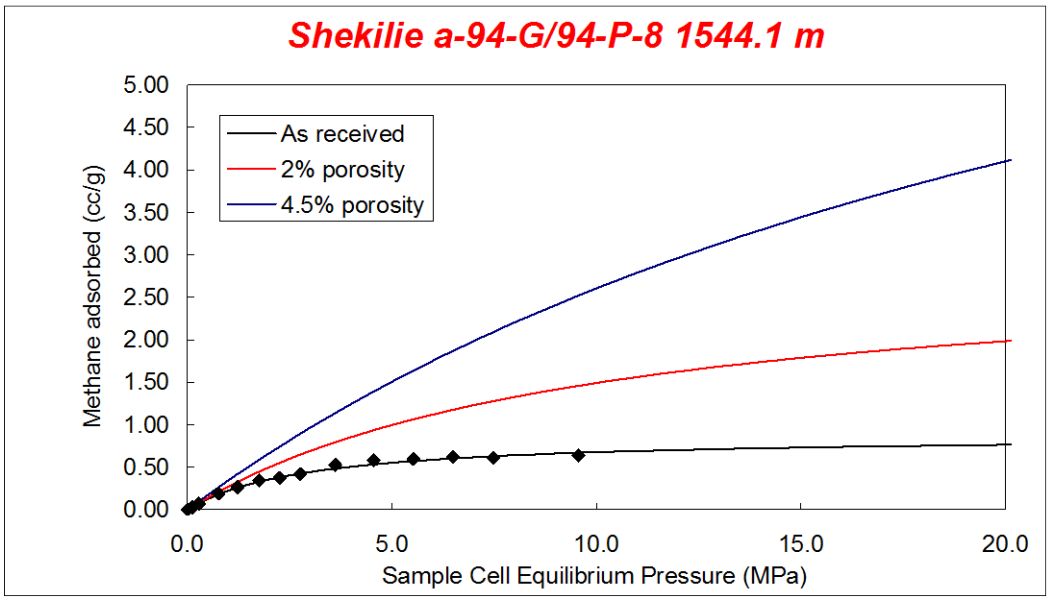

Pressure (MPa)	*Adsorbed gas (cc/g) In-Situ Conditions (Equilbrium Moisture)*
0.122	0.03
0.278	0.07
0.767	0.19
1.228	0.26
1.754	0.34
2.259	0.37
2.763	0.42
3.617	0.53
4.555	0.58
5.519	0.60
6.493	0.62
7.476	0.61

Langmuir Parameters

	In-Situ Conditions (Equilbrium Moisture)
Vol. (cc/g)	0.87
Pressure (MPa)	2.91

SUMMARY OF ADSORPTION ANALYSES SI UNITS

Isotherm Temperature: **30.0 ºC**

Goodness of fit of Langmuir regression: **0.98** **Density (g/cc)** **2.553**

Moisture% **3.64**

Shekilie a-94-G/94-P-8 1545.6 m

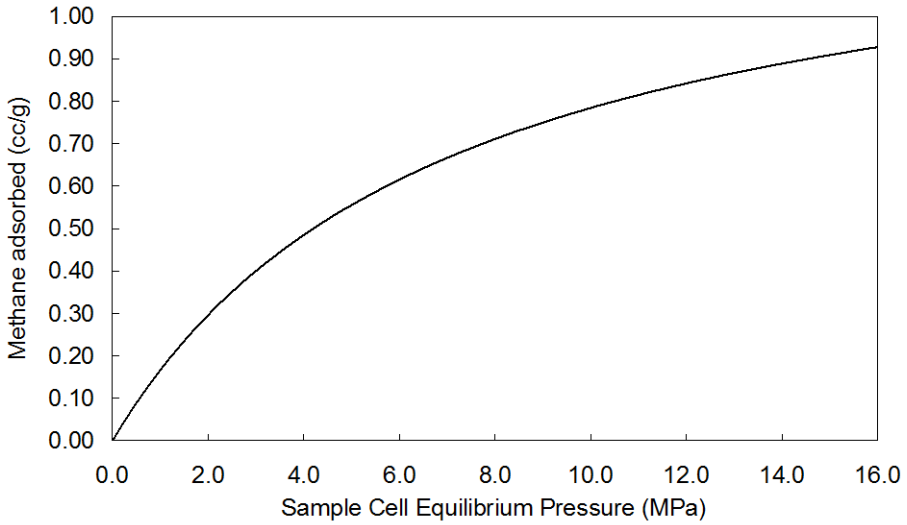

Pressure (MPa)	*Adsorbed gas (cc/g) In-Situ Conditions (Equilbrium Moisture)*
0.395	0.07
0.536	0.10
0.828	0.14
1.005	0.16
1.475	0.22
1.914	0.27
2.653	0.36
3.430	0.44
4.308	0.52
5.225	0.59
6.124	0.64
8.000	0.72
12.880	0.84

Langmuir Parameters

	In-Situ Conditions (Equilbrium Moisture)
Vol. (cc/g)	1.33
Pressure (MPa)	6.99

SUMMARY OF ADSORPTION ANALYSES SI UNITS

Isotherm Temperature: **30.0 ºC**

Goodness of fit of Langmuir regression: **0.99** **Density (g/cc)** **2.678**

Moisture% **3.73**

Shekilie a-94-G/94-P-8 1551.6 m

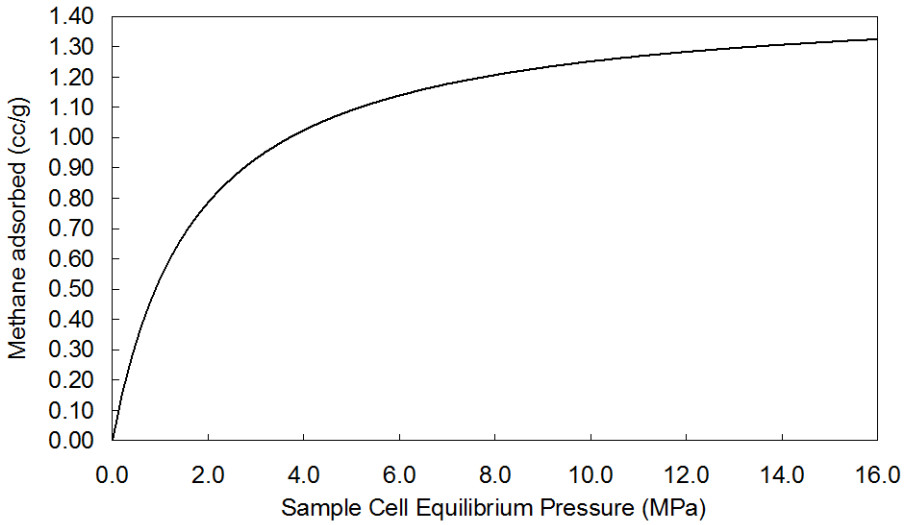

Pressure (MPa)	*Adsorbed gas (cc/g) In-Situ Conditions (Equilbrium Moisture)*
0.101	0.14
0.275	0.25
0.615	0.38
0.994	0.51
1.385	0.63
1.787	0.64
2.612	0.75
3.214	0.92
3.756	1.05
4.584	1.06
5.543	1.12
6.495	1.18
9.325	1.26

Langmuir Parameters

	In-Situ Conditions (Equilbrium Moisture)
Vol. (cc/g)	1.47
Pressure (MPa)	1.74

SUMMARY OF ADSORPTION ANALYSES SI UNITS

Isotherm Temperature: **30.0 ºC**

Goodness of fit of Langmuir regression: **0.98** **Density (g/cc)** **2.547**

Moisture% **3.81**

Kotcho c-32-K/94-I-14 1981.1 Muskwa

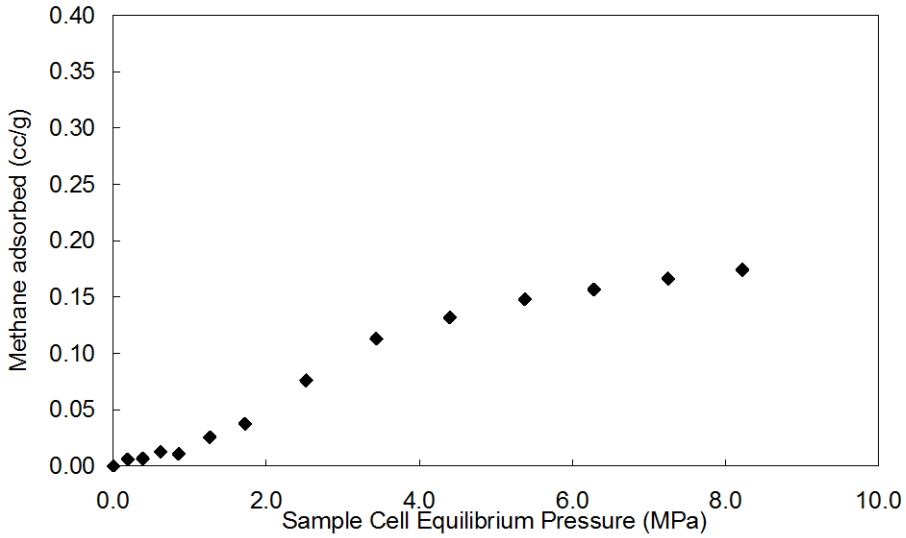

Pressure (MPa)	*Adsorbed gas (cc/g) In-Situ Conditions (Equilbrium Moisture)*
0.188	0.01
0.386	0.01
0.616	0.01
0.855	0.01
1.260	0.03
1.719	0.04
2.520	0.08
3.437	0.11
4.395	0.13
5.377	0.15
6.280	0.16
7.249	0.17

Langmuir Parameters

	In-Situ Conditions (Equilbrium Moisture)
Vol. (cc/g)	
Pressure (MPa)	

SUMMARY OF ADSORPTION ANALYSES SI UNITS

Isotherm Temperature: **30.0 ºC**

Goodness of fit of Langmuir regression: **0.09** **2.649**

Kotcho c-32-K/94-I-14 1982.2 m

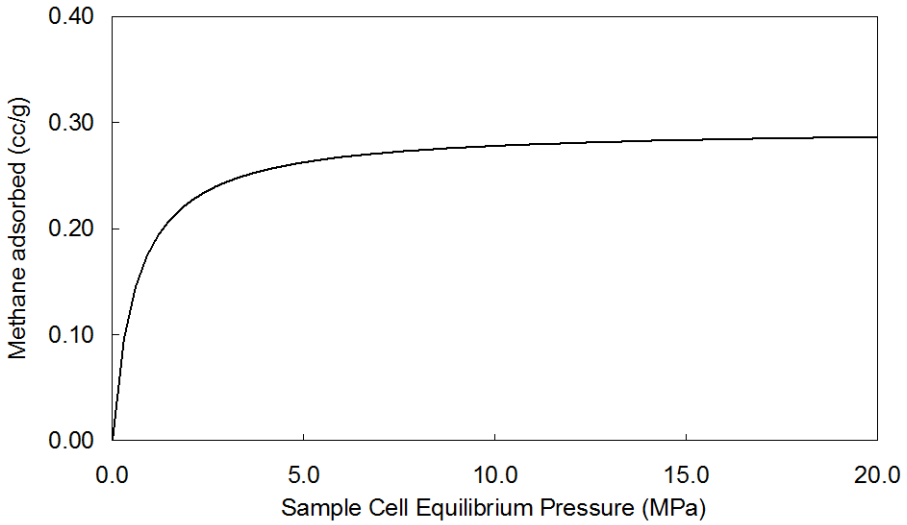

Pressure (MPa)	*Adsorbed gas (cc/g) In-Situ Conditions (Equilbrium Moisture)*
0.208	0.09
0.388	0.12
0.730	0.12
1.115	0.16
1.505	0.21
1.901	0.25
2.757	0.25
3.338	0.26
3.877	0.26
4.725	0.26
5.705	0.26
6.671	0.26

Langmuir Parameters

	In-Situ Conditions (Equilbrium Moisture)
Vol. (cc/g)	0.30
Pressure (MPa)	0.63

SUMMARY OF ADSORPTION ANALYSES SI UNITS

Isotherm Temperature: **30.0 ºC**

Goodness of fit of Langmuir regression: **0.99** **Density (g/cc)** **2.628**

Moisture% **4.71**

c-32-K/94-I-14 Kotcho 1984.4 m

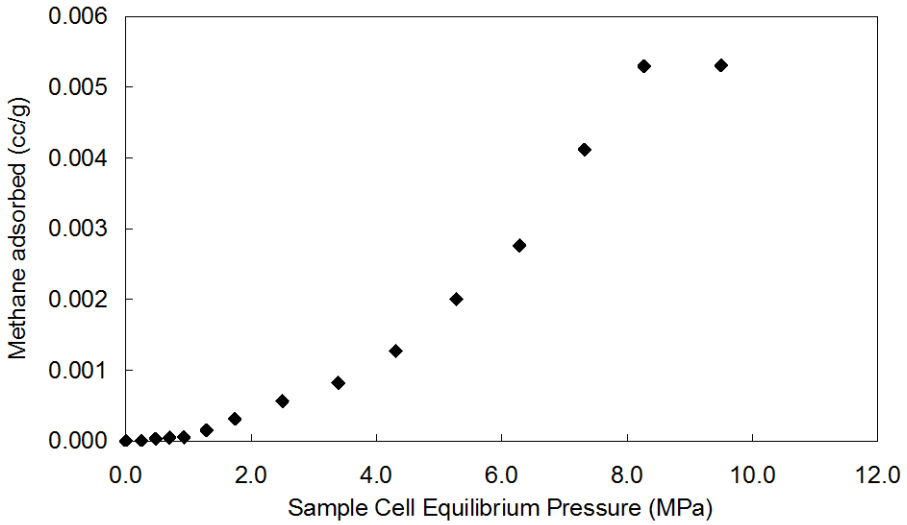

Pressure (MPa)	*Adsorbed gas (cc/g) In-Situ Conditions (Equilbrium Moisture)*
0.250	0.00
0.479	0.00
0.701	0.00
0.929	0.00
1.291	0.00
1.742	0.00
2.502	0.00
3.391	0.00
4.313	0.00
5.274	0.00
6.284	0.00
7.318	0.00
9.500	0.01
10.500	0.01

Langmuir Parameters

	In-Situ Conditions (Equilbrium Moisture)
Vol. (cc/g)	
Pressure (MPa)	

SUMMARY OF ADSORPTION ANALYSES SI UNITS

Isotherm Temperature: **30.0 ºC**
Goodness of fit of Langmuir regression: **0.10** **Density (g/cc)** **2.435**
Moisture% **9.18**

Kotcho c-32-K/94-I-14 1988.1 m

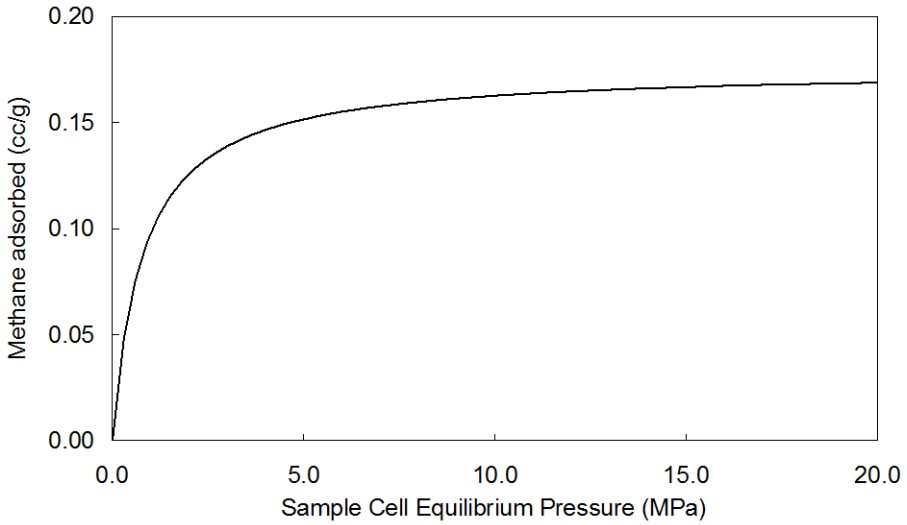

Pressure (MPa)	*Adsorbed gas (cc/g) In-Situ Conditions (Equilbrium Moisture)*
0.129	0.05
0.305	0.07
0.648	0.07
1.031	0.07
1.569	0.10
2.217	0.13
3.124	0.15
3.735	0.15
4.606	0.16
5.551	0.16
6.513	0.16
7.492	0.16

Langmuir Parameters

	In-Situ Conditions (Equilbrium Moisture)
Vol. (cc/g)	0.18
Pressure (MPa)	0.79

SUMMARY OF ADSORPTION ANALYSES SI UNITS

Isotherm Temperature: **30.0 ºC**

Goodness of fit of Langmuir regression: **0.98** **Density (g/cc)** **2.531**

Moisture% **4.71**

Ft. Nelson c-70-I/94-J-10 1967.4 m

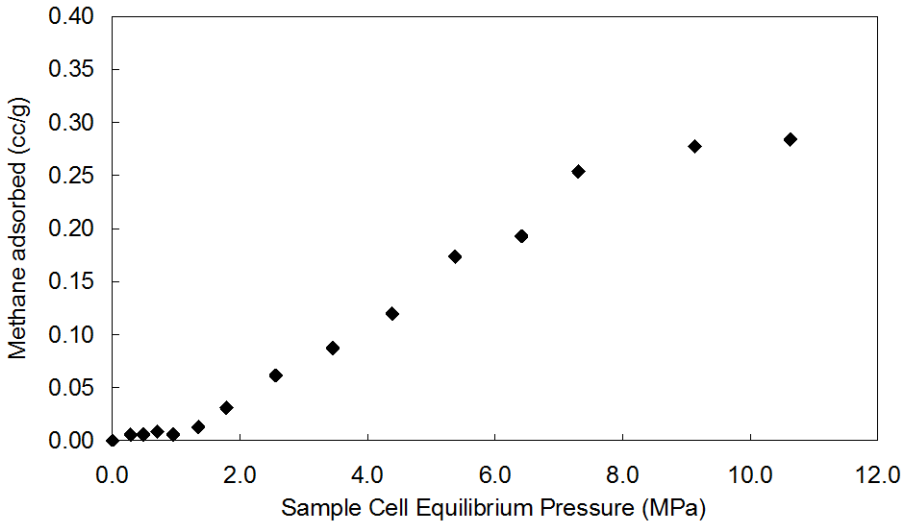

Pressure (MPa)	*Adsorbed gas (cc/g) In-Situ Conditions (Equilbrium Moisture)*
0.285	0.01
0.484	0.01
0.704	0.01
0.951	0.01
1.347	0.01
1.790	0.03
2.559	0.06
3.455	0.09
4.384	0.12
5.372	0.17
6.416	0.19
7.304	0.25
10.629	0.28

Langmuir Parameters

	In-Situ Conditions (Equilbrium Moisture)
Vol. (cc/g)	
Pressure (MPa)	

SUMMARY OF ADSORPTION ANALYSES SI UNITS

Isotherm Temperature: **30.0 ºC**

Goodness of fit of Langmuir regression: **0.36** **Density (g/cc)** **2.598**

Moisture% **4.21**

Ft. Nelson c-70-I/94-J-10 1968.9 m

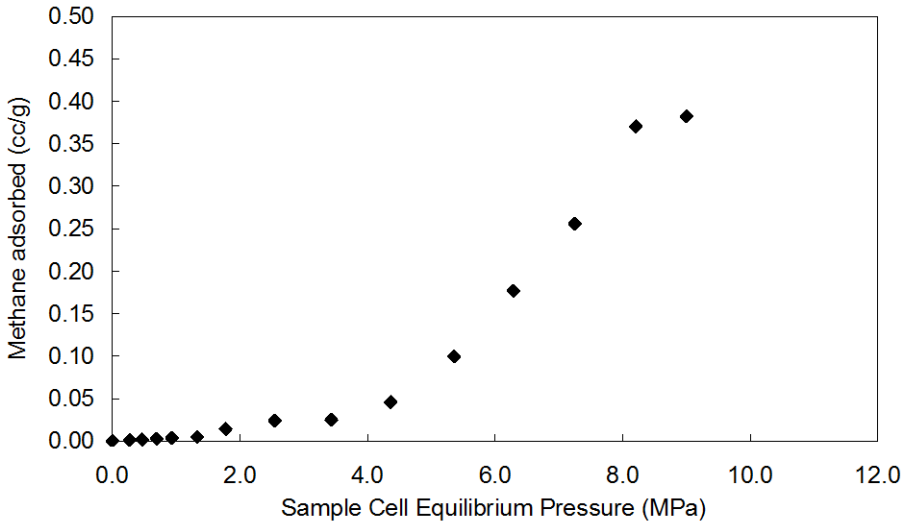

Pressure (MPa)	*Adsorbed gas (cc/g) In-Situ Conditions (Equilbrium Moisture)*
0.267	0.00
0.465	0.00
0.692	0.00
0.929	0.00
1.324	0.00
1.776	0.01
2.545	0.02
3.433	0.02
4.362	0.05
5.354	0.10
6.284	0.18
7.246	0.26
9.000	0.38
11.000	0.38

Langmuir Parameters

	In-Situ Conditions (Equilbrium Moisture)
Vol. (cc/g)	
Pressure (MPa)	

SUMMARY OF ADSORPTION ANALYSES SI UNITS

Isotherm Temperature: **30.0 ºC**

Goodness of fit of Langmuir regression: **0.78** **Density (g/cc)** **2.670**

Moisture% **3.71**

Helmet 200/b-049-G 094-P-07/00 1810.9 m

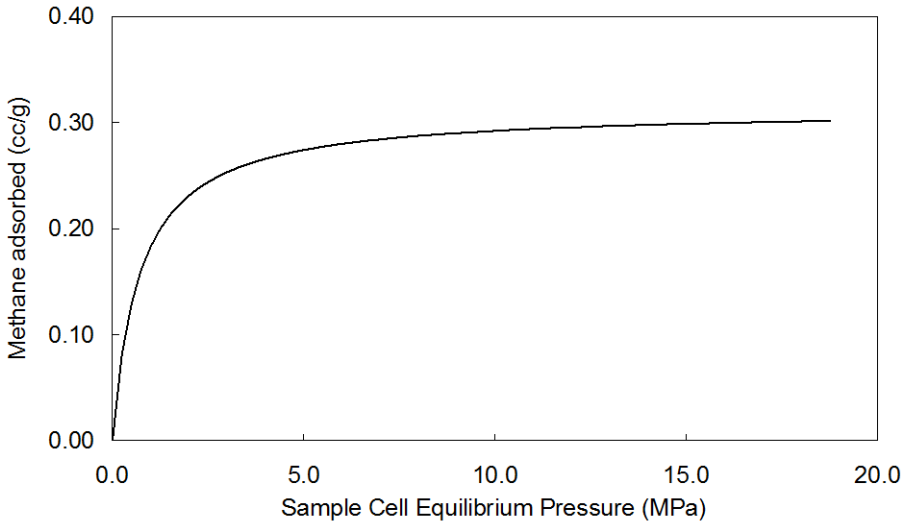

Pressure (MPa)	*Adsorbed gas (cc/g) In-Situ Conditions (Equilbrium Moisture)*
0.104	0.04
0.277	0.07
0.608	0.13
0.987	0.17
1.376	0.21
1.769	0.26
2.593	0.27
3.194	0.27
3.719	0.27
4.564	0.27
5.564	0.27
6.520	0.28

Langmuir Parameters

	In-Situ Conditions (Equilbrium Moisture)
Vol. (cc/g)	0.31
Pressure (MPa)	0.71

SUMMARY OF ADSORPTION ANALYSES SI UNITS

Isotherm Temperature: **30.0 ºC**
Goodness of fit of Langmuir regression: **0.99** **Density (g/cc)** **n/a**
Moisture% **3.27**

Helmet 200/b-049-G 094-P-07/00 1812.3 m

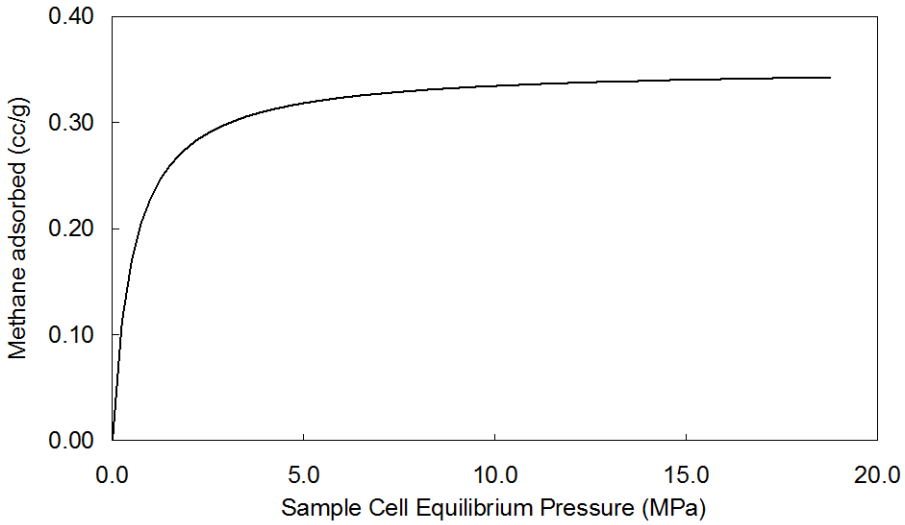

Pressure (MPa)	*Adsorbed gas (cc/g) In-Situ Conditions (Equilbrium Moisture)*
0.121	0.09
0.271	0.13
0.615	0.19
1.011	0.21
1.554	0.23
2.214	0.28
3.107	0.31
3.732	0.31

Langmuir Parameters

	In-Situ Conditions (Equilbrium Moisture)
Vol. (cc/g)	0.35
Pressure (MPa)	0.54

SUMMARY OF ADSORPTION ANALYSES SI UNITS

Isotherm Temperature: **30.0 ºC**

Goodness of fit of Langmuir regression: **0.99** **Density (g/cc)** **2.434**

Moisture% **3.41**

Helmet 200/b-049-G 094-P-07/00 1813.6 m

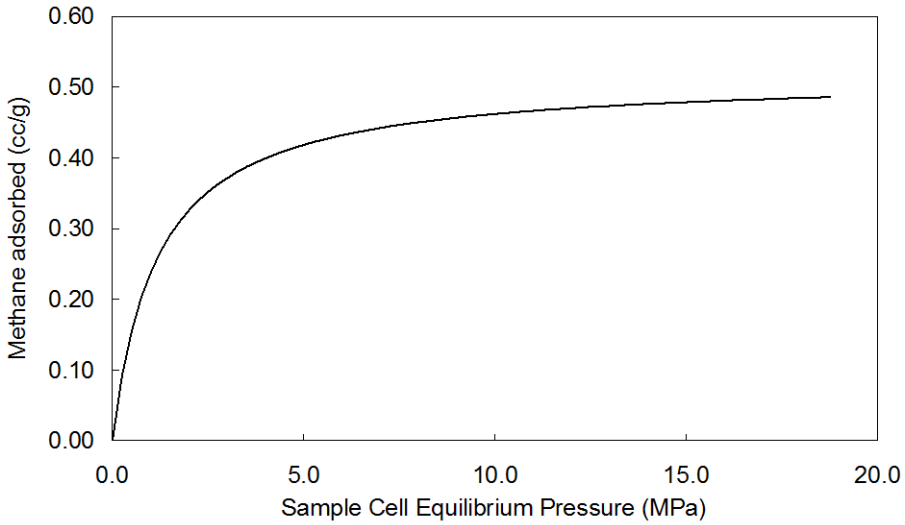

Pressure (MPa)	*Adsorbed gas (cc/g) In-Situ Conditions (Equilbrium Moisture)*
0.122	0.06
0.300	0.09
0.638	0.15
1.017	0.22
1.551	0.30
2.201	0.36
3.098	0.40
4.054	0.40
5.027	0.43
6.008	0.46
6.991	0.43
7.968	0.43

Langmuir Parameters

	In-Situ Conditions (Equilbrium Moisture)
Vol. (cc/g)	0.52
Pressure (MPa)	1.17

SUMMARY OF ADSORPTION ANALYSES SI UNITS

Isotherm Temperature: **30.0 ºC**

Goodness of fit of Langmuir regression: **0.99** **Density (g/cc)** **2.518**

Moisture% **3.87**

HELMET 200/b-049-G 094-P-07/00 1815.1 m

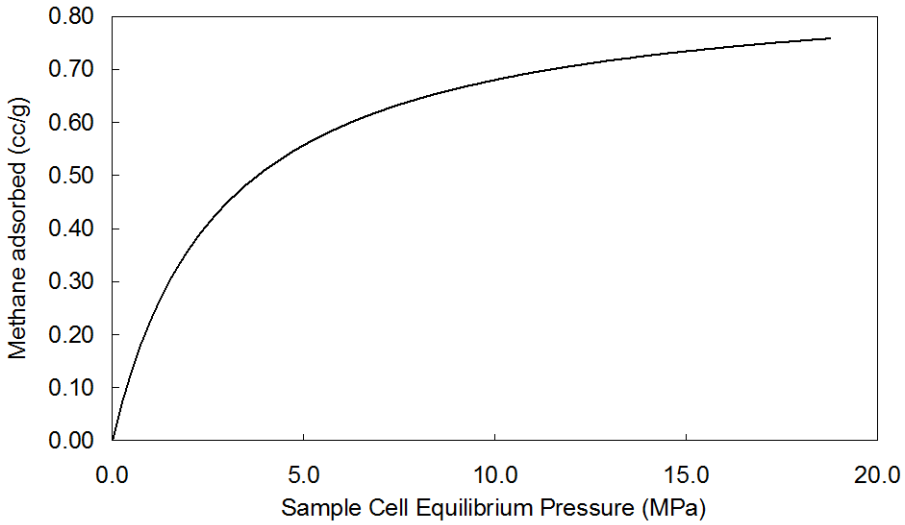

Pressure (MPa)	*Adsorbed gas (cc/g) In-Situ Conditions (Equilbrium Moisture)*
0.126	0.06
0.321	0.12
0.666	0.16
1.046	0.23
1.588	0.30
2.258	0.34
3.109	0.41
3.707	0.45
4.588	0.51
5.539	0.56
6.511	0.62
7.487	0.65

Langmuir Parameters

	In-Situ Conditions (Equilbrium Moisture)
Vol. (cc/g)	0.87
Pressure (MPa)	2.83

SUMMARY OF ADSORPTION ANALYSES SI UNITS

Isotherm Temperature: **30.0 ºC**

Goodness of fit of Langmuir regression: **0.96** **Density (g/cc)** **n/a**

Moisture% **3.14**

Helmet 200/b-049-G 094-P-07/00 1816.3 m

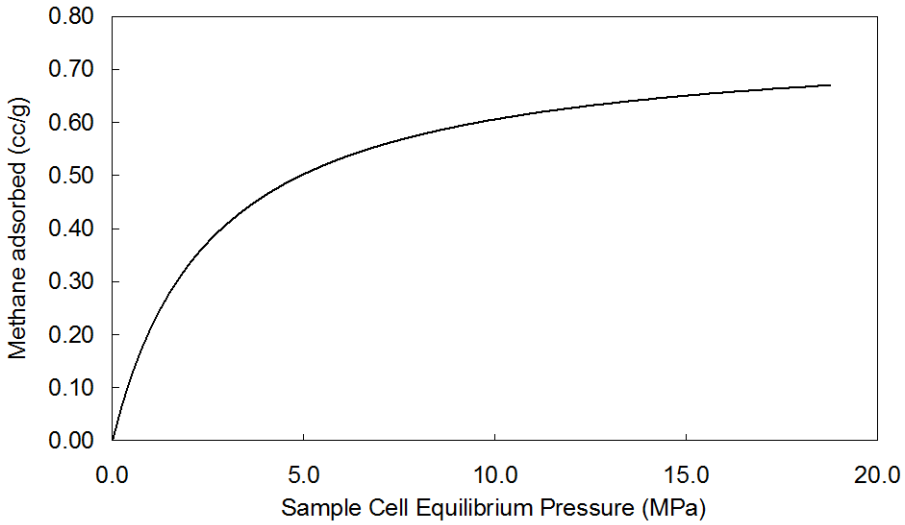

Pressure (MPa)	*Adsorbed gas (cc/g) In-Situ Conditions (Equilbrium Moisture)*
0.119	0.03
0.299	0.10
0.788	0.18
1.248	0.24
1.770	0.30
2.286	0.35
2.794	0.39
3.640	0.43
4.615	0.47
5.606	0.51
6.538	0.55
7.500	0.58

Langmuir Parameters

	In-Situ Conditions (Equilbrium Moisture)
Vol. (cc/g)	0.76
Pressure (MPa)	2.59

SUMMARY OF ADSORPTION ANALYSES SI UNITS

Isotherm Temperature: **30.0 ºC**
Goodness of fit of Langmuir regression: **0.99 Density (g/cc)**
Moisture% **3.57**